Title
Synthesis of Poly(ethylene glycol) Derivatives for Bioconjugation and Surface Patterning

Author
Lin, En-Wei

Publication Date
2014

Peer reviewed|Thesis/dissertation

UNIVERSITY OF CALIFORNIA

Los Angeles

Synthesis of Poly(ethylene glycol) Derivatives for Bioconjugation and Surface Patterning

A dissertation submitted in partial satisfaction of the requirements for the degree Doctor of Philosophy in Chemistry

by

En-Wei Lin

2014

ABSTRACT OF THE DISSERTATION

Synthesis of Poly(ethylene glycol) Derivatives

for Bioconjugation and Surface Patterning

by

En-Wei Lin

Doctor of Philosophy in Chemistry

University of California, Los Angeles, 2014

Professor Heather D. Maynard, Chair

Poly(ethylene glycol) (PEG) is a biocompatible and water-soluble polymer that has a wide range of applications in chemistry, biology, and medicine. In this dissertation, we describe the synthesis of end-functionalized PEG derivatives and PEG-like polymers for biomolecule conjugation and surface patterning applications. In Chapter 1, we provide an overview on PEG-protein conjugates, as well as current synthetic approaches and applications for protein-polymer conjugates and oligonucleotide-polymer conjugates. PEG-protein conjugates are currently the only FDA-approved protein-polymer conjugates, and the conjugation method plays an important role in protein performance. In Chapter 2, we describe a site-specific and photoinduced bioconjugation method utilizing non-covalent protein-ligand binding affinity and a photo-

reactive benzophenone group. In control experiments, such as without the benzophenone group or without photo-irradiation, no PEG conjugation was observed by gel electrophoresis.

Some deficiencies of PEG such as immunological responses have been observed. Moreover, PEG does not significantly stabilize proteins in storage conditions or when stressed by heat and other factors. In Chapter 3, we describe a new type of glycopolymer with trehalose side chains, and showed its stabilizing effect toward several enzymes after heating or lyophilization. In Chapter 4, we describe the conjugation of these trehalose polymers to small interfering ribonucleic acid (siRNA) and the investigation of their properties towards nuclease resistance and serum stability.

Previously, we discovered that conjugation of comb-type PEG (oligo(ethylene glycol) (metha)crylate-based polymers) to siRNA enhanced its nuclease resistance and gene silencing efficiency. In Chapter 5, we describe the preparation of similar siRNA-polymer conjugates using the *grafting from* approach, meaning that polymer growth occurred from a siRNA macroinitiator. Additionally, methacrylate-based polymers with oligo(ethylene glycol) side chains have also been found to be tunable thermoresponsive polymers. In Chapter 6, we describe the use of atom transfer radical polymerization (ATRP) to synthesize three distinctly temperature-responsive oligo(ethylene glycol) methacrylate-based polymers and the preparation of thermoresponsive and fluorescent hydrogel patterns. Above their volume phase transition temperature (VPTT), the hydrogels collapsed due to the release of water, and led to fluorescent quenching. Multicomponent morphing surfaces were prepared to display dual color patterns and encrypted messages at different temperatures.

The dissertation of En-Wei Lin is approved.

Timothy J. Deming

Andrea M. Kasko

Heather D. Maynard, Committee Chair

University of California, Los Angeles

2014

TABLE OF CONTENTS

LIST OF FIGURES

LIST OF TABLES

LIST OF SCHEMES

LIST OF ABBREVIATIONS

AA	Ascorbic acid
ACN	Acetonitrile
AF488	Alexa Fluor® 488
AFM	Atomic force microscopy
AGET ATRP	Activators generated by electron transfer ATRP
AIBN	2,2'-Azobis(2-methylpropionitrile)
AMP	Adenosine monophosphate
ATRP	Atom transfer radical polymerization
Bipy	2,2'-Bipyridine
Boc	*tert*-Butyloxycarbonyl
BODIPY	Boradiazaindacene
BP	Benzophenone
BSA	Bovine serum albumin
CBS	Calf bovine serum
$CDCl_3$	Deuterated chloroform
CRP	Controlled radical polymerization
CTA	Chain transfer agent
CuAAC	Copper-catalyzed azide-alkyne cycloaddition
Cys	Cysteine
D-PBS	Dulbecco's phosphate buffer saline
D_2O	Deuterated water

DA	Diazirine
DAHC	Diammonium hydrogen citrate
DCC	*N*,*N'*-Dicyclohexylcarbodiimide
DCM	Dichloromethane
DCM	Dichloromethane
DEGMA	Diethylene glycol methyl ether methacrylate
DIEA	*N*,*N*-Diisopropylethylamine
DMAEMA	*N*,*N*-Dimethylaminoethyl methacrylate
DMAP	4-Dimethylaminopyridine
DMF	*N*,*N*-Dimethylformamide
DMSO	Dimethyl sulfoxide
DNA	Deoxyribonucleic acid
DTT	Dithiothreitol
E-beam	Electron beam
EC	Enzyme commission
EDC	1-Ethyl-3-(3-dimethylaminopropyl)carbodiimide
EDTA	Ethylenediaminetetraacetic acid
eGFP	Enhanced green fluorescent protein
EPO	Erythropoiesis protein
ESI-MS	Electrospray ionization mass spectrometry
EtOAc	Ethyl acetate
Ex/Em	Excitation/Emission
FDA	Food and drug administration

FITC	Fluorescein isothiocyanate
Fmoc	Fluorenylmethoxycarbonyl
FPLC	Fast protein liquid chromatography
FRET	Förster resonance energy transfer
FT-IR	Fourier transform infrared spectroscopy
G-CSF	Granulocyte colony-stimulating factor
GFP	Green fluorescent protein
Glu	Glutamic acid
GOx	Glucose oxidase
GPC	Gel permeation chromatography
GRAS	Generally regarded as safe
GSH	Glutathione
GST	Gluthathione *S*-transeferase
HPLC	High performance liquid chromatography
HRP	Horseradish peroxidase
IL-8	Interleukin 8
k_d	Dissociation constant
kDa	kilodaltons
LCST	Lower critical solution temperature
Lyz	Lysozyme
MALDI-TOF	Matrix-assisted laser desorption ionization-time of flight
MeOD	Deuterated methanol
MeOH	Methanol

M_n	Number average molecular weight
mPEG	Monomethoxy poly(ethylene glycol)
mRNA	Messenger RNA
MW	Molecular weight
MWCO	Molecular weight cut-off
NEt_3	Triethylamine
NHS	*N*-hydroxysuccinimide
NIPAAm	*N*-isopropylacrylamide
NMP	Nitroxide-mediated radical polymerization
NMR	Nuclear magnetic resonance
OEOMA	Oligo(ethylene oxide) monomethyl ether methacrylate
ONPG	2-Nitrophenyl-β-D-galactopyranoside
PAGE	Polyacrylamide gel electrophoresis
PBD	Protein data bank
PBS	Phosphate-buffered saline
PDI	Polydispersity index
PEG	Poly(ethylene glycol)
PEGA	Poly(ethylene glycol) methyl ether acrylate
PEGMA	Poly(ethylene glycol) methyl ether methacrylate
PLP	Pyridoxal-5-phosphate
pMMA	Poly(methyl methacrylate)
PTFE	Polytetrafluoroethene
RAFT	Reversible addition-fragmentation chain transfer

rcf	Relative centrifugal force
rh-GH	Recombinant human growth hormone
RhodG	Rhodamine green
RNA	Ribonucleic acid
RNAi	RNA interference
RNase	Ribonuclease
ROMP	Ring-opening metathesis polymerization
rpm	Revolutions per minute
SA	Sinapic acid
sCT	Salmon calcitonin
SDS	Sodium dodecyl sulfate
siRNA	Small interfering ribonucleic acid
SRP	Stimuli responsive polymer
TBE	Tris/Borate/EDTA
TE	Tris-EDTA
TEAA	Triethylamine-acetic acid
TEGMA	Tri(ethylene glycol) methyl ether methacrylate
TFA	Trifluoroacetic acid
THAP	2,4,6-Trihydroxyacetophenone
THF	Tetrahydrofuran
TIPS	Triisopropylsilane
TLC	Thin layer chromatography
TMB	3,3’,5,5’-Tetramethylbenzidine

TPMA	Tris(2-pyridylmethyl)amine
Tris	Tris(hydroxymethyl)aminomethane
Ubq	Ubiquitin
UV/Vis	Ultraviolet/visible
VA044	2,2'-Azobis[2-(2-imidazolin-2-yl)propane] dihydrochloride
VEGF	Vascular endothelial growth factor
VPTT	Volume phase transition temperature
VS	Vinyl sulfone
W	Watts
wt equiv	Weight equivalent
β-Gal	β-Galactosidase

ACKNOWLEDGEMENTS

Over the past five years, I have received support, guidance, and encouragement from several people. Without them, the completion of my dissertation would not have been possible. First of all, I am sincerely grateful to my advisor, Professor Heather D. Maynard, for the opportunity to work in her research group, and for guiding me through this journey. Her creativity, knowledge, and time management skills are very inspiring and motivating to me. I would also like to thank my doctoral committee of Professor Timothy J. Deming and Professor Andrea M. Kasko for their input and guidance towards my dissertation work.

In addition, I would like to thank all of the former and current Maynard group members for being inspirational and supportive colleagues and friends. I thank Dr. Zachery Tolstyka, Dr. Panchami Prabhakaran, and Dr. Gregory Grover for their mentorship early on in my graduate career. I thank Dr. Rock Mancini and Prof. Erhan Bat for their helpful discussions during their time in the group. I also thank Juneyoung Lee, Nicholas Matsumoto, and Thi Kathy Nguyen for the support as fellow classmates for the past five years. I thank all current members, including Dr. Yang Liu, Dr. Muhammet Kahveci, Caitlin Decker, Uland Lau, Natalie Boehnke, Samantha Paluck, Emma Pelegri-O'Day, Jeong Hoon Ko, and Eric Raftery for reading sections of my dissertation and giving me feedbacks.

Portions of Chapter 1 is in-press as: Pelegri-O'Day, E. M.; Lin, E.-W.; Maynard, H. D., "Therapeutic Protein-Polymer Conjugates: Advancing Beyond PEGylation," *J. Am. Chem. Soc.*, DOI: 10.1021/ja504390x. Chapter 2 is a version of: Lin, E.-W.; Boehnke, N.; Maynard, H. D., "Protein-Polymer Conjugation *via* Ligand Affinity and Photoactivation of Glutathione *S*-Transferase*,"Bioconjugate Chem., accepted.* Portions of Chapter 3 have been published as: Lee,

J.; Lin, E.-W.; Lau, U. Y.; Hedrick, J. L.; Bat, E.; Maynard, H. D., "Trehalose Glycopolymers as Excipients for Protein Stabilization," *Biomacromolecules* **2013,** *14*, 2561-2569. Portions of Chapter 5 is in preparation for publication as: Lin, E.-W.; Maynard, H. D., "Alternative Synthesis Route Toward siRNA-Polymer Conjugates: *Grafting From* siRNA," *in preparation*. Chapter 6 is a version of: Bat, E.; Lin, E.-W.; Saxer, S.; Maynard, H. D., "Morphing Hydrogel Patterns by Thermo-Reversible Fluorescence Switching," *Macromol. Rapid Commun*. **2014**, *35*, 1260-1265.

The research described in this dissertation was supported by the National Science Foundation (CHE-1112550) and Phytex (MH-57063). I also thank the 2014 Cram Fellowship for funding.

I thank Liane Fukumoto, Gloria Lee, and Joseph Yi-Chao Fan for keeping me company and for all the helpful discussions about chemistry and graduate school. I thank Janie Yen-Ting Chen, my roommate for five years, for all the encouragements. I am also very grateful to have plenty of volleyball friends to exercise with on weekends and to keep me optimistic and joyful. Especially, I would like to thank Charles for the solid support throughout the past five years. I am very glad to have met all of you in Los Angeles!

Last but not least, I thank my friends and family in Taiwan and other states. I am blessed to have so many friends caring about me even when I'm so far away. I thank my sister, who assisted me in applying to graduate school, gave me so many textbooks and supplies to get me started, and supported me for the past twenty-seven years. I thank my parents to have given me a wonderful background and environment to grow up in. I thank my mom for flying over to visit me many times in the past five years and keeping my freezer filled. I would not have had the opportunity to be here without my family's support.

VITA

Education

2009	National Tsing Hua University, Hsinchu, Taiwan B.S. in Chemistry
2005	National Experimental High School Hsinchu, Taiwan

Research Experience

2009-2014	Graduate Research Assistant University of California, Los Angeles Professor Heather D. Maynard
2008-2009	Undergraduate Researcher National Tsing Hua University, Hsinchu, Taiwan Professor Chun-Cheng Lin

Honors & Awards

2014	Cram Fellowship
2007	Dean's List of Extraordinary Performance in Organic Chemistry Lab
2003	Gold Medal SpringSoft Inc. Science Creativity Competition

Publications

Lin, E.-W.; Boehnke, N.; Maynard, H. D., "Protein-Polymer Conjugation *via* Ligand Affinity and Photoactivation of Glutathione *S*-Transferase*,"Bioconjugate Chem., accepted*

Pelegri-O'Day, E. M.; **Lin, E.-W.**; Maynard, H. D., "Therapeutic Protein-Polymer Conjugates: Advancing Beyond PEGylation," *J. Am. Chem. Soc.*, DOI: 10.1021/ja504390x

Bat, E.*****; **Lin, E.-W.***; Saxer, S.; Maynard, H. D., "Morphing Hydrogel Patterns by Thermo-Reversible Fluorescence Switching," *Macromol. Rapid Commun*. **2014**, *35*, 1260-1265.

Lee, J.; **Lin, E.-W.**; Lau, U. Y.; Hedrick, J. L.; Bat, E.; Maynard, H. D., "Trehalose Glycopolymers as Excipients for Protein Stabilization," *Biomacromolecules* **2013,** *14*, 2561-2569.

Vázquez-Dorbatt, V.; Lee, J.; **Lin, E.-W.**; Maynard, H. D., "Synthesis of Glycopolymers by Controlled Radical Polymerization Techniques and Their Applications," *ChemBioChem* **2012**, *13*, 2478-2487.

Lai, C.-H.; Lin, Y.-C.; Chou, F.-I.; Liang, C.-F.; **Lin, E.-W.**; Chuang, Y.-J.; Lin, C.-C., "Design of Multivalent Galactosyl Carborane as a Targeting Specific Agent for Potential Application to Boron Neutron Capture Therapy," *Chem. Commun.* **2012**, *48*, 612-614.

Patents

Maynard, H. D.; Mancini, R. J.; Lee, J.; **Lin, E.-W.**, "Stabilization of Biomolecules using Sugar Polymers," International Patent Application PCT/US2013/23235, January 27, 2012.

Presentations

UCLA 2014 Organic Graduate Symposium, "Bioconjugation and Surface Patterning of Poly(ethylene glycol) Derivatives" Oral Presentation, Los Angeles, CA, June 7, 2014.

UCLA-USC-Caltech Nanotechnology & Nanomedicine Symposium, "Trehalose Glycopolymers for the Stabilization of Proteins and Nucleic Acids" Poster Presentation, Los Angeles, CA, October 17, 2013.

2013 Seaborg Symposium, "Thermo-reversible Fluorescence Switching of Multicomponent Hydrogel Patterns" Poster Presentation, Los Angeles, CA, October 26, 2013.

44th ACS Western Regional Meeting, "Thermo-reversible Fluorescence Switching of Multicomponent Hydrogel Patterns" Poster Presentation, Santa Clara, CA, October 4, 2013.

Chapter 1

Advancing Beyond PEGylation:

Polymer Bioconjugates Prepared by

Controlled Radical Polymerization[‡]

1.1 Introduction

Polymer bioconjugates are hybrid macromolecules of natural and synthetic polymers. Protein-polymer conjugates display a unique combination of properties derived from the biologic and synthetic materials, which can be individually tuned to elicit a desired effect. Inherent protein biorecognition can be used in therapies to replace deficient or absent natural proteins, upregulate existing metabolic pathways, or inhibit molecules and organisms.[1] Proteins may function in chemotherapeutic delivery devices as targeting agents. Additionally, enzymes can be used to catalyze chemical reactions both *in vivo* and *in vitro*. Oligonucleotides have high sequence-specificity, which is useful in both biological and structural functions. Synthetic polymers exhibit high thermal and chemical stabilities and can be synthesized with controlled molecular weight and low dispersity (i.e. narrow molecular weight distribution). In addition, synthetic polymers allow for the incorporation of desired functional groups and can be designed to respond to biological and non-biological stimuli including changes in pH, temperature, redox potential, or analyte concentration. The fusion of biological properties and chemical stability or reactivity provides polymer bioconjugates a unique position at the intersection of chemistry, biotechnology, nanotechnology, and medicine (**Figure 1-1**).[2]

The subject of protein-polymer conjugates has been extensively reviewed, with details on synthetic methods and comprehensive summaries of reported work.[2-10] Recently, investigations of polymer biconjugates have also extended to oligonucleotides.[11,12] This chapter will provide a brief overview on poly(ethylene glycol) (PEG) conjugates, controlled radical polymerization techniques, current synthetic approaches and applications for protein-polymer conjugates, and an introduction to oligonucleotide-polymer conjugates, mainly focusing on siRNA (small-interfering RNA).

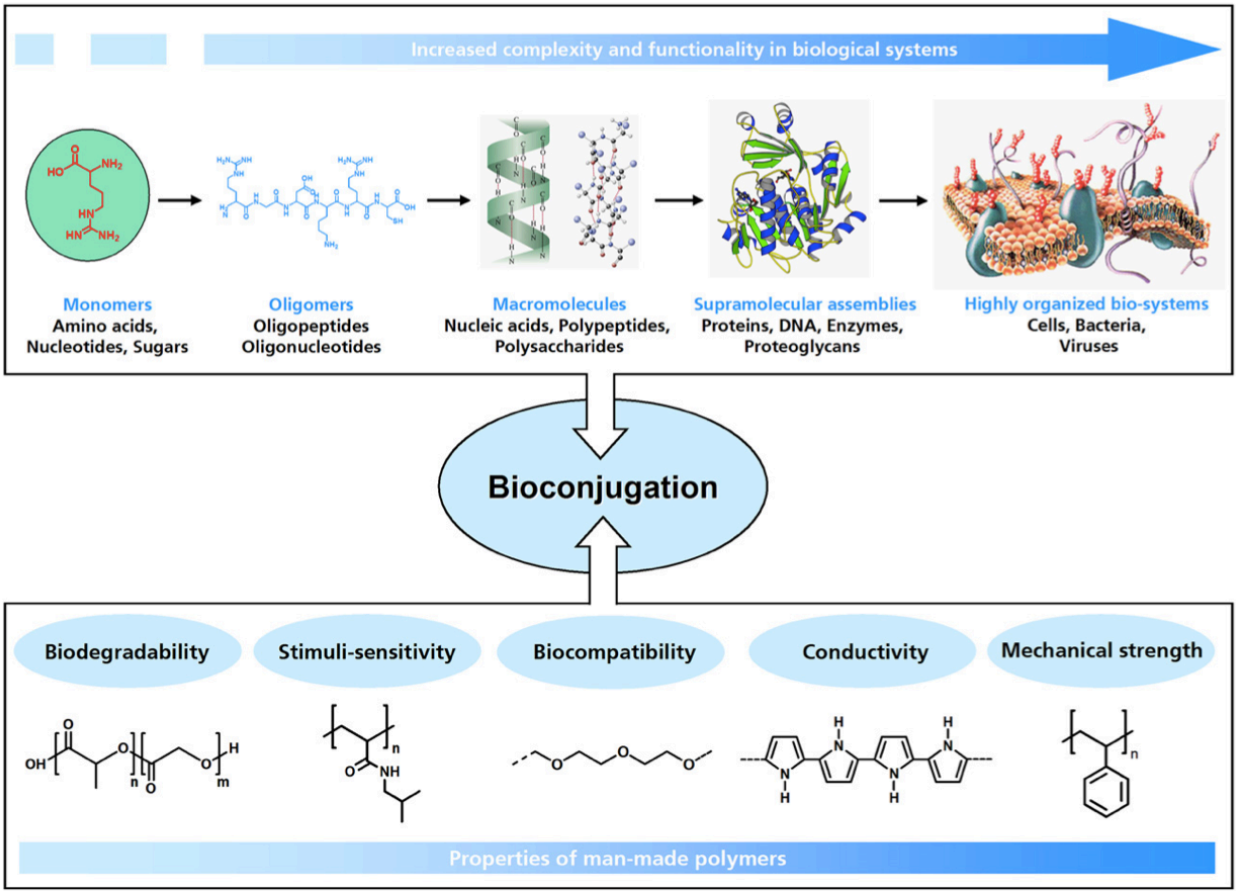

Figure 1-1. Reprinted from Progress in Polymer Science, Vol. 33, Jean-François Lutz and Hans G. Börner, Modern trends in polymer bioconjugates design, Page 1-39, Copyright (2007), with permission from Elsevier.[2]

1.2 The Evolvement and Current Status of PEGylation

The covalent attachment of PEG is known as PEGylation. PEG is generally regarded as safe by the FDA and is known to increase protein half-life by reducing renal clearance, resisting breakdown by enzymes and inhibiting recognition by the immune system. There are currently twelve FDA-approved PEGylated drugs on the market with diverse applications as therapeutics,

of which ten are PEG-protein conjugates.[13,14] These conjugates function as replacement therapies for native enzyme deficiencies, stimulate immune responses, increase production of red or white blood cells, or neutralize over-active cytokines or receptors.[5] They have been used to treat diseases, such as Hepatitis C or Crohn's disease, or to stimulate regrowth of white blood cells after chemotherapy. Macugen is a PEGylated RNA aptamer targeting vascular endothelial growth factor (VEGF), and is the only PEGylated oligonucleotide based drug that has entered the market.[15] As a result, protein-polymer conjugates are an important class of biologics, generating more than 5 billion dollars revenue annually.

1.2.1 Protein PEGylation

In 1977, Abuchowski and coworkers demonstrated the first conjugation of monomethoxy poly(ethylene glycol) (mPEG) to bovine serum albumin (BSA) through the use of a cyanuric chloride coupling agent.[16] This BSA-PEG conjugate displayed a lower immunogenic response in animal models relative to the native protein. They later reported that PEGylated proteins increased circulation times in animal models relative to native proteins.[16,17] Two years later, Kanamaru and coworkers reported the increased biocirculation of the chromoprotein neocarzinostatin when covalently coupled to a polystyrene-maleimide copolymer.[18] Together, these discoveries prompted a flurry of interest in conjugating polymers to proteins for therapeutic use (**Figure 1-2**).

In Japan, the protein-polymer conjugate SMANCS (zinostatin stimalamer), which consists of the anti-tumor chromoprotein neocarzinostatin and a styrene-maleic acid copolymer, is approved for the treatment of hepatocellular cancer.[19] However, the focus of medical

applications has been mainly on the conjugation of PEG to proteins, and PEG-protein conjugates are currently the only FDA-approved protein conjugates in the United States.[5]

1.2.2 Advances in PEG Conjugation Chemistry

PEG conjugation technology has greatly improved over the past forty years. First-generation PEGylation methods used semi-telechelic mPEG to modify lysine side chains. The mPEG hydroxyl groups were activated through formation of derivatives such as mPEG dichlorotriazine, mPEG succinimidyl carbonate, mPEG benzotriazol and mPEG tresylate, but these methods were inefficient. They suffered from crosslinking due to contamination with bisfunctional PEG, unstable and easily cleavable protein-polymer linkages, alterations in protein charges, and lack of selectivity, which all led to heterogeneity of the PEGylated proteins.[6,20] Most of these early protein conjugations relied on post-polymerization modifications or coupling reactions with the terminal hydroxyl group of PEG that required multiple steps, toxic reagents, or difficult purification procedures.[16,21]

Second-generation techniques focused on chemical transformations of mPEG to derivatives such as mPEG-propionaldehyde, which could produce more stable linkages as well as more selective PEGylation resulting in retention of bioactivity. For instance, it was shown that the N-terminal amine of interleukin 8 (IL-8) may be selectively oxidized under mild conditions to a glyoxyl group with sodium periodate, which can subsequently react with an aminooxy PEG to form a conjugate *via* oxime bond formation.[22] A transamination reaction was also introduced wherein the N-terminus could be selectively modified with pyridoxal-5-phosphate (PLP) to yield an aldehyde or ketone.[23] A variety of hydroxylamine-functionalized

molecules or polymers including PEG were conjugated to the resulting N-terminus carbonyls *via* an oxime bond. Moreover, second-generation techniques minimized negative effects on biological activity caused by conjugation. For instance, PEGylation of granulocyte colony-stimulating factor (G-CSF) and other proteins resulted in less protein aggregation at elevated temperatures for an extended time when the positive charge on the N-terminal methionine residue was retained after conjugation by alkylation instead of acylation.[24]

Free cysteines in the desired protein have also been targeted using thiol-reactive groups such as maleimide, vinylsulfone, iodoacetamide, and pyridyl disulfide.[25-27] For proteins that do not contain free cysteines, they can be inserted through genetic engineering.[28,29] Other ways to incorporate reactive handles include the preparation of synthetic proteins using native chemical ligation[30]. The inclusion of reactive functional groups in the peptide sequence allows for site-specific PEGylation as well as retention of native protein bioactivity provided that the conjugated polymer does not inhibit access to the active site. For example, synthetic erythropoiesis protein (EPO) was prepared by synthesizing polypeptide chains containing levulinyl ester-modified lysine residues.[31] Branched PEG-like polymers with negatively charged end-groups were then conjugated *via* oxime chemistry site-specifically. The resulting PEGylated EPO had similar bioactivity to the native protein with improved pharmacokinetics.

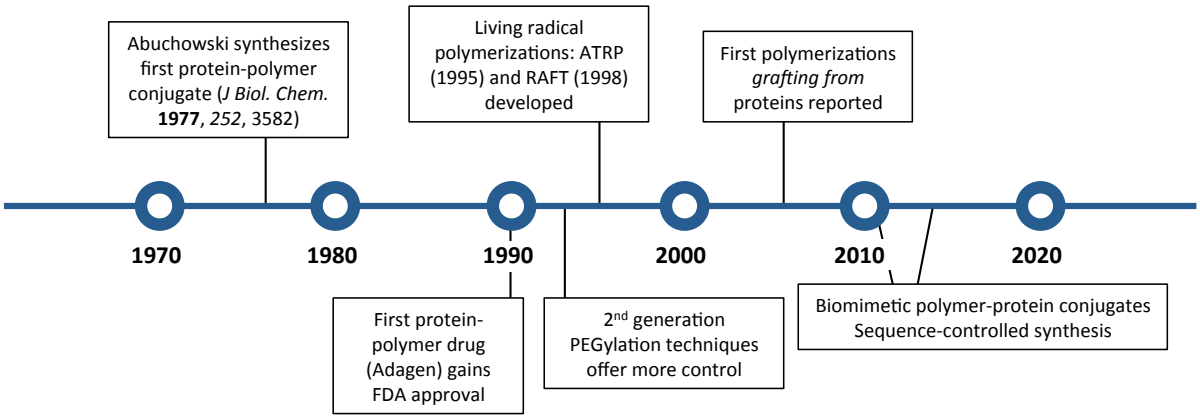

Figure 1-2. Advances in protein-polymer conjugation chemistry.

1.2.3 Disadvantages of PEGylation

PEG is an essential molecule in the field of protein-polymer conjugates. However, some deficiencies have been observed, including hypersensitivity and immunological responses, accelerated blood clearance upon repeated exposure, and degradation under light, heat, and mechanical stress with the possibility of toxic side products.[32] The non-biodegradability of PEG is another main drawback; PEG has been shown to form vacuoles in organs such as the liver, kidney, and spleen after protein-PEG conjugate administration.[14] These deficiencies have led researchers to investigate alternative polymers for protein conjugation. For example, our group has developed protein-polymer conjugates with sulfonated polymers and glycopolymers to enhance protein stability.[33,34]

1.3 Protein-Polymer Conjugation Strategies by Controlled Radical Polymerization

The developments of new polymerization methods have greatly enhanced the field in preparing biohybrid materials with tailored properties for therapeutic use. Out of these, controlled radical polymerization (CRP) is currently the most popular technique to prepare conjugates with polymers other than linear PEG. Atom transfer radical polymerization (ATRP) and reversible addition-fragmentation chain transfer (RAFT) polymerization are the two CRP techniques commonly used for this purpose. During ATRP, the polymer growth occurs from a halogenated initiator, which undergoes a reversible redox reaction mediated by a transition metal catalyst.[35,36] RAFT polymerization requires a chain transfer agent (CTA), typically a thiocarbonylthio group, to mediate the reversible chain-transfer process (**Figure 1-3**).[37] Both techniques tolerate a wide range of functional groups, solvents, and reaction conditions. Importantly for therapeutic applications, these techniques provide polymers with narrow molecular weight distributions. This can be important for FDA approval as well as for uniformity in the properties of the resulting protein conjugate.

Synthetic strategies toward protein-polymer conjugates generally fall into three categories: *grafting to*, *grafting from* and *grafting through* (**Figure 1-4**).[4,9,38]

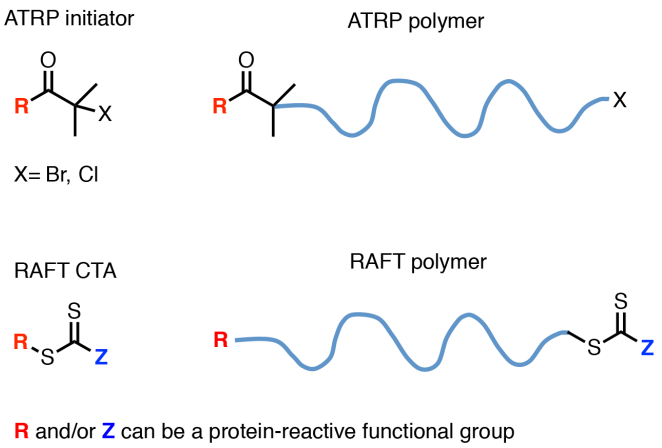

Figure 1-3. General structure of protein-reactive ATRP initiator and RAFT chain transfer agent (CTA), and their resulting polymers.

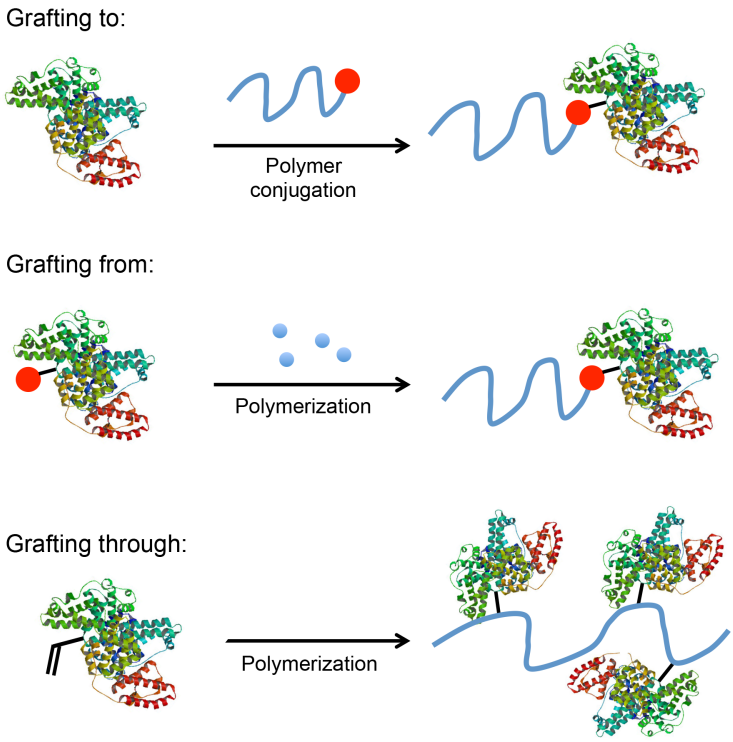

Figure 1-4. General approaches to synthesize protein-polymer conjugates (Protein structure of BSA from PBD #4F5S).

1.3.1 Grafting to

The *grafting to* technique involves covalent attachment of a synthetic polymer to a protein. It is the most common method, and all of the PEG conjugates described above were made through this method. CRP techniques are particularly effective in preparing end-functionalized polymers. A protein-reactive handle (an initiator or CTA) can be used to initiate the polymer chain growth.[39-43] Alternatively, post-polymerization modification methods can be used to install or reveal a reactive end-group.[44-46] For example, pyridyl disulfide has been incorporated directly into initiators and CTAs, resulting in protein-reactive polymers by ATRP or RAFT without post-polymerization modification.[39,40] The high binding affinity of the biotin-streptavidin system has been explored for protein-polymer conjugates by synthesizing a biotinylated initiator and associating the resulting polymer with streptavidin.[41,42] Polymers synthesized from Boc-protected aminooxy initiators were conjugated to levulinyl-modified BSA through oxime formation.[44] Vinyl sulfone was installed for protein conjugation by *in situ* post-polymerization modification of the dithioester group of a RAFT polymer.[45] Among all the conjugation methods that have been recently demonstrated, copper-catalyzed azide-alkyne cycloaddition (CuAAC) is one of the most widely utilized for protein-polymer conjugates due to its high efficiency, but requires the installation of an unnatural functionality (azide or alkyne) to the protein.[43,46,47]

Major advantages of the *grafting to* approach are that the polymer can be made, characterized and stored prior to use. However, the major drawback of this strategy is steric hindrance between the two macromolecules, which requires very efficient bioconjugation chemistries and/or a large excess of polymer to obtain good yields. Purification of the protein-polymer conjugate is also often a challenge, due to the similar molecular weights and sizes of the

components. In addition, it can be difficult to determine the number and location of the polymers on the protein.

1.3.2 Grafting from

Grafting from involves the polymerization of monomers from an initiation site on the protein (**Figure 1-5**). Using previously mentioned conjugation methods, ATRP initiators or RAFT CTAs can be conjugated to a specific site on the protein. Our group is the first to demonstrate *grafting from* by synthesizing biotinylated ATRP initiators that could non-covalently associate with streptavidin and generate a protein macroinitiator.[48] After polymerization with a variety of monomers, the protein was modified with polymer at the biotin binding sites. Shortly thereafter, we reported pyridyl disulfide- and maleimide-functionalized ATRP initiators that were synthesized and conjugated to free cysteines of BSA and T4 lysozyme to generate protein macroinitiators.[49] Upon polymerization, the T4 lysozyme retained its bioactivity completely. Both examples demonstrated the robustness of the method.

Russell and Matyjaszewski compared *grafting from* and *grafting to* techniques by varying the conjugation stoichiometry. A single initiator or polymer per protein was introduced to the lysine residues of chymotrypsin. The *grafting from* conjugates were unimodal when measured by size exclusion chromatography, while the corresponding *grafting to* method failed to provide such exact control on the degree of modification.[50] ATRP initiators have also been introduced into proteins by genetically encoding an unnatural amino acid into green fluorescent protein (GFP).[51,52] This approach avoids bioconjugation steps in preparing the macroinitiator. *Grafting from* using RAFT polymerization has also been demonstrated. CTAs (Z-C(=S)S-R) where a

pyridyl disulfide was placed in the Z-group[53,54] or the R-group[55] were attached to the free thiol of BSA and subsequently utilized as a macroCTA in polymerization reactions. Using the R-group approach, the thiocarbonylthio moiety is more accessible for chain transfer with propagating chains, and will also be available for subsequent transformations. Block copolymers grafted from proteins have also been demonstrated by both ATRP[56] and RAFT polymerizations[57,58]. Because ATRP and RAFT polymerizations can be performed under aqueous conditions at mild temperatures, utilization of the *grafting from* approach is rapidly growing. Recently, a systematic investigation (including ligand structure, halide species, aqueous medium) to determine optimal and biologically relevant conditions for generating polymers with low polydispersity while maintaining protein activity was undertaken using both conventional ATRP as well as activators generated by electron transfer (AGET) ATRP.[59]

The general benefits of the *grafting from* approach include less steric interference in the initiator-protein conjugation, higher efficiency in the preparation of high molecular weight conjugates especially if those polymers are hydrophobic, and easier purification due to significant mass differences between the protein conjugate and small molecule impurities. Additionally, the initiator or CTA conjugate can be more easily characterized, clearly indicating the sites for subsequent polymer attachment. The disadvantages of this approach include the potential reaction with or partial inactivation of the protein, particularly with more sensitive biomolecules. Thus, the polymerization conditions for this approach necessitate the exclusion of toxic reagents and harsh conditions such as elevated temperatures. In addition, the characterization of the polymer (for example molecular weight and polydispersity) can be difficult, particularly if the initiator or CTA is conjugated through an irreversible bond.

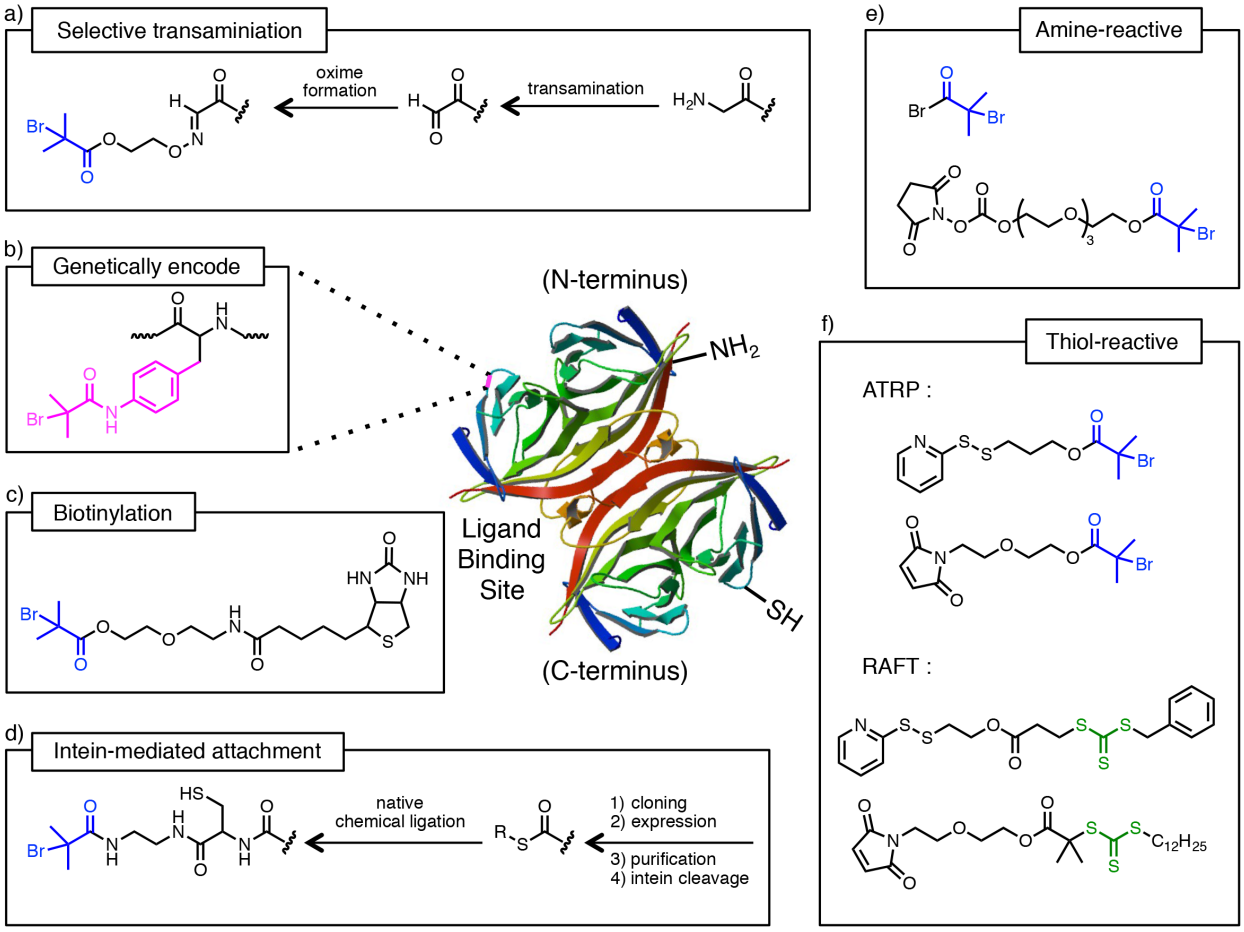

Figure 1-5. Schematic presentation of selected "*grafting from*" methods mentioned in this chapter (Protein structure of Strepavidin from PBD #1N4J). References: a) Gao *et al.*,[60] b) Peeler *et al.*[51] c) Bontempo *et al.*,[48] d) Gao *et al.*,[61] e) Lele *et al.*,[50] Magnusson *et al.*,[62] f) Heredia *et al.*,[49] Liu *et al.*,[53] De *et al.*[55]

1.3.3 Grafting through

Currently, the *grafting through* method with CRP has only been used to prepare peptide-polymer conjugates. In this approach, a peptide is modified to contain a polymerizable group, and the macromonomer is then polymerized. This would result in a highly functionalized polymer chain with pendant peptide sequences. The major challenges in this approach are the steric bulk and compatibility of the monomers. Protecting groups are often required to avoid interference of peptide functional groups with the polymerization technique. For example, the amide bonds may complex with the copper catalyst in ATRP.[63] *Grafting through* has not yet been demonstrated for protein-polymer conjugates; Hoffman and coworkers have conjugated vinyl groups onto L-asparaginase with good retention of bioactivity but did not polymerize the resulting macromonomers.[64] However, multiple groups have demonstrated the use of protein macromonomers in the synthesis of hydrogels. Hydrogels containing proteins as cross-linking elements can selectively adsorb therapeutic agents and exhibit highly elastomeric properties.[65,66] They can also express structural changes in response to biological stimuli such as disulfide reduction[67,68] or in the presence of analytes such as calcium or phenothiazine,[69] or when exposed to free antigens.[70]

The polymerization of monomers incorporated with protein-reactive groups followed by the attachment of proteins would also produce polymers with pendant proteins. Although this approach is not technically *grafting through*, such protein-polymer conjugates have been prepared by free radical polymerization[71], ring-opening metathesis polymerization (ROMP)[72], and ATRP[73]. This type of protein-polymer conjugates could be highly useful in preparing protein clusters and enhancing polyvalent interactions.

1.4 Properties and Applications of Protein-Polymer Conjugates

The CRP techniques mentioned above have opened up new possibilities to prepare protein-polymer conjugates for diverse applications. Ideally, the attached polymer should improve existing functions or introduce new properties to the protein. The majority of the synthetic efforts have been focused on polymers with polyacrylate or polymethacrylate backbones with oligo(ethylene glycol) side chains (pPEGA or pPEGMA, respectively). These comb-type PEG conjugates not only have biological applications, but also other interesting and useful material properties, which leads to a brief introduction on smart protein-polymer conjugates and their applications (see **Section 1.4.2** below).

1.4.1 Biological Applications of Comb-Type PEG Conjugates

Several pPEGA and pPEGMA conjugates have shown promise *in vivo*. An early study involved site-specific conjugation of aldehyde pPEGMA to salmon calcitonin (sCT) through reductive amination.[74] In the preliminary *in vivo* studies, the conjugate displayed comparable activity (increasing intracellular cyclic AMP levels) to the unmodified protein. *Grafting from* recombinant human growth hormone (rh-GH) was shown to produce conjugates with improved properties.[62] An initiator, *N*-hydroxysuccinimide (NHS) bromoisobutyrate was coupled to free amine groups on rh-GH and polymerization of PEGMA was conducted. The conjugate showed higher stability to denaturation and proteolysis compared to unmodified rh-GH. The *in vivo* efficacy of the hormone also improved, confirmed by monitoring weight growth in administrated female rats. Polymerization of PEGMA from the N-terminus of myoglobin and C-terminus of genetically modified GFP was also explored.[60,61] In mice, these conjugates displayed improved

pharmacokinetics compared to unmodified protein. These examples clearly demonstrated that similar to PEG conjugates, pPEGMA conjugates significantly extend the circulation lifetime of the protein and are effective *in vivo*.

1.4.2 Tunable Thermoresponsive Polymers

Oligo(ethylene glycol) methacrylate-based polymers have also been found to have thermoresponsive properties. Living anionic polymerization[75,76], ATRP[77,78], and nitroxide-mediated radical polymerization (NMP)[79] have been used to prepare this type of polymers. When thermoresponsive water-soluble polymers are heated over their lower critical solution temperature (LCST), hydrogen-bonded water molecules are released and the polymers become insoluble. The LCST can be tuned by altering the length of oligo(ethylene glycol) side chains or by adjusting the ratio of monomers with different lengths.[76,77] Such compositions are well known for their biocompatibility, hence suitable for biomaterial applications.[80] These polymers have been employed to prepare thermally responsive protein-polymer conjugates.[81-83]

1.4.3 Smart Protein-Polymer Conjugates

pPEGMA and pPEGA are two of the many stimuli-responsive, or "smart", polymers which have been used to modulate protein activity in response to external stimuli. Hoffman, Stayton, and coworkers demonstrated thermoreversible protein aggregation with retention of bioactivity[84] and developed applications in immunoassays,[85] chromatography-free conjugate purifications,[84,86] and intracellular drug delivery.[87] In their most well-known work, Stayton and

coworkers conjugated poly(*N*-isopropylacrylamide-*co*-acrylic acid) (pNIPAAm) to a free thiol on streptavidin. The resulting conjugate displayed a conformational change above its LCST.[88] At elevated temperatures, the polymer collapsed, blocking access to the biotin active site. In later publications, similar stimuli-responsive effects were induced by pH and UV/Vis irradiation.[89-91]. Smart polymers can also respond to biological stimuli, such as elevated glucose levels, or the presence of antigens, enzymes, or thiols.[92] More examples of stimuli-responsive protein-polymer conjugates can be found in extensive reviews on the topic.[93,94]

1.5 Oligonucleotide-Polymer Conjugates

While protein-polymer conjugates have been explored in depth, far fewer examples of oligonucleotide-polymer conjugates have been reported. Cationic polymers are often used to complex and condense oligonucleotides into polyplexes to promote cellular internalization, but covalent conjugates have not yet been extensively explored.[95-100] The first oligonucleotide-polymer conjugate was demonstrated in 1987 by reductive amination of an oligodeoxyribonucleotide and poly(L-lysine) and further showed effective antiviral acitivty.[101] The unique recognition, precise sequence control, and biological activities of DNA and RNA may lead to many potential applications for polymer conjugation, which have been reviewed and discussed elsewhere.[12,102] Here, the discussion will focus on small interfering RNA (siRNA) and its polymer conjugates.

1.5.1 Small-Interfering RNA (siRNA) and its PEGylation

Gene therapy is a promising method to cure or prevent a large number of diseases, such as cancer and genetic disorders. In 1998, Andrew Fire, Craig Mello, and colleagues discovered the ability of double-stranded RNA to silence gene expression in the nematode worm *Caenorhabditis elegans* through RNA interference (RNAi), which led to their Nobel Prize in 2006.[103] Small-interfering RNA (siRNA) are synthetic nucleotides with 21-23 base pairs that are complementary to the target messenger RNA (mRNA). The advantage of siRNA as a therapeutic agent is its highly sequence-specific and efficient gene silencing at low intracellular concentrations (nM). However, efficient delivery of siRNA is a major challenge.[104] Under *in vivo* conditions, siRNA is rapidly degraded by nucleases.[105-107] Covalent attachment of linear or branched poly(ethylene glycol) (PEG) to siRNA has been employed by many researchers to enhance stability and pharmacokinetics.[108-120]

1.5.2 Polymeric Delivery Systems for siRNA by CRP

CRP techniques have allowed the formation of precise polymeric drug delivery structures and designs, which is advantageous for design of siRNA delivery systems.[121,122] In the recent years, increasing examples related to siRNA delivery developed by CRP have been published, mainly including polymers synthesized for siRNA-polymer conjugates[123-128], cationic polymers which form polyplexes with siRNA[129-139], block copolymers to form micelles or polymersomes with a cationic core[131,133,140-144], or cationic nanogels as delivery platforms[145-147]. Polymers synthesized by RAFT polymerization have also been used in combination of inorganic nanoparticles (iron oxide[148] and gold[149]) as siRNA delivery vehicles.

Most polymeric gene delivery systems involve complexing cationic blocks with the negatively charged nucleotide sequences through electrostatic interactions. However, with the ability to prepare end-functional polymers from appropriate initiators or CTAs, CRP presents the option of forming both cleavable and non-cleavable siRNA-polymer conjugates. Through RAFT polymerization, our group has conjugated siRNA to pPEGA through a reducible disulfide bond, and achieved enhanced serum stability, nuclease resistance, and gene delivery efficiency.[123,125] We have also successfully conjugated siRNA to a glycopolymer synthesized through ATRP.[126] York *et al.* have also utilized thiol exchange to conjugate siRNA at multiple sites along their polymer backbone.[127] Recently, Averick *et al.* used CuAAC to prepare conjugates, which facilitated cell internalization of the siRNA even without cationic moieties in the polymer.[128]

1.6 This Thesis

PEG-protein conjugates are currently the only FDA-approved protein conjugates in the United States, emphasizing the importance of developing advanced PEGylation techniques to suit individual proteins. In **Chapter 2**, we describe a site-specific photoinduced PEGylation method utilizing non-covalent ligand binding affinity and a photo-reactive benzophenone group. This *grafting to* conjugation method is generally applicable to GST-fusion proteins, which offers minimal interference with the fusion protein as well as light-triggered bond formation.

However, some deficiencies of PEG have been observed. Moreover, PEG does not significantly stabilize proteins in storage conditions under environmental stressors. In **Chapter 3**, we developed a new type of glycopolymer with trehalose side chains, and showed its stabilizing effect toward several enzymes. The glycopolymers were also used to prepare siRNA-polymer

conjugates, and the research is described in **Chapter 4**. These trehalose glycopolymers can potentially serve as PEG replacements in the future, especially when heat and lyophilization stabilization of the protein is required.

CRP techniques, which introduce functional end-groups, have allowed for the preparation of biohybrid materials with tailored properties. G*rafting to* and *grafting from* are the two synthetic strategies that are most often used, and a variety of protein-polymer conjugates have been developed for a wide range of applications. Oligonucleotides are also attractive biomacromolecules that exhibit distinct biological and structural properties. We have shown that siRNA-pPEGA conjugates increase serum stability and enhanced gene silencing efficiency. In **Chapter 5**, we describe for the first time, the preparation of siRNA-polymer conjugates using the *grafting from* approach. Only nanomoles of siRNA-macroinitiators were required to carry out successful polymerizations of oligo(ethylene glycol). This is an alternative to the commonly used *grafting to* approach.

Besides its biocompatible properties, oligo(ethylene glycol) methacrylate-based polymers have also been found be tunable thermoresponsive polymers. We used ATRP to prepare three distinctly temperature-responsive oligo(ethylene glycol) methacrylate-based polymers with amine end-groups. The polymers were used to prepare thermoresponsive hydrogel patterns on silicon surfaces that allow simple fluorophore conjugation. Over their volume phase transition temperature (VPTT), the hydrogels released water, collapsed in height, and led to fluorescent quenching. Multicomponent morphing surfaces were prepared to display dual color patterns and encrypted messages at different temperatures. This research is described in **Chapter 6**.

1.7 Conclusion

In conclusion, the versatility of CRP techniques and the huge selection of monomers and polymers have allowed the community to prepare various types of biohybrid materials with important materials and biological properties. In the thesis, a variety of polymerization methods and bioconjugation techniques will be demonstrated. The majority of the work describes efforts towards biomolecules with enhanced physical, chemical and therapeutic properties through attachment of designed synthetic polymers.

1.8 References

‡ Portions of this chapter is in-press as: Pelegri-O'Day, E. M.; Lin, E.-W.; Maynard, H. D., "Therapeutic Protein-Polymer Conjugates: Advancing Beyond PEGylation," *J. Am. Chem. Soc.*, DOI: 10.1021/ja504390x.

(1) Dimitrov, D. S. "Therapeutic Proteins" *Methods in Molecular Biology (Clifton, N.J.)* **2012**, *899*, 1-26.

(2) Lutz, J. F.; Borner, H. G. "Modern Trends in Polymer Bioconjugates Design" *Prog. Polym. Sci.* **2008**, *33*, 1-39.

(3) Heredia, K. L.; Maynard, H. D. "Synthesis of Protein-Polymer Conjugates" *Org. Biomol. Chem.* **2007**, *5*, 45-53.

(4) Grover, G. N.; Maynard, H. D. "Protein-Polymer Conjugates: Synthetic Approaches by Controlled Radical Polymerizations and Interesting Applications" *Curr. Opin. Chem. Biol.* **2010**, *14*, 818-827.

(5) Alconcel, S. N. S.; Baas, A. S.; Maynard, H. D. "FDA-Approved Poly(Ethylene Glycol)-Protein Conjugate Drugs" *Polym. Chem.* **2011**, *2*, 1442-1448.

(6) Duncan, R. "The Dawning Era of Polymer Therapeutics" *Nat. Rev. Drug Discovery* **2003**, *2*, 347-360.

(7) Haag, R.; Kratz, F. "Polymer Therapeutics: Concepts and Applications" *Angew. Chem., Int. Ed.* **2006**, *45*, 1198-1215.

(8) Gauthier, M. A.; Klok, H.-A. "Peptide/Protein-Polymer Conjugates: Synthetic Strategies and Design Concepts" *Chem.l Commun.* **2008**, 2591-2611.

(9) Canalle, L. A.; Lowik, D. W. P. M.; van Hest, J. C. M. "Polypeptide-Polymer Bioconjugates" *Chem. Soc. Rev.* **2010**, *39*, 329-353.

(10) Borchmann, D. E.; Carberry, T. P.; Weck, M. ""Bio"-Macromolecules: Polymer-Protein Conjugates as Emerging Scaffolds for Therapeutics" *Macromol. Rapid Commun.* **2014**, *35*, 27-43.

(11) Alemdaroglu, F. E.; Herrmann, A. "DNA Meets Synthetic Polymers - Highly Versatile Hybrid Materials" *Org. Biomol. Chem.* **2007**, *5*, 1311-1320.

(12) Kwak, M.; Herrmann, A. "Nucleic Acid/Organic Polymer Hybrid Materials: Synthesis, Superstructures, and Applications" *Angew. Chem., Int. Ed.* **2010**, *49*, 8574-8587.

(13) Pfister, D.; Morbidelli, M. "Process for Protein PEGylation" *J. Controlled Release* **2014**, *180*, 134-149.

(14) Besheer, A.; Liebner, R.; Meyer, M.; Winter, G. In *Tailored Polymer Architectures for Pharmaceutical and Biomedical Applications*; Scholz, C., Kressler, J., Eds.; Amer Chemical Soc: Washington, 2013; Vol. 1135, p 215-233.

(15) Rose, V. L.; Winkler, G. S.; Allen, S.; Puri, S.; Mantovani, G. "Polymer siRNA Conjugates Synthesised by Controlled Radical Polymerisation" *Eur. Polym. J.* **2013**, *49*, 2861-2883.

(16) Abuchowski, A.; Vanes, T.; Palczuk, N. C.; Davis, F. F. "Alteration of Immunological Properties of Bovine Serum-Albumin by Covalent Attachment of Polyethylene-Glycol" *J. Biol. Chem.* **1977**, *252*, 3578-3581.

(17) Abuchowski, A.; McCoy, J. R.; Palczuk, N. C.; Vanes, T.; Davis, F. F. "Effect of Covalent Attachment of Polyethylene-Glycol on Immunogenicity and Circulating Life of Bovine Liver Catalase" *J. Biol. Chem.* **1977**, *252*, 3582-3586.

(18) Maeda, H.; Takeshita, J.; Kanamaru, R. "Lipophilic Derivative of Neocarzinostatin - a Polymer Conjugation of an Anti-Tumor Protein Antibiotic" *Int. J. Pept. Protein Res.* **1979**, *14*, 81-87.

(19) Greish, K.; Fang, J.; Inutsuka, T.; Nagamitsu, A.; Maeda, H. "Macromolecular Therapeutics - Advantages and Prospects with Special Emphasis on Solid Tumour Targeting" *Clin. Pharmacokinet.* **2003**, *42*, 1089-1105.

(20) Roberts, M. J.; Bentley, M. D.; Harris, J. M. "Chemistry for Peptide and Protein Pegylation" *Adv. Drug Delivery Rev.* **2002**, *64*, 116-127.

(21) Veronese, F. M.; Largajolli, R.; Boccú, E.; Benassi, C. A.; Schiavon, O. "Surface Modification of Proteins Activation of Monomethoxy-Polyethylene Glycols by Phenylchloroformates and Modification of Ribonuclease and Superoxide Dismutase" *Appl. Biochem. Biotechnol.* **1985**, *11*, 141-152.

(22) Gaertner, H. F.; Offord, R. E. "Site-Specific Attachment of Functionalized Poly(Ethylene Glycol) to the Amino Terminus of Proteins" *Bioconjugate Chem.* **1996**, *7*, 38-44.

(23) Gilmore, J. M.; Scheck, R. A.; Esser-Kahn, A. P.; Joshi, N. S.; Francis, M. B. "N-Terminal Protein Modification through a Biomimetic Transamination Reaction" *Angew. Chem., Int. Ed.* **2006**, *45*, 5307-5311.

(24) Kinstler, O. B.; Brems, D. N.; Lauren, S. L.; Paige, A. G.; Hamburger, J. B.; Treuheit, M. J. "Characterization and Stability of N-Terminally PEGylated rhG-CSF" *Pharm. Res.* **1996**, *13*, 996-1002.

(25) Kogan, T. P. "The Synthesis of Substituted Methoxy-Poly(Ethyleneglycol) Derivatives Suitable for Selective Protein Modification" *Synth. Commun.* **1992**, *22*, 2417-2424.

(26) Woghiren, C.; Sharma, B.; Stein, S. "Protected Thiol Polyethylene-Glycol - a New Activated Polymer for Reversible Protein Modification" *Bioconjugate Chem.* **1993**, *4*, 314-318.

(27) Morpurgo, M.; Veronese, F. M.; Kachensky, D.; Harris, J. M. "Preparation and Characterization of Poly(Ethylene Glycol) Vinyl Sulfone" *Bioconjugate Chem.* **1996**, *7*, 363-368.

(28) Goodson, R. J.; Katre, N. V. "Site-Directed Pegylation of Recombinant Interleukin-2 at Its Glycosylation Site" *Bio-Technology* **1990**, *8*, 343-346.

(29) Dieterich, D. C.; Link, A. J.; Graumann, J.; Tirrell, D. A.; Schuman, E. M. "Selective Identification of Newly Synthesized Proteins in Mammalian Cells Using Bioorthogonal Noncanonical Amino Acid Tagging (Boncat)" *Proc. Natl. Acad. Sci. U. S. A.* **2006**, *103*, 9482-9487.

(30) Dawson, P. E.; Muir, T. W.; Clarklewis, I.; Kent, S. B. H. "Synthesis of Proteins by Native Chemical Ligation" *Science* **1994**, *266*, 776-779.

(31) Kochendoerfer, G. G.; Chen, S. Y.; Mao, F.; Cressman, S.; Traviglia, S.; Shao, H. Y.; Hunter, C. L.; Low, D. W.; Cagle, E. N.; Carnevali, M.; Gueriguian, V.; Keogh, P. J.; Porter, H.; Stratton, S. M.; Wiedeke, M. C.; Wilken, J.; Tang, J.; Levy, J. J.; Miranda, L. P.; Crnogorac, M. M.; Kalbag, S.; Botti, P.; Schindler-Horvat, J.; Savatski, L.; Adamson, J. W.; Kung, A.; Kent, S. B. H.; Bradburne, J. A. "Design and Chemical Synthesis of a Homogeneous Polymer-Modified Erythropoiesis Protein" *Science* **2003**, *299*, 884-887.

(32) Knop, K.; Hoogenboom, R.; Fischer, D.; Schubert, U. S. "Poly(Ethylene Glycol) in Drug Delivery: Pros and Cons as Well as Potential Alternatives" *Angew. Chem., Int. Ed.* **2010**, *49*, 6288-6308.

(33) Nguyen, T. H.; Kim, S. H.; Decker, C. G.; Wong, D. Y.; Loo, J. A.; Maynard, H. D. "A Heparin-Mimicking Polymer Conjugate Stabilizes Basic Fibroblast Growth Factor" *Nat. Chem.* **2013**, *5*, 221-227.

(34) Mancini, R. J.; Lee, J.; Maynard, H. D. "Trehalose Glycopolymers for Stabilization of Protein Conjugates to Environmental Stressors" *J. Am. Chem. Soc.* **2012**, *134*, 8474-8479.

(35) Kato, M.; Kamigaito, M.; Sawamoto, M.; Higashimura, T. "Polymerization of Methyl-Methacrylate with the Carbon-Tetrachloride Dichlorotris(Triphenylphosphine)Ruthenium (II) Methylaluminum Bis(2,6-Di-Tert-Butylphenoxide) Initiating System - Possibility of Living Radical Polymerization" *Macromolecules* **1995**, *28*, 1721-1723.

(36) Wang, J. S.; Matyjaszewski, K. "Controlled Living Radical Polymerization - Atom-Transfer Radical Polymerization in the Presence of Transition-Metal Complexes" *J. Am. Chem. Soc.* **1995**, *117*, 5614-5615.

(37) Chiefari, J.; Chong, Y. K.; Ercole, F.; Krstina, J.; Jeffery, J.; Le, T. P. T.; Mayadunne, R. T. A.; Meijs, G. F.; Moad, C. L.; Moad, G.; Rizzardo, E.; Thang, S. H. "Living Free-Radical Polymerization by Reversible Addition-Fragmentation Chain Transfer: The RAFT Process" *Macromolecules* **1998**, *31*, 5559-5562.

(38) Gauthier, M. A.; Klok, H. A. "Peptide/Protein-Polymer Conjugates: Synthetic Strategies and Design Concepts" *Chem. Commun.* **2008**, 2591-2611.

(39) Bontempo, D.; Heredia, K. L.; Fish, B. A.; Maynard, H. D. "Cysteine-Reactive Polymers Synthesized by Atom Transfer Radical Polymerization for Conjugation to Proteins" *J. Am. Chem. Soc.* **2004**, *126*, 15372-15373.

(40) Boyer, C.; Liu, J.; Wong, L.; Tippett, M.; Bulmus, V.; Davis, T. P. "Stability and Utility of Pyridyl Disulfide Functionality in RAFT and Conventional Radical Polymerizations" *J. Polym. Sci., Part A: Polym. Chem.* **2008**, *46*, 7207-7224.

(41) Hou, S. J.; Sun, X. L.; Dong, C. M.; Chaikof, E. L. "Facile Synthesis of Chain-End Functionalized Glycopolymers for Site-Specific Bioconjugation" *Bioconjugate Chem.* **2004**, *15*, 954-959.

(42) Bontempo, D.; Li, R. C.; Ly, T.; Brubaker, C. E.; Maynard, H. D. "One-Step Synthesis of Low Polydispersity, Biotinylated Poly(*N*-Isopropylacrylamide) by ATRP" *Chem. Commun.* **2005**, 4702-4704.

(43) Li, M.; De, P.; Gondi, S. R.; Sumerlin, B. S. "Responsive Polymer-Protein Bioconjugates Prepared by RAFT Polymerization and Copper-Catalyzed Azide-Alkyne Click Chemistry" *Macromol. Rapid Commun.* **2008**, *29*, 1172-1176.

(44) Heredia, K. L.; Tolstyka, Z. P.; Maynard, H. D. "Aminooxy End-Functionalized Polymers Synthesized by ATRP for Chemoselective Conjugation to Proteins" *Macromolecules* **2007**, *40*, 4772-4779.

(45) Grover, G. N.; Alconcel, S. N. S.; Matsumoto, N. M.; Maynard, H. D. "Trapping of Thiol-Terminated Acrylate Polymers with Divinyl Sulfone to Generate Well-Defined Semitelechelic Michael Acceptor Polymers" *Macromolecules* **2009**, *42*, 7657-7663.

(46) Dirks, A. J. T.; van Berkel, S. S.; Hatzakis, N. S.; Opsteen, J. A.; van Delft, F. L.; Cornelissen, J. J. L. M.; Rowan, A. E.; van Hest, J. C. M.; Rutjes, F. P. J. T.; Nolte, R. J. M. "Preparation of Biohybrid Amphiphiles Via the Copper Catalysed Huisgen [3+2] Dipolar Cycloaddition Reaction" *Chem. Commun.* **2005**, 4172-4174.

(47) Deiters, A.; Cropp, T. A.; Summerer, D.; Mukherji, M.; Schultz, P. G. "Site-Specific PEGylation of Proteins Containing Unnatural Amino Acids" *Bioorg. Med. Chem. Lett.* **2004**, *14*, 5743-5745.

(48) Bontempo, D.; Maynard, H. D. "Streptavidin as a Macroinitiator for Polymerization: In Situ Protein-Polymer Conjugate Formation" *J. Am. Chem. Soc.* **2005**, *127*, 6508-6509.

(49) Heredia, K. L.; Bontempo, D.; Ly, T.; Byers, J. T.; Halstenberg, S.; Maynard, H. D. "In Situ Preparation of Protein - "Smart" Polymer Conjugates with Retention of Bioactivity" *J. Am. Chem. Soc.* **2005**, *127*, 16955-16960.

(50) Lele, B. S.; Murata, H.; Matyjaszewski, K.; Russell, A. J. "Synthesis of Uniform Protein-Polymer Conjugates" *Biomacromolecules* **2005**, *6*, 3380-3387.

(51) Peeler, J. C.; Woodman, B. F.; Averick, S.; Miyake-Stoner, S. J.; Stokes, A. L.; Hess, K. R.; Matyjaszewski, K.; Mehl, R. A. "Genetically Encoded Initiator for Polymer Growth from Proteins" *J. Am. Chem. Soc.* **2010**, *132*, 13575-13577.

(52) Averick, S. E.; Bazewicz, C. G.; Woodman, B. F.; Simakova, A.; Mehl, R. A.; Matyjaszewski, K. "Protein-Polymer Hybrids: Conducting ARGET ATRP from a Genetically Encoded Cleavable ATRP Initiator" *Eur. Polym. J.* **2013**, *49*, 2919-2924.

(53) Liu, J. Q.; Bulmus, V.; Herlambang, D. L.; Barner-Kowollik, C.; Stenzel, M. H.; Davis, T. P. "In Situ Formation of Protein-Polymer Conjugates through Reversible Addition Fragmentation Chain Transfer Polymerization" *Angew. Chem., Int. Ed.* **2007**, *46*, 3099-3103.

(54) Boyer, C.; Bulmus, V.; Liu, J. Q.; Davis, T. P.; Stenzel, M. H.; Barner-Kowollik, C. "Well-Defined Protein-Polymer Conjugates via In Situ RAFT Polymerization" *J. Am. Chem. Soc.* **2007**, *129*, 7145-7154.

(55) De, P.; Li, M.; Gondi, S. R.; Sumerlin, B. S. "Temperature-Regulated Activity of Responsive Polymer-Protein Conjugates Prepared by Grafting-from via RAFT Polymerization" *J. Am. Chem. Soc.* **2008**, *130*, 11288-+.

(56) Yasayan, G.; Saeed, A. O.; Fernandez-Trillo, F.; Allen, S.; Davies, M. C.; Jangher, A.; Paul, A.; Thurecht, K. J.; King, S. M.; Schweins, R.; Griffiths, P. C.; Magnusson, J. P.; Alexander, C. "Responsive Hybrid Block Co-Polymer Conjugates of Proteins-Controlled Architecture to Modulate Substrate Specificity and Solution Behaviour" *Polym. Chem.* **2011**, *2*, 1567-1578.

(57) Li, H. M.; Li, M.; Yu, X.; Bapat, A. P.; Sumerlin, B. S. "Block Copolymer Conjugates Prepared by Sequentially Grafting from Proteins via RAFT" *Polym. Chem.* **2011**, *2*, 1531-1535.

(58) Li, M.; Li, H. M.; De, P.; Sumerlin, B. S. "Thermoresponsive Block Copolymer-Protein Conjugates Prepared by Grafting-from via Raft Polymerization" *Macromol. Rapid Commun.* **2011**, *32*, 354-359.

(59) Averick, S.; Simakova, A.; Park, S.; Konkolewicz, D.; Magenau, A. J. D.; Mehl, R. A.; Matyjaszewski, K. "ATRP under Biologically Relevant Conditions: Grafting from a Protein" *ACS Macro Lett.* **2012**, *1*, 6-10.

(60) Gao, W. P.; Liu, W. G.; Mackay, J. A.; Zalutsky, M. R.; Toone, E. J.; Chilkoti, A. "In Situ Growth of a Stoichiometric PEG-Like Conjugate at a Protein's N-Terminus with Significantly Improved Pharmacokinetics" *Proc. Natl. Acad. Sci. U. S. A.* **2009**, *106*, 15231-15236.

(61) Gao, W.; Liu, W.; Christensen, T.; Zalutsky, M. R.; Chilkoti, A. "In Situ Growth of a PEG-Like Polymer from the C Terminus of an Intein Fusion Protein Improves Pharmacokinetics and Tumor Accumulation" *Proc. Natl. Acad. Sci. U. S. A.* **2010**, *107*, 16432-16437.

(62) Magnusson, J. P.; Bersani, S.; Salmaso, S.; Alexander, C.; Caliceti, P. "In Situ Growth of Side-Chain PEG Polymers from Functionalized Human Growth Hormone-a New Technique for Preparation of Enhanced Protein-Polymer Conjugates" *Bioconjugate Chem.* **2010**, *21*, 671-678.

(63) Fernandez-Trillo, F.; Dureault, A.; Bayley, J. P. M.; van Hest, J. C. M.; Thies, J. C.; Michon, T.; Weberskirch, R.; Cameron, N. R. "Elastin-Based Side-Chain Polymers:

Improved Synthesis Via RAFT and Stimulus Responsive Behavior" *Macromolecules* **2007**, *40*, 6094-6099.

(64) Shoemaker, S. G.; Hoffman, A. S.; Priest, J. H. "Synthesis and Properties of Vinyl Monomer Enzyme Conjugates - Conjugation of L-Asparaginase with N-Succinimidyl Acrylate" *Appl. Biochem. Biotechnol.* **1987**, *15*, 11-24.

(65) Elvin, C. M.; Carr, A. G.; Huson, M. G.; Maxwell, J. M.; Pearson, R. D.; Vuocolo, T.; Liyou, N. E.; Wong, D. C. C.; Merritt, D. J.; Dixon, N. E. "Synthesis and Properties of Crosslinked Recombinant Pro-Resilin" *Nature* **2005**, *437*, 999-1002.

(66) Tada, D.; Tanabe, T.; Tachibana, A.; Yamauchi, K. "Drug Release from Hydrogel Containing Albumin as Crosslinker" *J. Biosci. Bioeng.* **2005**, *100*, 551-555.

(67) Verheyen, E.; Delain-Bioton, L.; van der Wal, S.; el Morabit, N.; Hennink, W. E.; van Nostrum, C. F. "Protein Macromonomers for Covalent Immobilization and Subsequent Triggered Release from Hydrogels" *J. Controlled Release* **2010**, *148*, E18-E19.

(68) Verheyen, E.; van der Wal, S.; Deschout, H.; Braeckmans, K.; de Smedt, S.; Barendregt, A.; Hennink, W. E.; van Nostrum, C. F. "Protein Macromonomers Containing Reduction-Sensitive Linkers for Covalent Immobilization and Glutathione Triggered Release from Dextran Hydrogels" *J. Controlled Release* **2011**, *156*, 329-336.

(69) Ehrick, J. D.; Deo, S. K.; Browning, T. W.; Bachas, L. G.; Madou, M. J.; Daunert, S. "Genetically Engineered Protein in Hydrogels Tailors Stimuli-Responsive Characteristics" *Nat. Mater.* **2005**, *4*, 298-302.

(70) Miyata, T.; Asami, N.; Uragami, T. "A Reversibly Antigen-Responsive Hydrogel" *Nature* **1999**, *399*, 766-769.

(71) Buller, J.; Laschewsky, A.; Lutz, J. F.; Wischerhoff, E. "Tuning the Lower Critical Solution Temperature of Thermoresponsive Polymers by Biospecific Recognition" *Polym. Chem.* **2011**, *2*, 1486-1489.

(72) Carrillo, A.; Gujraty, K. V.; Rai, P. R.; Kane, R. S. "Design of Water-Soluble, Thiol-Reactive Polymers of Controlled Molecular Weight: A Novel Multivalent Scaffold" *Nanotechnology* **2005**, *16*, S416-S421.

(73) Griffith, B. R.; Allen, B. L.; Rapraeger, A. C.; Kiessling, L. L. "A Polymer Scaffold for Protein Oligomerization" *J. Am. Chem. Soc.* **2004**, *126*, 1608-1609.

(74) Sayers, C. T.; Mantovani, G.; Ryan, S. M.; Randev, R. K.; Keiper, O.; Leszczyszyn, O. I.; Blindauer, C.; Brayden, D. J.; Haddleton, D. M. "Site-Specific N-Terminus

Conjugation of Poly(mPEG(1100)) Methacrylates to Salmon Calcitonin: Synthesis and Preliminary Biological Evaluation" *Soft Matter* **2009**, *5*, 3038-3046.

(75) Han, S.; Hagiwara, M.; Ishizone, T. "Synthesis of Thermally Sensitive Water-Soluble Polymethacrylates by Living Anionic Polymerizations of Oligo(Ethylene Glycol) Methyl Ether Methacrylates" *Macromolecules* **2003**, *36*, 8312-8319.

(76) Ishizone, T.; Seki, A.; Hagiwara, M.; Han, S.; Yokoyama, H.; Oyane, A.; Deffieux, A.; Carlotti, S. "Anionic Polymerizations of Oligo(Ethylene Glycol) Alkyl Ether Methacrylates: Effect of Side Chain Length and Omega-Alkyl Group of Side Chain on Cloud Point in Water" *Macromolecules* **2008**, *41*, 2963-2967.

(77) Lutz, J. F.; Hoth, A. "Preparation of Ideal Peg Analogues with a Tunable Thermosensitivity by Controlled Radical Copolymerization of 2-(2-Methoxyethoxy)Ethyl Methacrylate and Oligo(Ethylene Glycol) Methacrylate" *Macromolecules* **2006**, *39*, 893-896.

(78) Yamamoto, S. I.; Pietrasik, J.; Matyjaszewski, K. "The Effect of Structure on the Thermoresponsive Nature of Well-Defined Poly(Oligo(Ethylene Oxide) Methacrylates) Synthesized by ATRP" *J. Polym. Sci., Part A: Polym. Chem.* **2008**, *46*, 194-202.

(79) Hua, F. J.; Jiang, X. G.; Li, D. J.; Zhao, B. "Well-Defined Thermosensitive, Water-Soluble Polyacrylates and Polystyrenics with Short Pendant Oligo (Ethylene Glycol) Groups Synthesized by Nitroxide-Mediated Radical Polymerization" *J. Polym. Sci., Part A: Polym. Chem.* **2006**, *44*, 2454-2467.

(80) Hu, Z. B.; Cai, T.; Chi, C. L. "Thermoresponsive Oligo(Ethylene Glycol)-Methacrylate-Based Polymers and Microgels" *Soft Matter* **2010**, *6*, 2115-2123.

(81) Zarafshani, Z.; Obata, T.; Lutz, J. F. "Smart PEGylation of Trypsin" *Biomacromolecules* **2010**, *11*, 2130-2135.

(82) Lavigueur, C.; Garcia, J. G.; Hendriks, L.; Hoogenboom, R.; Cornelissen, J. J. L. M.; Nolte, R. J. M. "Thermoresponsive Giant Biohybrid Amphiphiles" *Polym. Chem.* **2011**, *2*, 333-340.

(83) Jones, M. W.; Gibson, M. I.; Mantovani, G.; Haddleton, D. M. "Tunable Thermo-Responsive Polymer-Protein Conjugates Via a Combination of Nucleophilic Thiol-Ene "Click" and SET-LRP" *Polym. Chem.* **2011**, *2*, 572-574.

(84) Chen, G. H.; Hoffman, A. S. "Preparation and Properties of Thermoreversible, Phase-Separating Enzyme-Oligo(*N*-Isopropylacrylamide) Conjugates" *Bioconjugate Chem.* **1993**, *4*, 509-514.

(85) Monji, N.; Hoffman, A. S. "A Novel Immunoassay System and Bioseparation Process Based on Thermal Phase Separating Polymers" *Appl. Biochem. Biotechnol.* **1987**, *14*, 107-120.

(86) Chen, J. P.; Hoffman, A. S. "Polymer Protein Conjugates II. Affinity Precipitation Separation of Human Immuno-Gamma-Globulin by a Poly(*N*-Isopropylacrylamide)-Protein A Conjugate" *Biomaterials* **1990**, *11*, 631-634.

(87) Murthy, N.; Campbell, J.; Fausto, N.; Hoffman, A. S.; Stayton, P. S. "Bioinspired Ph-Responsive Polymers for the Intracellular Delivery of Biomolecular Drugs" *Bioconjugate Chem.* **2003**, *14*, 412-419.

(88) Stayton, P. S.; Shimoboji, T.; Long, C.; Chilkoti, A.; Chen, G. H.; Harris, J. M.; Hoffman, A. S. "Control of Protein-Ligand Recognition Using a Stimuli-Responsive Polymer" *Nature* **1995**, *378*, 472-474.

(89) Shimoboji, T.; Larenas, E.; Fowler, T.; Kulkarni, S.; Hoffman, A. S.; Stayton, P. S. "Photoresponsive Polymer–Enzyme Switches" *Proc. Natl. Acad. Sci. U. S. A.* **2002**, *99*, 16592-16596.

(90) Yin, X.; Hoffman, A. S.; Stayton, P. S. "Poly(*N*-Isopropylacrylamide-*co*-Propylacrylic Acid) Copolymers That Respond Sharply to Temperature and pH" *Biomacromolecules* **2006**, *7*, 1381-1385.

(91) Bulmus, V.; Ding, Z. L.; Long, C. J.; Stayton, P. S.; Hoffman, A. S. "Site-Specific Polymer-Streptavidin Bioconjugate for pH-Controlled Binding and Triggered Release of Biotin" *Bioconjugate Chem.* **2000**, *11*, 78-83.

(92) Roy, D.; Cambre, J. N.; Sumerlin, B. S. "Future Perspectives and Recent Advances in Stimuli-Responsive Materials" *Prog. Polym. Sci.* **2010**, *35*, 278-301.

(93) Hoffman, A. S.; Stayton, P. S.; Bulmus, V.; Chen, G. H.; Chen, J. P.; Cheung, C.; Chilkoti, A.; Ding, Z. L.; Dong, L. C.; Fong, R.; Lackey, C. A.; Long, C. J.; Miura, M.; Morris, J. E.; Murthy, N.; Nabeshima, Y.; Park, T. G.; Press, O. W.; Shimoboji, T.; Shoemaker, S.; Yang, H. J.; Monji, N.; Nowinski, R. C.; Cole, C. A.; Priest, J. H.; Harris, J. M.; Nakamae, K.; Nishino, T.; Miyata, T. "Really Smart Bioconjugates of Smart Polymers and Receptor Proteins" *J. Biomed. Mater. Res.* **2000**, *52*, 577-586.

(94) Hoffman, A. S.; Stayton, P. S. "Conjugates of Stimuli-Responsive Polymers and Proteins" *Prog. Polym. Sci.* **2007**, *32*, 922-932.

(95) Cho, Y. W.; Kim, J. D.; Park, K. "Pollycation Gene Delivery Systems: Escape from Endosomes to Cytosol" *J. Pharm. Pharmacol.* **2003**, *55*, 721-734.

(96) Behr, J. P. "Synthetic Gene Transfer Vectors II: Back to the Future" *Acc. Chem. Res.* **2012**, *45*, 980-984.

(97) Gao, K.; Huang, L. "Nonviral Methods for siRNA Delivery" *Mol. Pharmaceutics* **2009**, *6*, 651-658.

(98) Pack, D. W.; Hoffman, A. S.; Pun, S.; Stayton, P. S. "Design and Development of Polymers for Gene Delivery" *Nat. Rev. Drug Discovery* **2005**, *4*, 581-593.

(99) Schaffert, D.; Wagner, E. "Gene Therapy Progress and Prospects: Synthetic Polymer-Based Systems" *Gene Ther.* **2008**, *15*, 1131-1138.

(100) Midoux, P.; Breuzard, G.; Gomez, J. P.; Pichon, C. "Polymer-Based Gene Delivery: A Current Review on the Uptake and Intracellular Trafficking of Polyplexes" *Curr. Gene Ther.* **2008**, *8*, 335-352.

(101) Lemaitre, M.; Bayard, B.; Lebleu, B. "Specific Antiviral Activity of a Poly(L-Lysine)-Conjugated Oligodeoxyribonucleotide Sequence Complementary to Vesicular Stomatitis-Virus N-Protein Messenger-Rna Initiation Site" *Proc. Natl. Acad. Sci. U. S. A.* **1987**, *84*, 648-652.

(102) Schnitzler, T.; Herrmann, A. "DNA Block Copolymers: Functional Materials for Nanoscience and Biomedicine" *Acc. Chem. Res.* **2012**, *45*, 1419-1430.

(103) Fire, A.; Xu, S. Q.; Montgomery, M. K.; Kostas, S. A.; Driver, S. E.; Mello, C. C. "Potent and Specific Genetic Interference by Double-Stranded RNA in Caenorhabditis Elegans" *Nature* **1998**, *391*, 806-811.

(104) Whitehead, K. A.; Langer, R.; Anderson, D. G. "Knocking Down Barriers: Advances in siRNA Delivery" *Nat. Rev. Drug Discovery* **2009**, *8*, 129-138.

(105) Soutschek, J.; Akinc, A.; Bramlage, B.; Charisse, K.; Constien, R.; Donoghue, M.; Elbashir, S.; Geick, A.; Hadwiger, P.; Harborth, J.; John, M.; Kesavan, V.; Lavine, G.; Pandey, R. K.; Racie, T.; Rajeev, K. G.; Rohl, I.; Toudjarska, I.; Wang, G.; Wuschko, S.; Bumcrot, D.; Koteliansky, V.; Limmer, S.; Manoharan, M.; Vornlocher, H. P. "Therapeutic Silencing of an Endogenous Gene by Systemic Administration of Modified siRNAs" *Nature* **2004**, *432*, 173-178.

(106) Dykxhoorn, D. M.; Palliser, D.; Lieberman, J. "The Silent Treatment: siRNAs as Small Molecule Drugs" *Gene Ther.* **2006**, *13*, 541-552.

(107) Guo, P. X.; Coban, O.; Snead, N. M.; Trebley, J.; Hoeprich, S.; Guo, S. C.; Shu, Y. "Engineering RNA for Targeted siRNA Delivery and Medical Application" *Adv. Drug Delivery Rev.* **2010**, *62*, 650-666.

(108) Oishi, M.; Nagasaki, Y.; Itaka, K.; Nishiyama, N.; Kataoka, K. "Lactosylated Poly(Ethylene Glycol)-siRNA Conjugate through Acid-Labile Beta-Thiopropionate Linkage to Construct pH-Sensitive Polyion Complex Micelles Achieving Enhanced Gene Silencing in Hepatoma Cells" *J. Am. Chem. Soc.* **2005**, *127*, 1624-1625.

(109) Kim, S. H.; Jeong, J. H.; Lee, S. H.; Kim, S. W.; Park, T. G. "PEG Conjugated VEGF siRNA for Anti-Angiogenic Gene Therapy" *J. Controlled Release* **2006**, *116*, 123-129.

(110) Lee, S. H.; Kim, S. H.; Park, T. G. "Intracellular siRNA Delivery System Using Polyelectrolyte Complex Micelles Prepared from VEGF siRNA-PEG Conjugate and Cationic Fusogenic Peptide" *Biochem. Biophys. Res. Commun.* **2007**, *357*, 511-516.

(111) Oishi, M.; Nagasaki, Y.; Nishiyama, N.; Itaka, K.; Takagi, M.; Shimamoto, A.; Furuichi, Y.; Kataoka, K. "Enhanced Growth Inhibition of Hepatic Multicellular Tumor Spheroids by Lactosylated Poly(Ethylene Glycol)-siRNA Conjugate Formulated in PEGylated Polyplexes" *ChemMedChem* **2007**, *2*, 1290-1297.

(112) Kim, S. H.; Jeong, J. H.; Lee, S. H.; Kim, S. W.; Park, T. G. "Local and Systemic Delivery of VEGF siRNA Using Polyelectrolyte Complex Micelles for Effective Treatment of Cancer" *J. Controlled Release* **2008**, *129*, 107-116.

(113) Kim, S. H.; Jeong, J. H.; Lee, S. H.; Kim, S. W.; Park, T. G. "LHRH Receptor-Mediated Delivery of siRNA Using Polyelectrolyte Complex Micelles Self-Assembled from siRNA-PEG-LHRH Conjugate and PEI" *Bioconjugate Chem.* **2008**, *19*, 2156-2162.

(114) Tatsumi, T.; Oishi, M.; Kataoka, K.; Nagasaki, Y. "PEG-siRNA Conjugate Bearing 27 bp siRNA to Form Novel PEGylated Polyplexes with Improved Stability" *Trans. Mater. Res. Soc. Jpn.* **2008**, *33*, 807-810.

(115) Jung, S.; Lee, S. H.; Mok, H.; Chung, H. J.; Park, T. G. "Gene Silencing Efficiency of siRNA-PEG Conjugates: Effect of PEGylation Site and PEG Molecular Weight" *J. Controlled Release* **2010**, *144*, 306-313.

(116) Kow, S. C.; McCarroll, J.; Valade, D.; Boyer, C.; Dwarte, T.; Davis, T. P.; Kavallaris, M.; Bulmus, V. "Dicer-Labile PEG Conjugates for siRNA Delivery" *Biomacromolecules* **2011**, *12*, 4301-4310.

(117) Lee, S. H.; Mok, H.; Park, T. G. "Di- and Triblock siRNA-PEG Copolymers: PEG Density Effect of Polyelectrolyte Complexes on Cellular Uptake and Gene Silencing Efficiency" *Macromol. Biosci.* **2011**, *11*, 410-418.

(118) Iversen, F.; Yang, C. X.; Dagnaes-Hansen, F.; Schaffert, D. H.; Kjems, J.; Gao, S. "Optimized siRNA-PEG Conjugates for Extended Blood Circulation and Reduced Urine Excretion in Mice" *Theranostics* **2013**, *3*, 201-209.

(119) Gaziova, Z.; Baumann, V.; Winkler, A. M.; Winkler, J. "Chemically Defined Polyethylene Glycol siRNA Conjugates with Enhanced Gene Silencing Effect" *Bioorg. Med. Chem.* **2014**, *22*, 2320-2326.

(120) Choi, S. W.; Lee, S. H.; Mok, H.; Park, T. G. "Multifunctional siRNA Delivery System: Polyelectrolyte Complex Micelles of Six-Arm PEG Conjugate of siRNA and Cell Penetrating Peptide with Crosslinked Fusogenic Peptide" *Biotechnol. Prog.* **2010**, *26*, 57-63.

(121) Smith, D.; Holley, A. C.; McCormick, C. L. "RAFT-Synthesized Copolymers and Conjugates Designed for Therapeutic Delivery of siRNA" *Polym. Chem.* **2011**, *2*, 1428-1441.

(122) Rose, V. L.; Winkler, G. S.; Allen, S.; Puri, S.; Mantovani, G. "Polymer siRNA Conjugates Synthesised by Controlled Radical Polymerisation" *Eur. Polym. J.* **2013**, 2861-2883.

(123) Heredia, K. L.; Nguyen, T. H.; Chang, C.-W.; Bulmus, V.; Davis, T. P.; Maynard, H. D. "Reversible siRNA-Polymer Conjugates by RAFT Polymerization" *Chem. Commun.* **2008**, 3245-3247.

(124) Jiangtao, X.; Boyer, C.; Bulmus, V.; Davis, T. P. "Synthesis of Dendritic Carbohydrate End-Functional Polymers via RAFT: Versatile Multi-Functional Precursors for Bioconjugations" *J. Polym. Sci., Part A: Polym. Chem.* **2009**, *47*, 4302-4313.

(125) Gunasekaran, K.; Nguyen, T. H.; Maynard, H. D.; Davis, T. P.; Bulmus, V. "Conjugation of siRNA with Comb-Type PEG Enhances Serum Stability and Gene Silencing Efficiency" *Macromol. Rapid Commun.* **2011**, *32*, 654-659.

(126) Vazquez-Dorbatt, V.; Tolstyka, Z. P.; Chang, C.-W.; Maynard, H. D. "Synthesis of a Pyridyl Disulfide End-Functionalized Glycopolymer for Conjugation to Biomolecules and Patterning on Gold Surfaces" *Biomacromolecules* **2009**, *10*, 2207-2212.

(127) York, A. W.; Huang, F.; McCormick, C. L. "Rational Design of Targeted Cancer Therapeutics through the Multiconjugation of Folate and Cleavable siRNA to RAFT-Synthesized (HPMA-*s*-APMA) Copolymers" *Biomacromolecules* **2010**, *11*, 505-514.

(128) Averick, S. E.; Paredes, E.; Dey, S. K.; Snyder, K. M.; Tapinos, N.; Matyjaszewski, K. "Autotransfecting Short Interfering RNA through Facile Covalent Polymer Escorts" *J. Am. Chem. Soc.* **2013**, 12508-12511.

(129) Benoit, D. S. W.; Srinivasan, S.; Shubin, A. D.; Stayton, P. S. "Synthesis of Folate-Functionalized RAFT Polymers for Targeted siRNA Delivery" *Biomacromolecules* **2011**, *12*, 2708-2714.

(130) Cheng, Q.; Huang, Y. Y.; Zheng, H.; Wei, T.; Zheng, S. Q.; Huo, S. D.; Wang, X. X.; Du, Q.; Zhang, X. N.; Zhang, H. Y.; Liang, X. J.; Wang, C.; Tang, R. P.; Liang, Z. C. "The Effect of Guanidinylation of Pegylated Poly(2-Aminoethyl Methacrylate) on the Systemic Delivery of siRNA" *Biomaterials* **2013**, *34*, 3120-3131.

(131) Cho, H. Y.; Srinivasan, A.; Hong, J.; Hsu, E.; Liu, S. G.; Shrivats, A.; Kwak, D.; Bohaty, A. K.; Paik, H. J.; Hollinger, J. O.; Matyjaszewski, K. "Synthesis of Biocompatible PEG-Based Star Polymers with Cationic and Degradable Core for siRNA Delivery" *Biomacromolecules* **2011**, *12*, 3478-3486.

(132) Convertine, A. J.; Benoit, D. S. W.; Duvall, C. L.; Hoffman, A. S.; Stayton, P. S. "Development of a Novel Endosomolytic Diblock Copolymer for siRNA Delivery" *J. Controlled Release* **2009**, *133*.

(133) Gary, D. J.; Lee, H.; Sharma, R.; Lee, J. S.; Kim, Y.; Cui, Z. Y.; Jia, D.; Bowman, V. D.; Chipman, P. R.; Wan, L.; Zou, Y.; Mao, G. Z.; Park, K.; Herbert, B. S.; Konieczny, S. F.; Won, Y. Y. "Influence of Nano-Carrier Architecture on in Vitro siRNA Delivery Performance and in Vivo Biodistribution: Polyplexes vs Micelleplexes" *ACS Nano* **2011**, *5*, 3493-3505.

(134) Hinton, T. M.; Guerrero-Sanchez, C.; Graham, J. E.; Le, T.; Muir, B. W.; Shi, S. N.; Tizard, M. L. V.; Gunatillake, P. A.; McLean, K. M.; Thang, S. H. "The Effect of RAFT-Derived Cationic Block Copolymer Structure on Gene Silencing Efficiency" *Biomaterials* **2012**, *33*, 7631-7642.

(135) Scales, C. W.; Huang, F.; Li, N.; Vasilieva, Y. A.; Ray, J.; Convertine, A. J.; McCormick, C. L. "Corona-Stabilized Interpolyelectrolyte Complexes of siRNA with Nonimmunogenic, Hydrophilic/Cationic Block Copolymers Prepared by Aqueous RAFT Polymerization" *Macromolecules* **2006**, *39*, 6871-6881.

(136) Smith, A. E.; Sizovs, A.; Grandinetti, G.; Xue, L.; Reineke, T. M. "Diblock Glycopolymers Promote Colloidal Stability of Polyplexes and Effective pDNA and siRNA Delivery under Physiological Salt and Serum Conditions" *Biomacromolecules* **2011**, *12*, 3015-3022.

(137) Valade, D.; Boyer, C.; Davis, T. P.; Bulmus, V. "Synthesis of siRNA Polyplexes Adopting a Combination of RAFT Polymerization and Thiol-Ene Chemistry" *Aust. J. Chem.* **2009**, *62*, 1344-1350.

(138) York, A. W.; Zhang, Y.; Holley, A. C.; Guo, Y.; Huang, F.; McCormick, C. L. "Facile Synthesis of Multivalent Folate-Block Copolymer Conjugates Via Aqueous RAFT Polymerization: Targeted Delivery of siRNA and Subsequent Gene Suppression" *Biomacromolecules* **2009**, *10*, 936-943.

(139) Boyer, C.; Teo, J.; Phillips, P.; Erlich, R. B.; Sagnella, S.; Sharbeen, G.; Dwarte, T.; Duong, H. T. T.; Goldstein, D.; Davis, T. P.; Kavallaris, M.; McCarroll, J. "Effective Delivery of siRNA into Cancer Cells and Tumors Using Well-Defined Biodegradable Cationic Star Polymers" *Mol. Pharmaceutics* **2013**, *10*, 2435-2444.

(140) Benoit, D. S. W.; Henry, S. M.; Shubin, A. D.; Hoffman, A. S.; Stayton, P. S. "pH-Responsive Polymeric siRNA Carriers Sensitize Multidrug Resistant Ovarian Cancer Cells to Doxorubicin via Knockdown of Polo-Like Kinase 1" *Mol. Pharmaceutics* **2010**, *7*, 442-455.

(141) Convertine, A. J.; Diab, C.; Prieve, M.; Paschal, A.; Hoffman, A. S.; Johnson, P. H.; Stayton, P. S. "pH-Responsive Polymeric Micelle Carriers for siRNA Drugs" *Biomacromolecules* **2010**, *11*, 2904-2911.

(142) Palanca-Wessels, M. C.; Convertine, A. J.; Cutler-Strom, R.; Booth, G. C.; Lee, F.; Berguig, G. Y.; Stayton, P. S.; Press, O. W. "Anti-CD22 Antibody Targeting of pH-Responsive Micelles Enhances Small Interfering RNA Delivery and Gene Silencing in Lymphoma Cells" *Mol. Ther.* **2011**, *19*, 1529-1537.

(143) Wang, L. G.; Chierico, L.; Little, D.; Patikarnmonthon, N.; Yang, Z.; Azzouz, M.; Madsen, J.; Armes, S. P.; Battaglia, G. "Encapsulation of Biomacromolecules within Polymersomes by Electroporation" *Angew. Chem., Int. Ed.* **2012**, *51*, 11122-11125.

(144) Zhu, C.; Jung, S.; Luo, S.; Meng, F.; Zhu, X.; Park, T. G.; Zhong, Z. "Co-Delivery of siRNA and Paclitaxel into Cancer Cells by Biodegradable Cationic Micelles Based on PDMAEMA-PCL-PDMAEMA Triblock Copolymers" *Biomaterials* **2010**, *31*, 2408-2416.

(145) Averick, S. E.; Paredes, E.; Irastorza, A.; Shrivats, A. R.; Srinivasan, A.; Siegwart, D. J.; Magenau, A. J.; Cho, H. Y.; Hsu, E.; Averick, A. A.; Kim, J.; Liu, S. G.; Hollinger, J. O.; Das, S. R.; Matyjaszewski, K. "Preparation of Cationic Nanogels for Nucleic Acid Delivery" *Biomacromolecules* **2012**, *13*, 3445-3449.

(146) Nuhn, L.; Hirsch, M.; Krieg, B.; Koynov, K.; Fischer, K.; Schmidt, M.; Helm, M.; Zentel, R. "Cationic Nanohydrogel Particles as Potential siRNA Carriers for Cellular Delivery" *ACS Nano* **2012**, *6*, 2198-2214.

(147) Oliveira, M. A. M.; Boyer, C.; Nele, M.; Pinto, J. C.; Zetterlund, P. B.; Davis, T. P. "Synthesis of Biodegradable Hydrogel Nanoparticles for Bioapplications Using Inverse Miniemulsion RAFT Polymerization" *Macromolecules* **2011**, *44*, 7167-7175.

(148) Boyer, C.; Priyanto, P.; Davis, T. P.; Pissuwan, D.; Bulmus, V.; Kavallaris, M.; Teoh, W. Y.; Amal, R.; Carroll, M.; Woodward, R.; St Pierre, T. "Anti-Fouling Magnetic Nanoparticles for siRNA Delivery" *J. Mater. Chem.* **2010**, *20*, 255-265.

(149) Kirkland-York, S.; Zhang, Y.; Smith, A. E.; York, A. W.; Huang, F.; McCormick, C. L. "Tailored Design of Au Nanoparticle-siRNA Carriers Utilizing Reversible Addition-Fragmentation Chain Transfer Polymers" *Biomacromolecules* **2010**, *11*, 1052-1059.

Chapter 2

Protein-Polymer Conjugation *via* Ligand Affinity and Photoactivation of Glutathione *S*-Transferase[‡]

2.1 Introduction

Protein-polymer conjugates are of great interest due to their applications in drug delivery, biomaterials, and nanotechnology.[1-5] The role of the attached polymer is to enhance existing functions or introduce new properties to the unmodified protein. For example, the covalent attachment of poly(ethylene glycol) (PEG), also known as PEGylation, is commonly used to improve the pharmacological properties of therapeutic proteins.[6] Site-specific conjugation is important for retaining bioactivity of the protein, and therefore development of new conjugation approaches are of high interest in the field of bioconjugation.[7] Typically site-specific conjugation is achieved by targeting rare natural amino acids, genetic modifications, or chemically installed functionalities.[8-14]

Other methods have also been used for protein-polymer conjugation, such as non-covalent interactions including ligand protein affinity. Using ligand-protein binding affinity, ligand-modified polymers can specifically bind to the corresponding protein. This type of conjugation method has been most commonly used with the biotin-streptavidin systems.[15-18] Another example is cofactor reconstitution, which has been employed to couple polystyrene to heme-dependent proteins, such as horseradish peroxidase (HRP) and myoglobin, to form bioactive giant amphiphiles.[19,20] Recently, our group and others have also utilized the interaction between glutathione (GSH) and gluthathione *S*-transeferase (GST) to form protein-polymer conjugates.[18,21] However, the major drawback of non-covalent interactions is that the conjugates are prone to dissociate under charge disruption, heat, or other denaturing conditions.

GSTs, (EC 2.5.1.18) are a family of enzymes that catalyze the nucleophilic addition of the thiol of GSH to electrophilic centers in organic compounds for means of cellular

detoxification.[22,23] There are several classes of GSTs, but all exhibit similar monomer sizes (23-28 kDa), amino acid sequences, and substrate specificity. They function as homodimeric or heterodimeric species, with heterodimers only forming between different subunits belonging to the same class. GSTs have two active sites per dimer, with each active site separated into two distinct functional regions: a hydrophilic "G-site" for recognition of GSH, and an adjacent "H-site" for binding hydrophobic electrophiles. Due to its specificity to GSH (with a dissociation constant of $k_d \sim 10^{-4}$ M^{-1})[24], GST has been commonly integrated into recombinant proteins to allow for affinity chromatography purification with immobilized GSH.[25,26] Herein, we describe an approach to prepare site selective PEG-GST proteins by light activation of photo-reactive GSH-PEG (**Scheme 2-1**).

Photoaffinity labeling has been widely used in mapping the active sites of enzymes and studying protein interactions.[27,28] A photoaffinity probe contains at least two parts: an affinity unit and a photo-reactive unit. Benzophenone, diazirine, and azide are widely used photo-reactive groups that can generate highly reactive species, namely triplet state carbonyls, carbenes, and nitrenes, respectively. Benzophenone (BP) was selected for study because it has an advantage that it is chemically more stable than the other groups or species, can be manipulated in ambient light, and inserts into unreactive C-H bonds even in the presence of nucleophilic solvents such as water and alcohols.[29] Recently, the use of affinity association followed by photoexcitation of benzophenone has been utilized by Aida and coworkers to develop "photoclickable molecular glue" that labels proteins with a fluorescent dendron.[30] Yet there have been no examples of using benzophenone to form protein-polymer conjugates. We also prepared a GSH analogue containing a diazirine (DA) moiety. Upon irradiation, diazirine generates a highly active carbene intermediate that can insert into C-H bonds within close

proximity.[31,32] In one earlier report, PEG has been functionalized with diazopyruvate and nitroaryl azide for protein conjugation, which after photolysis generated carbene and nitrene, respectively. The reactive species then underwent rearrangements followed by amine insertion of protein lysine residues or N-terminal to give PEGylated proteins.[33] However, the PEGs did not contain a specific affinity tag and highly reactive carbene and nitrene could also insert into C-H and N-H bonds, especially without close proximity of the reactive groups. Described herein is the first example, to our knowledge, of PEGylation through photoaffinity conjugation.

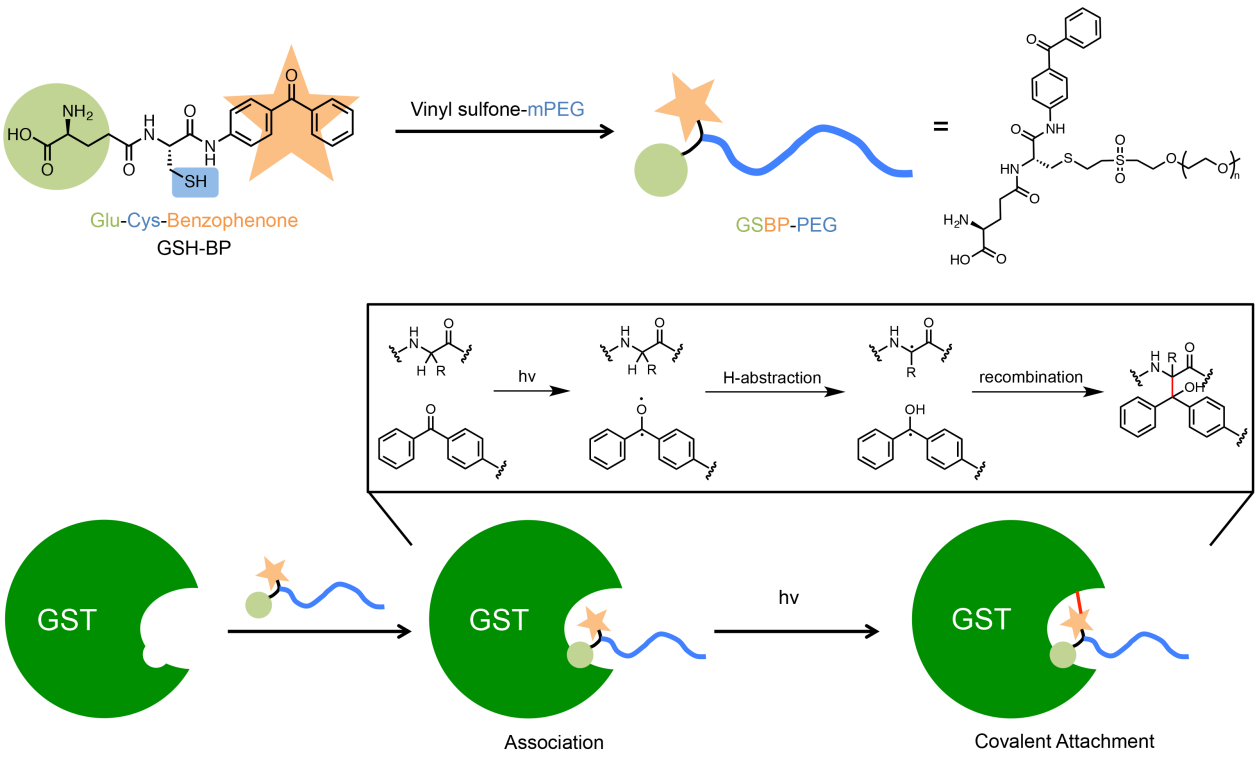

Scheme 2-1. Schematic overview of the photoaffinity PEGylation using GSH-BP.

2.2 Results and Discussion

2.2.1 Synthesis of GSH-BP

To form an irreversibly-bound, covalent protein-polymer conjugate, a GSH analogue containing a photo-reactive probe was designed to act as the cross-linking moiety between GST and the polymer. We hypothesized that the modified polymer end-group could be directed into the GSH binding pocket of GST through ligand affinity, and then activated by UV irradiation to form a stable and irreversible covalent bond. The overall approach was to prepare a BP labeled GSH and react vinyl sulfone PEG (2K mPEG, 5K mPEG, and 20K mPEG) with the GSH via thiol-ene chemistry. The modified polymers could then conjugate to GST and a GST fusion protein through photoactivation (**Scheme 2-1**).

It has been reported that the gamma glutamyl residue of the GSH tripeptide is crucial for binding to GST, whereas the C-terminal glycyl carboxylate is non-essential.[34] Therefore, the design of our GSH analogue (GSH-BP) replaces the glycine with amino-benzophenone. The free thiol of cysteine was used as a handle for PEG modification, and the glutamyl group remained free for GST binding. The GSH-BP was synthesized by solution phase peptide synthesis (**Scheme 2-2**). To incorporate the benzophenone moiety, 4-aminobenzophenone was coupled to Fmoc-Cys(Trt)-OH. Following Fmoc deprotection and subsequently coupling Boc-Glu-OtBu, fully protected GSH-BP was obtained. Global deprotection yielded GSH-BP in 28% overall yield for all steps. UV-Vis showed λ_{max}=295 nm; ESI-MS gave the mass $+H^+$ 430.1450 (calculated 430.1392). (See Appendix **Figure 2-7** through **Figure 2-12** for NMR spectra.)

Scheme 2-2. Synthesis of GSH-BP.

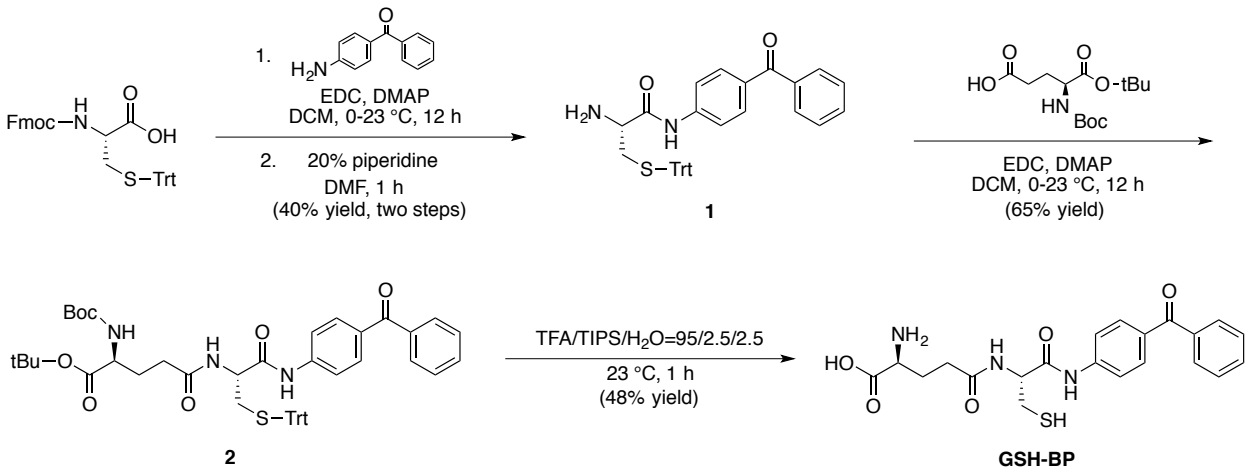

2.2.2 Conjugation of GSH-BP to GST

To confirm GSH-BP attachment to GST after irradiation, 200 mM GSH-BP was added to 4 mM GST, incubated on ice for 2 hours to allow association, and subsequently irradiated for 30 minutes with a 450 W mercury arc lamp (energy distribution at 296.7 nm is 4.3 W). At the same time, two control samples were prepared: one without the addition of GSH-BP substrate but with 30 min of UV irradiation, to confirm the integrity of GST after the irradiation condition. The other was with GSH-BP, but without UV irradiation, to confirm that irradiation is necessary for GSH-BP binding. The GST samples were analyzed by MALDI-TOF (**Figure 2-1**). The peak corresponding to GST without GSH-BP or UV irradiation showed up as the GST monomer subunit with m/z around 23,300. An increase of mass was observed only when both GSH-BP and UV irradiation are present. The difference in mass between the new peak and unmodified GST was 426.74, which closely corresponded to the mass of GSH-BP (429.1358). This confirmed the covalent attachment of a single GSH-BP to GST after irradiation.

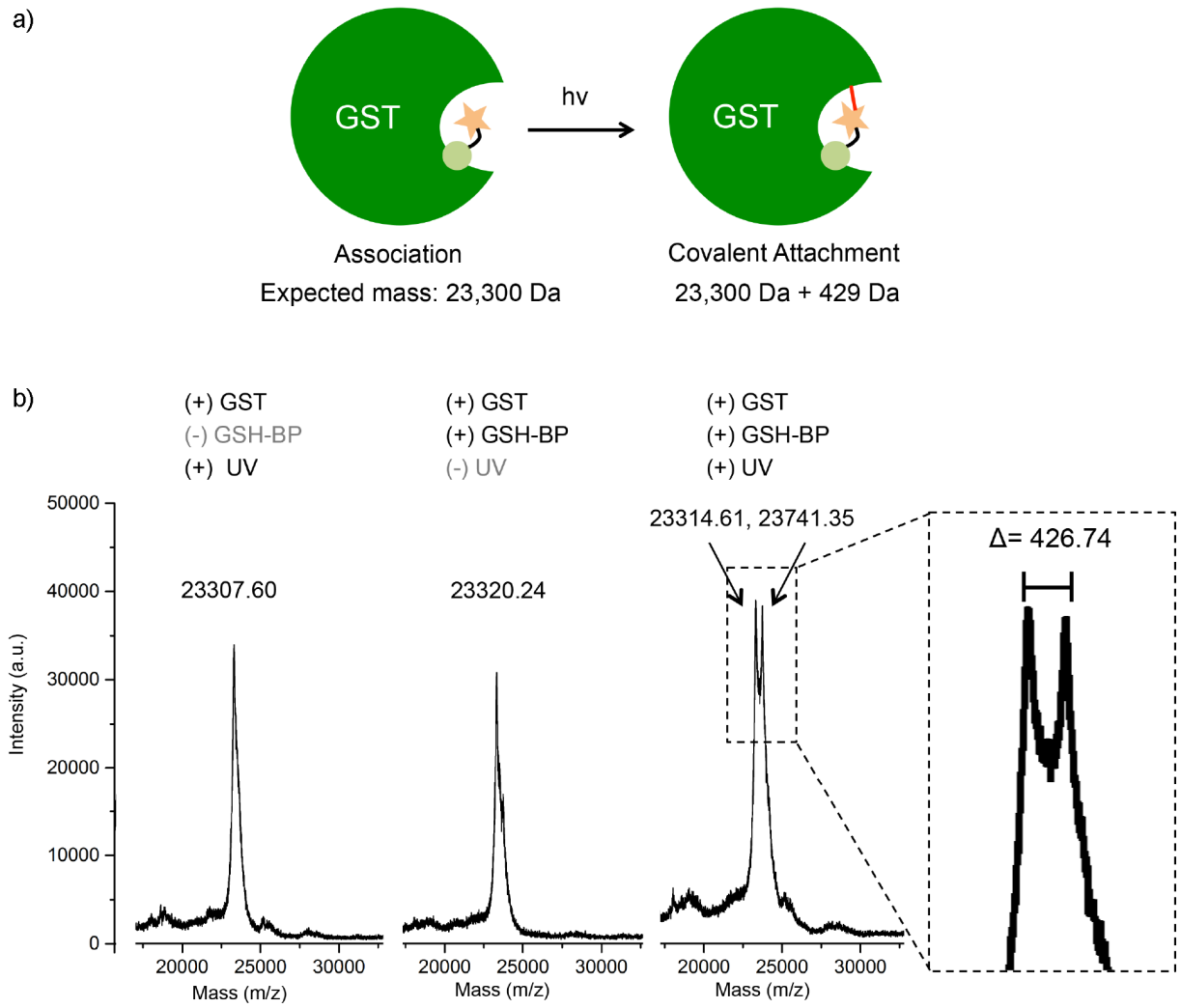

Figure 2-1. a) Photoconjugation of GSH-BP to GST and b) MALDI-TOF MS results with or without the presence of GSH-BP or UV irradiation with a mercury arc lamp. Only in the case of addition of GSH-BP and application of UV irradiation, an increase in mass was observed.

We have also conducted the same irradiation experiment with a common hand-held UV lamp, using the long wavelength (365 nm). The results showed that the energy of the hand-held UV lamp was not enough to obtain as high yield of modification as using the mercury arc lamp

(**Figure 2-2**). Therefore, for the following photoactivation experiments, we chose to use the broadband, medium-pressure quartz mercury arc lamp as the irradiation source.

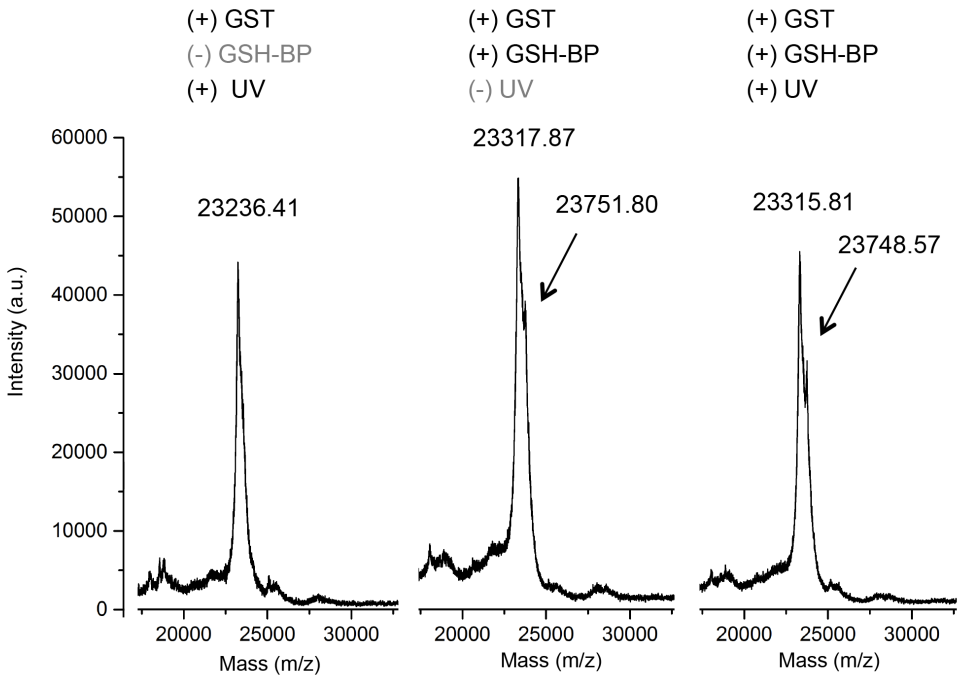

Figure 2-2. MALDI-TOF MS of the addition of GSH-BP to GST, using hand-held UV lamp.

The peak intensities of the unmodified GST and modified GST were very similar, which could be explained if only one subunit of the GST dimer was modified. Wang et al. have synthesized a photoaffinity probe consisting of glutathione and benzophenone, in which benzophenone acts as the photo-reactive group as well as the xenobiotic substrate.[35] They demonstrated that the probe binds to both the glutathione binding site (G-site) and hydrophobic substrate binding site (H-site), and reacts specifically with Met-112 of the μ class GST, isoenzyme 4-4. From experimental and docking results, they concluded that modification of one subunit prevents the modification of the other dimer subunit. This would explain the results

observed in the MALDI spectrum; namely that the GSH-BP binds to one of the two GSTs in the dimer and subsequently the dimer dissociates during the mass spectrometry experiment.

2.2.3 Synthesis of GSH-DA

We also synthesized a GSH analogue containing a diazirine group to compare its photoconjugation efficiency to GSH-BP. Diazirine was incorporated into the peptide sequence as an amino acid side chain using commercially available L-photo-Leucine (see Appendix **Figure 2-13** and **Figure 2-14** for NMR spectra of Fmoc-photo-Leucine). The peptide (GSH-DA) was synthesized by solid phase synthesis and verified by ESI-MS (**Scheme 2-3**). GSH-DA has a smaller photo-reactive group than GSH-BP, and conserves the carboxylic acid on the original glycine position

Scheme 2-3. Synthesis of GSH-DA.

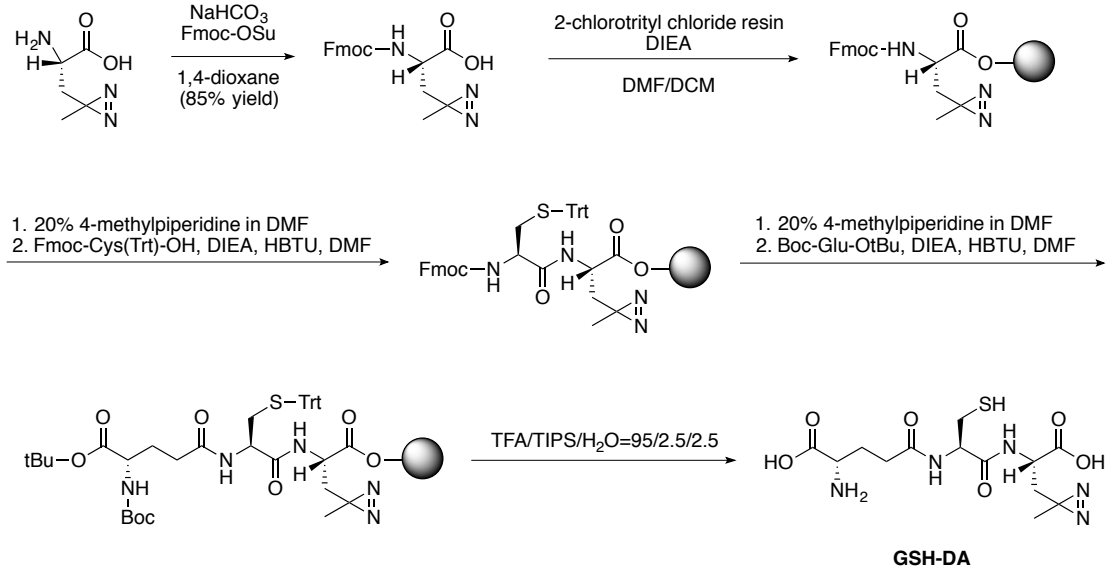

2.2.4 PEG Functionalization with GSH-BP, GSH-DA, and Controls

Vinyl sulfone-PEG (VS-PEG) was prepared from three sizes of mPEG, modifying reported procedures (**Scheme 2-4**).[36] Michael addition of the PEG hydroxyl group to divinyl sulfone yielded mono-functionalized VS-PEGs (see Appendix **Figure 2-15** through **Figure 2-17** for ^{1}H NMR spectra of 2K, 5K, and 20K VS-PEG). By comparing the integration of the vinyl peaks to that of the ethylene glycol peak in ^{1}H NMR, the vinyl sulfone conversion of 2K, 5K, and 20K VS-PEG, was calculated to be 89%, 85%, and 90%, respectively. GSH-BP was then added to each size of VS-PEG to form the corresponding size of GSBP-PEG (**Scheme 2-5**). GSH-BP is insoluble in water, so it was dissolved in methanol before addition to a phosphate buffer solution of VS-PEG. The pH of the reaction mixture was kept at pH 8.0 to avoid side reactions of vinyl sulfone with the free amine of GSH-BP.[37] The disappearance of vinyl protons was confirmed by ^{1}H NMR after 48 hours. GSBP-PEGs were purified by HPLC with gradient elution of MeOH/H_2O or dialysis against water followed by filtration to remove excess GSH-BP (see Appendix **Figure 2-18** through **Figure 2-20** for ^{1}H NMR spectra of 2K, 5K, and 20K GSBP-PEG). By comparing the integration of the aromatic protons of benzophenone to the ethylene glycol protons in ^{1}H NMR, the modification ratio of 2K, 5K, and 20K GSBP-PEG, was calculated to be 94%, 100%, and 95%, respectively. 5K GSDA-PEG was synthesized in a similar fashion (**Scheme 2-6**), and the conversion was calculated as 75% (see Appendix **Figure 2-21** for ^{1}H NMR spectrum).

Scheme 2-4. Synthesis of VS-PEG.

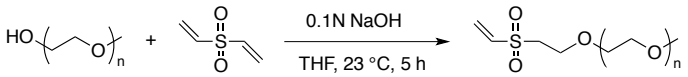

2K VS-PEG, n=50
5K VS-PEG, n=125
20K VS-PEG, n=500

Scheme 2-5. Synthesis of GSBP-PEG.

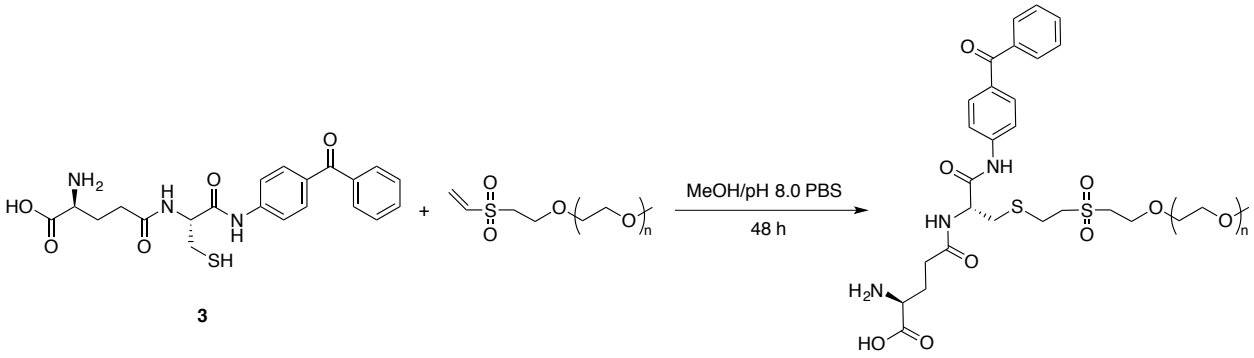

3

2K VS-PEG, n=50
5K VS-PEG, n=125
20K VS-PEG, n=500

2K GSBP-PEG, n=50
5K GSBP-PEG, n=125
20K GSBP-PEG, n=500

Scheme 2-6. Synthesis of 5K GSDA-PEG.

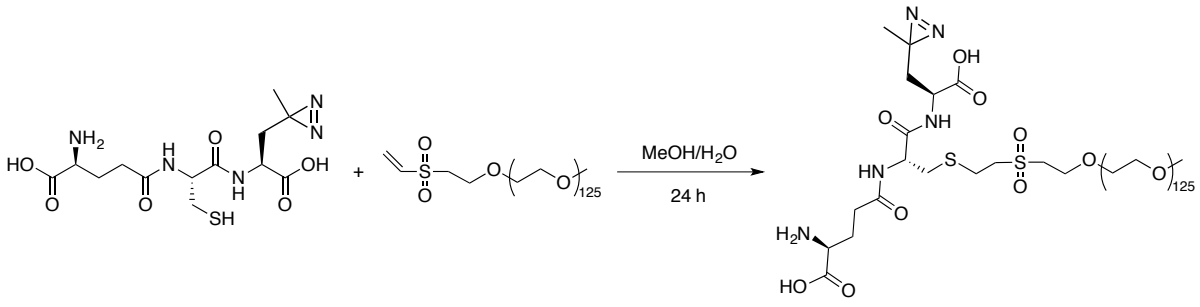

5K GSDA-PEG

To confirm the selectivity and ability of GSBP-PEG to covalently attach to GST, we prepared PEG with different end-groups, including GSH and BP, as controls. 2K and 5K GS-PEG, with the affinity probe (GSH), but not the photo-reactive component (BP), were synthesized by conjugating GSH to VS-PEG through the free thiol of the cysteine moiety, and the conversion was 83% and 86%, respectively (**Scheme 2-7**, see Appendix **Figure 2-22** and **Figure 2-23** for ^{1}H NMR spectra). 5K BP-PEG, with the photo-reactive probe (BP) but no affinity moiety (GSH), was synthesized via 1-ethyl-3-(3-dimethylaminopropyl)carbodiimide (EDC) coupling of mPEG and 4-benylbenzoic acid (**Scheme 2-8**). The end-group conversion was calculated to be 100% (see Appendix **Figure 2-24** for ^{1}H NMR spectrum).

Scheme 2-7. Synthesis of 2K and 5K GS-PEG.

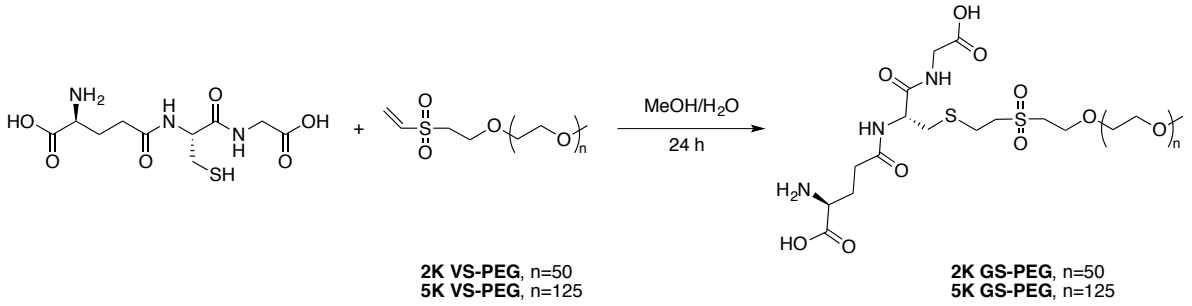

Scheme 2-8. Synthesis of 5K BP-PEG.

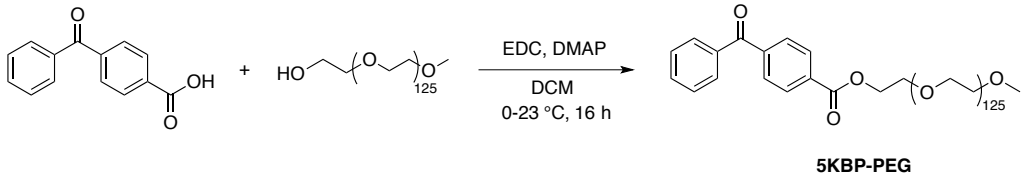

2.2.5 Conjugation of GSBP-PEG to GST

To investigate the photoinduced reactivity of GSBP-PEG to GST, a mixture of GSBP-PEG (20 mM) and GST (0.4 mM) in pH 7.4 D-PBS was irradiated with a 450 W mercury arc lamp in an ice bath over a period of 15 minutes (see **Section 2.2.2**). All subsequent conjugation experiments used the same protocol. SDS-PAGE analysis demonstrated that the synthesized GSBP-PEGs could be covalently conjugated to GST, appearing as an additional band with higher molecular weight above the unconjugated GST band (**Figure 2-3a**). Importantly, no conjugates were observed in samples that were not exposed to UV irradiation. The conjugation yields of 2K, 5K, and 20K GSBP-PEG were estimated by quantification of the band intensities taking into account of the dimeric form of GST, and were calculated to be 52%, 56%, and 76%, respectively (**Table 2-1**). Various concentrations of protein and polymer equivalents were then investigated for 5K GSBP-PEG (**Table 2-2**) and it was found that by increasing the polymer concentration to 50 equivalents and the irradiation time to 30 min keeping the polymer concentration the same, the yield was increased from 56% to 74%. Photoaffinity labeling approaches are often limited from their low efficiencies. Photolysis of benzophenone in protein-protein cross-linking events or the labeling of peptide binding sites generally resulted in efficiencies lower than 40%.[38,39] Recent reports that have utilized benzophenone to covalently conjugate immunoglobin-binding domains to antibodies showed conjugation yields of 70% at maximum.[40,41] Thus, the conjugation yields of GSBP-PEGs to GST ranging from 52-76% are fairly high.

While the naturally existing GST dimer is denatured and unfolded during SDS-PAGE analysis releasing free GST, the band we observe is based on the molecular weight of one monomer subunit. Therefore, we also analyzed unmodified GST and its conjugates by native PAGE, because native gels are run under non-denaturing conditions, and the mobility of the

proteins is based on its charge and hydrodynamic size. However, the conjugates and protein itself appear as a smear, which makes the results unsuitable for determination of the conjugation yield (**Figure 2-4a**).

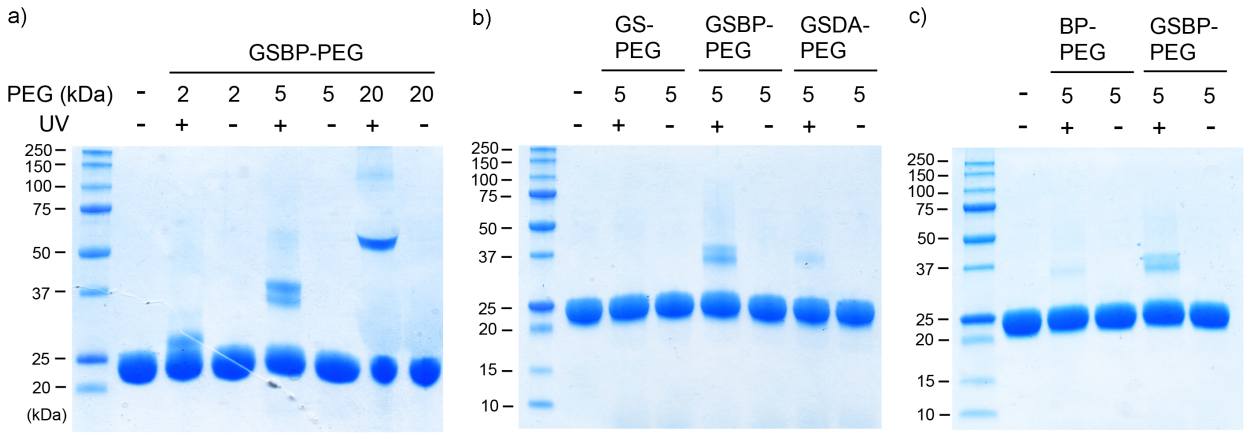

Figure 2-3. SDS-PAGE of a) GSBP-PEG conjugation to GST; b) comparison between GS-PEG, 5K GSBP-PEG, and GSDA-PEG; c) comparison between BP-PEG and 5K GSBP-PEG.

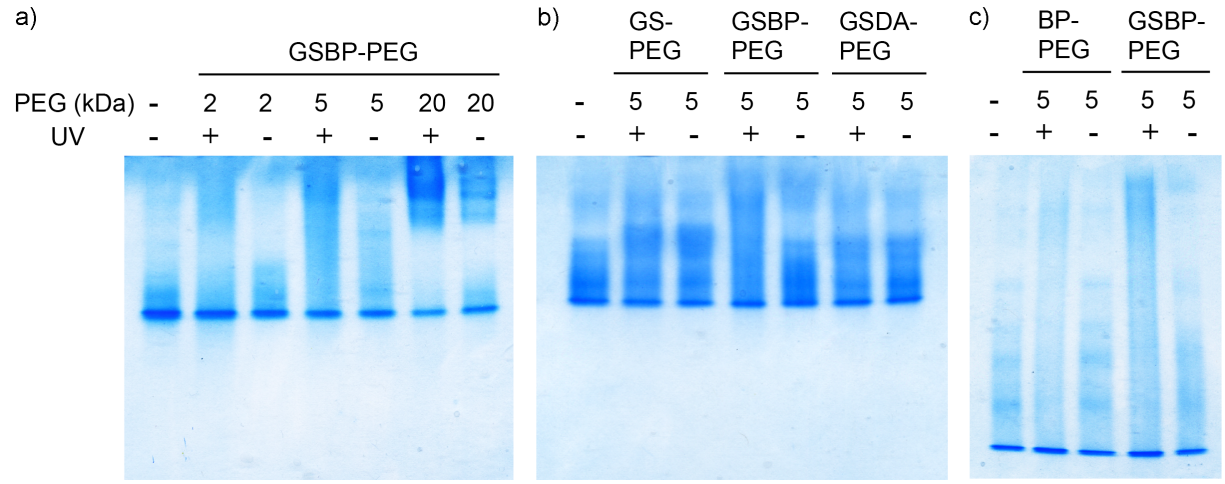

Figure 2-4. Native PAGE of a) GSBP-PEG conjugation to GST; b) comparison between GS-PEG, 5K GSBP-PEG, and GSDA-PEG; c) comparison between BP-PEG and 5K GSBP-PEG.

To compare the conjugation efficiency of GS-PEG and GSDA-PEG to GSBP-PEG, a mixture of each polymer (5 kDa, 20 mM) and GST (0.4 mM) was irradiated following the previously mentioned protocol. SDS-PAGE analysis demonstrated that, as expected, GS-PEG does not form any covalent conjugates with GST after UV irradiation due to the lack of photo-reactive group (**Figure 2-3b** and Appendix **Figure 2-25**). This is exactly what we would expect, since SDS would disrupt any non-covalent interactions. Surprisingly, GSDA-PEG only showed a small conjugation yield of 18%, compared to the 56% conjugation yield of 5K GSBP-PEG (**Table 2-1**). Native PAGE analysis was also conducted, and no obvious difference in the bands was observed in either GS-PEG or GSDA-PEG conjugates after irradiation **(Figure 2-4b**). However, the conjugation of GSBP-PEG was observed as an intense high molecular weight smear. We originally anticipated that the GSH with the smaller DA group would bind better than the larger BP group. However, given the results, we propose that the larger, hydrophobic benzophenone may play an important role in the binding the hydrophobic "H-site" of the binding pocket, which further increases the binding affinity of GSH-BP to GST.

To confirm that covalent conjugation was not exclusively due to hydrophobic binding of benzophenone, the photoinduced conjugation of GSBP-PEG and BP-PEG to GST were compared under the same conditions. From SDS-PAGE analysis, the conjugation yield of BP-PEG to GST was calculated as 14%, which is much lower than the 56% yield of GSBP-PEG (**Figure 2-3c** and **Table 2-1**). This demonstrates that the GSH binding component is crucial to the design of the GSH-BP probe. The conjugation results were also analyzed by native PAGE, and the higher molecular weight smear of GSBP-PEG conjugate was observed to be significantly more intense than BP-PEG, which further demonstrates the higher conjugation efficiency of

GSBP-PEG (**Figure 2-4c**). The conjugation efficiencies of different sizes of GSBP-PEG, as well as different end-functionalized 5K PEGs, are summarized in **Table 2-1**.

Table 2-1. Conjugation yields for the different PEGs to GST.

Size	2K	5K	20K	5K	5K	5K
Polymer	GSBP-PEG	GSBP-PEG	GSBP-PEG	GS-PEG	BP-PEG	GSDA-PEG
Conjugation yield[a]	52%	56%[b]	76%	0%	14%	18%

[a]GST is a protein dimer, and showed on SDS-PAGE gels as broken subunits. The yield was obtained by dividing the conjugate percentage on gel by the theoretical maximum yield because of the dimer(50%).

[b]The conjugation yield is presented as an average from three separate SDS-PAGE gels.

2.2.6 Binding Properties of GSBP-PEG to GST

To further prove the binding of GSBP-PEG to GST, we used a commercially available GSTrap column packed with immobilized GSH resins as an investigation tool. GSH, PEG, and GS-PEG were also prepared as comparison. A solution of GST was loaded into the GSTrap column, and pH7.4 D-PBS was used to wash the column and elute unbound GST. After unbound GST was removed, the buffer was switched to a solution of GSH, 5K PEG, 5K GS-PEG, or 5K GSBP-PEG. If competitive binding occurred between the solution and GSH resins, bound GST would interact with the solution and elute off the column, proving that there was binding effect with GST. From the chromatography traces of GSH and GSH-PEG elution, we observed GST by UV-Vis detection at 280 nm at 15 min retention time, meaning that the competition with GSH resin occurred. The absorbance of GSBP-PEG at 295 nm overlapped with 280 nm, and therefore

interfered with the detection of GST. To visualize the amount of GST that was eluted, the collected materials were analyzed on SDS-PAGE. Coomassie Blue was used to stain the protein, and iodide stain was used to stain PEG (**Figure 2-5**). In lane 4, the detection of GST confirmed the binding effect of GSBP-PEG with GST, while lane 2 showed that no GST eluted when exposed to unmodified PEG. From this result, it was concluded that GSBP-PEG binds to GST.

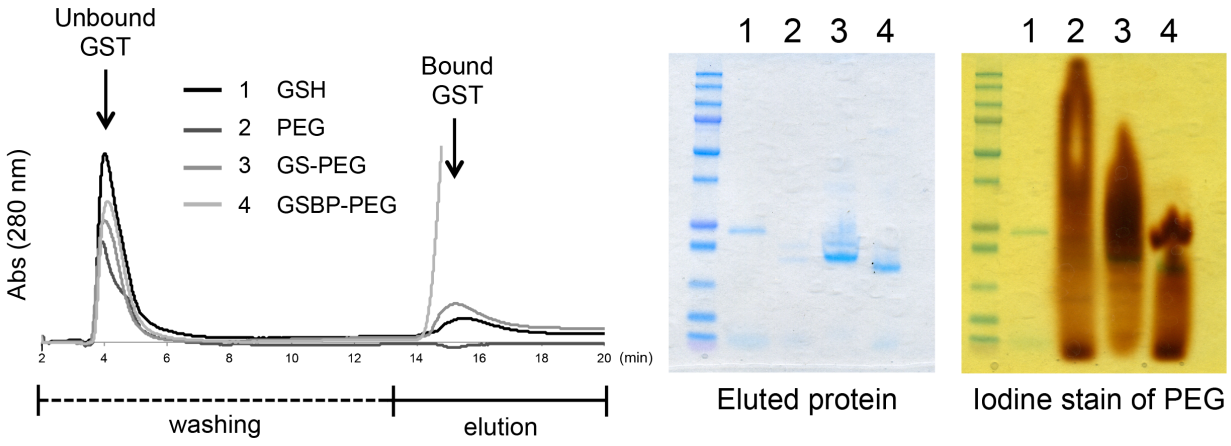

Figure 2-5. GSTrap elution experiment with 1) GSH, 2) PEG, 3) GS-PEG, and 4) GSBP-PEG as eluent.

2.2.7 GSBP-PEG Conjugation to Other Proteins- BSA, Lyz, Ubq, and GST-Ubq

In order to investigate the further applicability of this conjugation method, several proteins including GST were tested under various conjugation conditions (including protein concentration, polymer ratio, and irradiation time). First, bovine serum albumin (BSA, 66.5 kDa) was chosen as a model protein. A mixture of GSBP-PEG (2K or 5K, 20 mM) and BSA (or GST

as a control, 0.4 mM) was irradiated on ice over a period of 30 min and analyzed by SDS-PAGE. Similar conjugation efficiency of GSBP-PEG to BSA as to GST was observed, which can be explained by the known binding effect of benzophenone to the subdomain IIA hydrophobic cavities of BSA (**Figure 2-6a**).[42] This further strengthens our hypothesis that GSH-BP is interacting with the hydrophobic binding site (H-site) in GST. To eliminate this factor, lysozyme (Lyz, 14.4 kDa) was also tested as a general non-binding protein (**Figure 2-6b**). Under conditions of 0.4 mM protein concentration and 30 min of irradiation, 12% and 24% of non-specific conjugation to Lyz were observed with adding 5 eq and 10 eq of 5K GSBP-PEG, respectively. When protein concentration, irradiation time, and the polymer ratio were decreased, the non-specific conjugation was significantly reduced compared to GST and BSA under the same conditions down to 0% (**Table 2-2** and Appendix **Figure 2-26**). These results convey that after photoexcitation, benzophenone non-specifically attaches to non-binding proteins (Lyz) at high protein concentrations and large excess of GSBP-PEG. Decreasing concentration, stoichiometry, and irradiation time can reduce the non-specificity. The results indicate that polymer concentrations and polymer equivalents may be identified for each fusion protein to yield conjugation to the GST tag component only. For example, at 0.05 mM GST and 5 equivalent of polymer the conjugation yield to GST was 54%, while to Lys it was 8%, and 1 equivalent of polymer resulted yields of 20% and 0%, respectively.

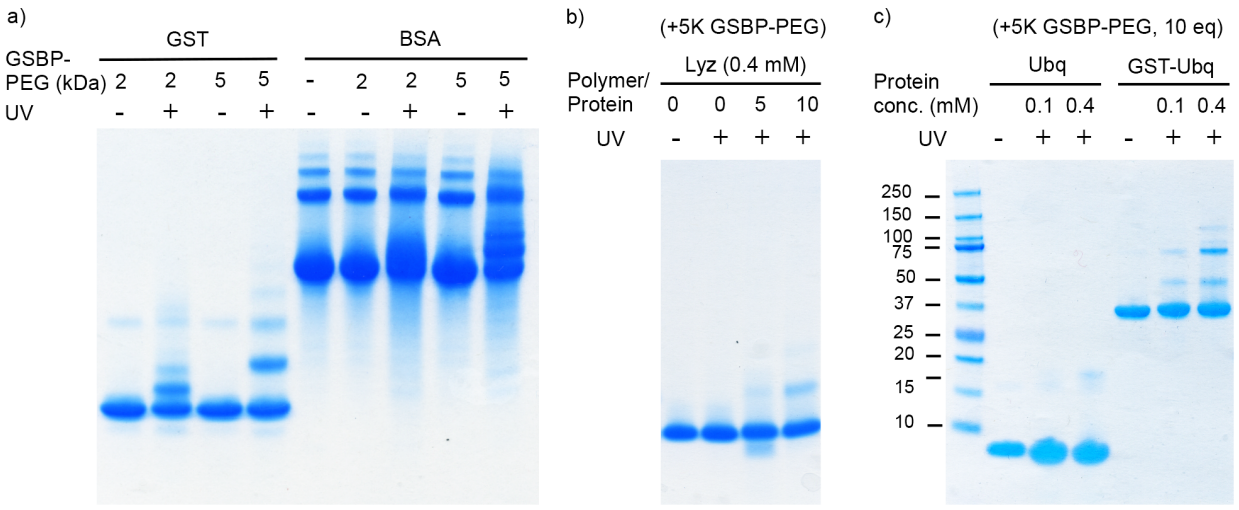

Figure 2-6. SDS-PAGE of the conjugation of a) 2K and 5K GSBP-PEG to GST and BSA, b) 5K GSBP-PEG to Lyz with different polymer to protein ratios, and c) 5K GSBP-PEG to Ubq and GST-Ubq.

To further study the applicability of the approach, the conjugations of GSBP-PEG to Ubiquitin (Ubq, 8.5 kDa) and GST-tagged Ubq (GST-Ubq, 38.5 kDa) were compared side-by-side, with higher conjugation efficiency of the fusion protein is expected. The important role of the GST tag in the conjugation of GSBP-PEG to Ubq was demonstrated by SDS-PAGE analysis (**Figure 2-6c**). The conjugation efficiencies calculated by the band intensities were 9% for Ubq and 36% for GST-Ubq (**Table 2-2**). The conjugation mixture of GST-Ubq was subjected to MALDI-TOF MS analysis, and the addition of one, two, and three GSBP-PEGs to GST-Ub (monomer) was observed (see Appendix **Figure 2-27**).

Table 2-2. Conjugation yields for 5K GSBP-PEG to GST, BSA, Lyz, Ubq, and GST-Ubq at various conditions.[a]

Protein	**GST**							**Ubq**	**GST-Ubq**
Protein conc. (mM)	0.4	0.4	0.4	0.1	0.05	0.05	0.05	0.4	0.4
Polymer (eq)	50	10	5	1	1	5	10	10	10
UV time (min)	30	30	30	15	15	15	15	15	15
Conj. yield (%)	**74**	**62**	**54**	**26**	**20**	**54**	**52**	**9**	**36**

Protein	**BSA**						**Lyz**					
Protein conc. (mM)	0.4	0.4	0.1	0.05	0.05	0.05	0.4	0.4	0.1	0.05	0.05	0.05
Polymer (eq)	10	5	1	1	5	10	10	5	1	1	5	10
UV time (min)	30	30	15	15	15	15	30	30	15	15	15	15
Conj. yield (%)	**37**	**38**	**16**	**13**	**28**	**24**	**24**	**12**	**4**	**0**	**8**	**12**

[a]The conjugation efficiency is presented as an average from two separate SDS-PAGE gels.

From the investigation of various end-functionalized PEGs to GST, we have determined that GSH (affinity) and BP (labeling) were both crucial to the irreversible conjugation of GSH-BP to GST. By the tuning the concentration, stoichiometry, and irradiation time, the conjugation yields of 5K GSBP-PEG to GST ranged from 20-74%. However, at higher concentrations, larger excess of polymer, and longer irradiation time, non-specific proton abstraction and radical recombination would be more prone to occur. Investigations of the interactions between GSH-BP and several other proteins, including BSA, Lyz, Ubq, and GST-Ubq, were also conducted. Under each condition, the conjugation yields of GST were clearly higher than Ubq and Lyz. As a result, the described conjugation method should be generally applicable to other GST-fusion proteins for applications such as therapeutic protein delivery or construction of macromolecule architectures, provided the protein does not have a binding site for BP (as demonstrated for BSA). PEGylation should exclusively occur at the binding site of GST, leaving the major protein unaffected when the photoconjugation condition is optimized. Other polymers, macromolecules, or small molecule probes that allow GSH-BP functionalization are also applicable for site-specific protein modifications. This would be convenient since many GST-tagged proteins are produced for purification purposes and then the GST group is removed post expression and purification prior to PEG conjugation. The approach reported herein would allow for the GST tag to remain and serve as the site for polymer conjugation, reducing steps and cost in the construction of the protein-polymer conjugates.

2.3 Conclusions

Herein, we reported the synthesis of a new GSH analogue containing a photo-reactive benzophenone and analyzed its use for photoinduced GST fusion protein-PEG conjugation. To test our hypothesis, different end-functionalized PEGs were synthesized as controls, including GS-PEG, BP-PEG, and GSDA-PEG. Without the addition of both GSH and benzophenone moieties, conjugation efficiency was significantly reduced. The conjugation yields of different proteins, including BSA, Lyz, Ubq, and GST-Ubq, were analyzed. GSBP-PEG nonspecifically conjugates to BSA through the hydrophobic binding effect with benzophenone, but has less than 10% conjugation efficiency to Lyz and Ubq under controlled conditions. In other cases, the GST moiety is crucial for the conjugation effect to occur. The conjugation efficiency of 5K GSBP-PEG ranges from 20-74% for GST. As a result, this system is a light-responsive and site-specific protein-polymer conjugation that occurs only after photoexcitation and majorly at the GST-tag. It is a versatile method, for the GSH analogue can be attached to any thiol-reactive polymers or substrates, and other GST-fusion proteins can serve as a conjugation target.

2.4 Experimental Section

Materials

All the reagents and solvents were purchased from Sigma-Aldrich and Fisher Scientific and used without purification unless noted otherwise. 4-Aminobenzophenone was recrystallized from DCM/MeOH=1/5. GST from equine liver was purchased from Sigma-Aldrich as a lyophilized powder containing salts, and the protein concentration was determined by its extinction coefficient (ε_{280}=47,000 $M^{-1}cm^{-1}$) at 280 nm. Polyacrylamide gels for electrophoresis were purchased from Invitrogen and Bio-Rad. L-Photo-leucine was purchased from Thermo Scientific. GSTrap 4B column was purchased from GE Healthcare Life Sciences. Ubiquitin (human, recombinant) GST-tag was purchased from Enzo Life Sciences.

Instrumentation

NMR spectra were obtained on Bruker AV 500 and DRX 500 MHz spectrometers. ^{1}H NMR spectra were acquired with a relaxation delay of 2 s for small molecules and 30 s for polymers. UV-Vis spectroscopy was performed using a Biomate 5 Thermo Spectronic spectrometer or Thermo Scientific NanoDrop 2000 (for small quantities). ESI-MS data were gathered on a Waters LCT premier with ACQUITY LC. Infrared absorption spectra were recorded using a PerkinElmer FT-IR equipped with an ATR accessory. Photoreactions were carried out in a photochemical safety cabinet equipped with a broadband, medium pressure Ace-Hanocia 7825-34 quartz mercury arc lamp and ACE Glass Inc. power supply. An Entela UVGL-254 Watt UV lamp was operated at 365 nm for hand-held lamp irradiation. Matrix-assisted laser desorption/ionization time-of-flight mass (MALDI-TOF-MS) spectrometry data was gathered using sinapic acid (SA) as a matrix on an Applied Biosystems Voyager-DE-STR spectrometer.

Fast protein liquid chromatography (FPLC) was performed on a Bio-Rad BioLogic DuoFlow™ Chromatography System.

Methods

Synthesis of 1. In a round bottom flask over ice, Fmoc-Cys(Trt)-OH (1.63 g, 2.79 mmol) was dissolved in anhydrous DCM (5 mL) and stirred to dissolve. 1-Ethyl-3-(3-dimethylaminopropyl)carbodiimide hydrochloride (EDC·HCl, 0.97 g, 5.07 mmol) was then added to the reaction mixture. In a separate flask, 4-aminobenzophenone (4-ABP, 0.51 g, 2.58 mmol) was dissolved in anhydrous DCM (5 mL). After keeping in an ice bath for 20 min, the 4-ABP solution was added dropwise to the reaction flask. 4-Dimethylaminopyridine (DMAP, 61.4 mg, 0.5 mmol) was then added, and the reaction was stirred from 0 °C to 23 °C for 12 h. The completion of the reaction was confirmed by thin layer chromatography (TLC, EtOAc:Hexanes=1:2, stained with ninhydrin). The crude mixture was washed with saturated $NaHCO_3$ three times. The organic layer was then dried over $MgSO_4$ and concentrated *in vacuo*. 20% piperidine in DMF (11 mL) was added to the crude solid, and allowed to stir at 23 °C for 1 h. The solvent was removed *in vacuo* at 40 °C. The crude product was purified via silica gel flash chromatography with EtOAc : Hexane = 1 : 2, then changed to DCM : MeOH = 95 : 5 to obtain **1** with 40% yield containing impurities, and was brought forward to the next step. ^{1}H NMR (500 MHz in MeOD) δ: 7.81-7.14 (m, 24H), 3.44-3.41 (t, *J*= 6.15 Hz, 1H), 2.67-2.46 (m, 2H). ^{13}C NMR (500 MHz in MeOD) δ: 196.25, 172.80, 144.60, 142.37, 137.77, 132.63, 132.17, 131.10, 129.48, 129.35, 128.09, 127.61, 126.52, 118.84, 118.15, 116.98 66.44, 54.71, 36.85. DART-MS (± 1.0) observed (predicted): H^+ 543.2064 (543.2062).

Synthesis of Protected GSH-BP 2. In a round bottom flask over ice, Boc-Glu-OtBu (93.9 mg, 0.31 mmol) was dissolved in anhydrous DCM (2 mL) and stirred to dissolve. EDC·HCl (98.9 mg, 0.52 mmol) was then added to the reaction mixture. In a separate flask, **1** (140 mg, 0.26 mmol) was dissolved in anhydrous DCM (2 mL). After keeping over ice for 20 min, the solution of **1** was added dropwise to the reaction flask. DMAP (5.8 mg, 0.05 mmol) was then added, and the reaction was stirred from 0 °C to 23 °C for 24 h. The crude mixture was washed with saturated $NaHCO_3$ three times. The organic layer was then dried over $MgSO_4$ and concentrated *in vacuo*. The crude product was purified using silica gel flash chromatography with EtOAc : Hexane = 1 : 2 to obtain 140 mg white solid with 65% yield containing slight amount of impurities. ^{1}H NMR (500 MHz in MeOD) δ: 7.81-7.16 (m, 24H), 4.49-4.46 (m, 1H), 4.03-3.84 (m, 1H), 2.71-2.49 (m, 2H), 2.41-2.26 (m, 2H), 2.16-1.77 (m, 2H), 1.52-1.36 (m, 18H). ^{13}C NMR (500 MHz in MeOD) δ: 197.51, 174.77, 173.14, 170.96, 158.09, 145.82, 143.80, 139.90, 134.29, 134.05, 133.53, 132.50, 132.39, 130.82, 130.68, 130.31, 129.47, 129.22, 129.03, 127.94, 120.47, 120.38, 114.07, 82.75, 80.54, 68.00, 55.34, 55.25, 54.64, 54.52, 34.89, 32.86, 28.73, 28.58, 28.24. IR: ν = 3292, 2972, 1703, 1652, 1595, 1522, 1445, 1366, 1310, 1278, 1251, 1149, 1047, 923, 845, 741. ESI-MS (± 1.0) observed (predicted): H^+ 828.3785 (828.3638).

Synthesis of GSH-BP. Protected GSH-BP **2** (41.5 mg, 0.05 mmol) was weighed in a glass vial. Under argon, trifluoroacetic acid (TFA, 1.33 mL), triisopropylsilane (TIPS, 35 μL, 0.17 mmol), and H_2O (35 μL) were added to the reaction with a final ratio of TFA/TIPS/H_2O = 95/2.5/2.5. Upon the addition of TFA, the solution immediately turned bright yellow. After the addition of TIPS, the color quickly turned pale yellow with the formation of a white precipitate. The reaction was allowed to stir for 1 h at 23 °C and then dried *in vacuo* to remove TFA. The solid was dissolved in 30% acetonitrile (ACN) and filtered for HPLC purification. HPLC chromatography

was carried out with a gradient elution from 30% to 70% ACN in 30 min with a flow rate of 10 mL/min. The collected fractions were lyophilized to obtain 6.1 mg white solid with 28% yield. ^{1}H NMR (500 MHz in MeOD) δ: 7.79-7.51 (m, 9H), 4.67-4.58 (m, 1H), 3.70-3.58 (m, 1H), 3.04-2.83 (m, 2H), 2.56-2.53 (t, *J*= 7.13 Hz, 2H), 2.22-2.07 (m, 2H). ^{13}C NMR (500 MHz in MeOD) δ: 196.16, 173.88, 172.48, 169.69, 142.55, 137.73, 132.71, 132.17, 130.99, 129.41, 128.10, 119.06, 56.77, 54.20, 31.31, 26.36, 25.33. IR: ν = 3293, 2977, 1645, 1595, 1517, 1446, 1407, 1365, 1311, 1279, 1252, 1174, 1149, 1047, 938, 924, 851, 793, 741. ESI-MS (± 1.0) observed (predicted): H^+ 430.1450 (430.1392). UV-Vis (MeOH) λ_{max}= 295 nm.

Reaction of GSH-BP with GST. GST (0.94 μL, 100 mg/mL in MilliQ H_2O) and GSH-BP (1 μL, 86 mg/mL in MeOH) were added to MilliQ H_2O (8.06 μL) to prepare a mixture with final concentration of 0.4 mM GST and 20 mM GSH-BP, containing 10% MeOH. Upon addition of the GSH-BP solution to water, a precipitate was observed. The sample was kept in the dark and incubated on ice for 2 h and then irradiated in an ice bath for 30 min in the photochemical safety cabinet with a mercury arc lamp (or with a hand-held lamp at long wavelength 365 nm). The crude mixture was purified by centrifugal filtration (0.5 mL, MWCO 3,000) and three washes of H_2O. The solution was then collected and analyzed by MALDI-TOF MS using sinapic acid as the matrix. Controls were prepared following the same procedure, but without adding GSH-BP, or without UV irradiation.

Synthesis of Fmoc-PhotoLeu. Fmoc-PhotoLeu was synthesized using a previously reported procedure.[43] Fmoc-OSu (118 mg, 0.35 mmol) was dissolved in 1,4-dioxane (2 mL). L-Photo-Leucine (50 mg, 0.35 mmol) and $NaHCO_3$ (47 mg, 0.56 mmol) were dissolved in H_2O (1.5 mL). 1,4-dioxane (2.5 mL) was added to this solution before adding Fmoc-OSu solution over 15 minutes. The reaction was then stirred for 26 hours at 23°C. HCl was added to the solution to

acidify to pH 3 before extracting 3 times into EtOAc. Organic layers were combined and dried over $MgSO_4$ and concentrated *in vacuo*. Silica gel chromatography (5% MeOH in CH_2Cl_2 + 0.1% AcOH) yielded 107 mg (85%) as a beige solid. All steps were carried out in the dark. ^{1}H NMR (500 MHz in MeOD) δ: 7.81-7.63 (d, *J*= 7.5 Hz, 2H), 7.74-7.68 (dd, *J*= 4.6, 7.0 Hz, 2H), 7.41-7.34 (t, *J*= 7.5 Hz, 2H), 7.33-7.27 (dt, *J*= 1.05, 7.5 Hz, 2H), 4.42-4.30 (m, 2H), 4.28-4.22 (t, *J*= 7.15 Hz, 1H), 4.15-4.07 (dd, *J*= 4.3, 10.5 Hz, 1H), 2.03-1.95 (dd, *J*= 4.4, 14.95 Hz, 1H), 1.67-1.59 (dd, *J*= 10.6, 14.95 Hz, 1H), 1.06-1.00 and 0.93-0.89 (s, rotamer, 3H). ^{13}C NMR (500 MHz in MeOD) δ: 173.39, 157.04, 143.81, 141.18, 127.38, 126.76, 124.94, 119.50, 66.70, 50.10, 36.19, 23.60, 18.48.

Synthesis of GSH-DA:

Resin Loading.[44] Fmoc-PhotoLeu (106 mg, 0.29 mmol) and DIEA (202 μL, 1.2 mmol) were dissolved in anhydrous DCM (2 mL). A small amount of DMF (200 μL) was added to dissolve the acid. The solution was added to the 2-chlorotrityl chloride resin (219 mg, .29 mmol) and mixed for 45 minutes in a peptide synthesis flask. The solution was drained and resin was rinsed with DCM/MeOH/DIEA, DCM, DMF, DCM, MeOH, DCM, DMF. The loaded resin was stored under argon until further use.

Amino Acid Coupling. 20% 4-methyl piperidine in DMF (10 mL) was added to resin in synthesis flask for 20 minutes to remove the fmoc group. Solution was drained and resin was washed with DMF/DCM/MeOH/DCM/DMF. Fmoc-Cys(Trt)-OH (250 mg, 0.38 mmol) and HBTU (161 mg, 0.42 mmol) were dissolved in DMF (10 mL) and DIEA (148 μL, 1.5 mmol) was added before adding solution to resin and mixing for 3 hours at 23°C. Solution was drained and resin was washed again. The Fmoc was removed in a similar manner. Boc-Glu-OtBu (129

mg, 0.41 mmol) and HBTU (161 mg, 0.42mmol) was dissolved in DMF (10 mL) before adding DIEA (148 μL, 1.5 mmol). This solution was added to resin and mixed at 23°C for 2 hours before draining solution and washing the resin.

Peptide Cleavage. The peptide was cleaved from the chlorotrityl resin using 95% TFA, 2.5% TIPS and 2.5% H_2O. The resin was mixed in cleavage cocktail for 45 minutes before draining the solution and rinsing the resin with DCM twice. The filtrate was concentrated *in vacuo* before precipitating in cold diethyl ether. The crude peptide was purified using HPLC with a C18 column with a gradient elution from 5% to 95% ACN in 30 min with a flow rate of 10 mL/min. The trityl group was subsequently deprotected using a solution of 95% TFA, 2.5% TIPS and 2.5% H_2O to yield 16.7 mg of pure GSH-DA as a white solid after precipitation in cold diethyl ether. ESI-MS (± 1.0) observed (predicted): H^+ 376.1289 (376.1291).

Synthesis of VS-PEG. Here, we describe the synthesis of 2K VS-PEG. 5K and 20K VS-PEG were prepared according to this same method modified from a previous report.[36] To poly(ethylene glycol) methyl ether of average M_n ~2,000 (1.32 g, 0.66 mmol), THF (35 mL) was added and warmed to 30 °C. After the polymer had dissolved, the solution was cooled down to room temperature. Divinyl sulfone (0.2 mL, 1.98 mmol) was added, followed by addition of 0.1 N aqueous NaOH solution (2.4 mL). The reaction mixture was stirred at 23 °C for 5 h, then neutralized with 0.1 N HCl solution (2.4 mL) and filtered. The filtrate was concentrated *in vacuo* to remove most of the THF. The residual solution was diluted in approximately 10 mL of H_2O, washed with diethyl ether (x3 times), and extracted with chloroform (x3 times). The organic layer was then washed with H_2O, dried over $MgSO_4$, and concentrated *in vacuo*. The white solid was then dissolved in minimum amount of DCM, and precipitated into cold ether (50 mL x3). The precipitant was dried *in vacuo* to obtain 1.1 g of white powder with 79% yield. ^1H NMR of

2K VS-PEG (500 MHz in $CDCl_3$) (conversion: 89%) δ: 6.86-6.79 (dd, *J*= 9.95, 16.60 Hz, 1H), 6.42-6.36 (d, *J*= 16.65 Hz, 1H), 6.11-6.06 (d, *J*= 9.90 Hz, 1H), 4.00-3.22 (m, 200H), 3.40-3.37 (s, 3H). ^{1}H NMR of 5K VS-PEG (500 MHz in $CDCl_3$) (conversion: 85%) δ: 6.84-6.76 (dd, *J*= 9.90, 16.65 Hz, 1H), 6.40-6.34 (d, *J*= 16.65 Hz, 1H), 6.09-6.04 (d, *J*= 9.90 Hz, 1H), 3.96-3.20 (m, 500H), 3.37-3.34 (s, 3H). ^{1}H NMR of 20K VS-PEG (500 MHz in $CDCl_3$) (conversion: 90%) δ: 6.83-6.75 (dd, *J*= 10.00, 16.65 Hz, 1H), 6.38-6.32 (d, *J*= 16.75 Hz, 1H), 6.07-6.03 (d, *J*= 10.00 Hz, 1H), 3.95-3.19 (m, 2000H), 3.36-3.33 (s, 3H).

Synthesis of GSBP-PEG. Here, we describe the synthesis of 2K GSBP-PEG. 5K and 20K GSBP-PEG were prepared according to the same method. Compound **3** (5.6 mg, 0.013 mmol) was dissolved in MeOH (0.2 mL). In a separate vial, VS-PEG (2K, 8.7 mg, 4.35×10^{-3} mmol) was dissolved in pH 8.0 phosphate buffer saline (0.2 mL). The two solutions were combined, and stirred under argon at 23 °C for 48 h. A small aliquot was taken for crude ^{1}H NMR in D_2O to confirm the disappearance of the vinyl peaks. The crude mixture was purified by HPLC with elution gradient of 60%-90% MeOH over 30 min. Alternatively, the crude mixture was purified by dialysis (MWCO 1,000) against H_2O for two days, followed by filtration to remove insoluble solids. The purified solution was then lyophilized to obtain 5.6 mg of white powder with 64% yield. ^{1}H NMR of 2K GSBP-PEG (500 MHz in D_2O) (conversion: 94%) δ: 7.88-7.49 (m, 9H), 4.76-4.69 (dd, *J*= 6.20, 8.00 Hz, 1H), 3.96-3.37 (m, 200H), 3.36-3.34 (s, 3H), 3.20-3.15 (dd, *J*= 6.20, 13.75 Hz, 1H), 3.05-2.98 (m, 2H), 2.96-2.90 (dd, *J*= 8.20, 13.75 Hz, 1H), 2.58-2.52 (m, 2H), 2.18-2.10 (m, 2H). ^{1}H NMR of 5K GSBP-PEG (500 MHz in D_2O) (conversion: 100%) δ: 7.86-7.48 (m, 9H), 4.75-4.69 (dd, *J*= 6.20, 8.05 Hz, 1H), 3.96-3.40 (m, 500H), 3.36-3.34 (s, 3H), 3.21-3.14 (dd, *J*= 6.10, 13.70 Hz, 1H), 3.05-2.98 (m, 2H), 2.96-2.90 (dd, *J*= 8.20, 13.75 Hz, 1H), 2.58-2.52 (m, 2H), 2.17-2.09 (m, 2H). ^{1}H NMR of 20K GSBP-PEG (500 MHz in D_2O)

(conversion: 95%) δ: 7.80-7.37 (m, 9H), 4.60-4.56 (m, 1H), 3.98-3.29 (m, 2000H), 3.27-3.25 (s, 3H), 3.08-2.86 (m, 4H), 2.48-2.33 (m, 2H), 2.08-2.96 (m, 2H).

Synthesis of GSDA-PEG. GSH-DA (16.6 mg, 4.4×10^{-2} mmol) was dissolved in pH 8.0 phosphate buffer (1 mL). The solution was then added to VS-PEG (5K, 20.4 mg, 4.1×10^{-3} mmol), and the reaction mixture was stirred under Argon at 23 °C for 14 h. A small aliquot for crude ^{1}H NMR was taken in D_2O to confirm the disappearance of the vinyl peaks. The crude solution was concentrated via centrifugal filtration (0.5 mL, MWCO 3,000) and washed with H_2O for 5 times. The solution was then collected and lyophilized. ^{1}H NMR (500 MHz in D_2O) (conversion: 75%) δ: 4.55-4.50 (dd, *J*= 5.05, 9.20 Hz, 1H), 4.08-4.02 (dd, *J*= 4.20, 9.50 Hz, 1H), 3.96-3.36 (m, 500H), 3.28-3.25 (s, 3H), 3.09-3.02 (dd, *J*= 5.00, 14.05 Hz, 1H), 2.97-2.89 (m, 2H), 2.88-2.81 (dd, *J*= 9.25, 14.05 Hz, 1H), 2.47-2.41 (m, 2H), 2.09-2.01 (m, 2H), 1.98-1.91 (dd, *J*= 4.20, 15.15 Hz, 1H), 1.54-1.46 (dd, *J*= 9.55, 15.15 Hz, 1H), 0.95-0.90 (s, 3H).

Synthesis of GS-PEG. Here, we describe the synthesis of 2K GS-PEG. 5K GS-PEG was prepared according to the same method. Glutathione (307.3 mg, 1.0 mmol) was dissolved in pH 8.0, 20 mM phosphate buffer (1 mL). The pH, which was around 3.0, was adjusted to 8.0 with 1 N NaOH and the total volume was diluted to 2 mL with additional phosphate buffer. The glutathione solution was added to VS-PEG (2K, 100 mg, 0.05 mmol), and the reaction mixture was stirred under Argon at 23 °C for 15 h. A small aliquot for crude ^{1}H NMR was taken in D_2O to confirm the disappearance of the vinyl peaks. The crude was then extracted with chloroform three times, dried over $MgSO_4$, and dried *in vacuo*. ^{1}H NMR of 2K GS-PEG (500 MHz in D_2O) (conversion: 83%) δ: 4.53-4.47 (dd, *J*= 4.95, 8.75 Hz, 1H), 3.90-3.40 (m, 200H), 3.27-3.23 (s, 3H), 3.05-2.98 (dd, *J*= 4.95, 14.10 Hz, 1H), 2.92-2.86 (m, 2H), 2.85-2.78 (dd, *J*= 8.75, 14.10 Hz, 1H), 2.47-2.35 (m, 2H), 2.06-1.99 (m, 2H). ^{1}H NMR of 5K GS-PEG (500 MHz in D_2O)

(conversion: 86%) δ: 4.52-4.47 (dd, *J*= 5.10, 8.50 Hz, 1H), 3.90-3.39 (m, 500H), 3.27-3.23 (s, 3H), 3.05-2.97 (dd, *J*= 4.95, 14.10 Hz, 1H), 2.93-2.86 (m, 2H), 2.86-2.78 (dd, *J*= 8.65, 14.10 Hz, 1H), 2.47-2.35 (m, 2H), 2.08-1.99 (m, 2H).

Synthesis of BP-PEG. In a round bottom flask over ice, 4-benzoylbenzoic acid (181 mg, 0.8 mmol) was dissolved in DCM (4 mL). EDC·HCl (230.1 mg, 1.2 mmol), poly(ethylene glycol) methyl ether of average M_n ~5,000 (200 mg, 0.04 mmol), and DMAP (24.4 mg, 0.2 mmol) were then added to the reaction mixture. The reaction mixture was allowed to stir from 0 °C to 23 °C for 23 h. The crude mixture was washed once with H_2O, twice with saturated $NaHCO_3$, and twice with brine. The organic layer was then dried over $MgSO_4$ and concentrated *in vacuo*. The solid was purified by dialysis (MWCO 1,000) against H_2O for two days, followed by 0.22 μm PTFE syringe filtration to remove insoluble solids. The purified solution was then lyophilized. ^{1}H NMR (500 MHz in D_2O) (conversion: 100%) δ: 8.12-7.46 (m, 9H), 4.47-4.42 (m, 2H), 3.85-3.40 (m, 500H), 3.29-3.24 (s, 3H).

General procedure of irradiation experiments of PEG. With GSBP-PEG as example, GST (10 μL, 0.8 mM, 18.64 mg/mL in pH 7.4 D-PBS) and GSBP-PEG (10 μL, 8 mM, 40 mg/mL in MilliQ H_2O) were combined to prepare a 20 μL mixture with final concentration of 0.4 mM GST and 4 mM GSBP-PEG. The concentration of GST was ascertained by UV-Vis measurement of A280 using ε=47,000 $M^{-1}cm^{-1}$. The mixture was kept in the dark and incubated on ice for 2 h to allow polymer association. An aliquot (10 μL) was transfered into a disposable UV cuvette and irradiated on ice bath for 15 min in the photochemical safety cabinet, while the other 10 μL was kept in the dark on ice as a control without UV irradiation. The samples were then directly analyzed by SDS-PAGE (200V, 35 min) and/or native PAGE (100V, 3.5 h) with Bio-Rad Any kD™ precast polyacrylamide gels (or Invitrogen 4-12% precast polyacrylamide gels).

Coomassie was used to stain the protein, and iodine was used to stain PEG.[45] All control experiments with other proteins (BSA and Lyz) and different PEGs (GS-PEG, GSDA-PEG, and BP-PEG) were conducted following the same procedure.

Analysis of conjugation yield. The SDS-PAGE gels were scanned with an Epson Perfection 2480 scanner as tiff images, and analyzed with the ImageJ software. Each lane was selected by the rectangular selection tool, and plotted with the gel analysis function. The percentage peak area of the conjugate divided by the sum of the conjugate and unmodified protein is the conjugation efficiency (conjugation yield).

GSTrap elution experiment. The GSTrap 4B column was run on a Bio-Rad BioLogic DuoFlow™ Chromatography System at 4 °C. Approximately 0.5 mg/mL of GST was loaded onto the column at a flow rate of 0.2 ml/min, and was washed with 10 column volumes (10 mL) of pH 7.4 PBS at a flow rate of 1 ml/min. The buffer was then switched to an elution buffer of pH 8.0 TBS containing 0.1 mM GSH, 5K mPEG, 5K GS-PEG, or 5K GSBP-PEG. After each run, pH 8.0 TBS containing 20 mM GSH was used to wash the column and elute any remaining GST. The column was then equilibrated with pH 7.4 PBS before the next use. For each run, fractions from 14-17 min were collected, concentrated and desalted by centrifugal filtration (MWCO 3000). The samples were then analyzed by SDS-PAGE.

2.5 Appendix to Chapter 2: Supplementary Figures

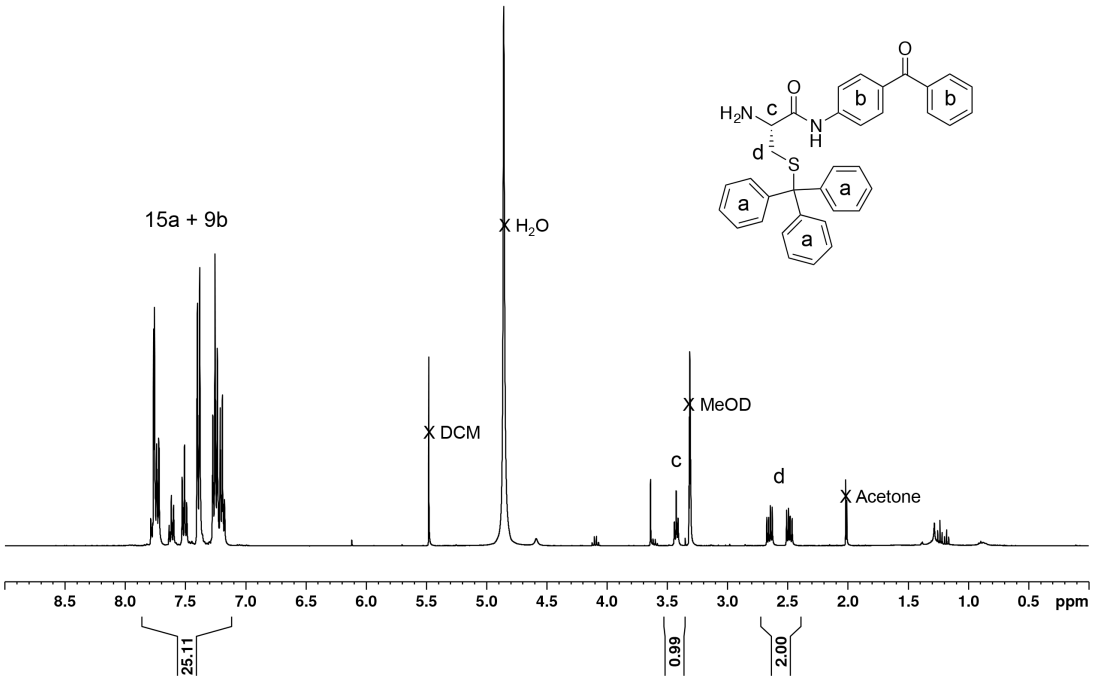

Figure 2-7. ^{1}H NMR spectrum of **1** (in MeOD).

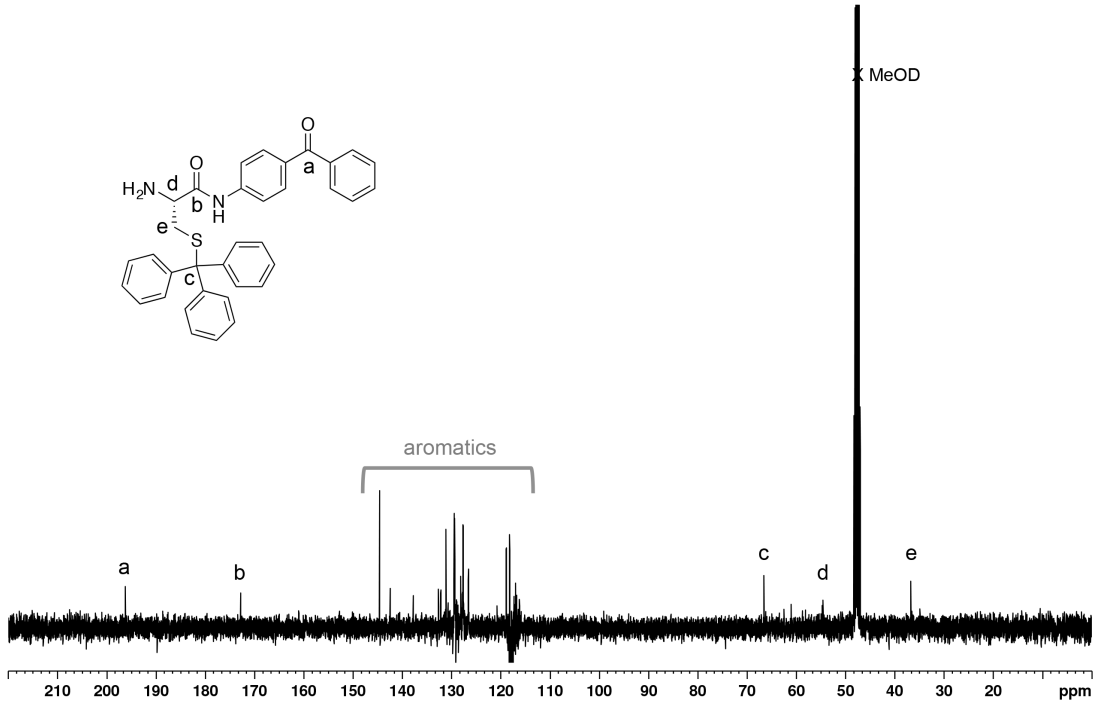

Figure 2-8. ^{13}C NMR spectrum of **1** (in MeOD).

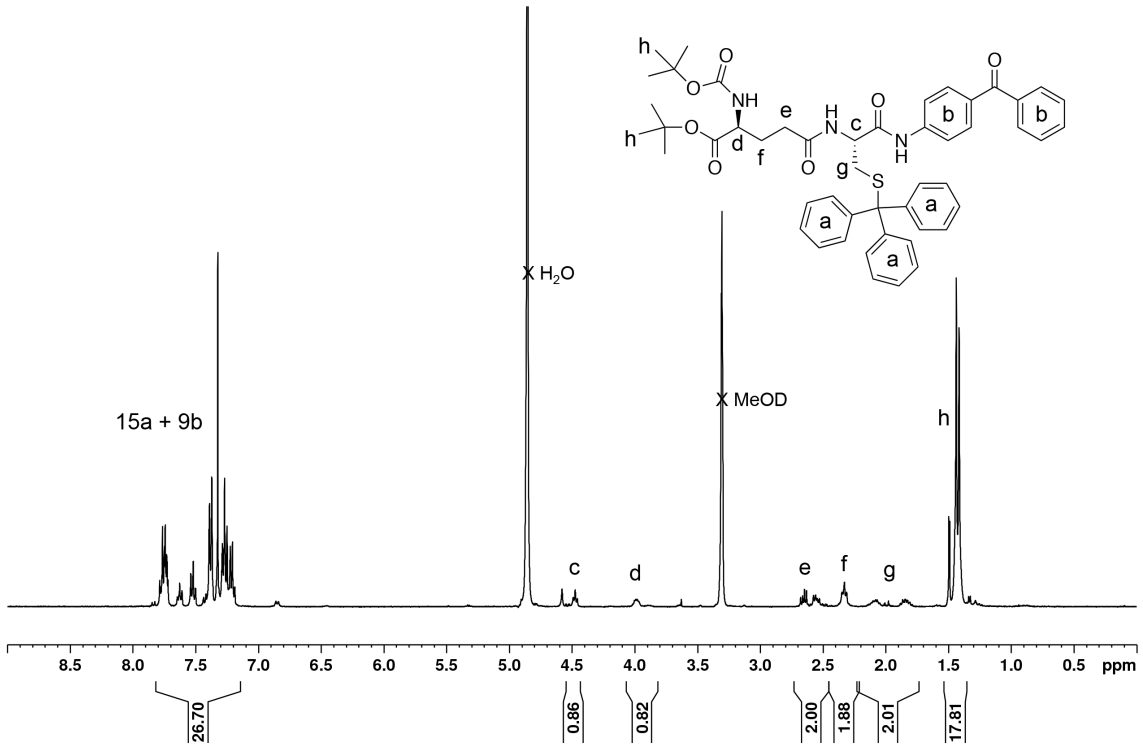

Figure 2-9. ^{1}H NMR spectrum of **2** (in MeOD).

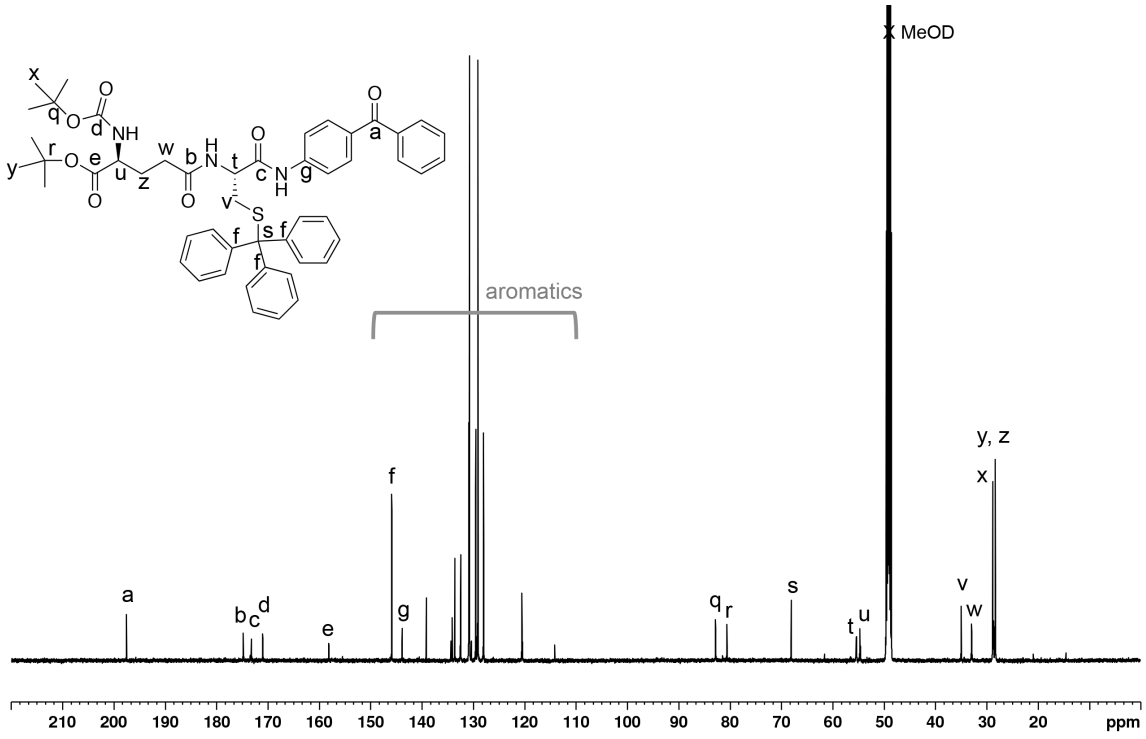

Figure 2-10. ^{13}C NMR spectrum of **2** (in MeOD).

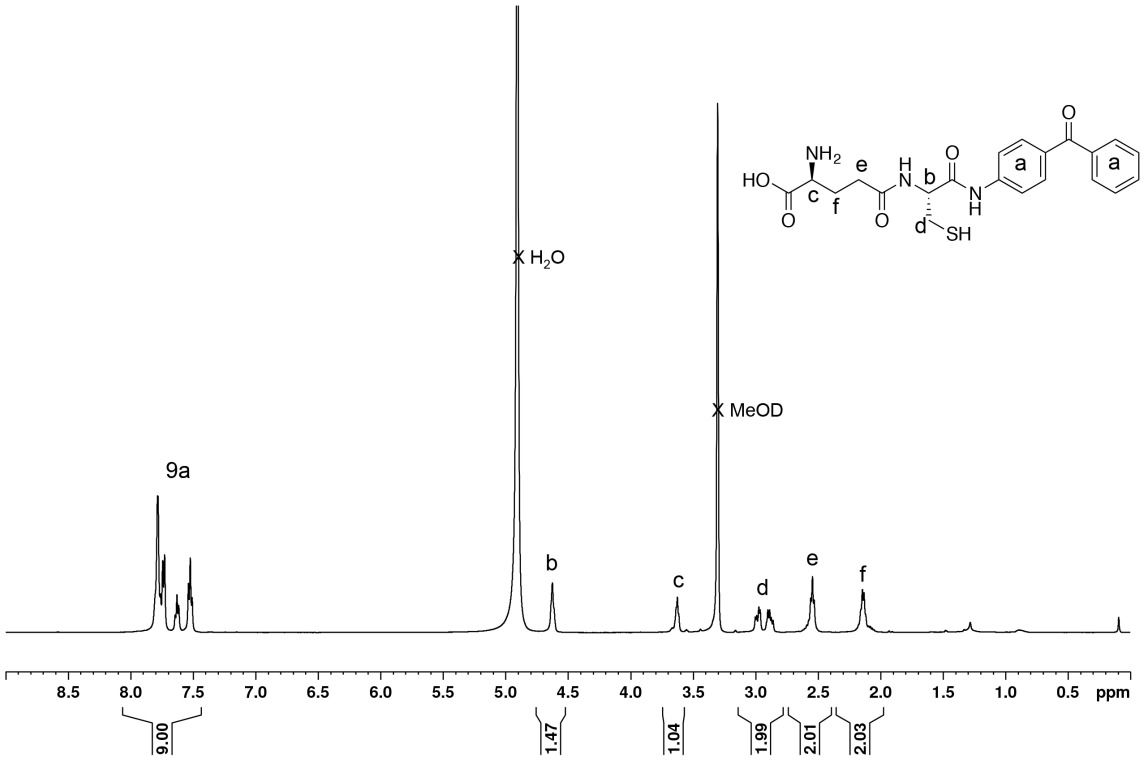

Figure 2-11. ^{1}H NMR spectrum of **3** (in MeOD).

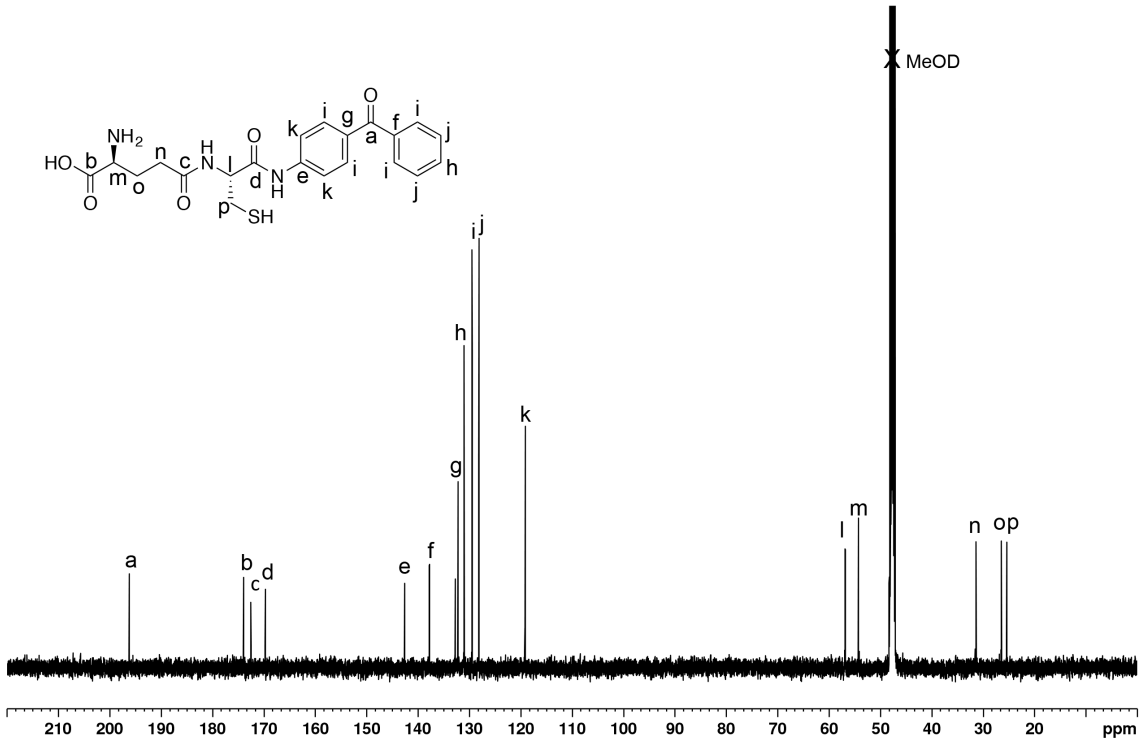

Figure 2-12. ^{13}C NMR spectrum of **3** (in MeOD).

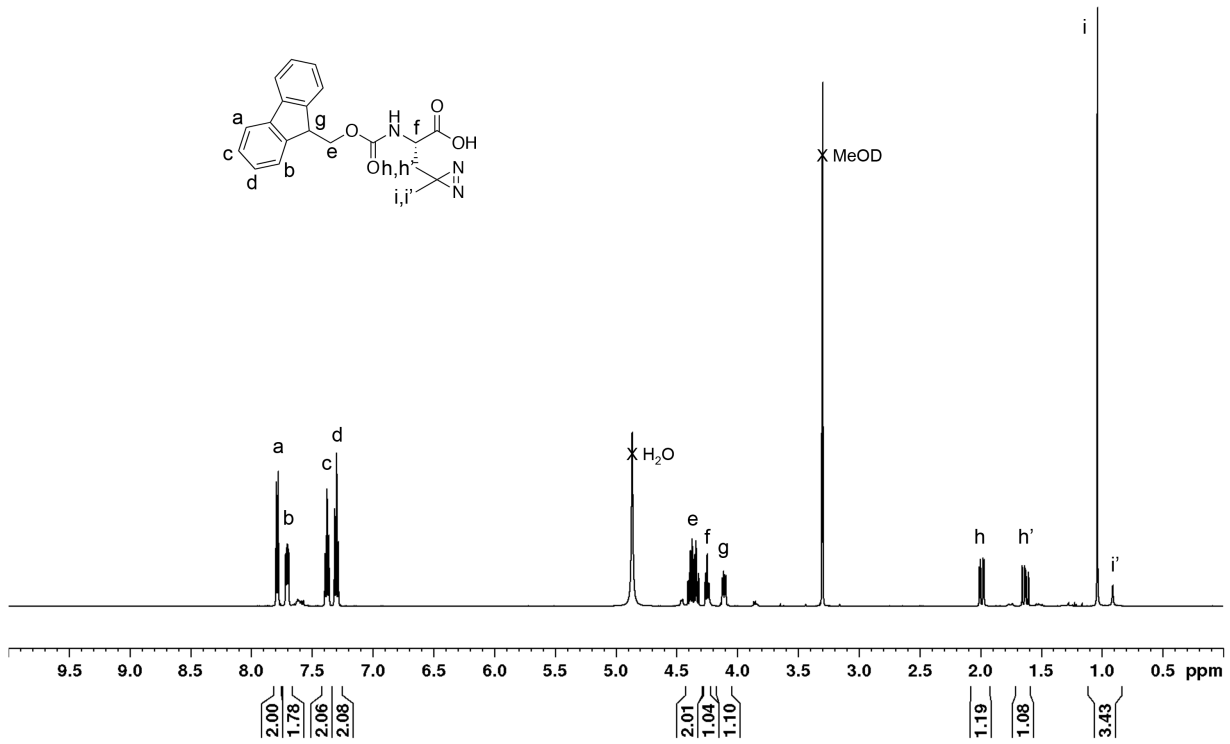

Figure 2-13. ^{1}H NMR spectrum of Fmoc-photo-Leucine (in MeOD).

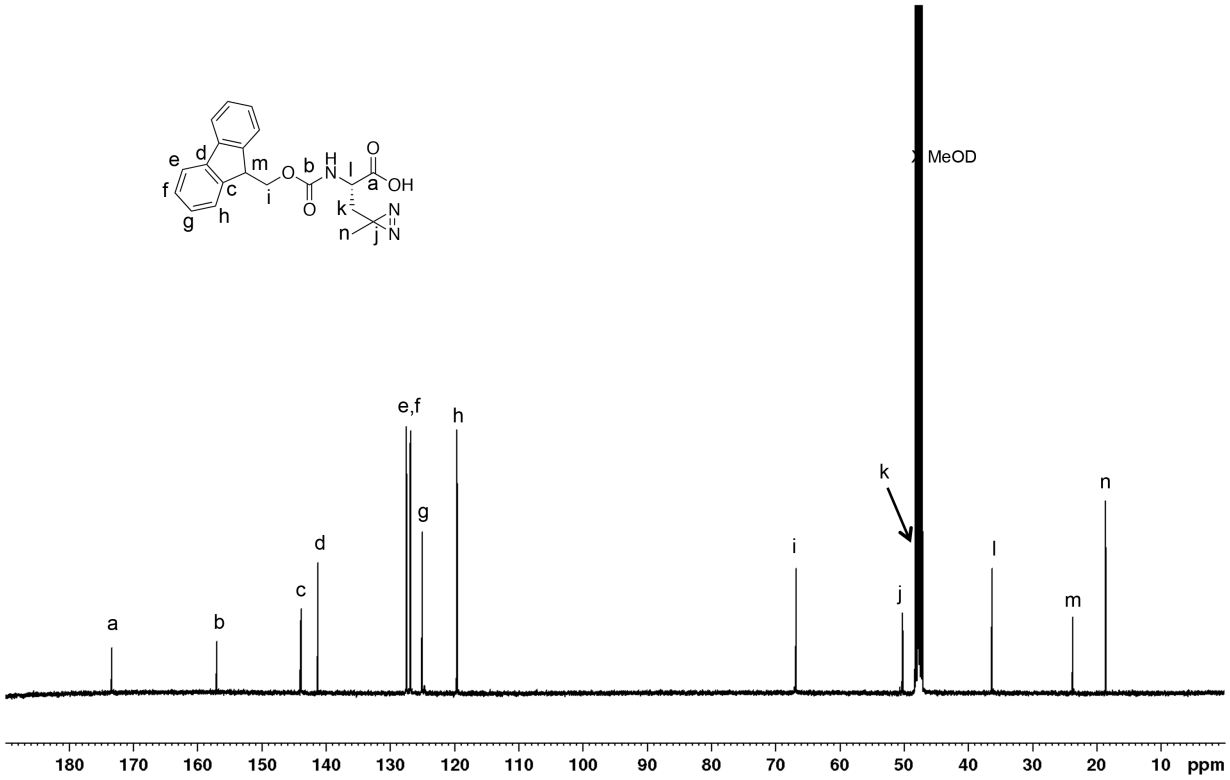

Figure 2-14. ^{13}C NMR spectrum of Fmoc-photo-Leucine (in MeOD).

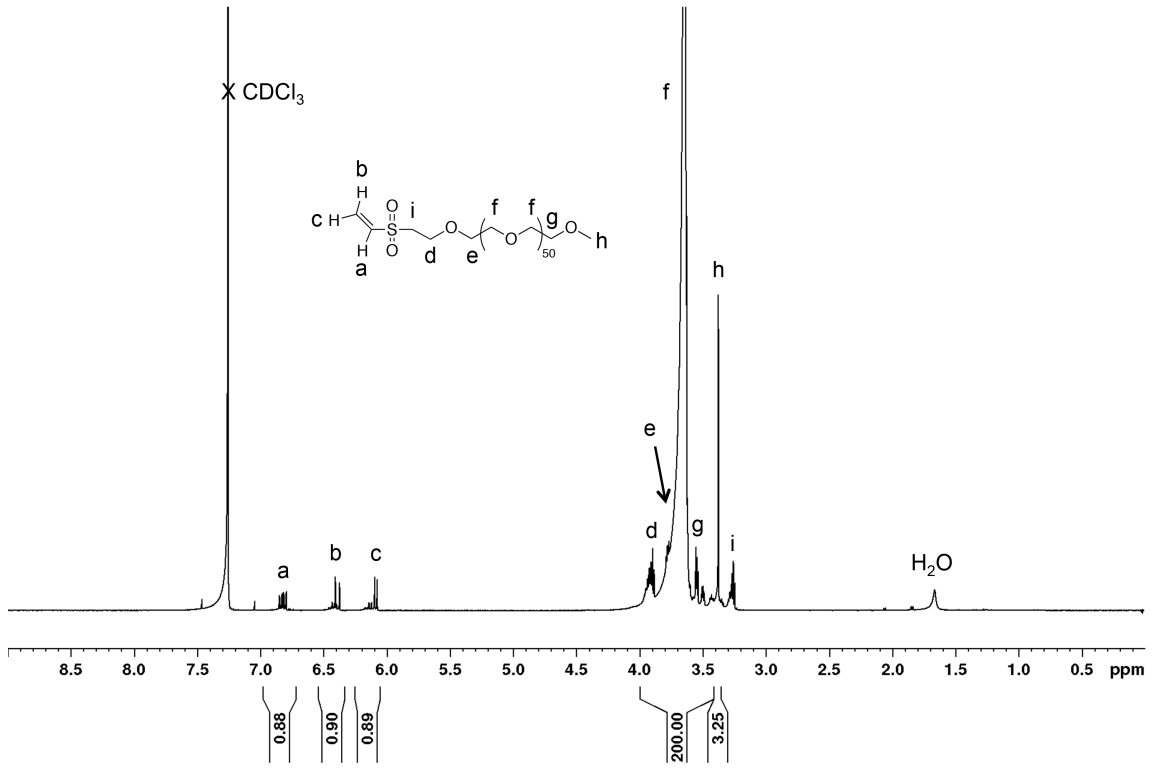

Figure 2-15. ^{1}H NMR spectrum of 2K VS-PEG (in $CDCl_3$).

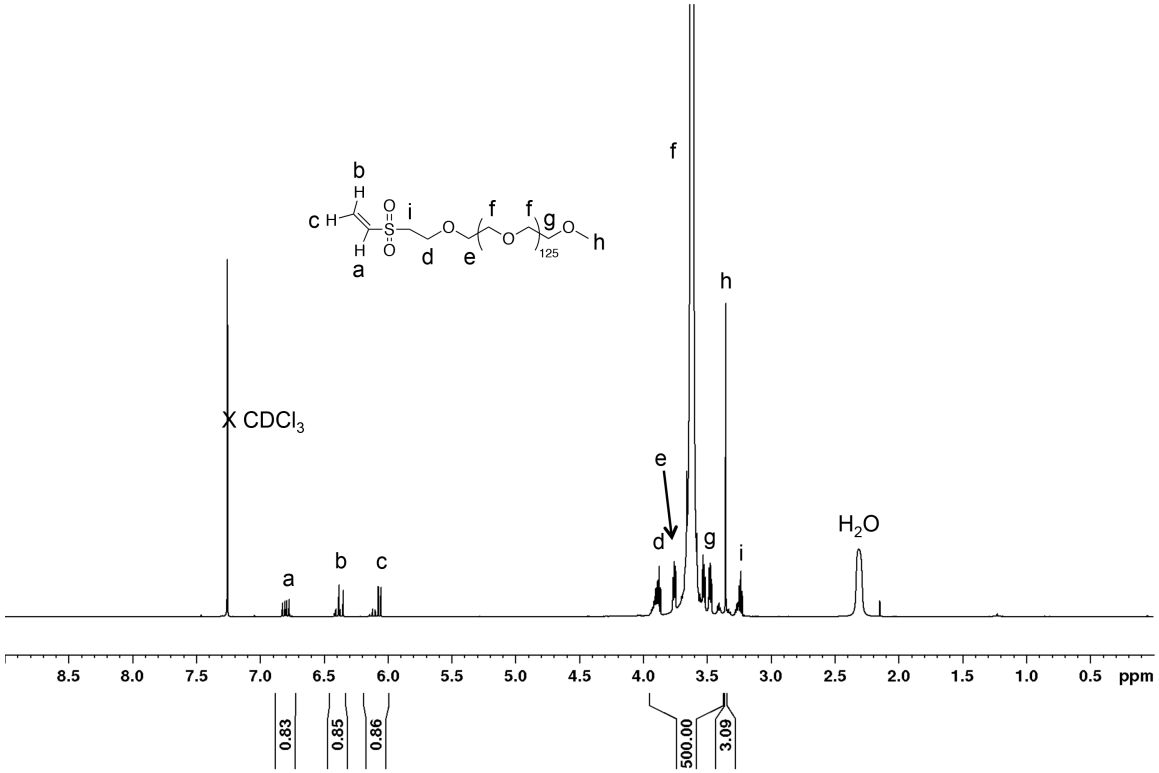

Figure 2-16. ^{1}H NMR spectrum of 5K VS-PEG (in $CDCl_3$).

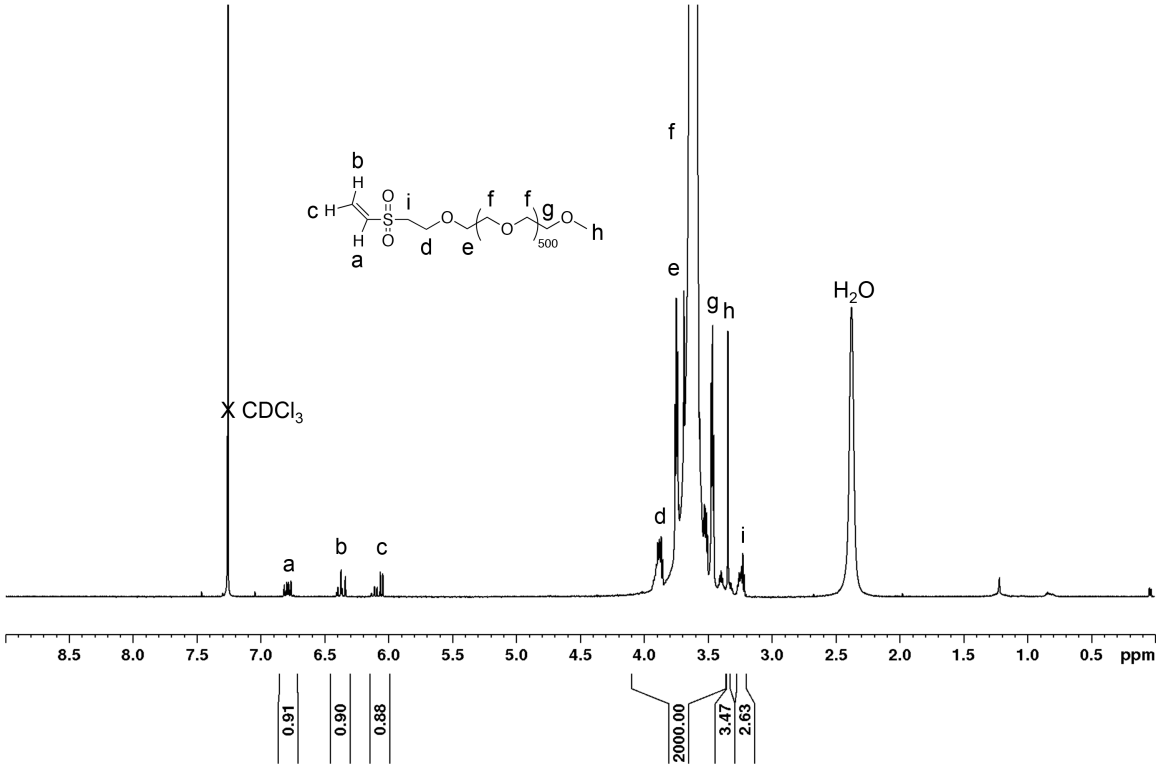

Figure 2-17. ^{1}H NMR spectrum of 20K VS-PEG (in $CDCl_3$).

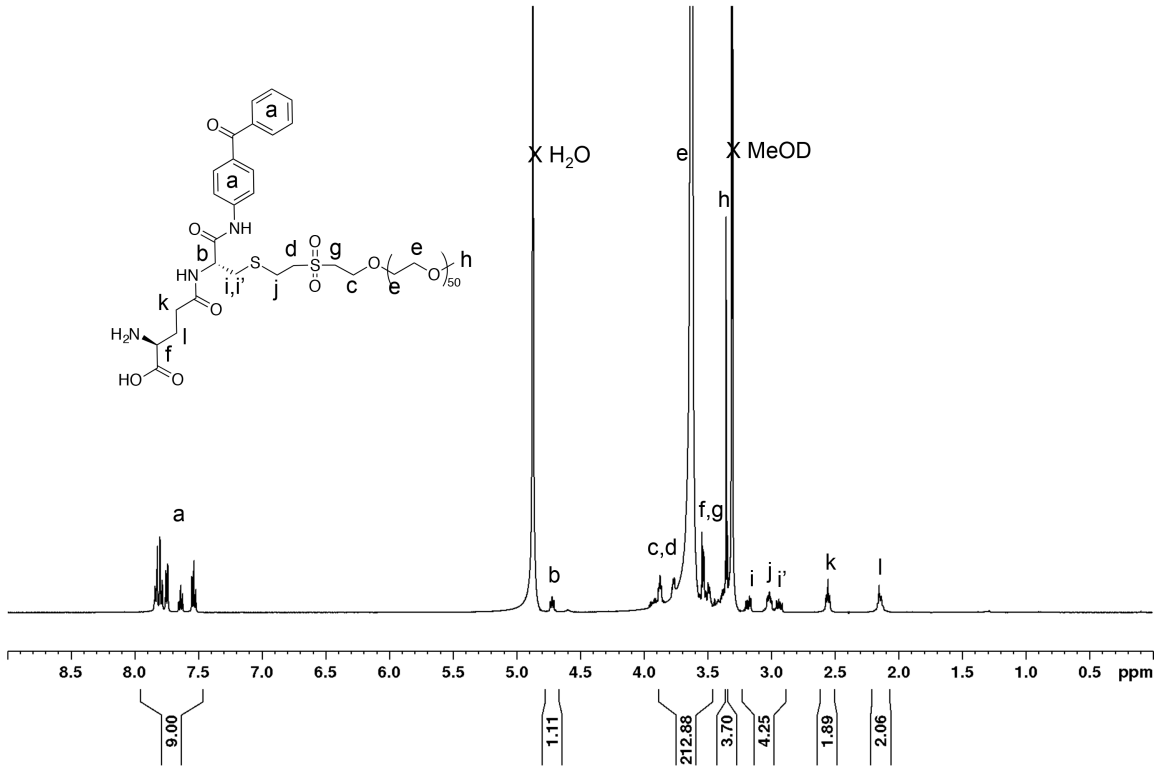

Figure 2-18. ^{1}H NMR spectrum of 2K GSBP-PEG (in MeOD).

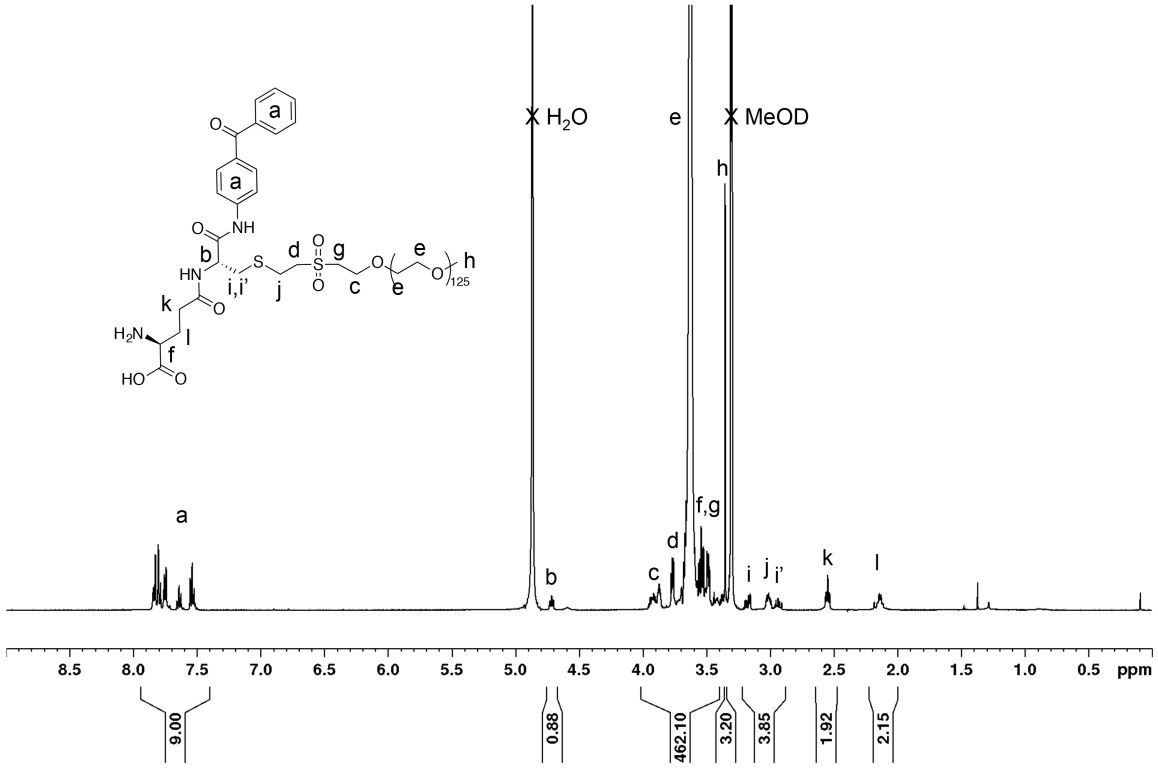

Figure 2-19. ^{1}H NMR spectrum of 5K GSBP-PEG (in $CDCl_3$).

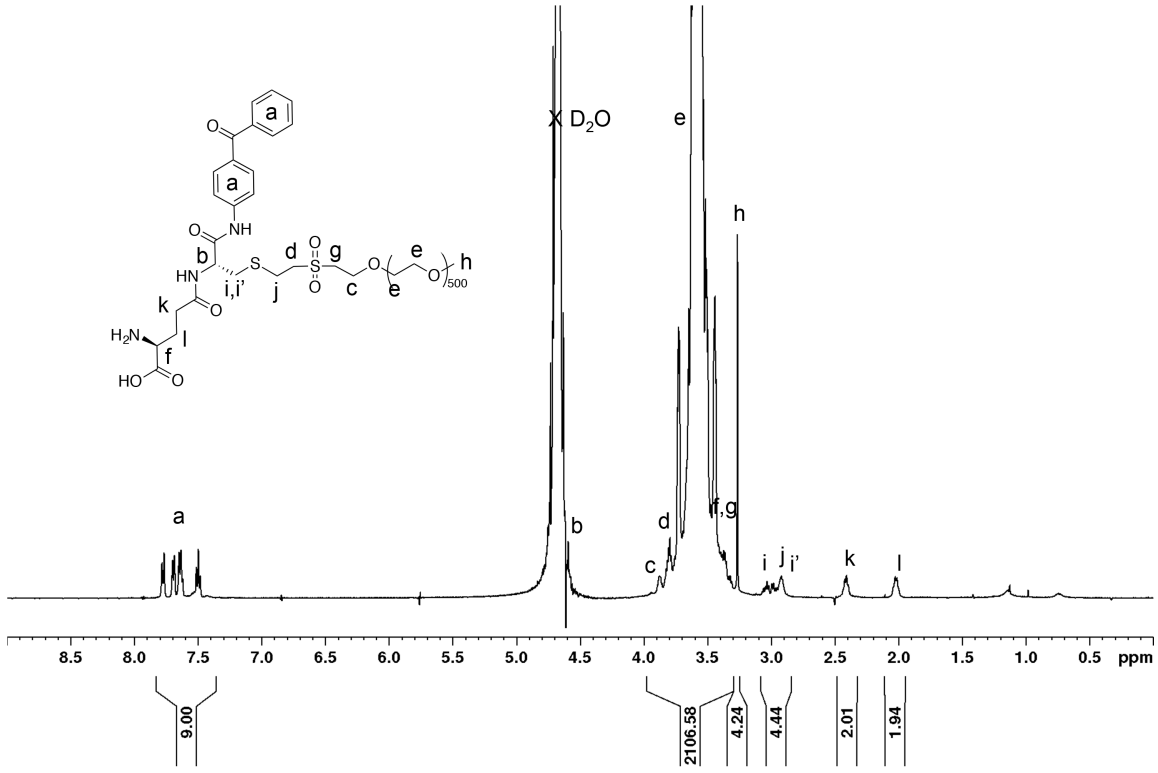

Figure 2-20. ^{1}H NMR spectrum of 20K GSBP-PEG (in MeOD).

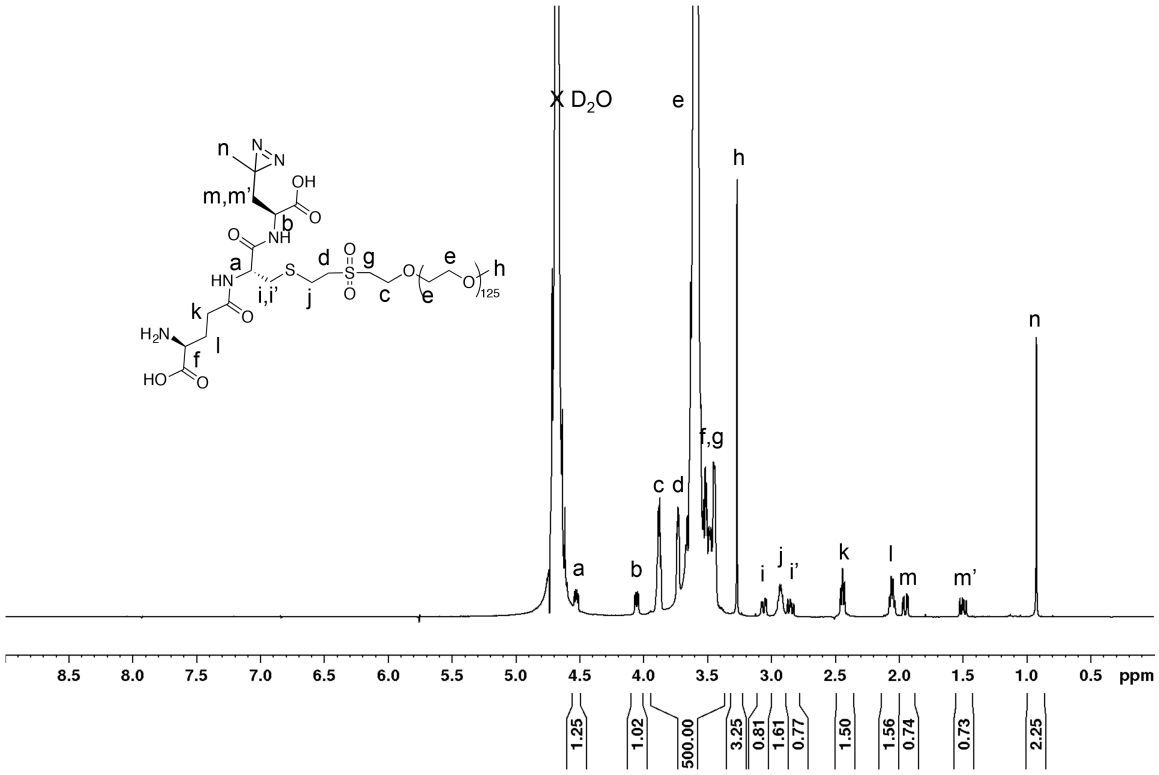

Figure 2-21. ^{1}H NMR spectrum of 5K GSDA-PEG (in D_2O).

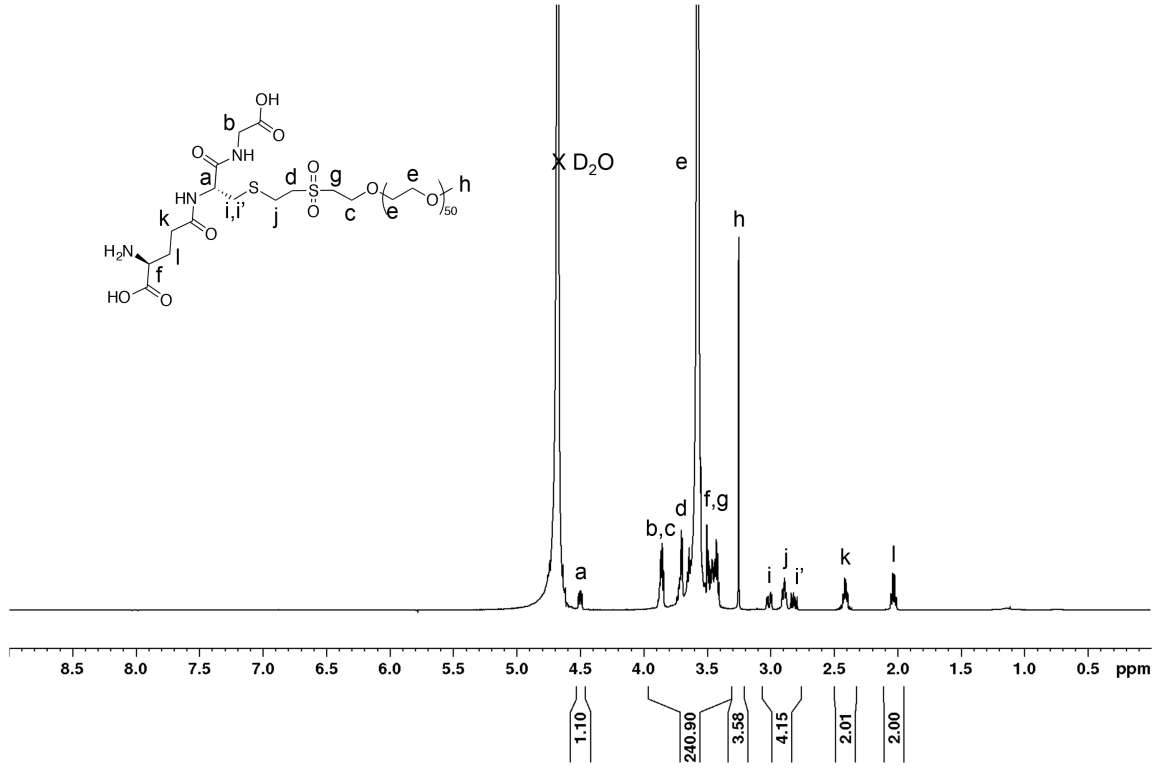

Figure 2-22. ^{1}H NMR spectrum of 2K GS-PEG (in D_2O).

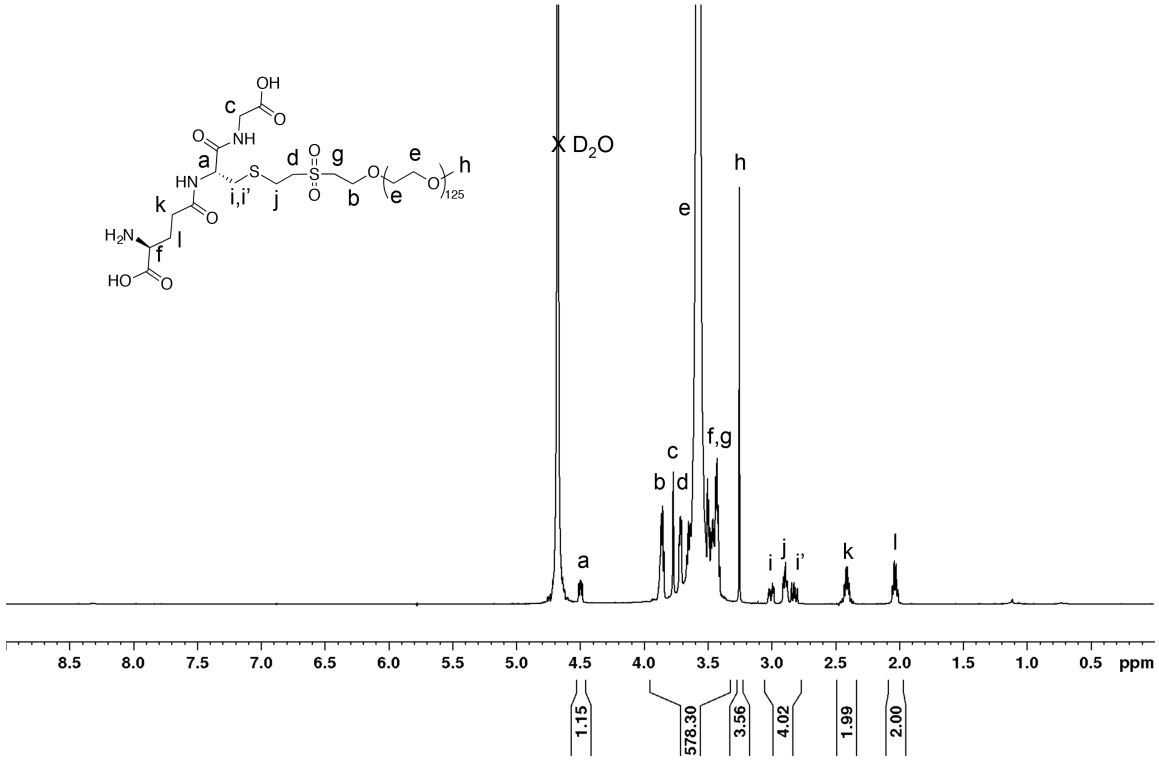

Figure 2-23. ^{1}H NMR spectrum of 5K GS-PEG (in D_2O).

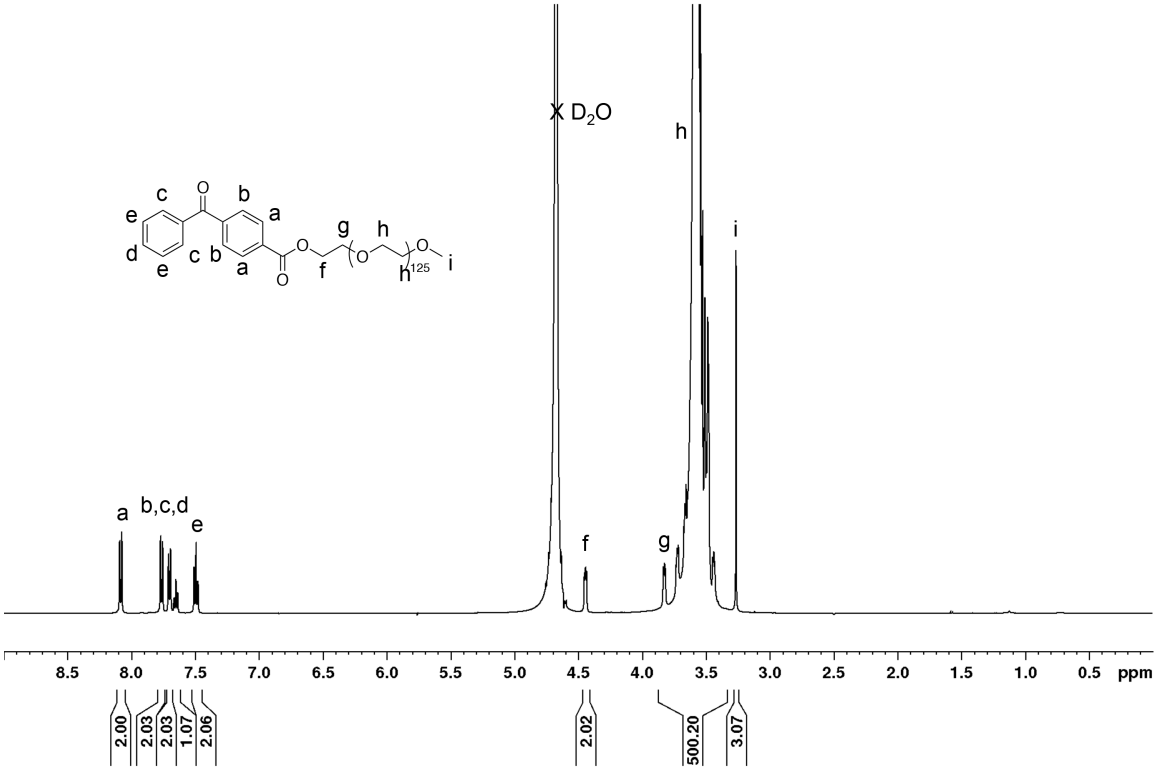

Figure 2-24. ^{1}H NMR spectrum of 5K BP-PEG (in D_2O).

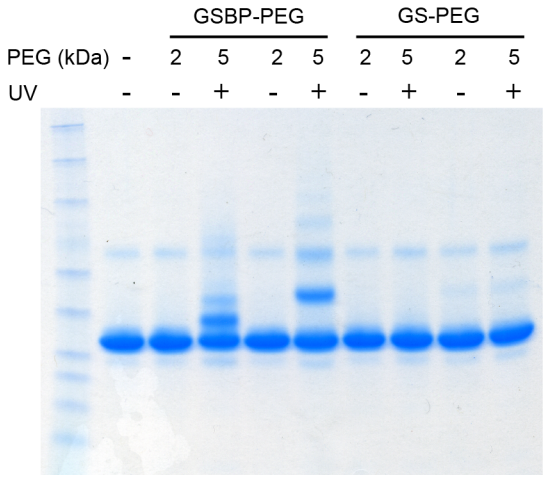

Figure 2-25. SDS-PAGE of the conjugation of different sizes of GSBP-PEG and GS-PEG to GST.

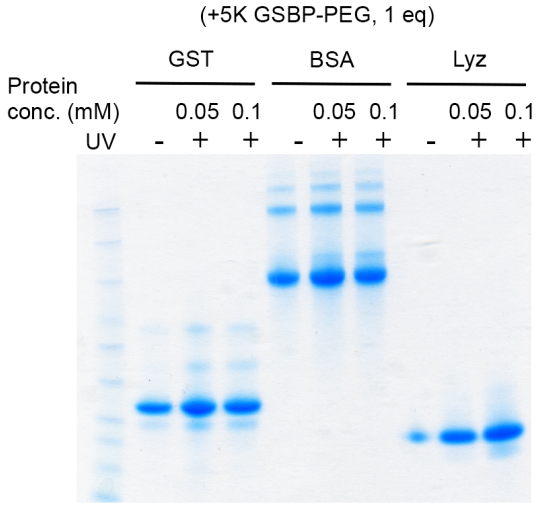

Figure 2-26. SDS-PAGE of the conjugation of 5K GSBP-PEG to GST, BSA, and Lyz at low concentrations. No conjugation is observed for Lyz.

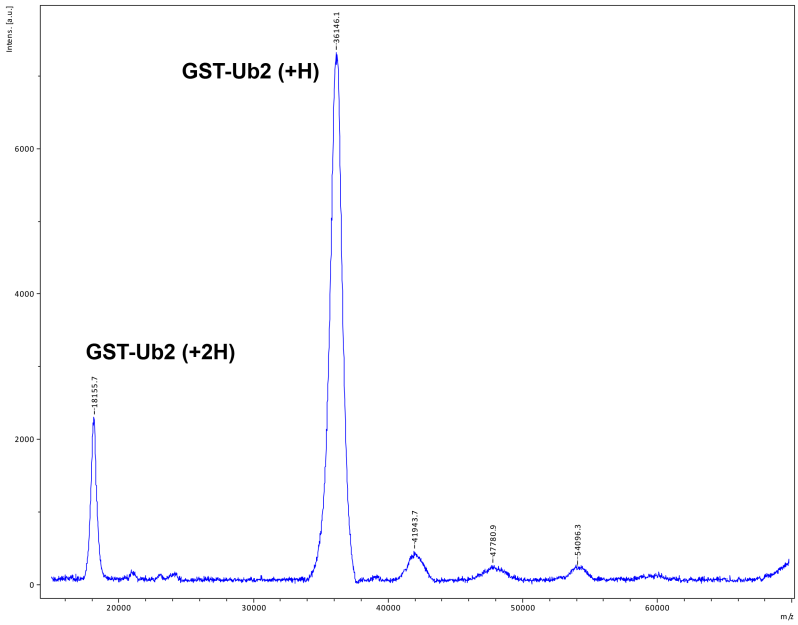

Figure 2-27. MALDI-TOF MS of the unpurified GST-Ubq conjugate.

2.6 References

‡ Portions of this chapter have been accepted for publication as: Lin, E.-W.; Boehnke, N.; Maynard, H. D., "Protein-Polymer Conjugation *via* Ligand Affinity and Photoactivation of Glutathione *S*-Transferase," *Bioconjugate Chem., accepted*.

(1) Duncan, R. "The Dawning Era of Polymer Therapeutics" *Nat. Rev. Drug Discovery* **2003**, *2*, 347-360.

(2) Heredia, K. L.; Maynard, H. D. "Synthesis of Protein-Polymer Conjugates" *Org. Biomol. Chem.* **2007**, *5*, 45-53.

(3) Gauthier, M. A.; Klok, H. A. "Peptide/Protein-Polymer Conjugates: Synthetic Strategies and Design Concepts" *Chem. Commun.* **2008**, 2591-2611.

(4) Canalle, L. A.; Lowik, D.; van Hest, J. C. M. "Polypeptide-Polymer Bioconjugates" *Chem. Soc. Rev.* **2010**, *39*, 329-353.

(5) Shu, J. Y.; Panganiban, B.; Xu, T. In *Annual Review of Physical Chemistry, Vol 64*; Johnson, M. A., Martinez, T. J., Eds.; Annual Reviews: Palo Alto, 2013; Vol. 64, p 631-657.

(6) Alconcel, S. N. S.; Baas, A. S.; Maynard, H. D. "FDA-Approved Poly(Ethylene Glycol)-Protein Conjugate Drugs" *Polym. Chem.* **2011**, *2*, 1442-1448.

(7) Kochendoerfer, G. G. "Site-Specific Polymer Modification of Therapeutic Proteins" *Curr. Opin. Chem. Biol.* **2005**, *9*, 555-560.

(8) Li, N.; Lim, R. K. V.; Edwardraja, S.; Lin, Q. "Copper-Free Sonogashira Cross-Coupling for Functionalization of Alkyne-Encoded Proteins in Aqueous Medium and in Bacterial Cells" *J. Am. Chem. Soc.* **2011**, *133*, 15316-15319.

(9) Dumas, A.; Spicer, C. D.; Gao, Z.; Takehana, T.; Lin, Y. A.; Yasukohchi, T.; Davis, B. G. "Self-Liganded Suzuki-Miyaura Coupling for Site-Selective Protein PEGylation" *Angew. Chem., Int. Ed.* **2013**, *52*, 3916-3921.

(10) Toda, N.; Asano, S.; Barbas, C. F. "Rapid, Stable, Chemoselective Labeling of Thiols with Julia-Kocienski-Like Reagents: A Serum-Stable Alternative to Maleimide-Based Protein Conjugation" *Angew. Chem., Int. Ed.* **2013**, *52*, 12592-12596.

(11) Wendeler, M.; Grinberg, L.; Wang, X. Y.; Dawson, P. E.; Baca, M. "Enhanced Catalysis of Oxime-Based Bioconjugations by Substituted Anilines" *Bioconjugate Chem.* **2014**, *25*, 93-101.

(12) Zhou, Z.; Zhang, J.; Sun, L. J.; Ma, G. H.; Su, Z. G. "Comparison of Site-Specific PEGylations of the N-Terminus of Interferon Beta-1b: Selectivity, Efficiency, and In Vivo/Vitro Activity" *Bioconjugate Chem.* **2014**, *25*, 138-146.

(13) Li, Y. M.; Li, Y. T.; Pan, M.; Kong, X. Q.; Huang, Y. C.; Hong, Z. Y.; Liu, L. "Irreversible Site-Specific Hydrazinolysis of Proteins by Use of Sortase" *Angew. Chem., Int. Ed.* **2014**, *53*, 2198-2202.

(14) Levine, P. M.; Craven, T. W.; Bonneau, R.; Kirshenbaum, K. "Intrinsic Bioconjugation for Site-Specific Protein Pegylation at N-Terminal Serine" *Chem. Commun.* **2014**, *50*, 6909-6912.

(15) Hannink, J. M.; Cornelissen, J.; Farrera, J. A.; Foubert, P.; De Schryver, F. C.; Sommerdijk, N.; Nolte, R. J. M. "Protein-Polymer Hybrid Amphiphiles" *Angew. Chem., Int. Ed.* **2001**, *40*, 4732-4734.

(16) Hou, S. J.; Sun, X. L.; Dong, C. M.; Chaikof, E. L. "Facile Synthesis of Chain-End Functionalized Glycopolymers for Site-Specific Bioconjugation" *Bioconjugate Chem.* **2004**, *15*, 954-959.

(17) Bontempo, D.; Li, R. C.; Ly, T.; Brubaker, C. E.; Maynard, H. D. "One-Step Synthesis of Low Polydispersity, Biotinylated Poly(*N*-Isopropylacrylamide) by ATRP" *Chem. Commun.* **2005**, 4702-4704.

(18) Huang, X.; Boyer, C.; Davis, T. P.; Bulmus, V. "Synthesis of Heterotelechelic Polymers with Affinity to Glutathione-*S*-Transferase and Biotin-Tagged Proteins by RAFT Polymerization and Thiol-Ene Reactions" *Polym. Chem.* **2011**, *2*, 1505-1512.

(19) Boerakker, M. J.; Hannink, J. M.; Bomans, P. H. H.; Frederik, P. M.; Nolte, R. J. M.; Meijer, E. M.; Sommerdijk, N. "Giant Amphiphiles by Cofactor Reconstitution" *Angew. Chem., Int. Ed.* **2002**, *41*, 4239-4241.

(20) Boerakker, M. J.; Botterhuis, N. E.; Bomans, P. H. H.; Frederik, P. M.; Meijer, E. M.; Nolte, R. J. M.; Sommerdijk, N. "Aggregation Behavior of Giant Amphiphiles Prepared by Cofactor Reconstitution" *Chem. - Eur. J.* **2006**, *12*, 6071-6080.

(21) Chang, C. W.; Nguyen, T. H.; Maynard, H. D. "Thermoprecipitation of Glutathione *S*-Transferase by Glutathione-Poly(*N*-Isopropylacrylamide) Prepared by RAFT Polymerization" *Macromol. Rapid Commun.* **2010**, *31*, 1691-1695.

(22) Wilce, M. C. J.; Parker, M. W. "Structure and Function of Glutathione *S*-Transferases" *Biochim. Biophys. Acta, Protein Struct. Mol. Enzymol.* **1994**, *1205*, 1-18.

(23) Dirr, H.; Reinemer, P.; Huber, R. "X-Ray Crystal-Structures of Cytosolic Glutathione *S*-Transferases - Implications for Protein Architecture, Substrate Recognition and Catalytic Function" *Eur. J. Biochem.* **1994**, *220*, 645-661.

(24) Yan, F.; Yang, W. K.; Li, X. Y.; Lin, T. T.; Lun, Y. N.; Lin, F.; Lv, S. W.; Yan, G. L.; Liu, J. Q.; Shen, J. C.; Mu, Y.; Luo, G. M. "A Trifunctional Enzyme with Glutathione *S*-Transferase, Glutathione Peroxidase and Superoxide Dismutase Activity" *Biochim. Biophys. Acta, Gen. Subj.* **2008**, *1780*, 869-872.

(25) Simons, P. C.; Vanderjagt, D. L. "Purification of Glutathione *S*-Transferases from Human Liver by Glutathione-Affinity Chromatography" *Anal. Biochem.* **1977**, *82*, 334-341.

(26) Smith, D. B.; Johnson, K. S. "Single-Step Purification of Polypeptides Expressed in Escherichia-Coli as Fusions with Glutathione *S*-Transferase" *Gene* **1988**, *67*, 31-40.

(27) Bayley, H.; Knowles, J. R. "Photoaffinity Labeling" *Methods Enzymol.* **1977**, *46*, 69-114.

(28) Kotzybahibert, F.; Kapfer, I.; Goeldner, M. "Recent Trends in Photoaffinity-Labeling" *Angew. Chem., Int. Ed. Engl.* **1995**, *34*, 1296-1312.

(29) Dorman, G.; Prestwich, G. D. "Benzophenone Photophores in Biochemistry" *Biochemistry* **1994**, *33*, 5661-5673.

(30) Uchida, N.; Okuro, K.; Niitani, Y.; Ling, X.; Ariga, T.; Tomishige, M.; Aida, T. "Photoclickable Dendritic Molecular Glue: Noncovalent-to-Covalent Photochemical Transformation of Protein Hybrids" *J. Am. Chem. Soc.* **2013**, *135*, 4684-4687.

(31) Das, J. "Aliphatic Diazirines as Photoaffinity Probes for Proteins: Recent Developments" *Chem. Rev.* **2011**, *111*, 4405-4417.

(32) Dubinsky, L.; Krom, B. P.; Meijler, M. M. "Diazirine Based Photoaffinity Labeling" *Bioorg. Med. Chem.* **2012**, *20*, 554-570.

(33) Pedone, E.; Brocchini, S. "Synthesis of Two Photolabile Poly(Ethylene Glycol) Derivatives for Protein Conjugation" *React. Funct. Polym.* **2006**, *66*, 167-176.

(34) Adang, A. E. P.; Brussee, J.; Vandergen, A.; Mulder, G. J. "The Glutathione-Binding Site in Glutathione *S*-Transferases - Investigation of the Cysteinyl, Glycyl and Gamma-Glutamyl Domains" *Biochem. J.* **1990**, *269*, 47-54.

(35) Wang, J. B.; Bauman, S.; Colman, R. F. "Photoaffinity Labeling of Rat Liver Glutathione *S*-Transferase, 4-4, by Glutathionyl *S*-4-(Succinimidyl)-Benzophenone" *Biochemistry* **1998**, *37*, 15671-15679.

(36) Ladd, D. L.; Snow, R. A.; Sterling Winthrop Inc. "Vinyl Sulfone Coupling of Polyoxylalkylenes to Proteins" **1995**, US5414135-A.

(37) Morpurgo, M.; Veronese, F. M.; Kachensky, D.; Harris, J. M. "Preparation and Characterization of Poly(Ethylene Glycol) Vinyl Sulfone" *Bioconjugate Chem.* **1996**, *7*, 363-368.

(38) Guo, L. W.; Hajipour, A. R.; Gavala, M. L.; Arbabian, M.; Martemyanov, K. A.; Arshavsky, V. Y.; Ruoho, A. E. "Sulfhydryl-Reactive, Cleavable, and Radioiodinatable Benzophenone Photoprobes for Study of Protein-Protein Interaction" *Bioconjugate Chem.* **2005**, *16*, 685-693.

(39) Galardy, R. E.; Craig, L. C.; Jamieson, J. D.; Printz, M. P. "Photoaffinity Labeling of Peptide Hormone Binding-Sites" *J. Biol. Chem.* **1974**, *249*, 3510-3518.

(40) Perols, A.; Karlstrom, A. E. "Site-Specific Photoconjugation of Antibodies Using Chemically Synthesized Igg-Binding Domains" *Bioconjugate Chem.* **2014**, *25*, 481-488.

(41) Yu, F. F.; Jarver, P.; Nygren, P. A. "Tailor-Making a Protein A-Derived Domain for Efficient Site-Specific Photocoupling to Fc of Mouse IGg_1" *Plos One* **2013**, *8*, e56597.

(42) Zhang, Y. Z.; Zhang, J.; Li, F. F.; Xiang, X.; Ren, A. Q.; Liu, Y. "Studies on the Interaction between Benzophenone and Bovine Serum Albumin by Spectroscopic Methods" *Mol. Biol. Rep.* **2011**, *38*, 2445-2453.

(43) Vila-Perello, M.; Pratt, M. R.; Tulin, F.; Muir, T. W. "Covalent Capture of Phospho-Dependent Protein Oligomerization by Site-Specific Incorporation of a Diazirine Photo-Cross-Linker" *J. Am. Chem. Soc.* **2007**, *129*, 8068-8069.

(44) Barlos, K.; Gatos, D.; Kallitsis, J.; Papaphotiu, G.; Sotiriu, P.; Wenqing, Y.; Schäfer, W. "Darstellung Geschützter Peptid-Fragmente Unter Einsatz Substituierter Triphenylmethyl-Harze" *Tetrahedron Lett.* **1989**, *30*, 3943-3946.

(45) Childs, C. E. "Determination of Polyethylene-Glycol in Gamma-Globulin Solutions" *Microchem. J.* **1975**, *20*, 190-192.

Chapter 3

Trehalose Glycopolymers as Excipients for Protein Stabilization[‡]

3.1 Introduction

Proteins are macromolecules with highly complex and sophisticated structures. Due to their ability to bind to specific targets, modulate cell signaling, and catalyze chemical reactions, proteins have been utilized in a wide range of industrial and pharmaceutical applications.[1] The physicochemical stability of the protein structure is crucial to maintain protein function. However, proteins are vulnerable to environmental stressors (e.g. heat, freezing, agitation, pH changes, or surface adsorption) during purification, processing, packaging, shipping, and storage.[2-4] Excipients such as salts[5], sugars,[6-9] polyols,[10,11] osmolytes,[12-14] polymers,[15-21] amino acids,[22,23] and surfactants[24] are commonly added to stabilize proteins and prevent unfolding and aggregation. Here, we focus on the development of a novel glycopolymer as a potential formulation excipient for proteins in both solution and in the dried state.

Trehalose is a natural non-reducing disaccharide with an α,α-1,1-linkage of two glucose units. It is generally regarded as safe (GRAS) by the U.S. Food and Drug Administration,[25] and widely used in food, cosmetic, and pharmaceutical industries.[26] It is naturally found in many organisms except mammals, in which its function mostly involves protection of cell membranes and proteins to desiccation or low temperature. Therefore, much laboratory research has been focused on using trehalose for mammalian cell preservation and protein protection.[27]

Until recently, there have been only a few examples of trehalose-based polymers, mainly polymer networks[28] or linear polymers.[29-35] Trehalose does not have anomeric hydroxyl groups, which makes selective chemical modification challenging due to similar reactivity of the remaining hydroxyl groups. It has two primary hydroxyl groups, which have been utilized as the reactive handle. However, all of the methods required protection and deprotection of the

secondary hydroxyl groups.[29,31] Another route is to form acetals with aromatic aldehydes targeting the primary hydroxyls.[30,32-35] Strategies to prepare main chain trehalose polymers include polyaddition of diamino-trehalose and diisocyanate,[29] ring opening of a diepoxide derivative of trehalose with aliphatic diamines,[30] Huisgen [3+2] cycloaddition of diazido-trehalose with dialkyne-oligoamine compounds,[31] hydrosilylation of 4-allyloxybenzldehyde-modified trehalose with dimethylsiloxane oligomers,[33] polycondensation of trehalose and dialdehydes to form polyacetals,[34] and Diels-Alder reaction between difurfurylidene trehalose and bismaleimide[32] or maleimide-terminated dimethylsiloxane oligomers[35]. Apart from these main chain polymers, there is interest in side chain polymers. Recently, our group has synthesized the monomer 4,6-*O*-(4-vinylbenzylidene)-*α*,*α*-trehalose, which was polymerized through reversible addition-fragmentation chain transfer (RAFT) polymerization.[36] When the resultant polymer was conjugated to lysozyme, the protein maintained over 80% activity after 30 minutes of heating at 90 °C and retained 100% activity after up to ten lyophilization cycles. We noted that adding excess of the free polymer not conjugated to the protein also stabilized the protein, which implied that the strategy might be applicable to using the trehalose polymer as an excipient. Based on this finding, we began to further develop the polymer and investigated various trehalose based vinyl monomers. We recently reported the synthesis of an additional styrenyl monomer and two methacrylate trehalose monomers and their respective polymers (**P1**-**P4**, **Figure 3-1** and **Scheme 3-1**).[37] In addition to these examples, Wada *et al.* reported synthesis of an acrylamide derivative of trehalose in eight steps, and the monomer was copolymerized with acrylamide for the inhibition study of amyloid β peptide aggregations.[38] Recently, Reineke and coworkers modified this acrylamide monomer synthesis and prepared a methacrylamide derivative of trehalose to prepare diblock copolycations for siRNA delivery.[39]

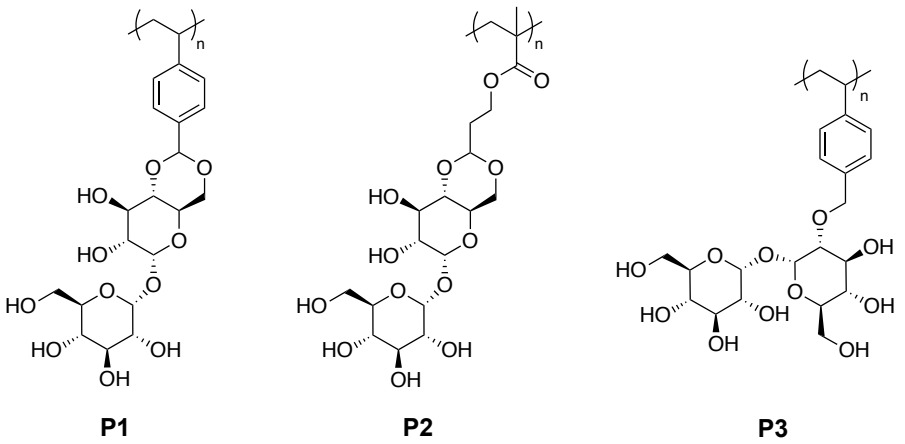

Figure 3-1. The chemical structure of the trehalose glycopolymers used in this study.[37]

In this chapter, the synthesis of a methacrylate trehalose monomer will be described. Protecting group chemistry was employed in synthesis for reaction selectivity. Four different proteins (horseradish peroxidase (HRP), β-galactosidase (β-Gal), glucose oxidase (GOx), and phytase (from Phytex, LLC)) were stressed with and without trehalose glycopolymers, and the protein activities after the stressor were evaluated.

3.2 Results and Discussion

3.2.1 Synthesis of Methacrylate Trehalose Monomer and Glycopolymer

Trehalose monomer **M4′** was synthesized through specifically protecting one of the primary alcohols and adding a methacrylate moiety to that position (**Scheme 3-1**). Compound **1** and **2** were synthesized according to a literature procedure with modifications (see Appendix **Figure 3-13** through **Figure 3-18** for NMR spectra).[29] The bulky trityl group was used to

discriminate the primary and secondary hydroxyl groups, and was subsequently deprotected to give **2** with one free hydroxyl group after purification. Compound **2** was then reacted with methacryloyl chloride in the presence of triethylamine to give the acetyl protected methacrylate glycomonomer **M4′** with 64% yield (see **Figure 3-2** and **Figure 3-3**, and Appendix **Figure 3-19** and **Figure 3-20** for NMR spectra). The protected monomer **M4′** was then polymerized by free radical polymerization using AIBN as a radical source at 65 °C for 19 h. The polymer **P4′** was purified by precipitation in diethyl ether and resulted in M_n = 18,300 g/mol and PDI = 2.40 (see **Figure 3-4** for NMR spectrum and **Figure 3-6** for GPC trace). **P4′** was then deprotected using a catalytic amount of NaOMe using a modified procedure from our previous report;[40,41] the product precipitates out of solution as the deprotection occurs. **P4** was neutralized with HCl and dialyzed against H_2O. From ^1H NMR spectroscopy, the peaks corresponding to the methyl protons of the acetate groups at approximately 2 ppm disappeared, suggesting successful deprotection (**Figure 3-5**). Also with IR analysis, the disappearance of the acetyl C=O and C-O stretch and the appearance of the O-H absorption were observed (**Figure 3-7**). The GPC samples of **P4** were prepared by dissolving in DMF and heating to 80 °C or 40 °C, and filtered before injection. The resulting trace is significantly different due to the low solubility of **P4** in DMF at 40 °C (**Figure 3-6**). After fully dissolving the polymers by heating the samples to 80 °C, we were able to characterize **P4** with M_n = 10,100 g/mol and PDI = 1.55.

Scheme 3-1. Synthesis and free radical polymerization of **M4′**.

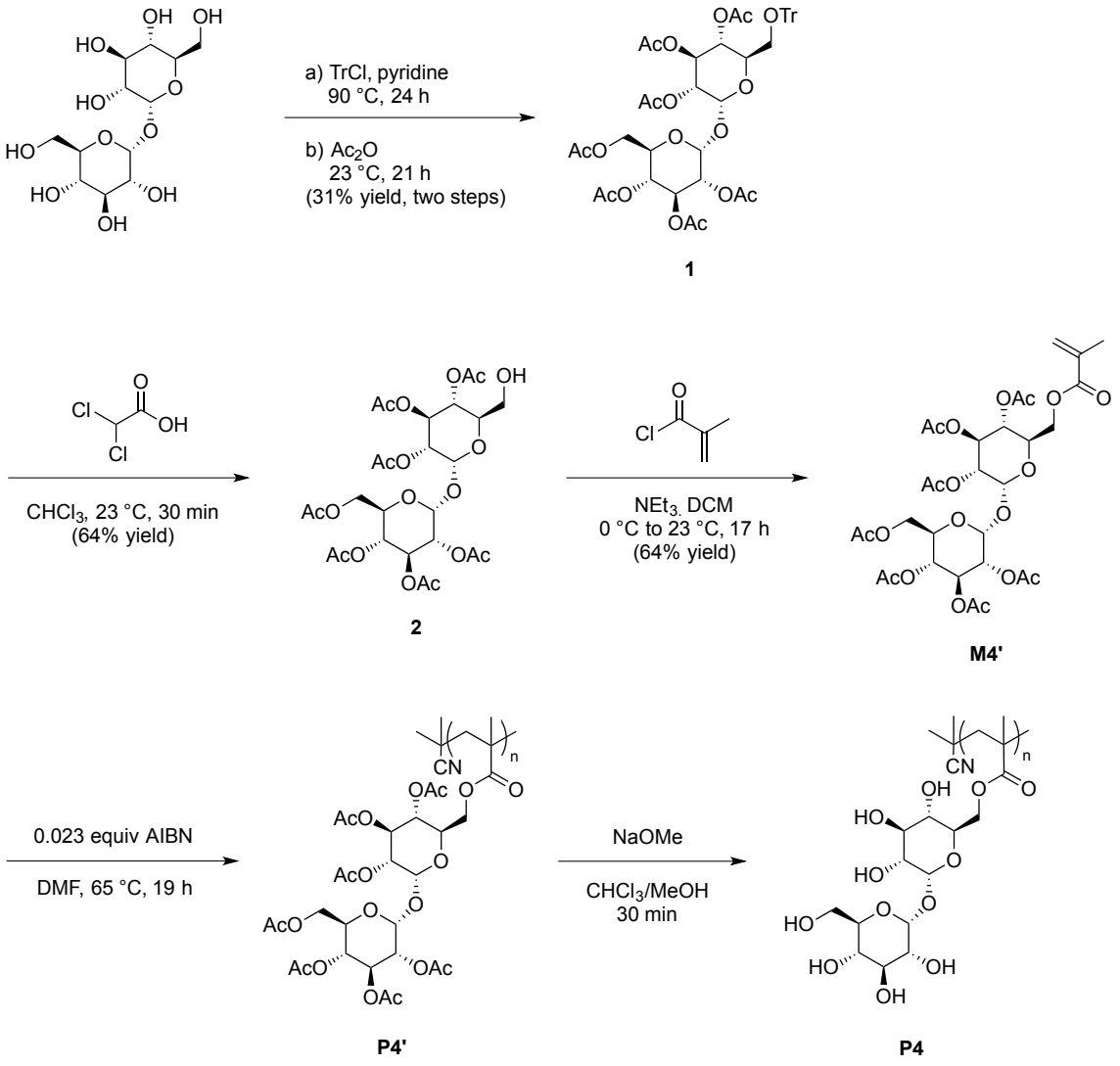

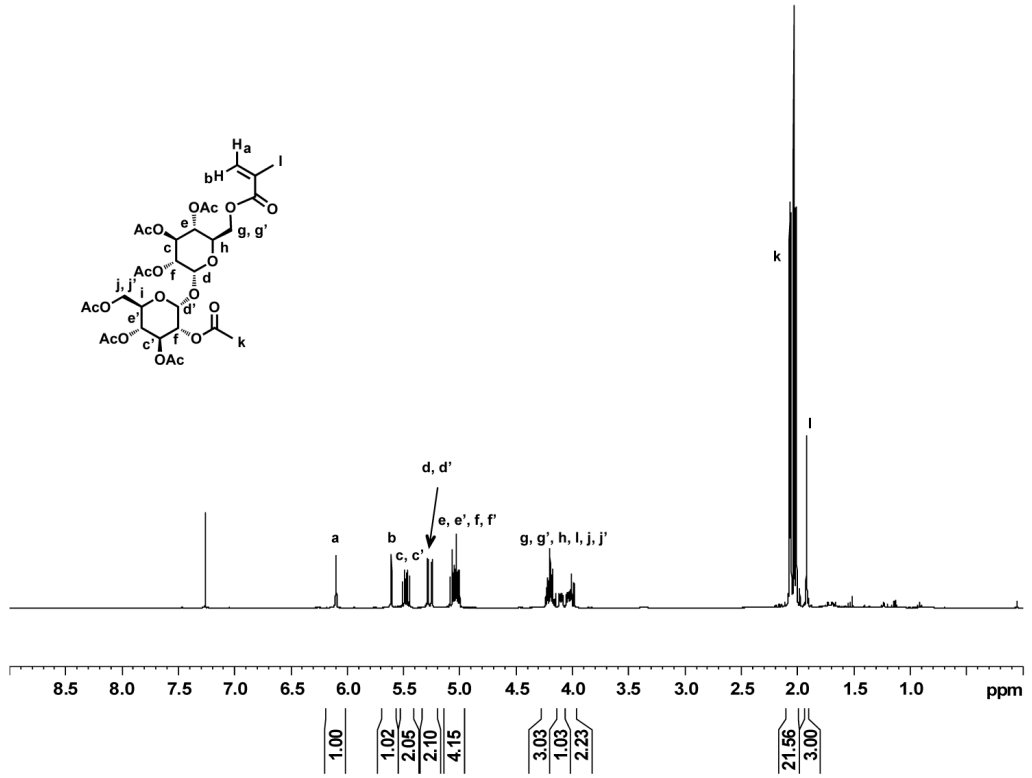

Figure 3-2. ^{1}H NMR spectrum of **M4′** (in $CDCl_3$).

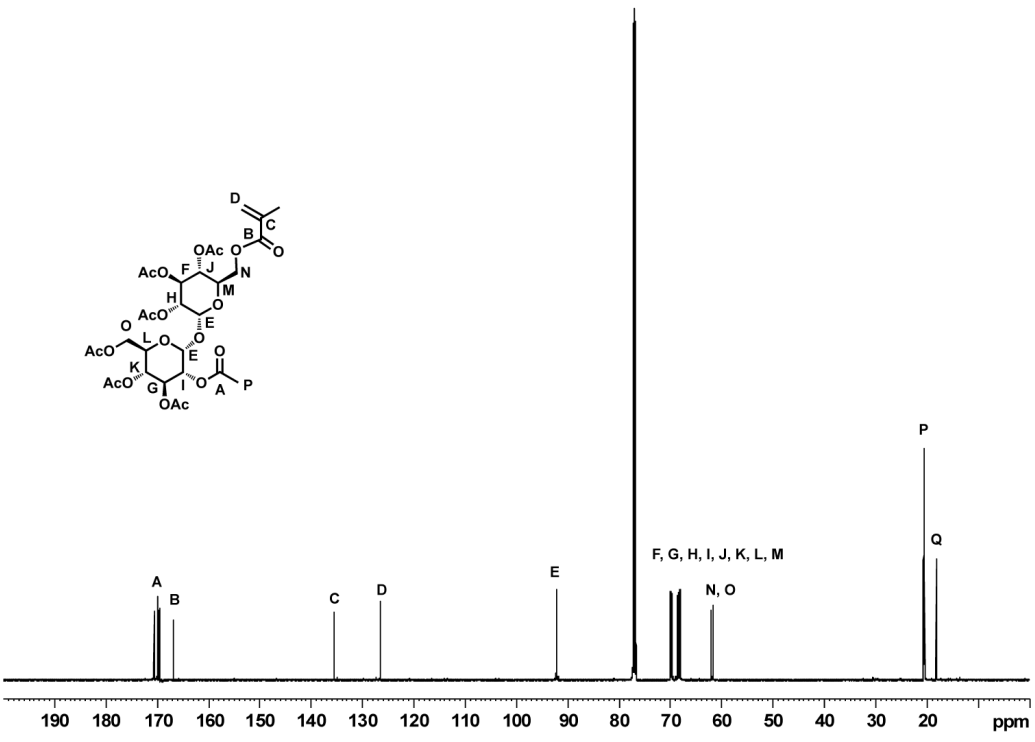

Figure 3-3. ^{13}C NMR spectrum of **M4′** (in $CDCl_3$).

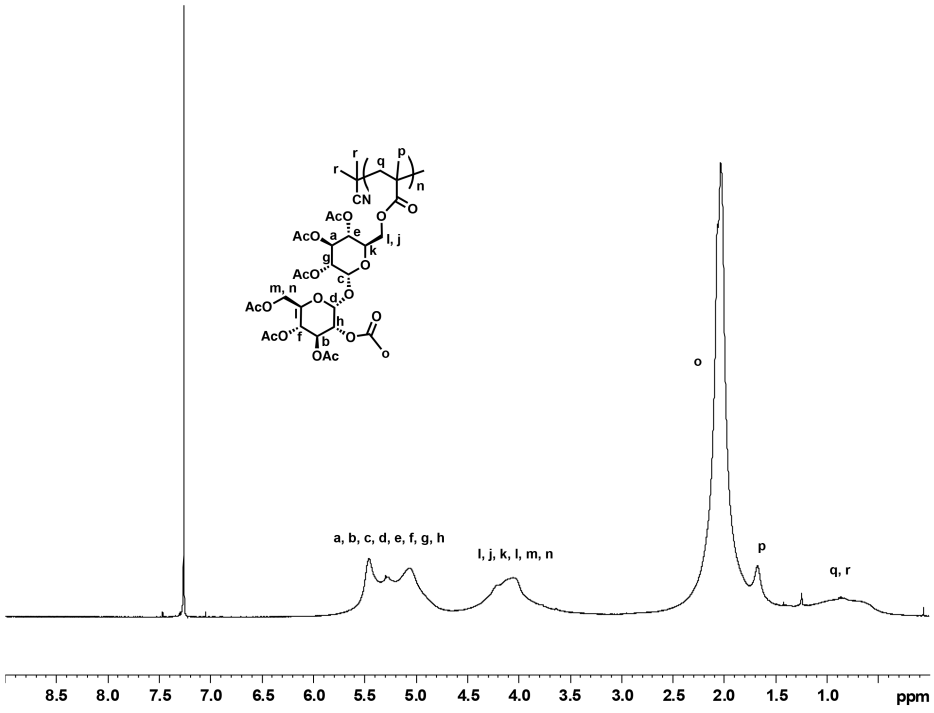

Figure 3-4. ^{1}H NMR spectrum of **P4′** (in $CDCl_3$).

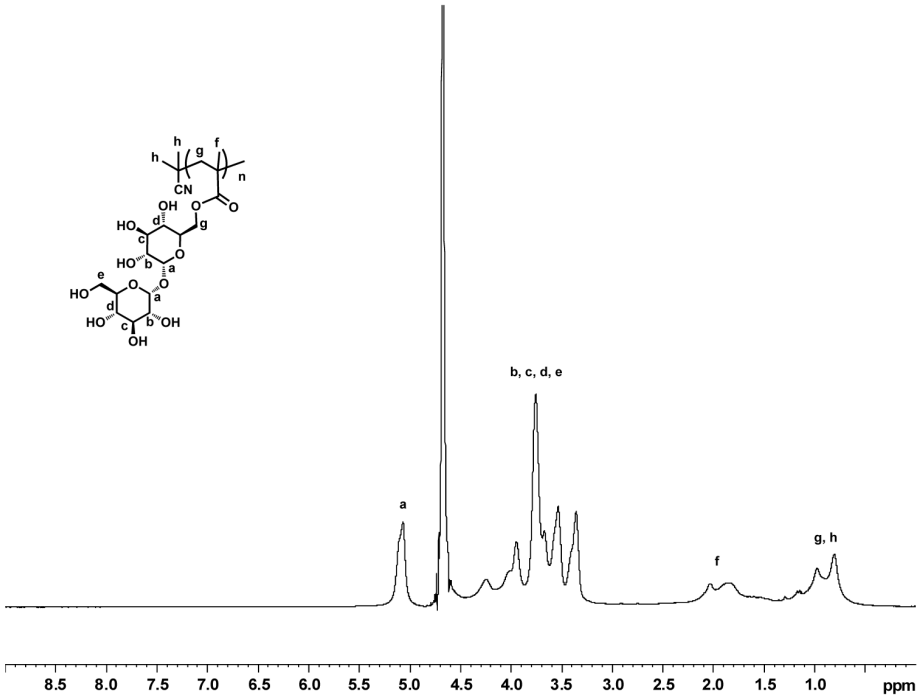

Figure 3-5. ^{1}H NMR spectrum of **P4** (in D_2O). The peaks corresponding to the methyl protons of the acetate groups at approximately 2 ppm disappeared, suggesting successful deprotection.

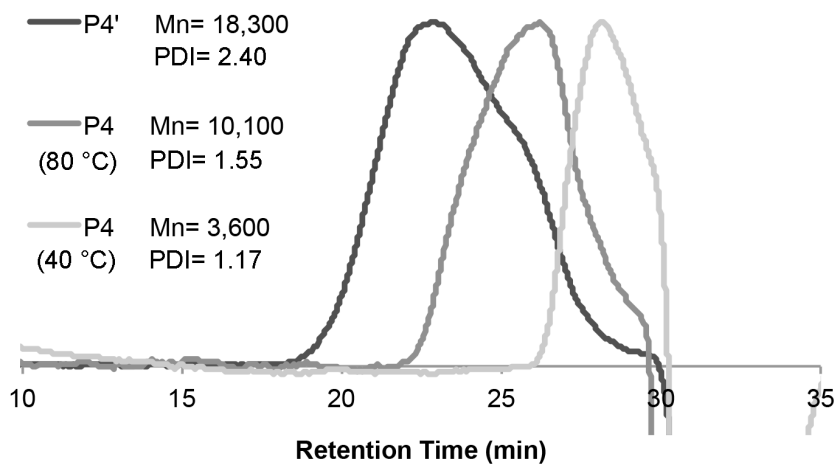

Figure 3-6. GPC trace overlay of **P4′** (dark gray trace) and **P4** (the two light gray traces). **P4** samples were prepared by dissolving in DMF and heating to 80 °C or 40 °C, and filtered before injection. The resulting trace is significantly different due to the low solubility of **P4** in DMF.

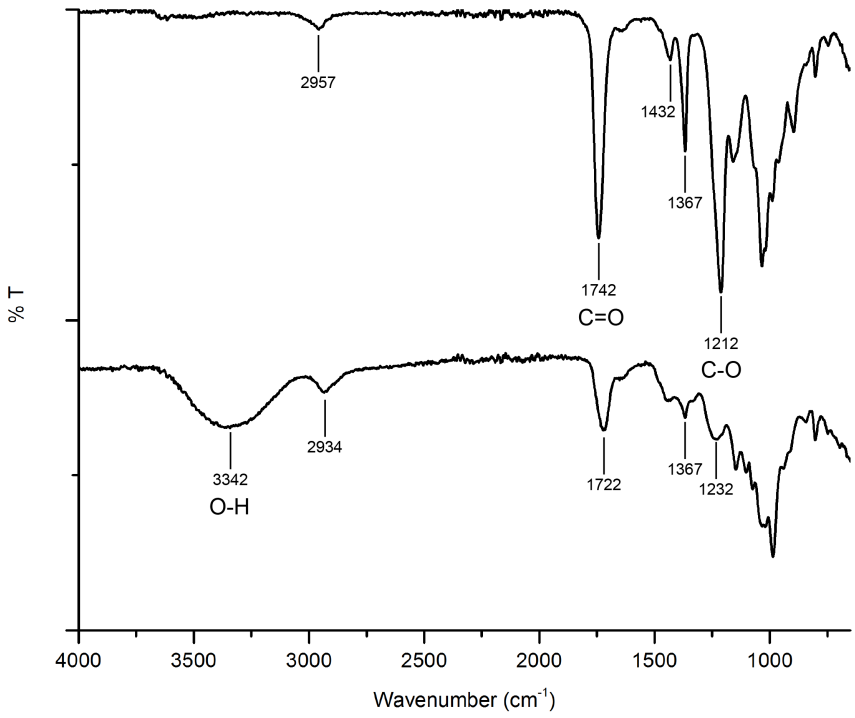

Figure 3-7. IR spectra of **P4′** (top) and **P4** (bottom). After acetyl deprotection, the disappearance of the acetyl C=O (1742 cm^{-1}) and C-O (1212 cm^{-1}) stretch and the appearance of the O-H (broad, 3342 cm^{-1}) absorption were observed.

3.2.2 Heat Burden Study of Horseradish Peroxidase

Horseradish peroxidase (HRP, EC 1.11.1.7) is an important enzyme that catalyzes the hydrogen peroxide oxidation of a variety of substrates. It has been widely used in biotechnological and diagnostic applications. However, inadequate stability at elevated temperatures has limited its potential use. Trehalose is one of many additives used to increase the stability of HRP by raising its T_m and preventing protein from unfolding.[42]

The activity of HRP (75 μg/mL, 10 mM sodium phosphate buffer, pH 7.0) after exposure to 70 °C for 30 minutes with and without additives was assayed. The activity of HRP was tested by addition of 3,3',5,5'-tetramethylbenzidine (TMB), which produces a blue by-product in the presence of HRP.[43] HRP samples were prepared without any additive, with **P4**, or with trehalose. To determine the effectiveness of the polymer in preserving protein activity, samples of the polymer from 1 weight equivalent (wt equiv) to 80 wt equiv relative to HRP were tested. Weight equivalent was used instead of molar equivalent because it would prevent any inaccuracies in the molecular weight of the polymer from affecting the ratio of trehalose side chain to HRP.

Samples that had been heated were tested for remaining HRP activity, and the percent original activities were calculated using the same concentration of HRP without heating and additive (**Figure 3-8**). Only 55% of the original activity was observed when HRP itself was heated to 70 °C. Yet, activity was completely retained (100%) for **P4** when 25, 50 or 80 wt equiv of polymer was added. With 1 wt equiv, **P4** still stabilized the protein slightly better (75%) than no additive. The same equivalents of trehalose also stabilized HRP, but the HRP activity was lower compared to the polymer.

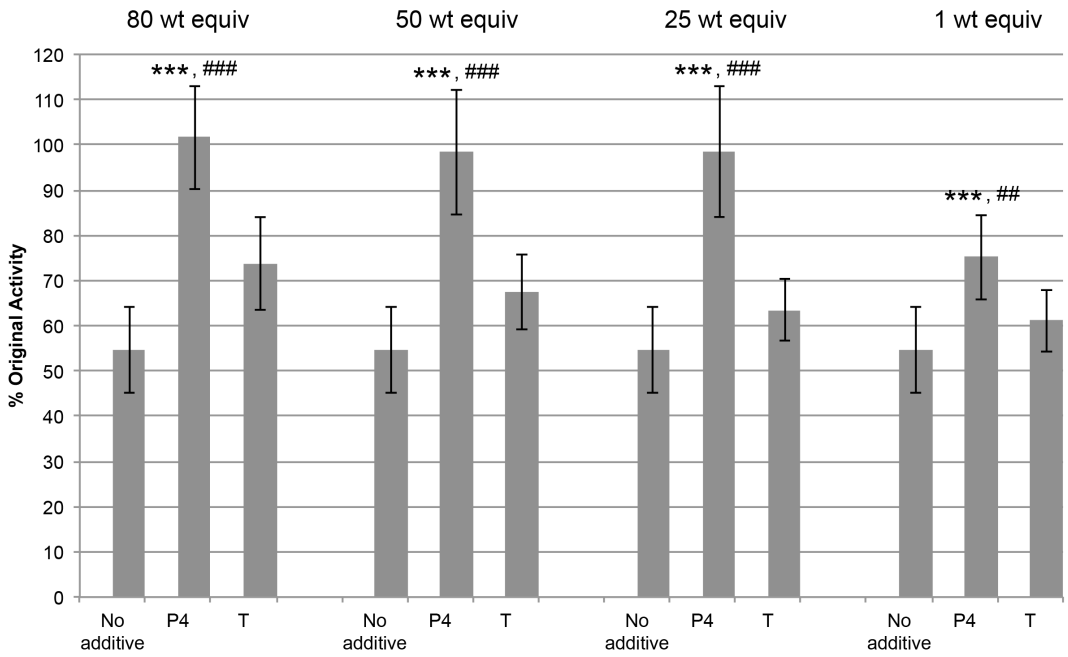

Figure 3-8. Activity of HRP (75 μg/mL) after 30 min incubation at 70 °C, with no additive, P4, or trehalose (T). 80, 50, 25, and 1 wt equiv of polymer was added to the protein. Data shown as the average of n=12 with standard deviation. *** = $p < 0.001$ relative to no additive. ### = $p < 0.001$ and ## = $p < 0.01$ relative to trehalose.

3.2.3 Lyophilization Study of β-Galactosidase

β-Galactosidase (β-gal, EC 3.2.1.12) catalyzes the hydrolysis of the β-glycosidic bond between a galactose and another monosaccharide or organic moiety. The protein is a 464-kDa homotetramer. During lyophilization, β-Gal activity decreases from both the freezing and dehydration stresses. However, the addition of sucrose has shown to effectively protect β-Gal from denaturation under these stresses.[44]

The stabilization of β-Gal was also tested after multiple lyophilization cycles. The activity of β-Gal was determined by reacting with 2-nitrophenyl-β-D-galactopyranoside (ONPG), which releases *o*-nitrophenol, a yellow chromophore that absorbs light at 405 nm.[45] After three cycles of lyophilization, β-Gal had only 47% original activity, while 10 wt equiv of **P4** maintained 85% activity (**Figure 3-9**). The result showed that the polymer outperformed trehalose, since the trehalose maintained only 73% of the original activity at maximum. At 5 wt equiv, **P4** still maintained 85% activity, while % activity for trehalose was the same as no additive. However, the protein was not stabilized by **P4** or trehalose at 1 wt equiv.

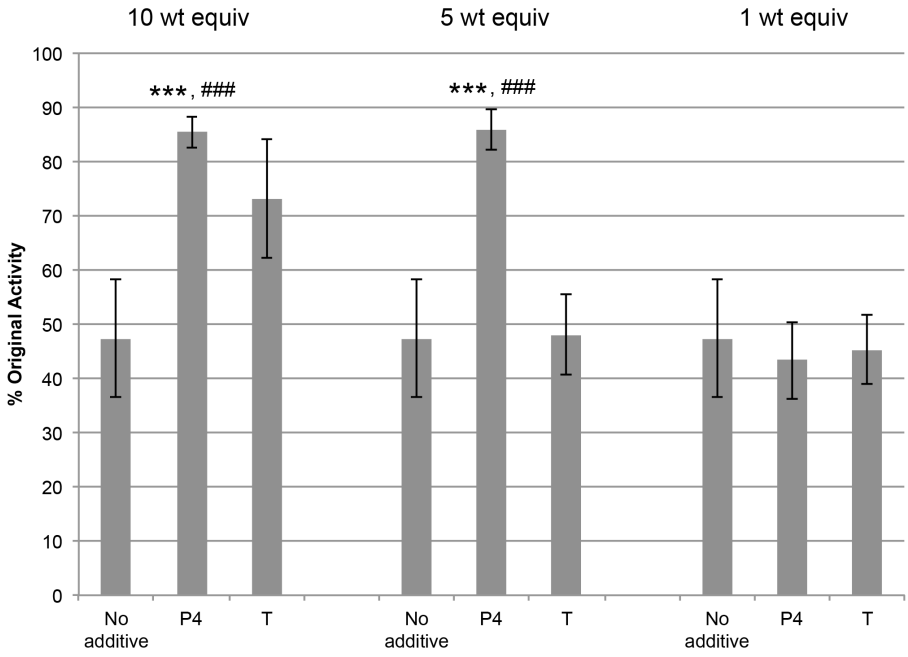

Figure 3-9. Activity of β-Gal (100 μg/mL) after 3 cycles of lyophilization with no additive, P4, and trehalose (T) added to the β-Gal. 10, 5, and 1 wt equiv of polymer was added to the protein. Data shown as the average of n=12 with standard deviation. *** = $p < 0.001$ relative to no additive. ### = $p < 0.001$ relative to trehalose.

3.2.4 Heat Burden Study of Glucose Oxidase

Glucose oxidase (GOx, EC 1.1.3.4) is a 160-kDa dimer that catalyzes the oxidation of β-D-glucose to β-D-glucolactone, which then hydrolyzes to gluconic acid. Similar to HRP, its usefulness in commercial applications has been limited due to its instability at elevated temperature. It has been previously shown that the addition of trehalose stabilizes GOx by decreasing the inactivation rate constant up to 50%.[46]

The stability of GOx (1 mg/mL, 10 mM sodium phosphate buffer, pH 7.0) after incubation at 50 °C for 30 minutes with and without additives was also investigated. The activity was determined by the release of hydrogen peroxide upon oxidation of glucose, which reacts with Amplex® Red reagent in the presence of peroxidase to produce the red-fluorescent resorufin (Ex/Em=571/585 nm).[47] It was found that 20 wt equiv of **P4** stabilized GOx better than no additive; however, the effect was not as dramatic as for other proteins because GOx alone is relatively stable at these conditions (**Figure 3-10**). Trehalose itself did not stabilize the protein as its % activity was not significantly different from no additive.

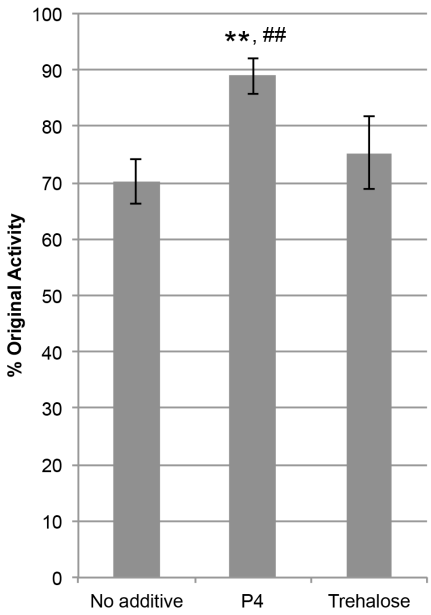

Figure 3-10. Activity of GOX (1 mg/mL) after 30 min incubation at 70 °C, with no additive, P4, and trehalose (T) added to the enzyme. Average and standard deviation values of 12 repeats are shown. ** = $p < 0.01$ compared to no addition, ## = $p < 0.01$ compared to T.

3.2.5 Heat Burden Study of Phytase

Phytase (EC 3.1.3.8) plays an important role in poultry industry as an animal feed supplement by hydrolyzing phytic acid to inorganic phosphate.[48] Phytic acid is the principle form of phosphorous stored in grains. However, it cannot be digested by humans and non-ruminant animals. It is also a strong chelator of many multivalent metal ions such as zinc, calcium, and iron, thereby lowering bioavailability of these minerals.[49] Phosphorus digestibility and mineral availability can be improved by adding the enzyme phytase to the feed. During the feed pelleting of phytase, the enzyme is shortly exposed to high temperatures (45 seconds at 70-90 °C, 17% moisture) after which it loses much of its activity. Therefore, it is of great interest to the feed

industry to enhance the thermostability of the enzyme. Several studies have been performed to improve its stability, including methods such as site-directed mutagenesis[50], glycosylation[51], and addition of protectants[52].

We hypothesized that the non-covalent addition of trehalose polymer may help preserve enzyme activity against heat treatment. In collaboration with Phytex, LLC, we tested the heat stability of phytase after the addition of three different trehalose polymers (**Figure 3-1**; The syntheses of the trehalose polymers are described in our recent publication.[37]) From the results, we were to decide on which polymer to provide in large scale for Phytex to use as an additive in the actual pelleting of phytase.

We first investigated the heat stability of an aqueous solution of phytase with or without the addition of a trehalose polymer (**P1**). We prepared 1.5 mg/mL phytase solutions (in10 mM sodium phosphate buffer, pH 7.0), and added 100 wt equiv of **P1**. Phytase solutions were heated at 40, 60, 80, or 90 °C for 1 minute. The activity assays were performed by Phytex researchers and compared to controls in the absence of heat burden (4 °C). The enzyme activities were lost after heating at 80 or 90 °C, regardless of whether or not the polymer has been added. After heating at 40 and 60 °C for 1 minute, the enzyme activity decreased to approximately 25% and 2% of the original activity, respectively, but retained 100% activity with the addition of polymer for both heating temperatures (**Figure 3-11**). In the liquid phase, the polymer protects phytase from heat at temperatures below 80 °C.

We then investigated the heat stability of dried mixture of phytase and trehalose polymers (**P1-P3**, all with approximately 20 kDa molecular weight). Lyophilized mixture of phytase and 100 wt equiv of trehalose polymers were heated at 80 and 90 °C for 1 minute and 3 minutes.

Assay results showed that the dried enzyme (or mixtures) retained its activity after such heating conditions, regardless of whether or not the polymer has been added. This implies that lyophilized phytase can be heated to 80-90 °C for up to 3 minutes without loss of activity, but it quickly becomes deactivated within a minute in a buffered solution (at least at concentrations below 1.5 mg/mL). Importantly, the moisture level of phytase during the industrial pelleting condition is 15-20%, which is closer to a dried state and suggesting that the trehalose polymer may be able to stabilize phytase at high temperature in a low-water environment.

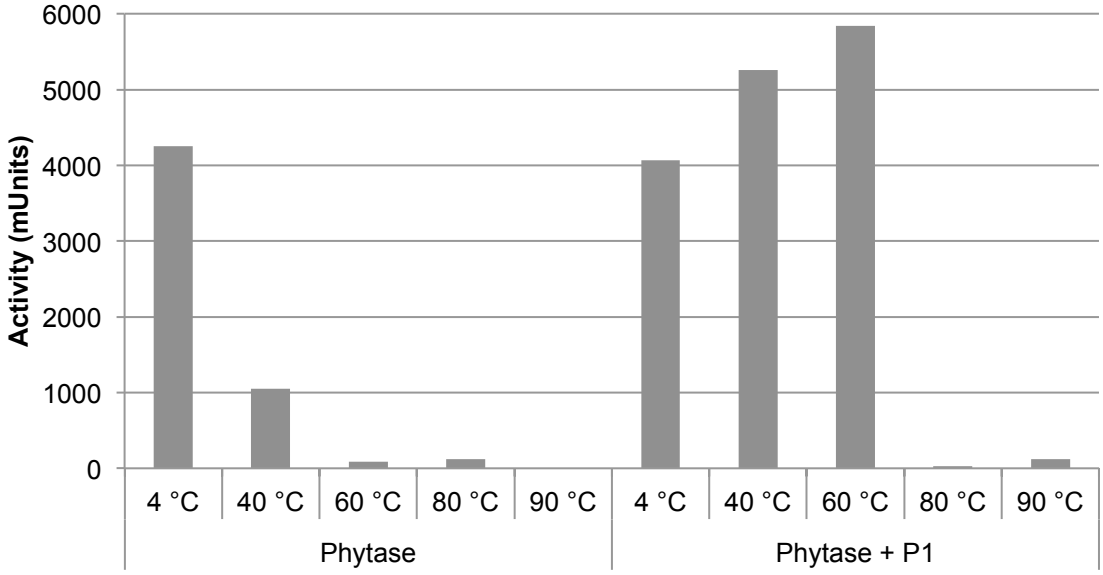

Figure 3-11. Activity of phytase (1.5 mg/mL) after 1 min incubation at 4, 40, 60, 80, and 90 °C with no additive or trehalose polymer (**P1**) added to the enzyme.

Next, we altered the moisture level by adding a small amount of water (0.1 μL) to the lyophilized samples (enzyme or mixture, 10 μg) to create ~90% moisture. The moist mixtures of phytase and 100 wt equiv of trehalose polymers were heated at 80 and 90 °C for 1 minute

(**Figure 3-12**). The results showed that at 90% moisture level, phytase readily degrades after 1 minute of heat treatment. With the addition of **P1**, the phytase activity was much lower than no additive for all temperatures, including the control at 4 °C. This may be due to some experimental error, because we had not observed adverse effects of **P1** to phytase. On the other hand, **P2** stabilized phytase to maintain 72% activity after 90 °C treatment, compared to 17% when no polymer was added. **P3** also stabilized phytase to maintain 76% activity after 80 °C treatment, compared to 29% when no polymer was added. From this result, we decided to use **P3** for the large-scale production for actual pelleting experiments.

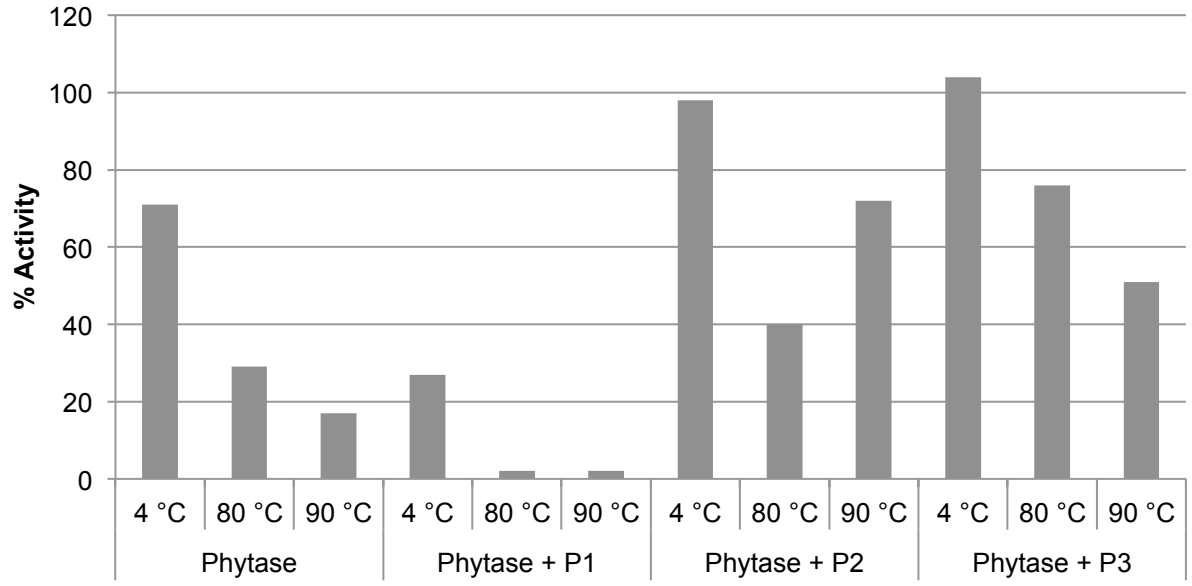

Figure 3-12. Activity of phytase (90% moist) after 1 min incubation at 4, 80, or 90 °C with no additive or trehalose polymers (**P1**, **P2**, **P3**) added to the enzyme.

3.3 Conclusions

In this chapter, we described the synthesis of an acetylated methacrylate trehalose monomer **M4′** and a trehalose glycopolymer **P4**. The polymer stabilized HRP and GOx against heating and β-Gal against freezing and drying compared to no additive and comparable amount of trehalose. The mechanism of the stabilization is thought to be a combination of the effect of trehalose and the nonionic surfactant capability of the polymers that prevents ice crystal formation and aggregation. We also showed that trehalose glycopolymers stabilized phytase against heat inactivation, and **P3** was chosen for actual pelleting conditions. The results show that trehalose glycopolymers are promising excipients for the pharmaceutical industry and can be used to prevent denaturation of protein-based drugs, to protect enzymes used industrially, and to aid in protein research and development.

3.4 Experimental Section

Materials

All the chemicals and proteins were purchased from Sigma-Aldrich and Fisher Scientific and were used without purification unless noted otherwise. Trehalose was purchased from The Healthy Essential Management Corporation (Houston, TX) and dried with ethanol and kept under vacuum before use. Trehalose used in stability studies was dried with ethanol, lyophilized, and kept in a closed vial prior to use. AIBN was recrystallized from acetone before using. Amplex® Red Glucose/Glucose Oxidase Assay kit was purchased from Invitrogen and was used following the manufacturer instructions. Phytase was provided by Phytex, LLC.

Analytical techniques

NMR spectra were obtained on Bruker AV 500 and DRX 500 MHz spectrometers. ^{1}H NMR spectra were acquired with a relaxation delay of 2 s for small molecules and 30 s for polymers. Infrared absorption spectra were recorded using a PerkinElmer FT-IR equipped with an ATR accessory. Gel permeation chromatography (GPC) was conducted on a Shimadzu high performance liquid chromatography (HPLC) system with a refractive index detector RID-10A, one Polymer Laboratories PLgel guard column, and two Polymer Laboratories PLgel 5 μm mixed D columns. Eluent was DMF with LiBr (0.1 M) at 40 °C (flow rate: 0.60 mL/min). Calibration was performed using near-monodisperse pMMA standards from Polymer Laboratories. ESI-MS data were gathered on a Waters LCT premier with ACQUITY LC.

Methods

Synthesis of 1. Trehalose (4.91 g, 14.34 mmol) was stirred in 20 mL pyridine for 30 min. Trityl chloride (TrCl, 2.67 g, 9.58 mmol) was then added, and the reaction mixture was stirred under Ar at 90 °C for 24 h. After cooling to room temperature, acetic anhydride (Ac_2O, 12 mL, 1.27×10^2 mmol) was added, and the reaction mixture was stirred under Ar at 23 °C for 21 h. Pyridine was removed *in vacuo*. To the crude solid, H_2O was added and extracted with $CHCl_3$. The organic layer was then sequentially washed with 0.1 N HCl, H_2O, sat. $NaHCO_3$, and brine. The organic layer was then dried with $MgSO_4$ and concentrated *in vacuo*. The crude was purified by silica gel flash chromatography with EtOAc : Hexane = 3 : 4 + 1% triethylamine (NEt_3, R_f~0.3) to obtain 2.62 g white solid with 31% yield. ^{1}H NMR (500 MHz in $CDCl_3$) δ: 7.40-7.20 (m, 15H), 5.50-5.45 (m, 2H), 5.40-5.37 (dd, *J*= 3.85, 7.85 Hz, 2H), 5.18-5.15 (dd, *J*= 3.85, 10.2 Hz, 2H), 5.14-5.05 (m, 2H), 4.27-4.23 (m, 1H), 4.14-4.02 (m, 3H), 3.10-3.02 (m, 2H), 2.11 (s,

3H), 2.10 (s, 3H), 2.05 (s, 3H), 2.01 (s, 3H), 2.00 (s, 3H), 1.88 (s, 3H), 1.74 (s, 3H). ^{13}C NMR (500 MHz in $CDCl_3$) δ: 170.81, 170.25, 170.12, 169.91, 169.72, 169.69, 169.30, 143.47, 128.71, 128.01, 127.24, 92.51, 92.48. 86.71, 70.43, 70.38, 70.27, 69.85, 69.61, 68.99, 68.67, 68.35, 61.94, 61.81, 20.88, 20.81, 20.79, 20.77, 20.67, 20.54. IR: ν = 2956, 2941, 1746, 1449, 1367, 1239, 1213, 1072, 1030, 985, 962, 902, 805, 766, 749. ESI-MS (± 1.0) observed (predicted): Na^+ 901.2892 (901.2895).

Synthesis of 2. Compound **1** (1.69 g, 1.92 mmol) was dissolved in 8 mL $CHCl_3$, then 8 mL dichloroacetic acid was added and stirred at 23°C for 30 min. The crude mixture was washed with H_2O once, and then with sat. $NaHCO_3$ three times. The organic layer was then dried with $MgSO_4$ and concentrated *in vacuo*. The crude was purified by silica gel flash chromatography with DCM (3% MeOH) (R_f~0.25) to obtain 780 mg of a crispy yellow solid in 64 % yield. ^{1}H NMR (500 MHz in $CDCl_3$) δ: 5.54-5.43 (m, 2H), 5.29-5.27 (t, *J*= 3.85 Hz, 2H), 5.06-4.97 (m, 4H), 4.27-4.22 (dd, *J*= 5.5, 12,2 Hz, 1H), 4.10-4.05 (m, 1H), 3.99-3.96 (dd, *J*=2.05, 12.2 Hz, 1H), 3.91-3.86 (m, 1H), 3.64-3.52 (m, 2H), 2.08-2.05 (m, 12H), 2.04 (s, 3H), 2.03 (s, 3H), 2.02 (s, 3H), 2.01 (s, 3H). ^{13}C NMR (500 MHz in $CDCl_3$) δ: 170.61, 170.33, 169.97, 169.93, 169.88, 169.70, 169.60, 169.57, 92.97, 92.86, 70.83, 70.48, 70.06, 69.95, 69.93, 69.86, 69.75, 69.59, 68.79, 68.52, 68.46, 68.14, 61.77, 61.71, 60.95, 20.90, 20.71, 20.68, 20.67, 20.61, 20.58. IR: ν = 3523, 2962, 2106, 1742, 1435, 1367, 1208, 1163, 1137, 1032, 986, 899, 802, 736 cm^{-1}. ESI-MS (± 1.0) observed (predicted): Na^+ 659.1762 (659.1799).

Synthesis of 6-methacrylate-α,α-acetylated trehalose (M4'). Compound **2** (360 mg, 5.66×10^{-1} mmol) was dissolved in 1.9 mL dry DCM in an ice bath, then NEt_3 (1.18 mL, 8.47 mmol) was added. Methacryloyl chloride (0.55 mL, 5.63 mmol) was dissolved in 2 mL dry DCM, and the solution was added to the reaction mixture dropwise. The mixture was then stirred under Ar from

0 °C to 23 °C for 17 h. The $HNEt_3^+Cl^-$ salt was filtered off, and the solution was washed with 10% HCl, H_2O, sat. $NaHCO_3$, and then brine. The organic layer was then dried with $MgSO_4$ and concentrated *in vacuo*. The crude was purified through silica gel flash chromatography with EtOAc : Hexane = 1 : 1 (R_f~0.4) to obtain 254.5 mg yellow oil with 64% yield. ^{1}H NMR (500 MHz in $CDCl_3$) δ: 6.10 (s, 1H), 5.61 (m, 1H), 5.51-5.45 (m, 2H), 5.29-5.24 (dd, *J*= 3.85, 17.75 Hz, 2H), 5.10-4.99 (m, 4H), 4.25-3.97 (m, 6H), 2.07 (s, 3H), 2.07 (s, 3H), 2,06 (s, 3H), 2.04 (s, 6H), 2.02 (s, 3H), 2.01 (s, 3H), 1.92 (s, 3H). ^{13}C NMR (500 MHz in $CDCl_3$) δ: 170.60, 169.96, 169.95, 169.64, 169.55, 169.53, 169.50, 166.82, 135.52, 126.60, 92.28, 92.17, 70.08, 69.95, 69.87, 69.67, 68.69, 68.47, 68.19, 68.13, 62.09, 61.74, 20.68, 20.67, 20.62, 20.60, 20.58, 20.52, 18.21. IR: ν = 2930, 1746, 1368, 1213, 1033, 897, 804 cm^{-1}. ESI-MS (± 1.0) observed (predicted): Na^+ 727.2078 (727.2062).

Free Radical Polymerization of M4′. **M4′** (221.9 mg, 3.15×10^{-1} mmol) and AIBN (1.2 mg, 7.31×10^{-3} mmol) were weighed into a Schlenk tube and dissolved in 0.5 mL DMF. Freeze-pump-thaw cycles were repeated five times, and the reaction was initiated by immersion in an oil bath at 65 °C. After 19 h, monomer conversion reached 83% by ^{1}H NMR, and the polymerization was quenched by cooling the flask in liquid nitrogen. DMF was removed under high vacuum. The crude was redissolved in DCM and precipitated into cold diethyl ether three times. 160 mg of white solid **P4′** was collected with M_n = 18,300 g/mol and PDI = 2.40 by GPC. ^{1}H NMR (500 MHz in $CDCl_3$) δ: 5.46, 5.30, 5.28, 5.07, 4.20, 4.06, 2.07, 2.03, 1.68, 1.25, 0.85. IR: 2957, 1742, 1432, 1367, 1212, 1159, 1034, 896, 802, 746 cm^{-1}.

Deprotection of P4′. To **P4′** (100 mg, 5.46×10^{-3} mmol) was added 1 mL $CHCl_3$ and 1 mL MeOH, and the mixture was stirred for 15 min to dissolve the polymer. NaOMe (30% in MeOH,

5.26 uL, 2.84×10^{-2} mmol) was added and stirred under Ar for 2 h. A white precipitate formed within 20 min. The precipitate was collected by centrifuge, and then dissolved in H_2O. The pH was adjusted to neutral with 0.1 N HCl. The solution was dialyzed (MWCO 3,500 g/mol) against H_2O (1 L × 2). The solution was then filtered with a 0.2 μM syringe filter. The aqueous solution was lyophilized to obtain 44 mg of **P4** as white solid. ^{1}H NMR (500 MHz in D_2O) δ: 5.16, 5.07, 4.26, 4.02, 3.95, 3.76, 3.67, 3.53, 3.36, 2.03, 1.86, 0.98, 0.81. IR: 3342, 2934, 1722, 1367, 1232, 1147,1102, 1019, 802 cm^{-1}.

Horseradish Peroxidase Heating Studies. Horseradish peroxidase (HRP, 150 μg/mL) solution was prepared by adding HRP into 10 mM sodium phosphate buffer, pH 7.0. Stock solutions of 80, 50, 25, and 1 weight equivalent (wt equiv) of **P4** and trehalose to HRP were prepared. 2 μL aliquots of the HRP solution were mixed with 2 μL aliquots of each polymer or trehalose solution to give final concentration of 75 μg/mL of HRP. Samples were incubated at 70 °C for 30 min and a non-heated control sample was stored at 4 °C until the activity assay was performed. TMB[43] was used as a substrate and 1 M H_2SO_4 solution as the stop solution. To assess the activity, absorbance at 450 nm was monitored. The assay was repeated in total twelve times (n=12, two separate experiments with six repeats each).

β-Galactosidase Lyophilization Studies. β-Galactosidase (β-Gal, 0.4 mg/mL) solution was prepared by adding β-Gal to 10 mM sodium phosphate buffer, pH 7.0. Each 25 μL aliquot of β-Gal solution was mixed with 75 μL of H_2O (the control) or 75 μL of stock solution each containing 10, 5, or 1 wt equiv of **P4** and trehalose to β-Gal in H_2O to yield 0.1 mg/mL protein solution. Aliquots of each sample were frozen by immersion in liquid nitrogen before solvent removal via lyophilization. The samples were lyophilized for 12 h for one cycle under 1 mbar. After the first cycle, 100 μL of H_2O was added and lyophilization was repeated for the next

cycles. The control sample was stored at 4 °C until the activity assay was conducted. After the desired number of cycles, the final lyophilized samples were dissolved into 50 μL of H_2O. 30 μL of ONPG (4 mg/mL) was added to the samples. The samples were incubated in dark for 5 min and the reaction was stopped with 50 μL of 1 M Na_2CO_3. Activity was ascertained by reading the absorbance at 405 nm.[44] The assay was repeated in total twelve times (n=12, two separate experiments with six repeats each).

Glucose Oxidase Heating Studies. Glucose oxidase (GOx, 2 mg/mL) solution was prepared by adding GOx to 10mM sodium phosphate buffer, pH 7.0. Stock solutions of **P4** (20 wt equiv of trehalose units to GOx) and trehalose were also prepared in 10 mM sodium phosphate buffer, pH 7.0. 2 μL aliquots of the GOx solution were mixed with 2 μL aliquots of each polymer or trehalose solution to give final concentration of 1 mg/mL GOx. Samples were incubated at 50 °C for 30 min and the non-heated control was stored at 4 °C until the activity assay was performed. The activity was measured using Amplex® Red Glucose/Glucose Oxidase Assay kit[47] following the manufacturer's procedure, and was repeated in total twelve times (n=12, two separate experiments with six repeats each).

Statistical Analysis. All the *p*-values were calculated using the independent Student's t-test assuming unequal variances.

Phytase Heating Studies in Aqueous Solution. Phytase solution (604.05 μL, 1.5 mg/mL in 10 mM sodium phosphate buffer, pH 7.0) was added to **P1** (20.1 kDa, 31.55 mg, 1.57×10^{-3} mmol) in Eppendorf® Protein Lobind microcentrifuge tubes. Aliquots of phytase solution (20 μL) or phytase-polymer solution (20 μL) were heated at 40, 60, 80, or 90 °C for 1 min, or stored at 4 °C

as a control. The heated samples were then cooled down to 4 °C, and all samples were shipped with an ice pack to Phytex for activity assay.

Phytase Heating Studies in Dried State. Three different types of trehalose polymers, all with approximately 20 kDa molecular weight, were tested: **P1** (20.1 kDa), **P2** (18.3 kDa), and **P3** (29.6 kDa). Phytase solutions (90 μL, 1 mg/mL in H_2O) were added to **P1** (3.6 mg, 1.8×10^{-4} mmol), **P2** (3.3 mg, 1.8×10^{-4} mmol), or **P3** (5.3 mg, 1.8×10^{-4} mmol) in Eppendorf® Protein Lobind microcentrifuge tubes, to prepare solutions with 100 equivalents of polymer to protein. 90 μL of phytase solution without polymer was also prepared as a control. The samples were then split into 10 μL aliquots for different treatments. The 10 μL aliquots were lyophilized for 18 h. To each tube of dry mixture (containing 10 μg of phytase), 0.1 μL of H_2O was added and stored at 4 °C for 24 h to create 90.9% moisture. Samples (3 repeats for each condition) were either stored at 4 °C, heated at 80 °C for 1 min or heated at 90 °C for 1 min. The heated samples were then cooled down to 4 °C, and all samples were shipped with an ice pack to Phytex for activity assay.

3.5 Appendix to Chapter 3: Supplementary Figures

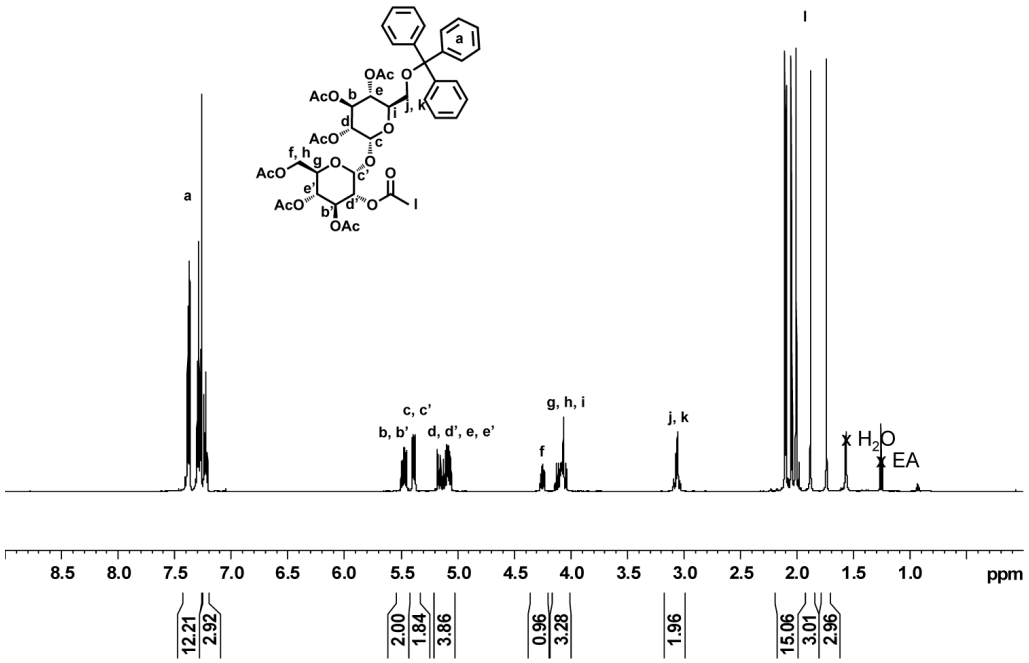

Figure 3-13. ^{1}H NMR spectrum of **1** (in $CDCl_3$).

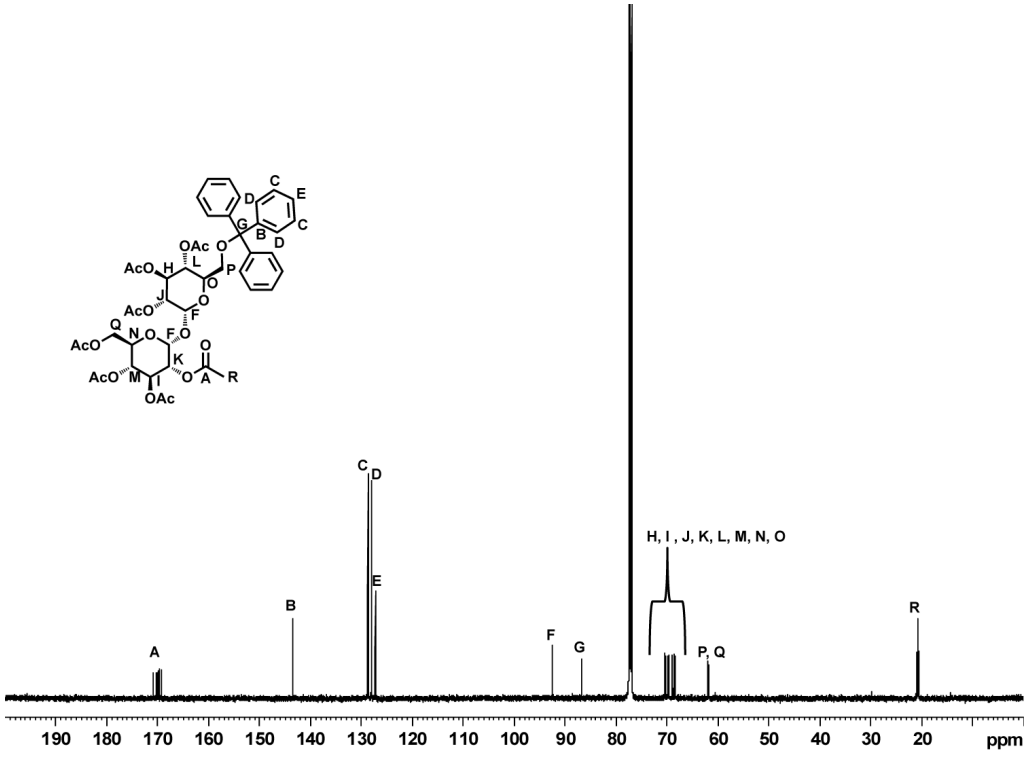

Figure 3-14. ^{13}C NMR spectrum of **1** (in $CDCl_3$).

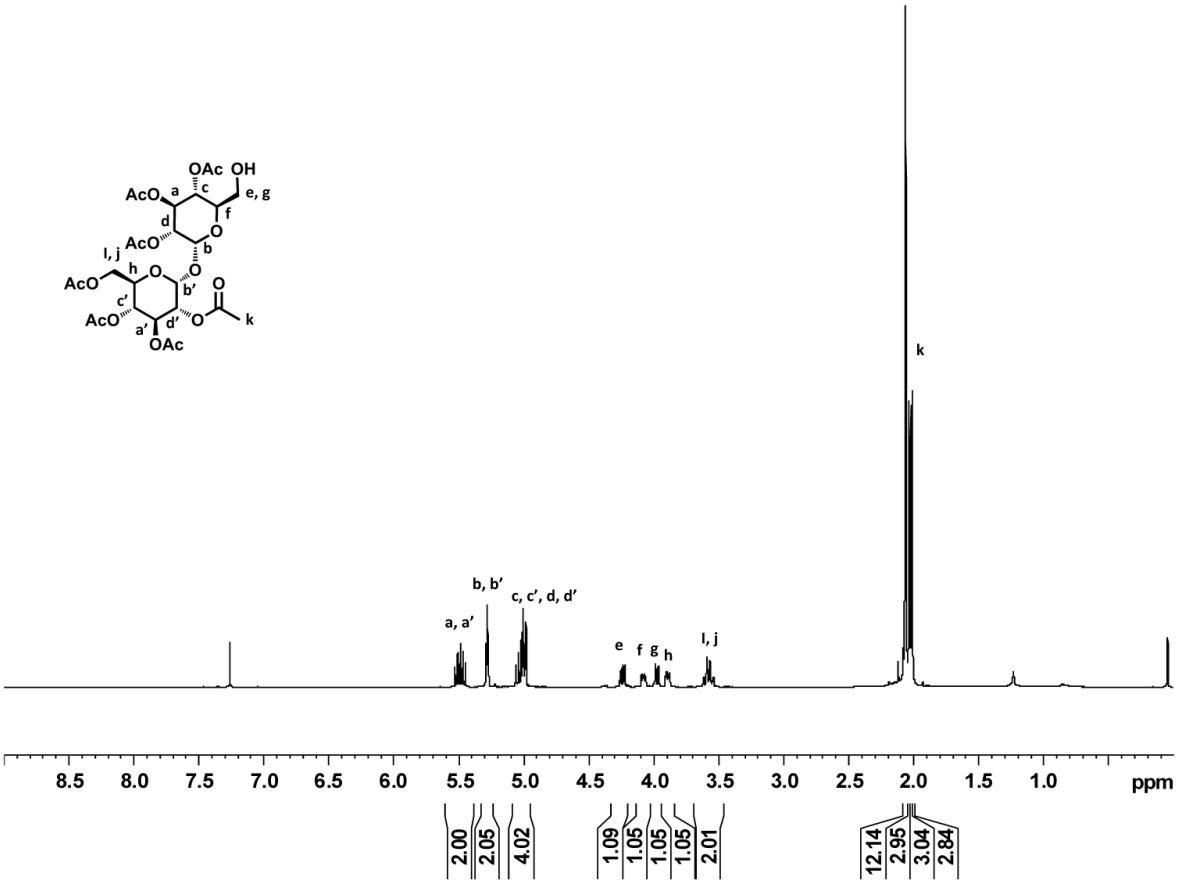

Figure 3-15. ^{1}H NMR spectrum of **2** (in $CDCl_3$).

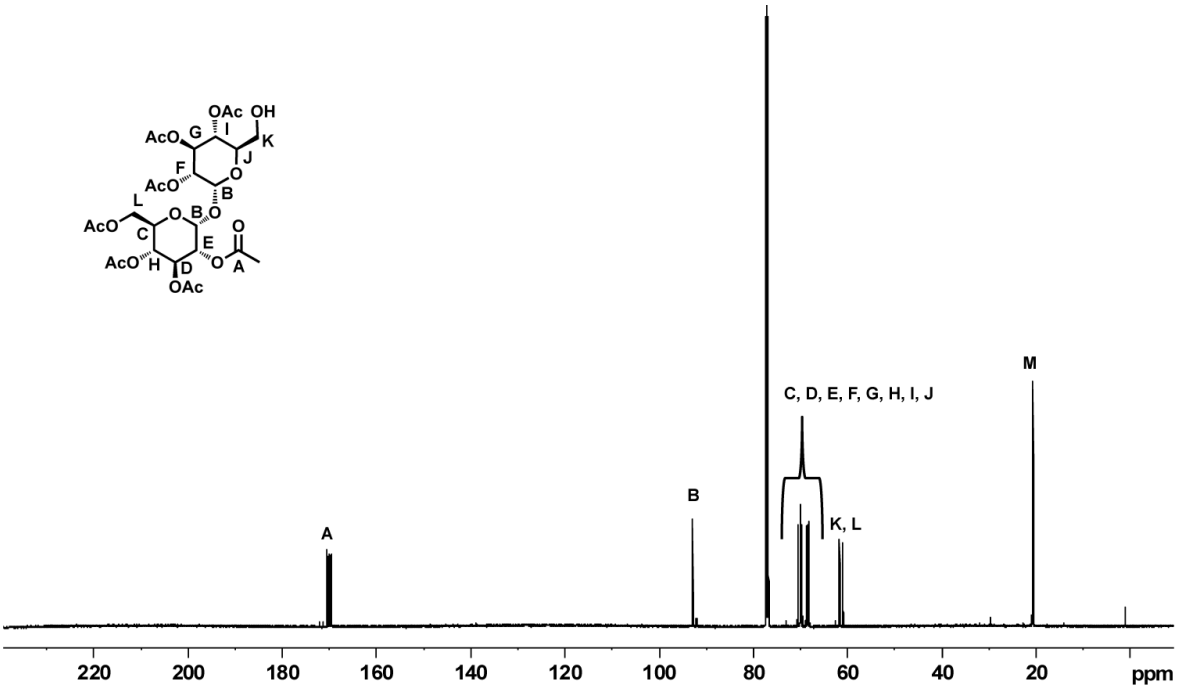

Figure 3-16. ^{13}C NMR spectrum of **2** (in $CDCl_3$).

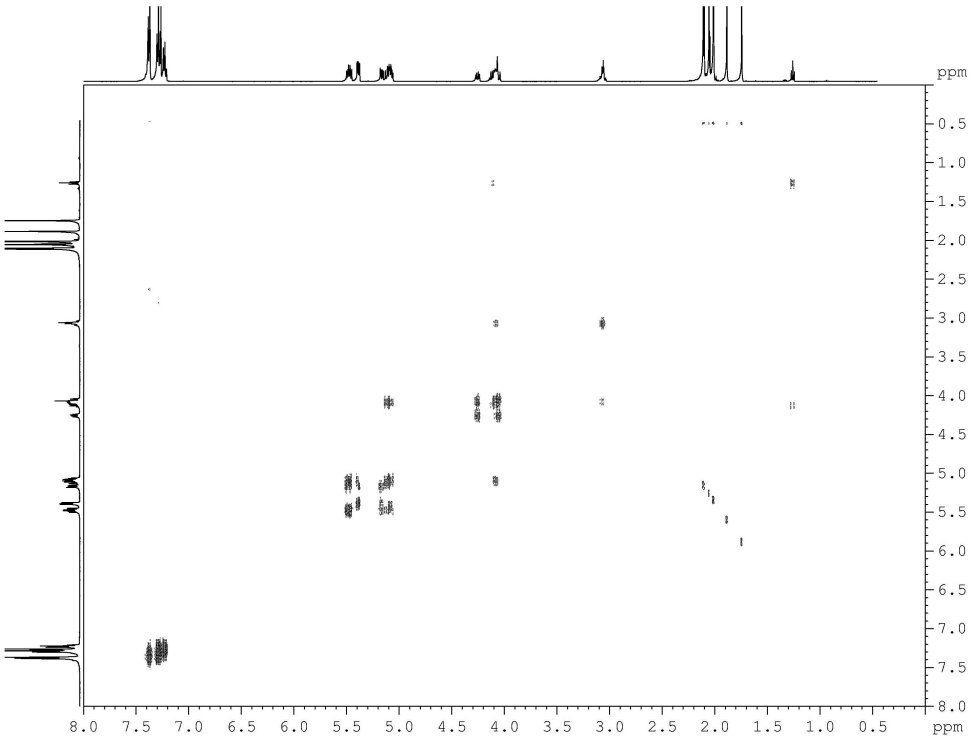

Figure 3-17. 2D COSY NMR spectrum of **1** (in $CDCl_3$).

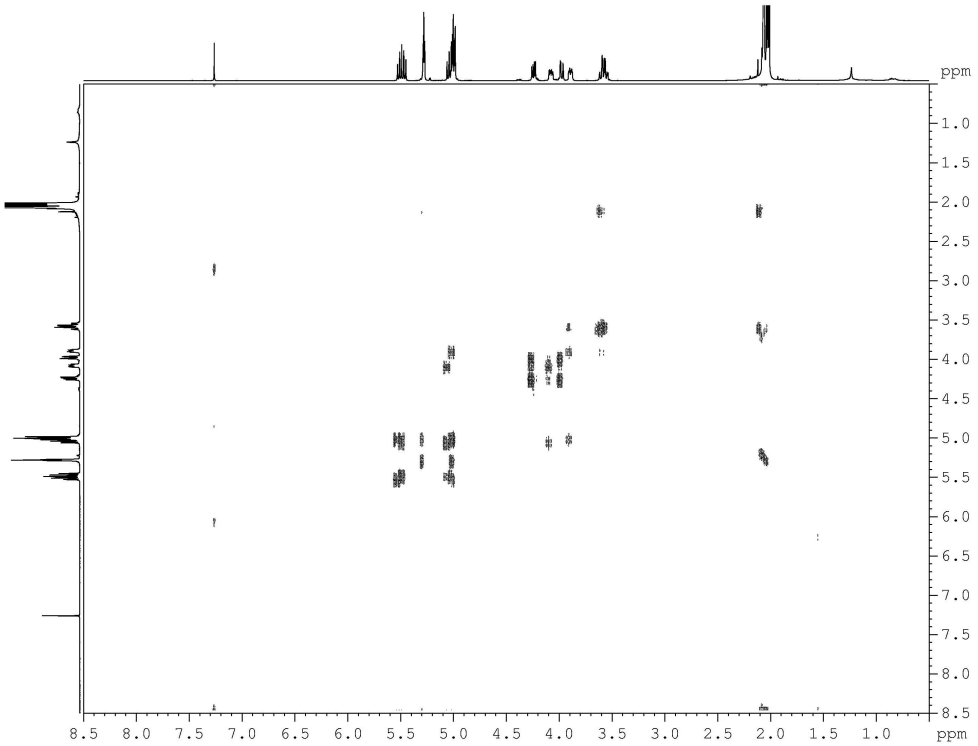

Figure 3-18. 2D COSY NMR spectrum of **2** (in $CDCl_3$).

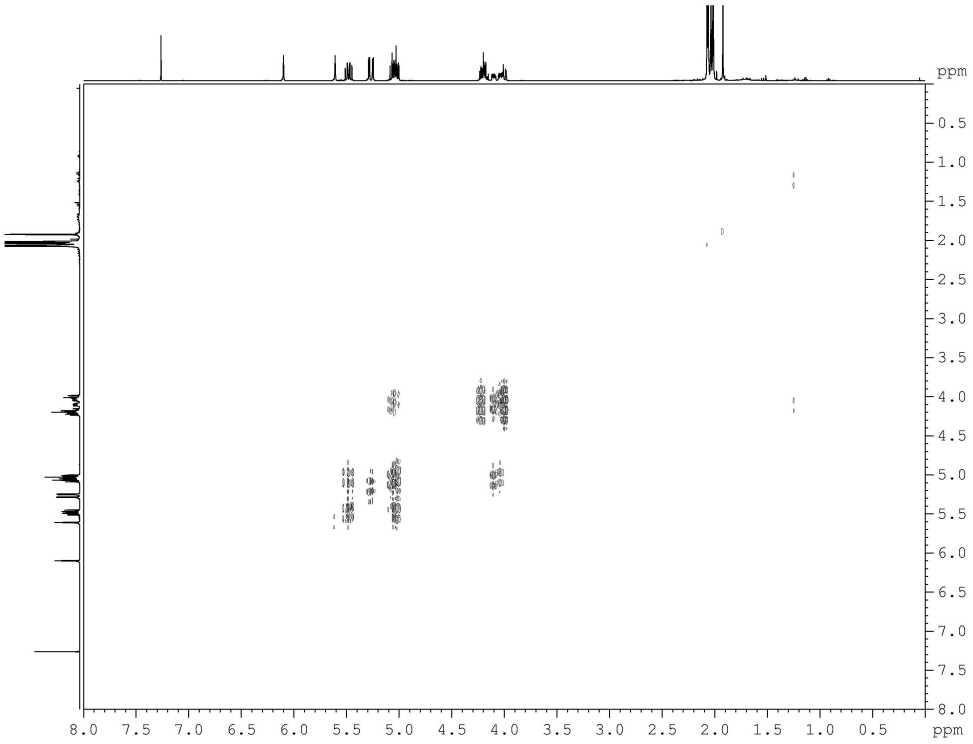

Figure 3-19. 2D COSY NMR spectrum of **M4′** (in $CDCl_3$).

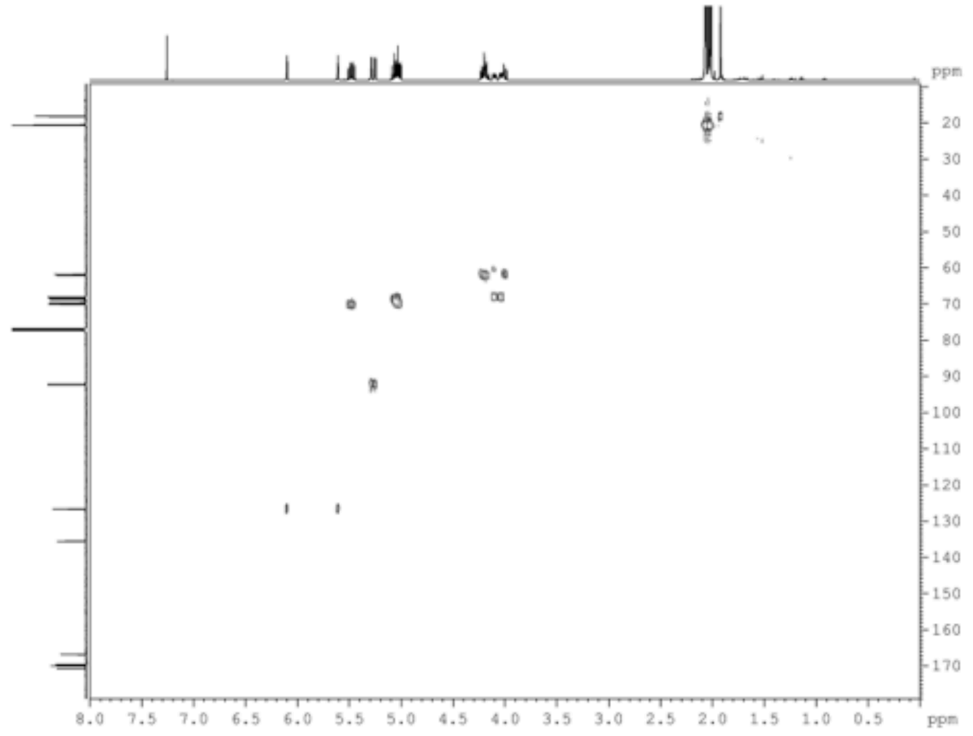

Figure 3-20. 2D HSQC NMR spectrum of **M4′** (in $CDCl_3$).

3.6 References

‡ Portions of this chapter have been published as: Lee, J.; Lin, E.-W.; Lau, U. Y.; Hedrick, J. L.; Bat, E.; Maynard, H. D., "Trehalose Glycopolymers as Excipients for Protein Stabilization," *Biomacromolecules* **2013,** *14*, 2561-2569.

(1) Brannigan, J. A.; Wilkinson, A. J. "Protein Engineering 20 Years On" *Nat. Rev. Mol. Cell Biol.* **2002**, *3*, 964-970.

(2) Banga, A. K. "Therapeutic Peptides and Proteins: Formulation, Processing, and Delivery Systems, Second Edition" *Therapeutic Peptides and Proteins: Formulation, Processing, and Delivery Systems, Second Edition* **2006**.

(3) Kamerzell, T. J.; Esfandiary, R.; Joshi, S. B.; Middaugh, C. R.; Volkin, D. B. "Protein-Excipient Interactions: Mechanisms and Biophysical Characterization Applied to Protein Formulation Development" *Adv. Drug Delivery Rev.* **2011**, *63*, 1118-1159.

(4) Ohtake, S.; Kita, Y.; Arakawa, T. "Interactions of Formulation Excipients with Proteins in Solution and in the Dried State" *Adv. Drug Delivery Rev.* **2011**, *63*, 1053-1073.

(5) Zhang, Y.; Cremer, P. S. In *Annual Review of Physical Chemistry* 2010; Vol. 61, p 63-83.

(6) Kaushik, J. K.; Bhat, R. "Why Is Trehalose an Exceptional Protein Stabilizer? An Analysis of the Thermal Stability of Proteins in the Presence of the Compatible Osmolyte Trehalose" *J. Biol. Chem.* **2003**, *278*, 26458-26465.

(7) Kendrick, B. S.; Chang, B. S.; Arakawa, T.; Peterson, B.; Randolph, T. W.; Manning, M. C.; Carpenter, J. F. "Preferential Exclusion of Sucrose from Recombinant Interleukin-1 Receptor Antagonist: Role in Restricted Conformational Mobility and Compaction of Native State" *Proc. Natl. Acad. Sci. U. S. A.* **1997**, *94*, 11917-11922.

(8) Kadoya, S.; Fujii, K.; Izutsu, K.-i.; Yonemochi, E.; Terada, K.; Yomota, C.; Kawanishi, T. "Freeze-Drying of Proteins with Glass-Forming Oligosaccharide-Derived Sugar Alcohols" *Int. J. Pharm.* **2010**, *389*, 107-113.

(9) Kim, Y. S.; Jones, L. S.; Dong, A.; Kendrick, B. S.; Chang, B. S.; Manning, M. C.; Randolph, T. W.; Carpenter, J. F. "Effects of Sucrose on Conformational Equilibria and Fluctuations within the Native-State Ensemble of Proteins" *Protein Sci.* **2003**, *12*, 1252-1261.

(10) Back, J. F.; Oakenfull, D.; Smith, M. B. "Increased Thermal-Stability of Proteins in the Presence of Sugars and Polyols" *Biochemistry* **1979**, *18*, 5191-5196.

(11) Gekko, K.; Timasheff, S. N. "Mechanism of Protein Stabilization by Glycerol - Preferential Hydration in Glycerol-Water Mixtures" *Biochemistry* **1981**, *20*, 4667-4676.

(12) Arakawa, T.; Timasheff, S. N. "The Stabilization of Proteins by Osmolytes" *Biophys. J.* **1985**, *47*, 411-414.

(13) Auton, M.; Bolen, D. W.; Rosgen, J. "Structural Thermodynamics of Protein Preferential Solvation: Osmolyte Solvation of Proteins, Aminoacids, and Peptides" *Proteins* **2008**, *73*, 802-813.

(14) Bolen, D. W. "Effects of Naturally Occurring Osmolytes on Protein Stability and Solubility: Issues Important in Protein Crystallization" *Methods* **2004**, *34*, 312-322.

(15) Yoshioka, S.; Aso, Y.; Kojima, S. "Dependence of the Molecular Mobility and Protein Stability of Freeze-Dried Gamma-Globulin Formulations on the Molecular Weight of Dextran" *Pharm. Res.* **1997**, *14*, 736-741.

(16) Garzon-Rodriguez, W.; Koval, R. L.; Chongprasert, S.; Krishnan, S.; Randolph, T. W.; Warne, N. W.; Carpenter, J. F. "Optimizing Storage Stability of Lyophilized Recombinant Human Interleukin-11 with Disaccharide/Hydroxyethyl Starch Mixtures" *J. Pharm. Sci.* **2004**, *93*, 684-696.

(17) Gombotz, W. R.; Pankey, S. C.; Phan, D.; Drager, R.; Donaldson, K.; Antonsen, K. P.; Hoffman, A. S.; Raff, H. V. "The Stabilization of a Human-IgM Monoclonal-Antibody with Poly(Vinylpyrrolidone)" *Pharm. Res.* **1994**, *11*, 624-632.

(18) Keefe, A. J.; Jiang, S. "Poly(Zwitterionic)Protein Conjugates Offer Increased Stability without Sacrificing Binding Affinity or Bioactivity" *Nat. Chem.* **2012**, *4*, 59-63.

(19) Sharma, K. S.; Durand, G.; Giusti, F.; Olivier, B.; Fabiano, A.-S.; Bazzacco, P.; Dahmane, T.; Ebel, C.; Popot, J.-L.; Pucci, B. "Glucose-Based Amphiphilic Telomers Designed to Keep Membrane Proteins Soluble in Aqueous Solutions: Synthesis and Physicochemical Characterization" *Langmuir* **2008**, *24*, 13581-13590.

(20) Bazzacco, P.; Sharma, K. S.; Durand, G.; Giusti, F.; Ebel, C.; Popot, J. L.; Pucci, B. "Trapping and Stabilization of Integral Membrane Proteins by Hydrophobically Grafted Glucose-Based Telomers" *Biomacromolecules* **2009**, *10*, 3317-3326.

(21) Bazzacco, P.; Billon-Denis, E.; Sharma, K. S.; Catoire, L. J.; Mary, S.; Le Bon, C.; Point, E.; Baneres, J.-L.; Durand, G.; Zito, F.; Pucci, B.; Popot, J.-L. "Nonionic Homopolymeric

Amphipols: Application to Membrane Protein Folding, Cell-Free Synthesis, and Solution Nuclear Magnetic Resonance" *Biochemistry* **2012**, *51*, 1416-1430.

(22) Arakawa, T.; Tsumoto, K.; Kita, Y.; Chang, B.; Ejima, D. "Biotechnology Applications of Amino Acids in Protein Purification and Formulations" *Amino Acids* **2007**, *33*, 587-605.

(23) Chen, B.; Bautista, R.; Yu, K.; Zapata, G. A.; Mulkerrin, M. G.; Chamow, S. M. "Influence of Histidine on the Stability and Physical Properties of a Fully Human Antibody in Aqueous and Solid Forms" *Pharm. Res.* **2003**, *20*, 1952-1960.

(24) Chang, B. S.; Kendrick, B. S.; Carpenter, J. F. "Surface-Induced Denaturation of Proteins During Freezing and Its Inhibition by Surfactants" *J. Pharm. Sci.* **1996**, *85*, 1325-1330.

(25) Teramoto, N.; Sachinvala, N. D.; Shibata, M. "Trehalose and Trehalose-Based Polymers for Environmentally Benign, Biocompatible and Bioactive Materials" *Molecules* **2008**, *13*, 1773-1816.

(26) Ohtake, S.; Wang, Y. J. "Trehalose: Current Use and Future Applications" *J. Pharm. Sci.* **2011**, *100*, 2020-2053.

(27) Jain, N. K.; Roy, I. "Trehalose and Protein Stability" *Current protocols in protein science* **2010**, *Chapter 4*, Unit 4.9.

(28) Teramoto, N.; Shibata, M. "Trehalose-Based Thermosetting Resins. I. Synthesis and Thermal Properties of Trehalose Vinylbenzyl Ether" *J. Appl. Polym. Sci.* **2004**, *91*, 46-51.

(29) Kurita, K.; Masuda, N.; Aibe, S.; Murakami, K.; Ishii, S.; Nishimura, S. I. "Synthetic Carbohydrate Polymers Containing Trehalose Residues in the Main-Chain - Preparation and Characteristic Properties" *Macromolecules* **1994**, *27*, 7544-7549.

(30) Teramoto, N.; Abe, Y.; Enomoto, A.; Watanabe, D.; Shibata, M. "Novel Synthetic Route of a Trehalose-Based Linear Polymer by Ring Opening of Two Epoxy Groups with Aliphatic Diamine" *Carbohydr. Polym.* **2005**, *59*, 217-224.

(31) Srinivasachari, S.; Liu, Y. M.; Zhang, G. D.; Prevette, L.; Reineke, T. M. "Trehalose Click Polymers Inhibit Nanoparticle Aggregation and Promote pDNA Delivery in Serum" *J. Am. Chem. Soc.* **2006**, *128*, 8176-8184.

(32) Teramoto, N.; Arai, Y.; Shibata, M. "Thermo-Reversible Diels-Alder Polymerization of Difurfurylidene Trehalose and Bismaleimides" *Carbohydr. Polym.* **2006**, *64*, 78-84.

(33) Teramoto, N.; Unosawa, M.; Matsushima, S.; Shibata, M. "Synthesis and Properties of Thermoplastic Alternating Copolymers Containing Trehalose and Siloxane Units by Hydrosilylation Reaction" *Polym. J.* **2007**, *39*, 975-981.

(34) Kukowka, S.; Maglinska-Solich, J. "Alpha,Alpha-Trehalose-Based Polyacetals and Macrocyclic Acetals" *Carbohydr. Polym.* **2010**, *80*, 711-719.

(35) Teramoto, N.; Niwa, M.; Shibata, M. "Synthesis and Properties of Trehalose-Based Flexible Polymers Prepared from Difurfurylidene Trehalose and Maleimide-Terminated Oligo(Dimethylsiloxane) by Diels-Alder Reactions" *Materials* **2010**, *3*, 369-385.

(36) Mancini, R. J.; Lee, J.; Maynard, H. D. "Trehalose Glycopolymers for Stabilization of Protein Conjugates to Environmental Stressors" *J. Am. Chem. Soc.* **2012**, *134*, 8474-8479.

(37) Lee, J.; Lin, E. W.; Lau, U. Y.; Hedrick, J. L.; Bat, E.; Maynard, H. D. "Trehalose Glycopolymers as Excipients for Protein Stabilization" *Biomacromolecules* **2013**, *14*, 2561-2569.

(38) Wada, M.; Miyazawa, Y.; Miura, Y. "A Specific Inhibitory Effect of Multivalent Trehalose toward Aβ(1-40) Aggregation" *Polym. Chem.* **2011**, *2*, 1822-1829.

(39) Sizovs, A.; Xue, L.; Tolstyka, Z. P.; Ingle, N. P.; Wu, Y. Y.; Cortez, M.; Reineke, T. M. "Poly(Trehalose): Sugar-Coated Nanocomplexes Promote Stabilization and Effective Polyplex-Mediated siRNA Delivery" *J. Am. Chem. Soc.* **2013**, *135*, 15417-15424.

(40) Vazquez-Dorbatt, V.; Maynard, H. D. "Biotinylated Glycopolymers Synthesized by Atom Transfer Radical Polymerization" *Biomacromolecules* **2006**, *7*, 2297-2302.

(41) Ambrosi, M.; Batsanov, A. S.; Cameron, N. R.; Davis, B. G.; Howard, J. A. K.; Hunter, R. "Influence of Preparation Procedure on Polymer Composition: Synthesis and Characterisation of Polymethacrylates Bearing β-D-Glucopyranoside and β-D-Galactopyranoside Residues" *J. Chem. Soc., Perkin Trans. 1* **2002**, 45-52.

(42) Asad, S.; Torabi, S. F.; Fathi-Roudsari, M.; Ghaemi, N.; Khajeh, K. "Phosphate Buffer Effects on Thermal Stability and H_2O_2-Resistance of Horseradish Peroxidase" *Int. J. Biol. Macromol.* **2011**, *48*, 566-570.

(43) Josephy, P. D.; Eling, T.; Mason, R. P. "The Horseradish Peroxidase-Catalyzed Oxidation of 3,5,3',5'-Tetramethylbenzidine-Free-Radical and Charge-Transfer Complex Intermediates" *J. Biol. Chem.* **1982**, *257*, 3669-3675.

(44) Pikal-Cleland, K. A.; Carpenter, J. F. "Lyophilization-Induced Protein Denaturation in Phosphate Buffer Systems: Monomeric and Tetrameric β-Galactosidase" *J. Pharm. Sci.* **2001**, *90*, 1255-1268.

(45) Craven, G. R.; Steers, E.; Anfinsen, C. B. "Purification Composition and Molecular Weight of β-Galactosidase of Escherichia Coli K12" *J. Biol. Chem.* **1965**, *240*, 2468-&.

(46) Paz-Alfaro, K. J.; Ruiz-Granados, Y. G.; Uribe-Carvajal, S.; Sampedro, J. G. "Trehalose-Mediated Thermal Stabilization of Glucose Oxidase from Aspergillus Niger" *J. Biotechnol.* **2009**, *141*, 130-136.

(47) Zhou, M. J.; Diwu, Z. J.; PanchukVoloshina, N.; Haugland, R. P. "A Stable Nonfluorescent Derivative of Resorufin for the Fluorometric Determination of Trace Hydrogen Peroxide: Applications in Detecting the Activity of Phagocyte Nadph Oxidase and Other Oxidases" *Anal. Biochem.* **1997**, *253*, 162-168.

(48) Haefner, S.; Knietsch, A.; Scholten, E.; Braun, J.; Lohscheidt, M.; Zelder, O. "Biotechnological Production and Applications of Phytases" *Appl. Microbiol. Biotechnol.* **2005**, *68*, 588-597.

(49) Zhou, J. R.; Erdman, J. W. "Phytic Acid in Health and Disease" *Crit. Rev. Food Sci. Nutr.* **1995**, *35*, 495-508.

(50) Rodriguez, E.; Wood, Z. A.; Karplus, P. A.; Lei, X. G. "Site-Directed Mutagenesis Improves Catalytic Efficiency and Thermostability of Escherichia Coli pH 2.5 Acid Phosphatase/Phytase Expressed in Pichia Pastoris" *Arch. Biochem. Biophys.* **2000**, *382*, 105-112.

(51) Han, Y. M.; Lei, X. G. "Role of Glycosylation in the Functional Expression of an Aspergillus Niger Phytase (phyA) in Pichia Pastoris" *Arch. Biochem. Biophys.* **1999**, *364*, 83-90.

(52) Zhang, L. H.; Wang, Y.; Zhang, C. Y.; Wang, Y. J.; Zhu, D. C.; Wang, C. X.; Nagata, S. "Supplementation Effect of Ectoine on Thermostability of Phytase" *J. Biosci. Bioeng.* **2006**, *102*, 560-563.

Chapter 4

Synthesis and Investigation of

siRNA-Trehalose Glycopolymer Conjugates

4.1 Introduction

Small interfering RNAs (siRNA) are promising therapeutic agents that induce the RNA interference (RNAi) pathway and achieve sequence-specific gene silencing by degrading a target messenger RNA (mRNA).[1] However, efficient delivery of siRNA to the cytoplasm is currently a major challenge.[2] *In vivo*, siRNA is rapidly degraded by endo- and exo-nucleases.[3-5] Also, negatively charged siRNA is repelled from cell membranes.[6-8] To enhance its stability and pharmacokinetics, covalent attachment of linear or branched poly(ethylene glycol) (PEG) to siRNA has been employed in many examples.[9-21]

Controlled living radical polymerization (CRP) techniques have allowed the formation of precise polymeric drug delivery structures, which is advantageous for the design of siRNA delivery systems to build in functionalities such as serum stability, targeting, or endosomal release.[22-24] Atom transfer radical polymerization (ATRP) and reversible addition-fragmentation chain transfer (RAFT) polymerization enable great control over the molecular weight, polymer architecture, and block composition of synthesized polymers.[25-27] Using CRP techniques, end-functionalized polymers can be easily synthesized from appropriate initiators or chain transfer agents (CTAs), enabling the formation of siRNA-polymer conjugates.[28-33] Our group has synthesized well-defined comb-type PEGs (poly(PEG methyl ether acrylates), pPEGAs) and demonstrated that their conjugation to siRNA enhances serum stability, nuclease resistance, and gene transfection efficiency.[28,29] Recently, Averick *et al.* used copper-catalyzed azide-alkyne cycloaddition (CuAAC) to prepare conjugates of PEG-methacrylate-pOEOMA$_{475}$, pOEOMA$_{300}$-*co*-MeO_2MA, and pOEOMA$_{475}$-*co*-DMAEMA and showed that the conjugated polymers facilitated cell internalization of the siRNA.[33]

Although many systems have been developed to lyophilize plasmid DNA or oligonucleotide polyplexes,[34-36] there are only limited examples of stabilizing siRNA polyplexes for long-term storage.[37-40] Recently, Kasper *et al*. have shown that adding 5-10% sucrose or lactosucrose to siRNA/oligoaminoamide polyplexes maintained particle size and gene silencing efficiency after six months at storage temperatures up to 40 °C.[41] Armstrong *et al.* published that without the addition of sucrose, PEGylation of DNA lipoplexes was insufficient to maintain original particles sizes after agitation, freeze-thawing, and lyophilization.[42] In our earlier publication, we have shown that the conjugation of trehalose polymer protects lysozyme during lyophilization and heat better than addition of large amount of trehalose molecules.[43] Therefore, we proposed that incorporating trehalose-based polymers into the siRNA-polymer conjugates would increase siRNA stability, and increase its feasibility as a therapeutic agent by simplifying transportation and storage. In this chapter, we report on the conjugation of different sizes of trehalose glycopolymers synthesized by RAFT polymerization to thiol-modified siRNA and the stability of the resulting conjugates.

4.2 Results and Discussion

4.2.1 Conjugation of Trehalose Glycopolymers and PEG-based Polymers

Previously synthesized as outlined in our earlier report, three styrene-based trehalose polymers with pyridyl disulfide end-groups were utilized in this study for siRNA conjugation.[43] Here, they are referred to as **Poly A**, **Poly B**, and **Poly C**, with molecular weights (M_n from GPC) of 8.0 kDa, 15.4 kDa, and 24.5 kDa, respectively (**Scheme 4-1**). Other pyridyl disulfide end-functionalized polymers were also prepared for siRNA conjugation. Polymethacrylate-based trehalose glycopolymer (referred to as **Poly M**, 18.3 kDa) was synthesized by ATRP (**Scheme 4-2**, see Appendix **Figure 4-6** for NMR spectrum) and poly(poly(ethylene glycol) methyl ether acrylate) (pPEGA, 12.0 kDa) was synthesized by RAFT polymerization (**Scheme 4-3**, see Appendix **Figure 4-7** for NMR spectrum). Linear PEG (pyridyl disulfide PEG methyl ether, 10 kDa) was purchased. The syntheses of the methacrylate trehalose monomer[44], pyridyl disulfide ATRP initiator[45], and pyridyl disulfide CTA[43] have been described in our previous reports.

Scheme 4-1. Synthesis of **Poly A**, **Poly B**, and **Poly C** by RAFT polymerization.[43]

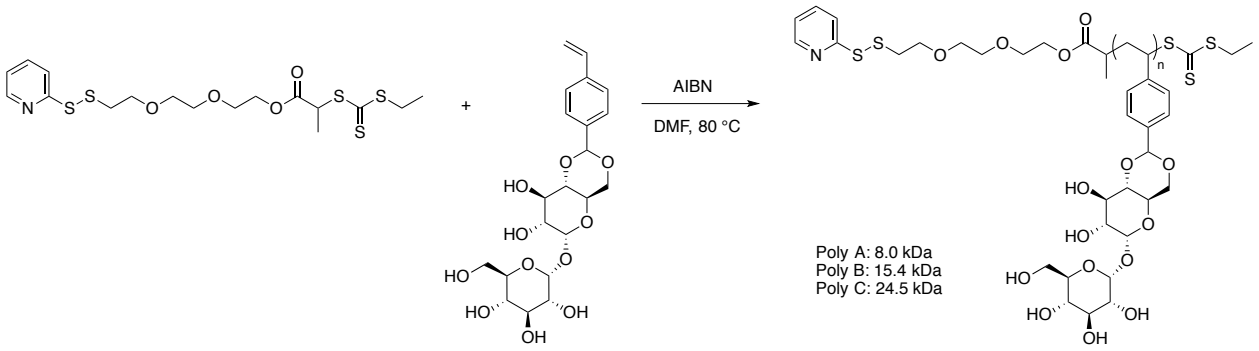

Scheme 4-2. Synthesis of **Poly M** by ATRP.

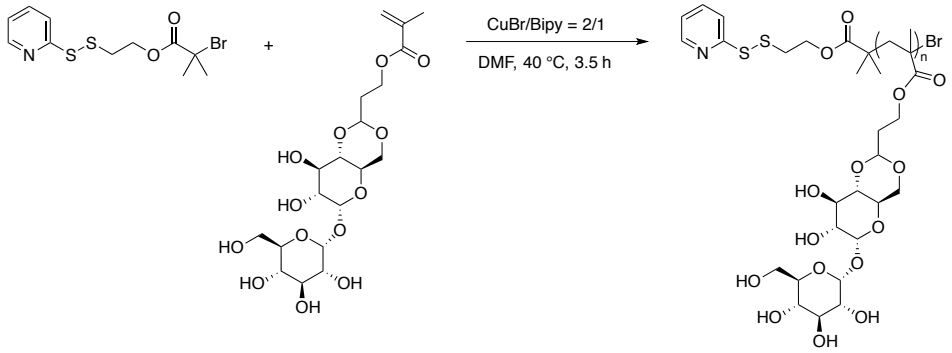

Scheme 4-3. Synthesis of pPEGA by RAFT polymerization.

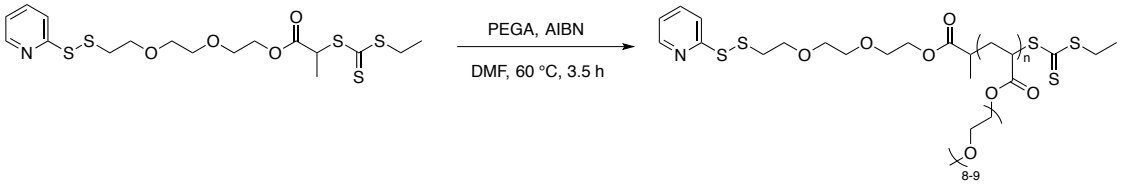

Thiol-modified siRNA was deprotected by reducing the disulfide bond to provide a free thiol on the 5' end of the sense strand. **Poly A**, **Poly B**, and **Poly C** were then conjugated to siRNA through disulfide exchange, following reported procedures (**Scheme 4-4)**.[28] Using the same method, the other pyridyl disulfide end-functionalized polymers were also conjugated to siRNA (**Figure 4-1**).

Scheme 4-4. Conjugation of siRNA to **Poly A**, **Poly B**, and **Poly C**.

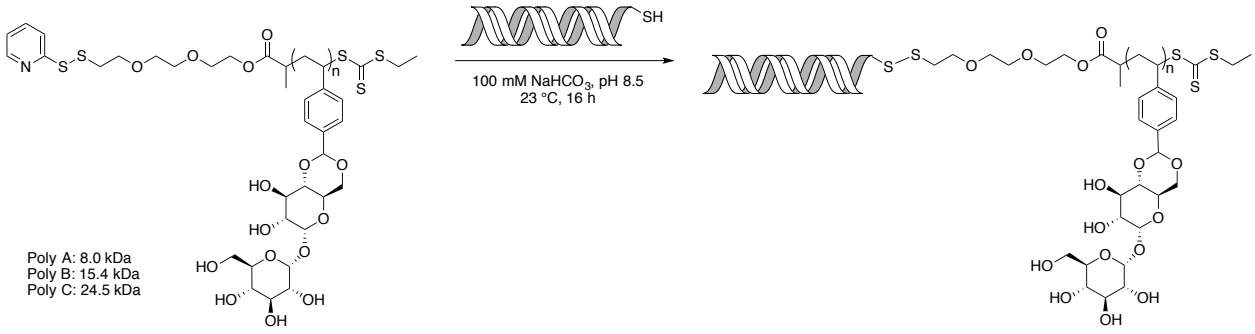

On a Tris/Borate/EDTA (TBE)-Urea PAGE gel, siRNA and the conjugates were analyzed under both reducing and non-reducing conditions (**Figure 4-1**). Under reducing conditions, the disulfide linkages between the polymers and siRNA were cleaved, and only the band representing free siRNA was observed. Under non-reducing conditions, the higher molecular weight smears of the conjugates were observed, along with unreacted free siRNA. Based on the band intensities of conjugate and unreacted siRNA, the conjugation yield of the polymers' to form conjugates **A**, **B**, and **C** were calculated as 83%, 72%, and 71%, respectively. Using the same method, PEG conjugate, conjugate **M**, and pPEGA conjugate were produced in

55%, 88%, and 68% yield, respectively. From the results, trehalose-based polymers generally resulted in higher conjugate yields than PEG-based polymers, which was not expected, since trehalose polymers are much more bulky and usually result in lower conjugation yields with proteins.[43]

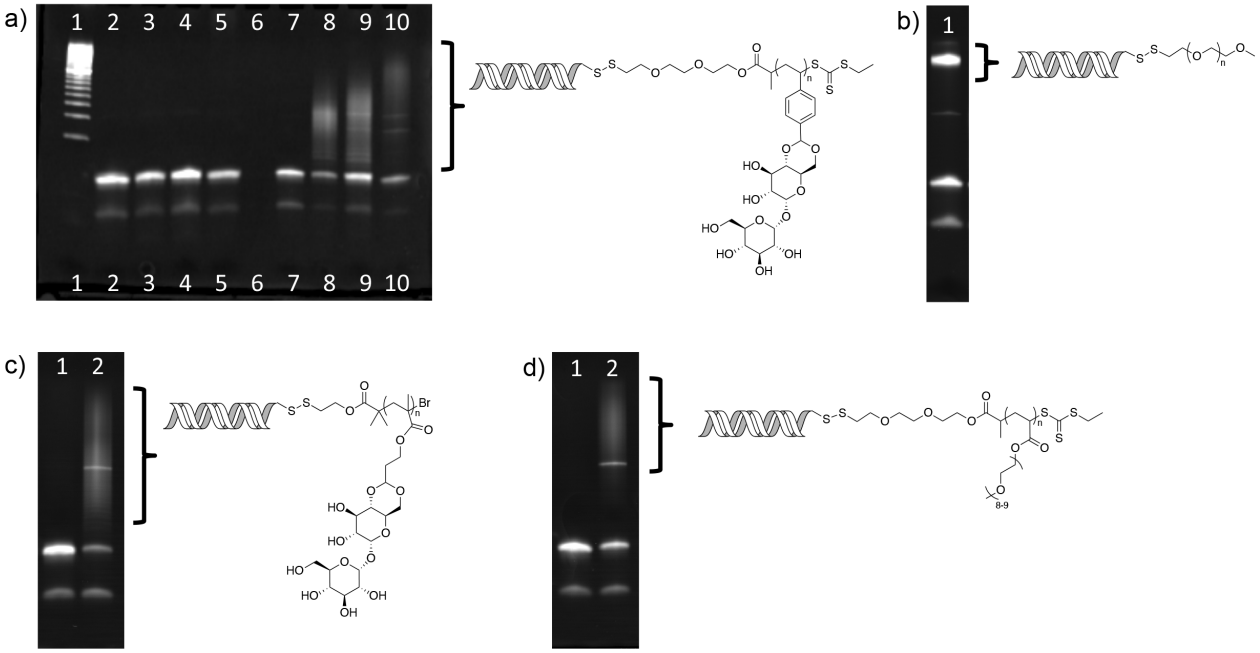

Figure 4-1. PAGE analysis of the conjugation results of siRNA to a) **Poly A**, **Poly B**, and **Poly C**. Lane 1: DNA ladder; lane 2: thiol-modified siRNA (reduced); lane 3: conjugate **A** (reduced); lane 4: conjugate **B** (reduced); lane 5: conjugate **C** (reduced); lane 7: thiol-modified siRNA; lane 8: conjugate **A**; lane 9: conjugate **B**; lane 10: conjugate **C**; b) pyridyl disulfide end-functionalized linear mPEG. Lane 1: PEG conjugate; c) **Poly M**. Lane 1: conjugate **M** (reduced); lane 2: conjugate **M**; d) pPEGA. Lane 1: pPEGA conjugate (reduced); lane 3: pPEGA conjugate. The lowest band is single-stranded siRNA.

4.2.2 Nuclease and Serum Stability of siRNA-Trehalose Polymer Conjugates

To investigate the stability of siRNA-polymer conjugates, the conjugates were incubated with nuclease. RNase ONE^{TM} Ribonuclease degrades RNA readily and was therefore chosen as an investigation tool. Unpurified conjugates (containing unreacted siRNA and excess polymer) were used for the following experiments. After 5 or 10 minutes of incubation with RNase ONE at 37°C, naked siRNA was mostly degraded as observed by PAGE analysis (**Figure 4-2**). Conjugate **A** also degraded readily over the timeframe, with 59% and 39% retention after 5 min and 10 min, respectively. Higher molecular weight conjugates (**B** and **C**) also degraded readily (data not shown). However, 10 kDa linear PEG conjugate showed higher stability (~75% retention after 10 min) towards RNase ONE degradation.

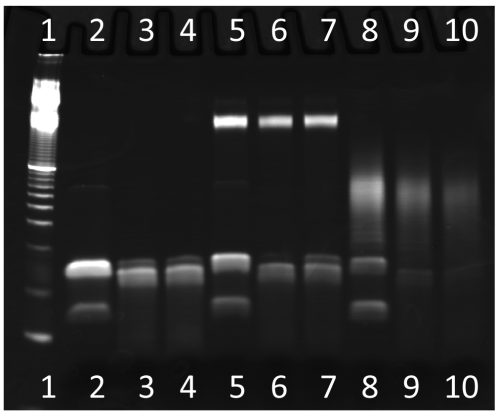

Figure 4-2. PAGE analysis of the effect of RNase ONE towards naked siRNA, 10 kDa PEG conjugate, and conjugate **A**. Lane 1: DNA ladder; lane 2: naked siRNA; lane 3: naked with RNase ONE (5 min); lane 4: naked siRNA with RNase ONE (10 min); lane 5: PEG conjugate; lane 6: PEG conjugate with RNase ONE (5 min); lane 7: PEG conjugate with RNase ONE (10 min); lane 8: conjugate **A**; lane 9: conjugate **A** with RNase ONE (5 min); lane 10: conjugate **A** with RNase ONE (10 min).

Next, the stabilities of naked siRNA and conjugate **A** in 80% calf bovine serum (CBS) were tested. The degradation trend was observed by taking time points at 0, 1, 2, 3, and 4 hours (**Figure 4-3**). After 4 hours of incubation in 80% CBS at 37 °C, conjugate **A** was still observable with ~40% retention, while naked siRNA had almost entirely degraded (~10% retention). Data of this experiment with 10 kDa PEG conjugate is not shown, because the PEG conjugate was unable to be observed and quantified due to its overlap with serum on the gel. The results above indicate that the conjugation of trehalose polymers to siRNA might not significantly increase its stability towards nucleases and serum conditions as we anticipated. A recent report has discussed the destabilization of double stranded DNA (dsDNA) in solution facilitated by addition of trehalose.[46] The effect was caused by the direct interaction of trehalose forming hydrogen bonds with DNA bases, disrupting base pair interactions, and lowering the melting temperature of DNA. Thus the trehalose polymers (attached or excess) may disrupt siRNA similarly. However, siRNA-trehalose polymer conjugates may still have positive effects such as stabilization in dry state or to lyophilized conditions.

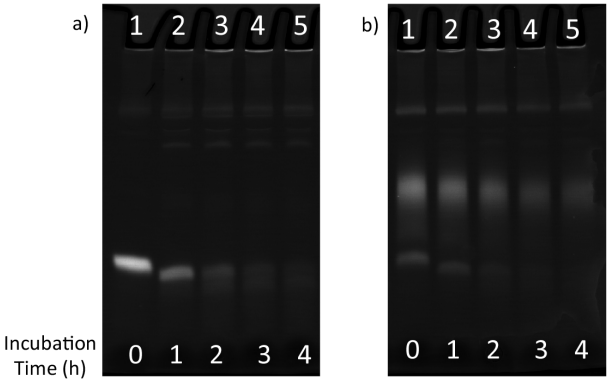

Figure 4-3. PAGE analysis of the effect of 80% Calf Bovine Serum (CBS) towards: a) naked siRNA. Lane 1: 0 h; lane 2: 1 h; lane 3: 2 h; lane 4: 3 h; lane 5: 4 h; b) conjugate **A**. Lane 1: 0 h; lane 2: 1 h; lane 3: 2 h; lane 4: 3 h; lane 5: 4 h.

4.2.3 Purification of siRNA-Trehalose Polymer Conjugates

The siRNA-polymer conjugate crude mixtures contained free siRNA and excess polymer. We intended to isolate the conjugates by HPLC using a C18 column (150 x 4.6 mm^2, 5 µm, Phenomenex) and a UV detector set at 220 nm and 260 nm. 220 nm and 260 nm were employed to detect the unconjugated polymers, and the free siRNA and siRNA-polymer conjugates, respectively. The fractions were collected and analyzed by gel electrophoresis (**Figure 4-4**). From 260 nm absorbance and gel analysis, we observed that siRNA elutes earlier then the free polymers and the conjugate. Conjugate **A** was observed to be entirely separated from siRNA beyond lane 7, confirmed by the absence of the free siRNA band in lanes 8, 9, and 10. However, elution of unconjugated polymer (does not stain on gel) overlapped with the conjugate, as observed from the HPLC trace. Dialysis was further performed to remove the remaining unconjugated polymer based on the large molecular weight difference, but was not successful.

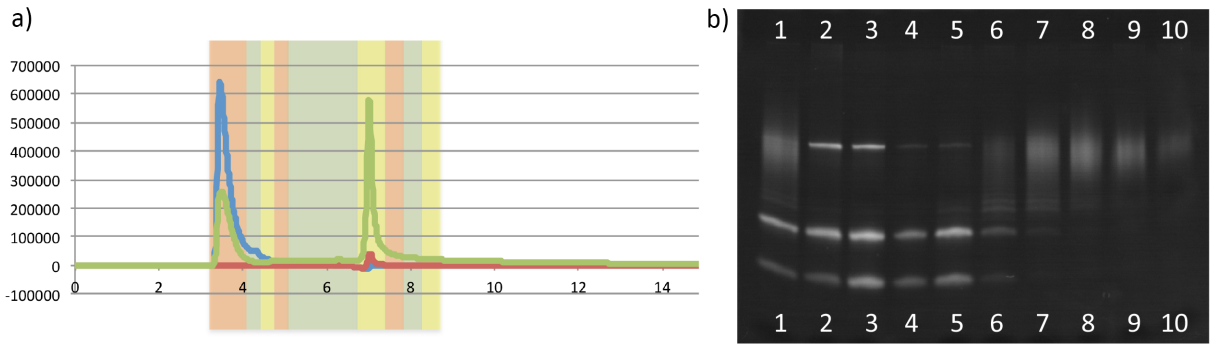

Figure 4-4. a) HPLC trace (260 nm) of siRNA (blue), **Poly A** (red), and conjugate **A** (green). The colored boxes represent the fractions collected; b) PAGE analysis of the fractions collected from HPLC purification. Lane 1: conjugate **A** crude mixture; lanes 2-10: collected approximately from 3-9 minutes of retention time. Conjugate **A** can be separated from unconjugated siRNA (after lane 7).

To remove trehalose polymer from the conjugate mixture, an ion exchange resin was employed. The separation was based on the negative charges of siRNA and siRNA-conjugates, while the trehalose polymers were neutral. To briefly describe the purification process, the conjugate mixtures were incubated with RESOURCE Q^{TM} cationic resins, and the supernatant (containing free polymer) was removed after centrifugation. By increasing NaCl concentration in the elution buffer, siRNA and siRNA conjugates were released and collected in the supernatant. Alternatively, a preloaded column with the cationic resin could be purchased and installed on an automatic chromatography system for convenience. From gel electrophoresis, the elution of siRNA and siRNA conjugate at salt strengths over 500 mM NaCl was observed (**Figure 4-5**). siRNA and siRNA conjugates were not separable by this method, and only free polymer was removed. Therefore, by combining HPLC (removes free siRNA) and ion exchange (removes free polymer), the conjugates can be purified.

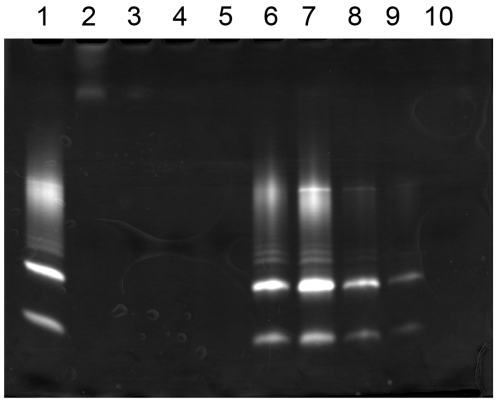

Figure 4-5. PAGE analysis of the supernatant fractions collected from ion exchange resin washes. Lane 1: conjugate **A** crude mixture; lanes 2-4: 20 mM pH 8.0 Tris-HCl; lane 5: 200 mM NaCl; lane 6: 500 mM NaCl; lanes 7-9: 1 M NaCl; lane 10: 20 mM pH 8.0 Tris-HCl. Free polymer was washed off in lanes 2 and 3. Later, siRNA and siRNA conjugate was washed off after increasing the salt concentration to 500 mM NaCl and higher.

4.3 Conclusions

We reported the conjugation of several types of trehalose-based glycopolymers and PEG-based polymers to thiol-modifed siRNA by disulfide exchange. The nuclease and serum stabilities of siRNA-trehalose polymer conjugate and linear PEG conjugate with similar sizes were investigated. The trehalose polymer conjugate showed a higher stability in CBS compared to naked siRNA, but did not exhibit higher nuclease stability. Efforts in purifying the conjugate mixtures led to a combination of HPLC and ion exchange methods. HPLC removes free siRNA, and ion exchange resin removes free polymer. The advantages and benefits of the siRNA-polymer conjugates still require further investigation. One potential area of interest is to stabilize siRNA polyplexes toward aggregation after lyophilization or storage in dried state.

4.4 Experimental Section

Materials

Chemicals were purchased from Sigma-Aldrich and Fisher Scientific and used as received unless otherwise specified. Complementary 5'-thiol modified sense siRNA (5'ThioMC6-D-GCU GAC CCU GAA GUU CAU CUU-3') and antisense siRNA (5'-GAU GAA CUU CAG GGU CAG CUU-3') specific for enhanced green fluorescent protein (eGFP) mRNA were purchased from Integrated DNA Technologies. 15% Mini-PROTEAN® TBE-Urea Precast Gels were purchased from Bio-Rad. SYBR® Safe nucleic acid staining dye, Calf Bovine Serum (CBS) for stability studies, and nuclease free water was purchased from Life Technologies. RNase ONE^{TM} Ribonuclease was purchased from Promega. RESOURCE Q resin was purchased from GE

Healthcare Life Sciences. Methacrylate trehalose monomer **M2**[44], pyridyl disulfide ATRP initiator **1**[45], and pyridyl disulfide CTA **2**[43] were synthesized as previously reported.

Instrumentation

^{1}H and ^{13}C NMR spectra were obtained on Bruker AV 500 and DRX 500 MHz spectrometers. Proton NMR spectra were acquired with a delay of 2 sec for small molecules, and a delay of 30 sec for all polymers. UV-Vis spectroscopy was performed using a Thermo Scientific NanoDrop 2000 (for small quantities such as siRNA samples). High-resolution electrospray ionization mass spectrum (HRESI-MS) was obtained on an IonSpec Ultima 7T ICR, (Varian Inc.) in the Molecular Instrumentation Center at UCLA. Infrared spectroscopy was performed using a PerkinElmer FT-IR equipped with an ATR accessory. Gel permeation chromatography was conducted on a Shimadzu HPLC system equipped with a refractive index detector RID-10A, one Polymer Laboratories PLgel guard column, and two Polymer Laboratories PLgel 5 μm mixed D columns. DMF containing 0.10 M LiBr at 40 °C was used as the eluent (flow rate: 0.80 mL/min) and near-monodisperse poly(methyl methacrylate) from Polymer Laboratories were used for calibration. Gel electrophoresis was performed using 15% Tris Borate EDTA (TBE) polyacrylamide gel electrophoresis (PAGE) at a constant voltage of 200 V for 45 minutes using 1X TBE buffer (pH 8.0). The siRNA gel was stained with SYBR Safe stain (Invitrogen) in 1X TBE buffer for 20 minutes. Visualization was conducted with a Bio-Rad FX Pro Plus Fluorimager located in the DOE-Biochemistry Facility at UCLA. High-performance liquid chromatography was conducted on a Shimadzu HPLC system equipped with a C18 column (150 x 4.6 mm^2, 5 μm, Phenomenex) and a photodiode array UV detector set at 220 nm and 260 nm.

Methods

Synthesis of polymethacrylate-based trehalose glycopolymer by ATRP. Initiator **1**[45] (1.52 mg, 4.5 μmol), trehalose monomer **M2**[44] (84.1 mg, 0.18 mmol), and DMF (0.325 mL) were added to a Schlenk tube and subjected to 6 freeze-pump-thaw cycles. A catalyst stock solution (4x) was made of CuBr (2.6 mg, 18.0 μmol) and 2,2′-bipyridine (bipy, 5.64 mg, 36.0 μmol). The solid catalyst mixture was evacuated-refilled with argon 7 times, and then dissolved in degassed DMF (500 μL). 125 μL of the catalyst stock solution was added to the Schlenk tube and stirred at 40 °C for 3.5 h under argon. DMF was removed under reduced pressure. The residual monomer and catalyst were removed by dialysis (MWCO 3500 Da) against 10 mM EDTA (4 L, 5 times), and then H_2O (4 L, 5 times). After lyophilization, polymer was obtained as 17 mg of white solid with M_n = 18,300 g/mol and PDI = 1.26 by GPC. ^{1}H NMR (500 MHz in DMSO-d_6) δ: 8.44, 7.81, 7.74, 7.24, 5.15, 5.02, 4.87, 4.82, 4.61, 3.93, 3.83, 3.64, 3.45, 3.27, 3.11, 2.74, 1.83, 1.19, 1.05, 0.89, 0.70.

Synthesis of pyridyl disulfide end-functionalized pPEGA by RAFT polymerization. CTA **2**[43] (10 mg, 0.021 mmol), PEGA (0.27 mL, 0.62 mmol), AIBN (0.35 mg, 2.1 μmol), and DMF (0.31 mL) were added to a Schlenk tube and subjected to 5 freeze-pump-thaw cycles. The polymerization was initiated by heating the vessel to 60 °C, and stirred under argon for 3 h 20 min. The crude was purified by dialysis (MWCO 3500 Da) against MeOH (4 L), followed by H_2O (4 L, 3 times). After lyophilization, the polymer was characterized by GPC, with M_n = 12,000 g/mol and PDI = 1.20. ^{1}H NMR (500 MHz in $CDCl_3$) δ: 8.43, 7.75, 7.65, 7.08, 4.80, 4.14, 3.62, 3.53, 3.52, 3.51, 3.35, 2.27, 2.20, 1.87, 1.60.

Conjugation of siRNA to pyridyl disulfide end-functionalized polymers. 30 μl of a 0.0383 mM solution of double stranded (ds)-siRNA was mixed with 5 μl of 200 mM dithiothreitol (DTT) solution and kept for 2 h at 24 °C. To remove unreacted DTT, siRNA was precipitated and

washed several times using 80% ethanol. The siRNA pellet was completely resuspended in 30 μL of polymer solution (50 eq in 100 mM sodium bicarbonate buffer at pH 8.5). For nuclease and serum stability tests, the siRNA pellet was re-suspended with polymer solutions in pH 7.0 TE buffer instead of pH 8.5 sodium bicarbonate buffer. The reaction mixture was left at 23 °C for 20 h. The conjugates were also treated with DTT to confirm that the covalent conjugation of siRNA with polymers could be reversed under physiologically relevant conditions. Conjugate reaction mixtures (0.03 nmol siRNA, 5 μL) in water were incubated with DTT (10 nmol, 1μL in water) for 1 h at 23 °C. Reduced and non-reduced conjugates were then analyzed by 15% Tris Borate EDTA (TBE) PAGE was carried out at a constant voltage of 200 V for 40 minutes using 1X TBE buffer (pH 8.0). siRNA was stained by incubating the gel in 1X SYBR® Safe nucleic acid dye/TBE buffer. Conjugation efficiency was quantified using the Quanti-One program (Bio-Rad).

RNase stability test. Samples (0.07 nmol siRNA, 4μL in pH 7.0 TE buffer) were mixed with nuclease-free water to a final volume of 8 μL. RNase ONE ribonuclease (1 μL, 1 unit, in reaction buffer: 100 mM Tris HCl, pH 7.5, 50 nM EDTA, 2 M sodium acetate) was added to each sample and the samples were incubated at 37 °C for 5 or 10 minutes. Nuclease reactions were terminated by the addition of SDS solution (1 μL from 1% solution in water). The samples were analyzed by PAGE using 15% TBE-Urea gel at a constant voltage of 200 V for 40 min using 1X TBE buffer (pH 8.0). The gel was stained by incubating in 1X SYBR-Safe nucleic acid dye/TBE buffer for 30 min. Percentage retention of siRNA or conjugates were determined by taking the proportion of the band intensity and were normalized to the siRNA or conjugate band intensity before RNase ONE treatment.

Serum stability test. In a typical experiment, the samples (0.1 nmol siRNA, 5 μL) were incubated in 80 v/v % CBS with a total volume of 50 μL at 37 °C for up to 4 hours. During the incubation period, aliquots (10 μL) were taken at predetermined time points and immediately frozen at -80 °C until further use. Then, all samples were analyzed together using gel electrophoresis with 15% TBE-Urea ready gel, at a constant voltage of 200 V for 45 minutes using 1X TBE running buffer (pH 8.0). Percent degradation at each time point were determined by taking the proportion of the siRNA band intensity at each time point to the siRNA band intensity at 0 hour.

Purification of siRNA-polymer conjugates by HPLC. HPLC was performed using a C18 column (150 x 4.6 mm^2, 5 μm, Phenomenex) and a photodiode array UV detector set at 220 nm and 260 nm. The UV detection was performed at 220 nm and 260 nm, to detect the unconjugated polymers, and the unconjugated siRNA and siRNA-polymer conjugates, respectively. Chromatography was carried out with isocratic mobile phase of 30% 0.05 M phosphate buffer (pH 7) and 70% acetonitrile; flow rate 1.0 mL/min; column at room temperature. The fractions were collected, desalted and concentrated by centrifugal filtration, and then analyzed by gel electrophoresis.

Purification of siRNA-polymer conjugates by ion exchange resins. RESOURCE Q resin was purchased from GE Healthcare Life Sciences, and was initially stored in 20% ethanol. 0.5-1 mL of resin slurry was transferred into a micro-centrifuge tube. After centrifugation, the resin was packed into 0.2 mL volume. For each wash or elution, 500 μL of solution was added and mixed well with the resin before centrifugation and supernatant collection. The washing and equilibration steps included once with 20% ethanol, three times with MilliQ H_2O, three times with 20 mM pH 8.0 Tris-HCl, once with 1 M NaCl (to provide counter ion Cl^-), and then five

times with 20 mM pH 8.0 Tris-HCl. Crude siRNA-polymer conjugate mixture was added to the prepared resin, and washed five times with 20 mM pH 8.0 Tris-HCl to remove all polymer. The salt strength was then gradually increased from 200 mM to 1 M NaCl, and finished with one wash of 20 mM pH 8.0 Tris-HCl. The supernatant fractions were individually collected, desalted and concentrated by centrifugal filtration, and then analyzed by gel electrophoresis.

4.5 Appendix to Chapter 4: Supplementary Figures

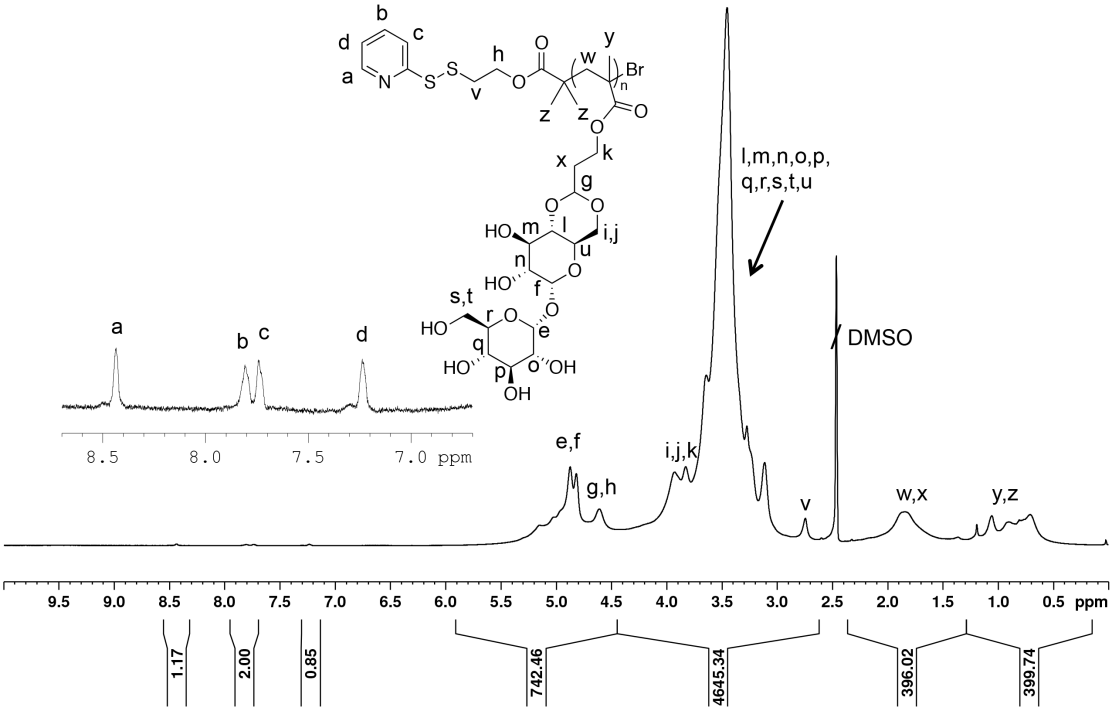

Figure 4-6. ^{1}H NMR spectrum of **Poly M** (in DMSO-d6).

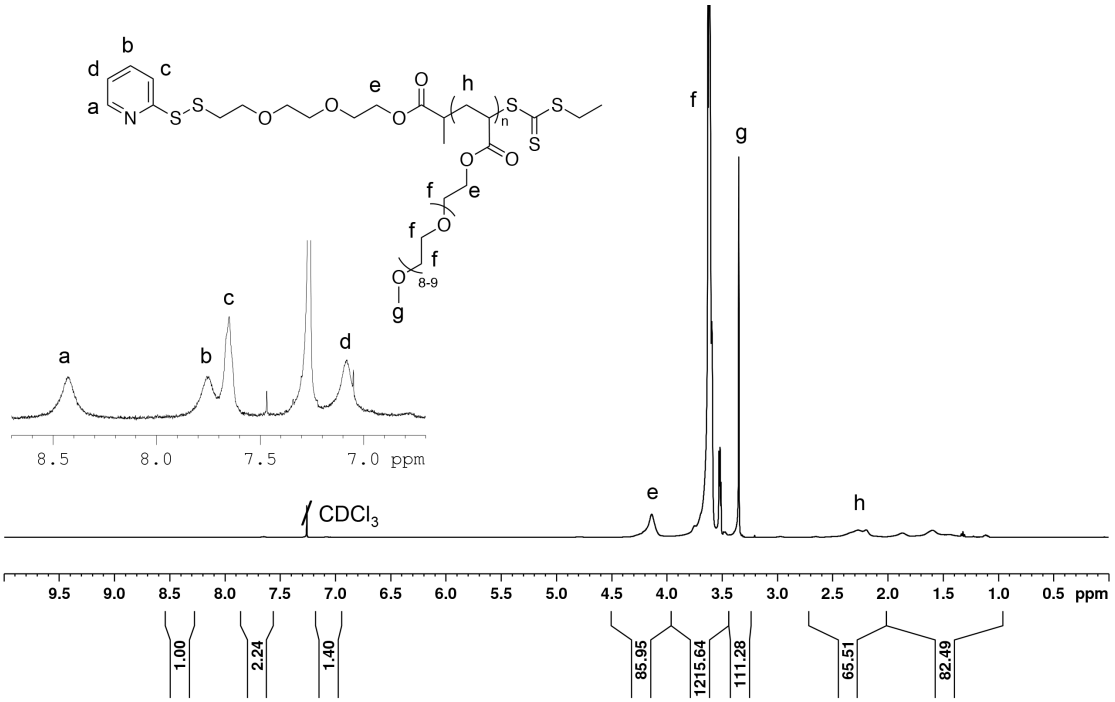

Figure 4-7. ^{1}H NMR spectrum of pPEGA (in $CDCl_3$).

4.6 References

(1) Elbashir, S. M.; Harborth, J.; Lendeckel, W.; Yalcin, A.; Weber, K.; Tuschl, T. "Duplexes of 21-Nucleotide RNAs Mediate RNA Interference in Cultured Mammalian Cells" *Nature* **2001**, *411*, 494-498.

(2) Whitehead, K. A.; Langer, R.; Anderson, D. G. "Knocking Down Barriers: Advances in siRNA Delivery" *Nat. Rev. Drug Discovery* **2009**, *8*, 129-138.

(3) Soutschek, J.; Akinc, A.; Bramlage, B.; Charisse, K.; Constien, R.; Donoghue, M.; Elbashir, S.; Geick, A.; Hadwiger, P.; Harborth, J.; John, M.; Kesavan, V.; Lavine, G.; Pandey, R. K.; Racie, T.; Rajeev, K. G.; Rohl, I.; Toudjarska, I.; Wang, G.; Wuschko, S.; Bumcrot, D.; Koteliansky, V.; Limmer, S.; Manoharan, M.; Vornlocher, H. P. "Therapeutic Silencing of an Endogenous Gene by Systemic Administration of Modified siRNAs" *Nature* **2004**, *432*, 173-178.

(4) Dykxhoorn, D. M.; Palliser, D.; Lieberman, J. "The Silent Treatment: siRNAs as Small Molecule Drugs" *Gene Ther.* **2006**, *13*, 541-552.

(5) Guo, P. X.; Coban, O.; Snead, N. M.; Trebley, J.; Hoeprich, S.; Guo, S. C.; Shu, Y. "Engineering RNA for Targeted siRNA Delivery and Medical Application" *Adv. Drug Delivery Rev.* **2010**, *62*, 650-666.

(6) Dominska, M.; Dykxhoorn, D. M. "Breaking Down the Barriers: siRNA Delivery and Endosome Escape" *J. Cell Sci.* **2010**, *123*, 1183-1189.

(7) Aagaard, L.; Rossi, J. J. "RNAi Therapeutics: Principles, Prospects and Challenges" *Adv. Drug Delivery Rev.* **2007**, *59*, 75-86.

(8) Wang, J.; Lu, Z.; Wientjes, M. G.; Au, J. L. S. "Delivery of siRNA Therapeutics: Barriers and Carriers" *AAPS J.* **2010**, *12*, 492-503.

(9) Oishi, M.; Nagasaki, Y.; Itaka, K.; Nishiyama, N.; Kataoka, K. "Lactosylated Poly(Ethylene Glycol)-siRNA Conjugate through Acid-Labile Beta-Thiopropionate Linkage to Construct pH-Sensitive Polyion Complex Micelles Achieving Enhanced Gene Silencing in Hepatoma Cells" *J. Am. Chem. Soc.* **2005**, *127*, 1624-1625.

(10) Kim, S. H.; Jeong, J. H.; Lee, S. H.; Kim, S. W.; Park, T. G. "PEG Conjugated VEGF siRNA for Anti-Angiogenic Gene Therapy" *J. Controlled Release* **2006**, *116*, 123-129.

(11) Lee, S. H.; Kim, S. H.; Park, T. G. "Intracellular siRNA Delivery System Using Polyelectrolyte Complex Micelles Prepared from VEGF siRNA-PEG Conjugate and Cationic Fusogenic Peptide" *Biochem. Biophys. Res. Commun.* **2007**, *357*, 511-516

(12) Oishi, M.; Nagasaki, Y.; Nishiyama, N.; Itaka, K.; Takagi, M.; Shimamoto, A.; Furuichi, Y.; Kataoka, K. "Enhanced Growth Inhibition of Hepatic Multicellular Tumor Spheroids by Lactosylated Poly(Ethylene Glycol)-siRNA Conjugate Formulated in PEGylated Polyplexes" *ChemMedChem* **2007**, *2*, 1290-1297.

(13) Kim, S. H.; Jeong, J. H.; Lee, S. H.; Kim, S. W.; Park, T. G. "Local and Systemic Delivery of VEGF siRNA Using Polyelectrolyte Complex Micelles for Effective Treatment of Cancer" *J. Controlled Release* **2008**, *129*, 107-116.

(14) Kim, S. H.; Jeong, J. H.; Lee, S. H.; Kim, S. W.; Park, T. G. "LHRH Receptor-Mediated Delivery of siRNA Using Polyelectrolyte Complex Micelles Self-Assembled from siRNA-PEG-LHRH Conjugate and PEI" *Bioconjugate Chem.* **2008**, *19*, 2156-2162.

(15) Tatsumi, T.; Oishi, M.; Kataoka, K.; Nagasaki, Y. "PEG-siRNA Conjugate Bearing 27 bp siRNA to Form Novel PEGylated Polyplexes with Improved Stability" *Trans. Mater. Res. Soc. Jpn.* **2008**, *33*, 807-810.

(16) Jung, S.; Lee, S. H.; Mok, H.; Chung, H. J.; Park, T. G. "Gene Silencing Efficiency of siRNA-PEG Conjugates: Effect of PEGylation Site and PEG Molecular Weight" *J. Controlled Release* **2010**, *144*, 306-313.

(17) Kow, S. C.; McCarroll, J.; Valade, D.; Boyer, C.; Dwarte, T.; Davis, T. P.; Kavallaris, M.; Bulmus, V. "Dicer-Labile PEG Conjugates for siRNA Delivery" *Biomacromolecules* **2011**, *12*, 4301-4310.

(18) Lee, S. H.; Mok, H.; Park, T. G. "Di- and Triblock siRNA-PEG Copolymers: PEG Density Effect of Polyelectrolyte Complexes on Cellular Uptake and Gene Silencing Efficiency" *Macromol. Biosci.* **2011**, *11*, 410-418.

(19) Iversen, F.; Yang, C. X.; Dagnaes-Hansen, F.; Schaffert, D. H.; Kjems, J.; Gao, S. "Optimized siRNA-PEG Conjugates for Extended Blood Circulation and Reduced Urine Excretion in Mice" *Theranostics* **2013**, *3*, 201-209.

(20) Gaziova, Z.; Baumann, V.; Winkler, A. M.; Winkler, J. "Chemically Defined Polyethylene Glycol siRNA Conjugates with Enhanced Gene Silencing Effect" *Bioorg. Med. Chem.* **2014**, *22*, 2320-2326.

(21) Choi, S. W.; Lee, S. H.; Mok, H.; Park, T. G. "Multifunctional siRNA Delivery System: Polyelectrolyte Complex Micelles of Six-Arm PEG Conjugate of siRNA and Cell

Penetrating Peptide with Crosslinked Fusogenic Peptide" *Biotechnol. Prog.* **2010**, *26*, 57-63.

(22) "RAFT-Synthesized Copolymers and Conjugates Designed for Therapeutic Delivery of siRNA" *Polym. Chem.* **2011**, *2*, 1428-1441.

(23) Rose, V. L.; Winkler, G. S.; Allen, S.; Puri, S.; Mantovani, G. "Polymer siRNA Conjugates Synthesised by Controlled Radical Polymerisation" *Eur. Polym. J.* **2013**, 2861-2883.

(24) Chu, D. S. H.; Schellinger, J. G.; Shi, J. L.; Convertine, A. J.; Stayton, P. S.; Pun, S. H. "Application of Living Free Radical Polymerization for Nucleic Acid Delivery" *Acc. Chem. Res.* **2012**, *45*, 1089-1099.

(25) Kato, M.; Kamigaito, M.; Sawamoto, M.; Higashimura, T. "Polymerization of Methyl-Methacrylate with the Carbon-Tetrachloride Dichlorotris(Triphenylphosphine)Ruthenium (II) Methylaluminum Bis(2,6-Di-Tert-Butylphenoxide) Initiating System - Possibility of Living Radical Polymerization" *Macromolecules* **1995**, *28*, 1721-1723.

(26) Wang, J. S.; Matyjaszewski, K. "Controlled Living Radical Polymerization - Atom-Transfer Radical Polymerization in the Presence of Transition-Metal Complexes" *J. Am. Chem. Soc.* **1995**, *117*, 5614-5615.

(27) Chiefari, J.; Chong, Y. K.; Ercole, F.; Krstina, J.; Jeffery, J.; Le, T. P. T.; Mayadunne, R. T. A.; Meijs, G. F.; Moad, C. L.; Moad, G.; Rizzardo, E.; Thang, S. H. "Living Free-Radical Polymerization by Reversible Addition-Fragmentation Chain Transfer: The RAFT Process" *Macromolecules* **1998**, *31*, 5559-5562.

(28) Heredia, K. L.; Nguyen, T. H.; Chang, C.-W.; Bulmus, V.; Davis, T. P.; Maynard, H. D. "Reversible siRNA-Polymer Conjugates by RAFT Polymerization" *Chem. Commun.* **2008**, 3245-3247.

(29) Gunasekaran, K.; Nguyen, T. H.; Maynard, H. D.; Davis, T. P.; Bulmus, V. "Conjugation of siRNA with Comb-Type PEG Enhances Serum Stability and Gene Silencing Efficiency" *Macromol. Rapid Commun.* **2011**, *32*, 654-659.

(30) Jiangtao, X.; Boyer, C.; Bulmus, V.; Davis, T. P. "Synthesis of Dendritic Carbohydrate End-Functional Polymers via RAFT: Versatile Multi-Functional Precursors for Bioconjugations" *J. Polym. Sci., Part A: Polym. Chem.* **2009**, *47*, 4302-4313.

(31) Vazquez-Dorbatt, V.; Tolstyka, Z. P.; Chang, C.-W.; Maynard, H. D. "Synthesis of a Pyridyl Disulfide End-Functionalized Glycopolymer for Conjugation to Biomolecules and Patterning on Gold Surfaces" *Biomacromolecules* **2009**, *10*, 2207-2212.

(32) York, A. W.; Huang, F.; McCormick, C. L. "Rational Design of Targeted Cancer Therapeutics through the Multiconjugation of Folate and Cleavable siRNA to RAFT-Synthesized (HPMA-*s*-APMA) Copolymers" *Biomacromolecules* **2010**, *11*, 505-514.

(33) Averick, S. E.; Paredes, E.; Dey, S. K.; Snyder, K. M.; Tapinos, N.; Matyjaszewski, K. "Autotransfecting Short Interfering RNA through Facile Covalent Polymer Escorts" *J. Am. Chem. Soc.* **2013**, 12508-12511.

(34) Anchordoquy, T. J.; Koe, G. S. "Physical Stability of Nonviral Plasmid-Based Therapeutics" *J. Pharm. Sci.* **2000**, *89*, 289-296.

(35) Kasper, J. C.; Schaffert, D.; Ogris, M.; Wagner, E.; Friess, W. "Development of a Lyophilized Plasmid/LPEI Polyplex Formulation with Long-Term Stability-a Step Closer from Promising Technology to Application" *J. Controlled Release* **2011**, *151*, 246-255.

(36) Miyata, K.; Kakizawa, Y.; Nishiyama, N.; Yamasaki, Y.; Watanabe, T.; Kohara, M.; Kataoka, K. "Freeze-Dried Formulations for in Vivo Gene Delivery of PEGylated Polyplex Micelles with Disulfide Crosslinked Cores to the Liver" *J. Controlled Release* **2005**, *109*, 15-23.

(37) Endres, T.; Zheng, M. Y.; Beck-Broichsitter, M.; Kissel, T. "Lyophilised Ready-to-Use Formulations of PEG-PCL-PEI Nano-Carriers for siRNA Delivery" *Int. J. Pharm.* **2012**, *428*, 121-124.

(38) Steele, T. W. J.; Zhao, X. B.; Tarcha, P.; Kissel, T. "Factors Influencing Polycation/siRNA Colloidal Stability toward Aerosol Lung Delivery" *Eur. J. Pharm. Biopharm.* **2012**, *80*, 14-24.

(39) Werth, S.; Urban-Klein, B.; Dai, L.; Hobel, S.; Grzelinski, M.; Bakowsky, U.; Czubayko, F.; Aigner, A. "A Low Molecular Weight Fraction of Polyethylenimine (PEI) Displays Increased Transfection Efficiency of DNA and siRNA in Fresh or Lyophilized Complexes" *J. Controlled Release* **2006**, *112*, 257-270.

(40) Yadava, P.; Gibbs, M.; Castro, C.; Hughes, J. A. "Effect of Lyophilization and Freeze-Thawing on the Stability of siRNA-Liposome Complexes" *AAPS PharmSciTech* **2008**, *9*, 335-341.

(41) Kasper, J. C.; Troiber, C.; Küchler, S.; Wagner, E.; Friess, W. "Formulation Development of Lyophilized, Long-Term Stable siRNA/Oligoaminoamide Polyplexes" *Eur. J. Pharm. Biopharm.* **2013**, *85*, 294-305.

(42) Armstrong, T. K. C.; Girouard, L. G.; Anchordoquy, T. J. "Effects of PEGylation on the Preservation of Cationic Lipid/DNA Complexes During Freeze-Thawing and Lyophilization" *J. Pharm. Sci.* **2002**, *91*, 2549-2558.

(43) Mancini, R. J.; Lee, J.; Maynard, H. D. "Trehalose Glycopolymers for Stabilization of Protein Conjugates to Environmental Stressors" *J. Am. Chem. Soc.* **2012**, *134*, 8474-8479.

(44) Lee, J.; Lin, E. W.; Lau, U. Y.; Hedrick, J. L.; Bat, E.; Maynard, H. D. "Trehalose Glycopolymers as Excipients for Protein Stabilization" *Biomacromolecules* **2013**, *14*, 2561-2569.

(45) Bontempo, D.; Heredia, K. L.; Fish, B. A.; Maynard, H. D. "Cysteine-Reactive Polymers Synthesized by Atom Transfer Radical Polymerization for Conjugation to Proteins" *J. Am. Chem. Soc.* **2004**, *126*, 15372-15373.

(46) Bezrukavnikov, S.; Mashaghi, A.; van Wijk, R. J.; Gu, C.; Yang, L. J.; Gao, Y. Q.; Tans, S. J. "Trehalose Facilitates DNA Melting: A Single-Molecule Optical Tweezers Study" *Soft Matter* **2014**, *10*, 7269-7277.

Chapter 5

Alternative Synthesis Route Toward

siRNA-Polymer Conjugates: *Grafting From* siRNA[‡]

5.1 Introduction

Grafting to and *grafting from* are the two major synthetic strategies for preparing polymer bioconjugates. The *grafting to* technique involves covalent attachment of a polymer to the biomolecule, and the siRNA-polymer conjugates described in the previous chapter were made through this method. However, the major drawback of the *grafting to* strategy is the steric hindrance between the two macromolecules, which requires very efficient bioconjugation chemistry and a large excess of polymer to obtain good yields. Purification of the protein-polymer conjugate is also a common challenge, due to the similar molecular weights and sizes of the components. In the *grafting from* technique, the initiator is incorporated on the biomolecule first, followed by polymerization of monomers from the initiating site. In 2005, our group was the first to demonstrate the strategy of grafting from a protein, using biotinylated ATRP initiators that could bind streptavidin non-covalently and generated a protein macroinitiator upon association with streptavidin.[1] The general benefits of the *grafting from* approach include less steric interference in the initiator conjugation, easier purification due to significant mass differences between the bioconjugate and small molecule impurities, and facile characterization.

To date, there has been no literature reporting *grafting from* siRNA. He and coworkers have published several reports on polymer growth from DNA immobilized on gold surface for DNA detection by employing both ATRP[2-7] and RAFT[8,9] polymerization techniques in aqueous conditions. The general strategy involved immobilization of a single strand of DNA on gold surface or gold nanoparticles[4] through its 3' thiol-functionalized end. The other end of the DNA was modified with an amine, which was used for coupling to the ATRP initiator or RAFT CTA through an activated ester, followed by subsequent polymerization. Recently, Matyaszewski's group has reported the preparation of polymer-DNA hybrids by both solution phase and solid

phase synthesis.[10] They incorporated the ATRP initiator onto DNA while it was still on the solid support of the DNA synthesis procedure. AGET ATRP was used to perform the polymerization of oligo(ethylene oxide) methacrylate (OEOMA, M_n=475). A hydrophobic monomer, benzyl methacrylate, was also polymerized to prepare DNA-latex particles with hydrophobic cores. In this chapter, we report *grafting from* siRNA on polymerization scales as low as nanomoles. Efforts towards *grafting from* siRNA using both RAFT polymerization and ATRP will be described and discussed.

5.2 Results and Discussion

5.2.1 Synthesis of siRNA-I and siRNA-CTA

The first step of *grafting from* is to prepare the macroinitiator or macro-CTA for ATRP and RAFT polymerization, respectively. As shown in the previous chapter, the free thiol of modified siRNA can be used as a reactive handle to undergo disulfide exchange with pyridyl disulfide end-functionalized polymers and yield siRNA-polymer conjugates. Using the same method, we attached a pyridyl disulfide end-functionalized ATRP initiator **1** or RAFT CTA **5** to prepare the corresponding macroinitiator or macro-CTA. Since the conjugation reaction would mainly be in aqueous conditions, a RAFT CTA containing an ethylene glycol unit was synthesized to increase its water solubility (**Scheme 5-1**, see Appendix **Figures 5-16** through **5-21** for NMR spectra).

Scheme 5-1. Synthesis of thiol-reactive CTA **5**.

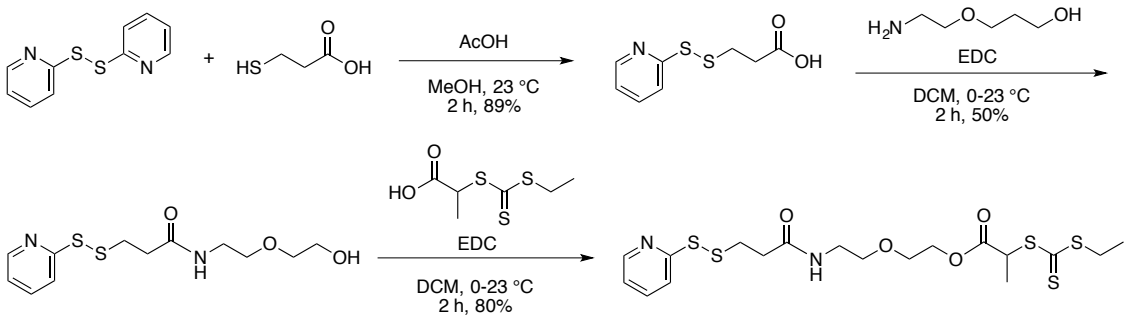

To prepare the macroinitiator (siRNA-initiator, siRNA-I), the modified free thiol was exposed by reduction with dithiothreitol (DTT), followed by addition of previously synthesized pyridyl disulfide isobromobutyrate ATRP initiator through disulfide exchange (**Scheme 5-2**). The macro-CTA (siRNA-CTA) was prepared through the same method. The excess initiator or CTA was then removed by 80% ethanol precipitation of siRNA-I or siRNA-CTA, as well as unreacted siRNA.

Scheme 5-2. Synthesis of siRNA-I and siRNA-CTA.

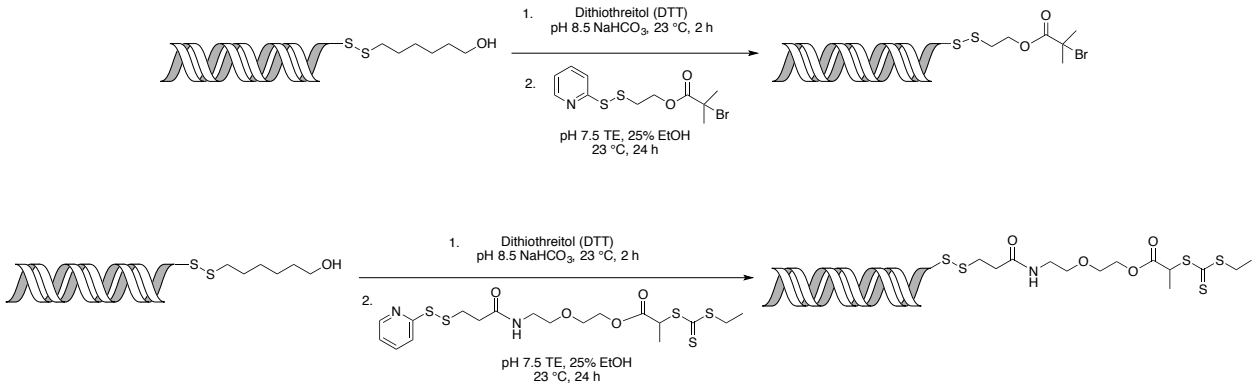

The reaction products were analyzed by MALDI-TOF MS (**Figure 5-1**). In MALDI-TOF MS analysis, double stranded siRNA separates into two single strands – the unmodified antisense strand (m/z = 6713) and the modified sense strand containing the 5'ThioMC6 group (m/z = 6933). Once the disulfide bond on the sense strand is reduced by DTT, there is a decrease of 133.07 in its mass. The subsequent attachment of ATRP initiator or RAFT CTA can be observed by the increase in m/z value to 7028 and 7187 respectively, which closely correspond to the theoretical increase in mass of 224.96 and 384.04. These results confirm the formation of siRNA-I and siRNA-CTA.

Unreacted siRNA was removed by HPLC using 25% acetonitrile in pH 7.0 100 mM TEAA buffer as elution buffer, and monitoring the wavelength at 260 nm (**Figure 5-2 a**). With the described method, the retention time of protected siRNA (starting material) is around 5 minutes (labeled as A in **Figure 5-2 a**). The modified product siRNA-I elutes at 10-15 minutes (labeled as C), and siRNA-CTA elutes at 30-35 minutes (labeled as E). The products were well separated from the earlier fractions (labeled B and D), and all fractions were collected for MALDI-TOF MS analysis (**Figure 5-2 b**). The results confirmed that C is purified siRNA-I, and E is purified siRNA-CTA. However, significant amount of material was lost after HPLC purification. Thus, since unreacted siRNA does not interfere with polymerizations, the following *grafting from* polymerizations were conducted with siRNA-I and siRNA-CTA without HPLC purification unless otherwise noted.

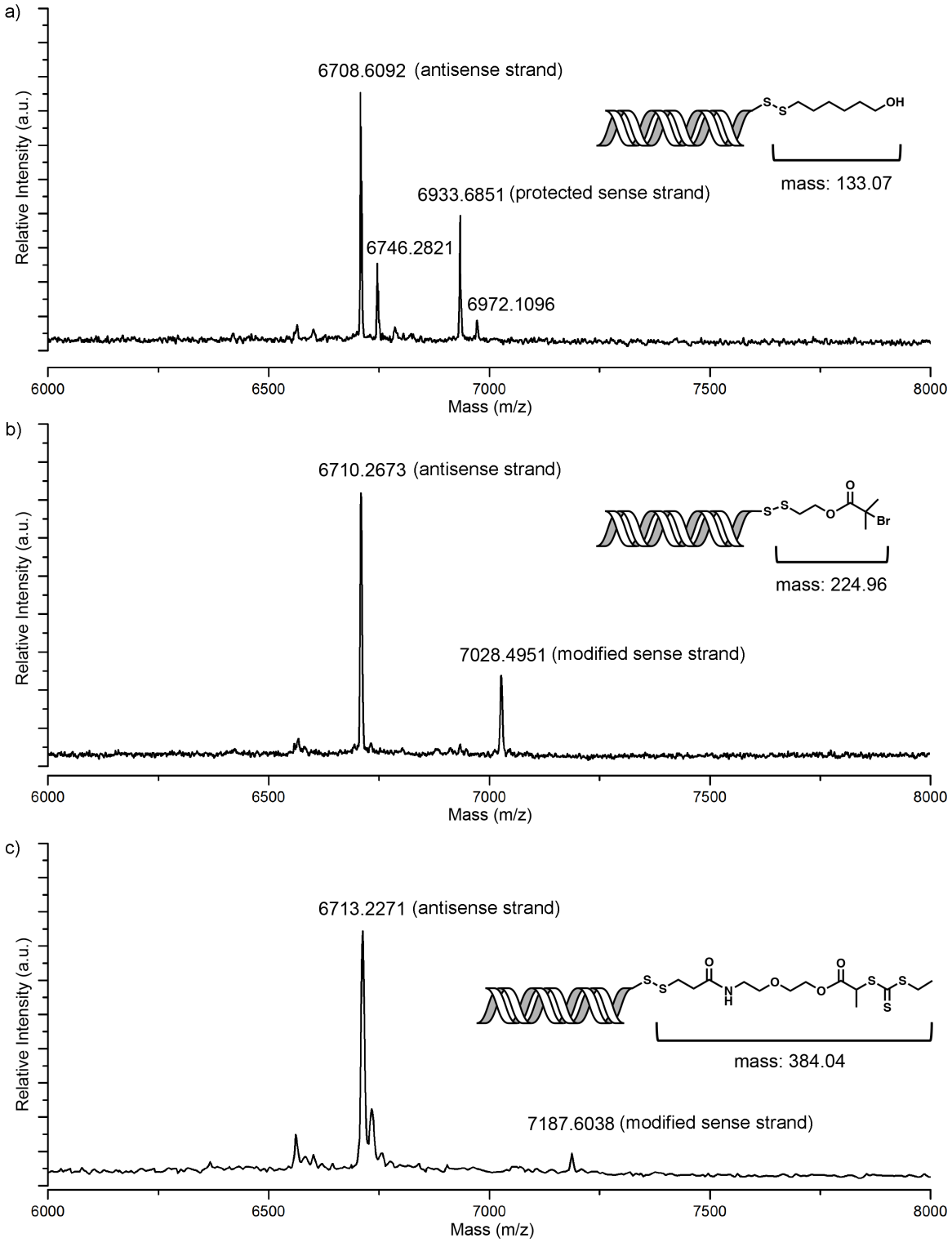

Figure 5-1. Synthesis of siRNA-I and the MALDI-TOF MS of a) protected siRNA, b) siRNA-I, and c) siRNA-CTA.

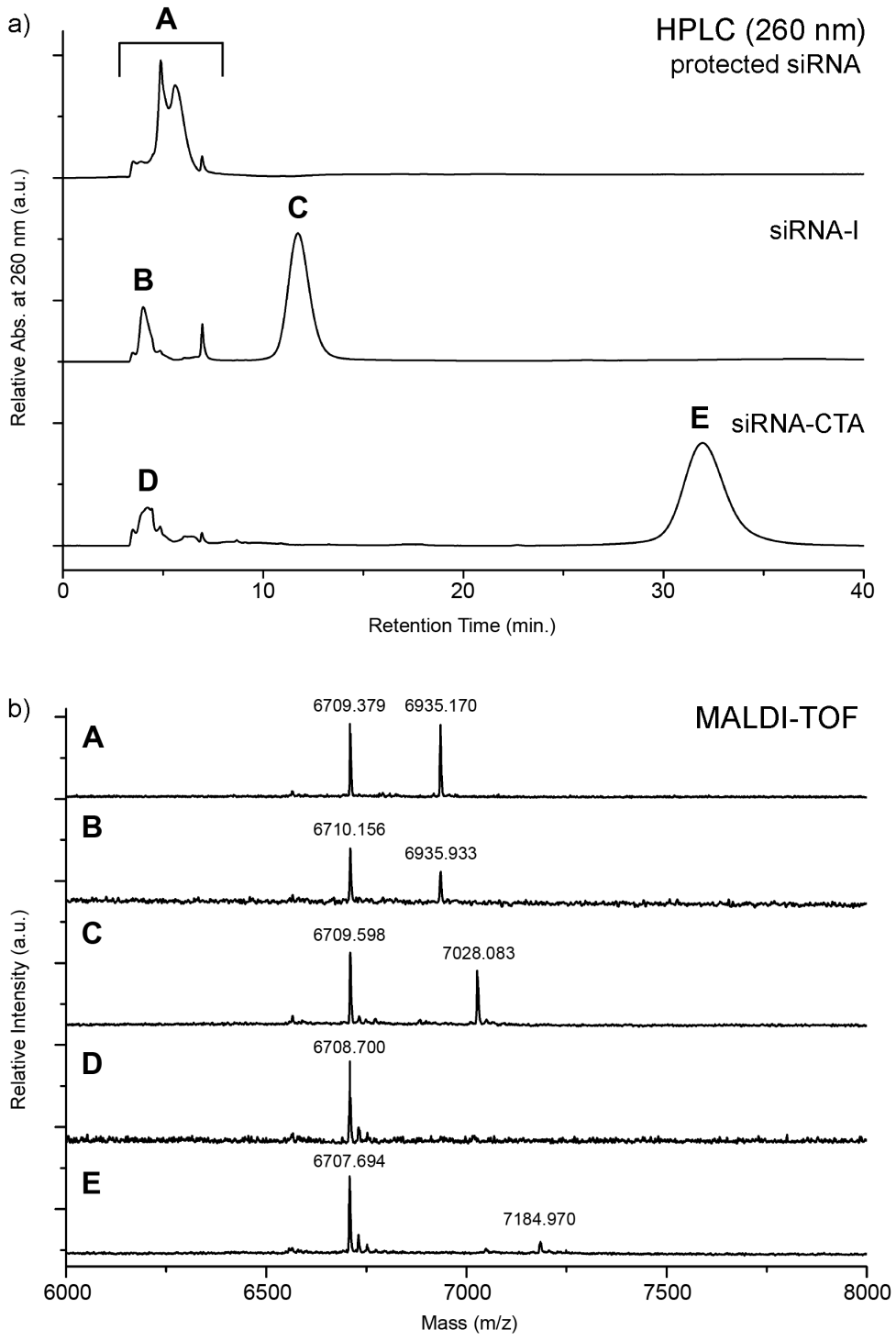

Figure 5-2. Purification of siRNA-I and siRNA-CTA: a) HPLC traces of protected siRNA, siRNA-I, and siRNA-CTA monitored at 260 nm, and b) MALDI-TOF MS results of the collected fractions (C: purified siRNA-I, E: purified siRNA-CTA).

5.2.2 Synthesis of Sacrificial Resins

A major challenge in this study was that siRNA is only available in very small quantities, and therefore would be impractical to polymerize on large scales. To maintain the equilibrium for controlled polymerization and to be able to work on a reasonable scale, we intended to increase the total initiator concentration by adding resins modified with ATRP initiators and RAFT CTAs in the polymerization media. This approach has been demonstrated in our earliest reports on *grafting from* proteins with ATRP.[1,11] The sacrificial resins were then easily removed from the polymerization mixture afterwards.

Wang resins are cross-linked polystyrene beads functionalized with *para*-hydroxybenzyl alcohols, and are commonly utilized in peptide synthesis for attaching C-terminus carboxylic acids.[12] Wang resin has been functionalized with ATRP initiators as a solid support for poly(methacrylates) synthesis in toluene.[13] The polymers were cleaved in acidic conditions and characterized with narrow PDIs. However, it has been shown that when hydrophobic polystyrene beads were used as the support for surface-initiated ATRP in water, there were no observed surface initiation and polymer growth.[14] This was because the hydrophobic surface limited the diffusion of catalyst towards the surface-bound initiators, and inhibited polymer growth. We also noticed this phenomenon and observed no polymer growth in aqueous conditions. Therefore, we changed the solid support to NovaSyn® TGA resin, which is a Wang-type resin with linear PEG chains as a hydrophilic coating.

Resin modification was achieved by coupling the *para*-hydroxybenzyl alcohol of Wang resin or TGA resin with 2-bromoisobutyric acid or 2-(ethyl trithiocarbonate)propionic acid, followed by Soxhlet extraction with THF for purification. As a result, Wang-I, Wang-CTA,

TGA-I, and TGA-CTA resins were prepared (**Scheme 5-3** and **Scheme 5-4**). All resins were characterized by IR spectroscopy, and the appearance of a C=O stretch confirmed the formation of the ester linkage between the resin and the carboxylic acid (**Figure 5-3**). The additional PEG linker in TGA resins led to higher solvation and mobility in solvents, and was beneficial for gel-phase NMR spectroscopy characterizations (**Figure 5-4** and **Figure 5-5**).[15] Expected signals were observed for both cases of TGA-I and TGA-CTA resins in their ^{1}H- and ^{13}C- NMR spectra, confirming successful modification and purification.

Scheme 5-3. Synthesis of hydrophobic and hydrophilic sacrificial ATRP initiator resins.

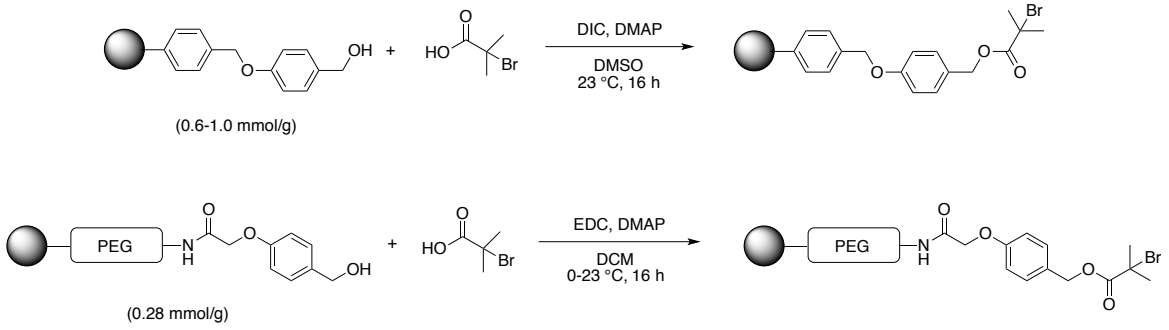

Scheme 5-4. Synthesis of hydrophobic and hydrophilic sacrificial RAFT CTA resins.

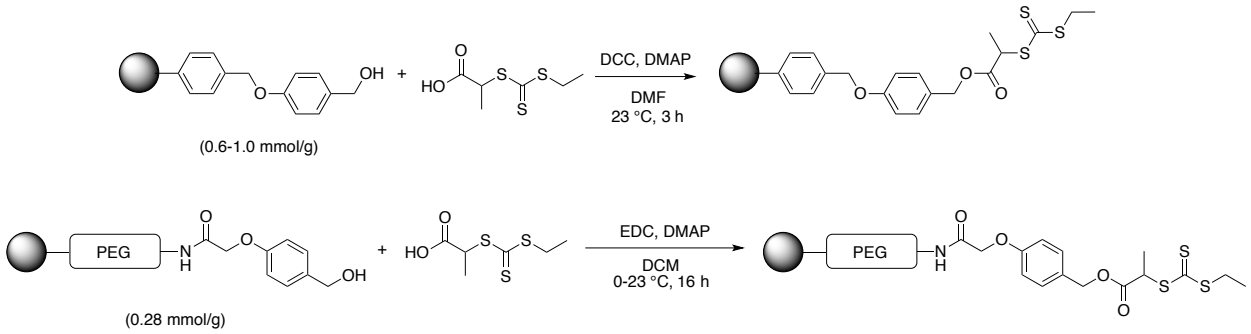

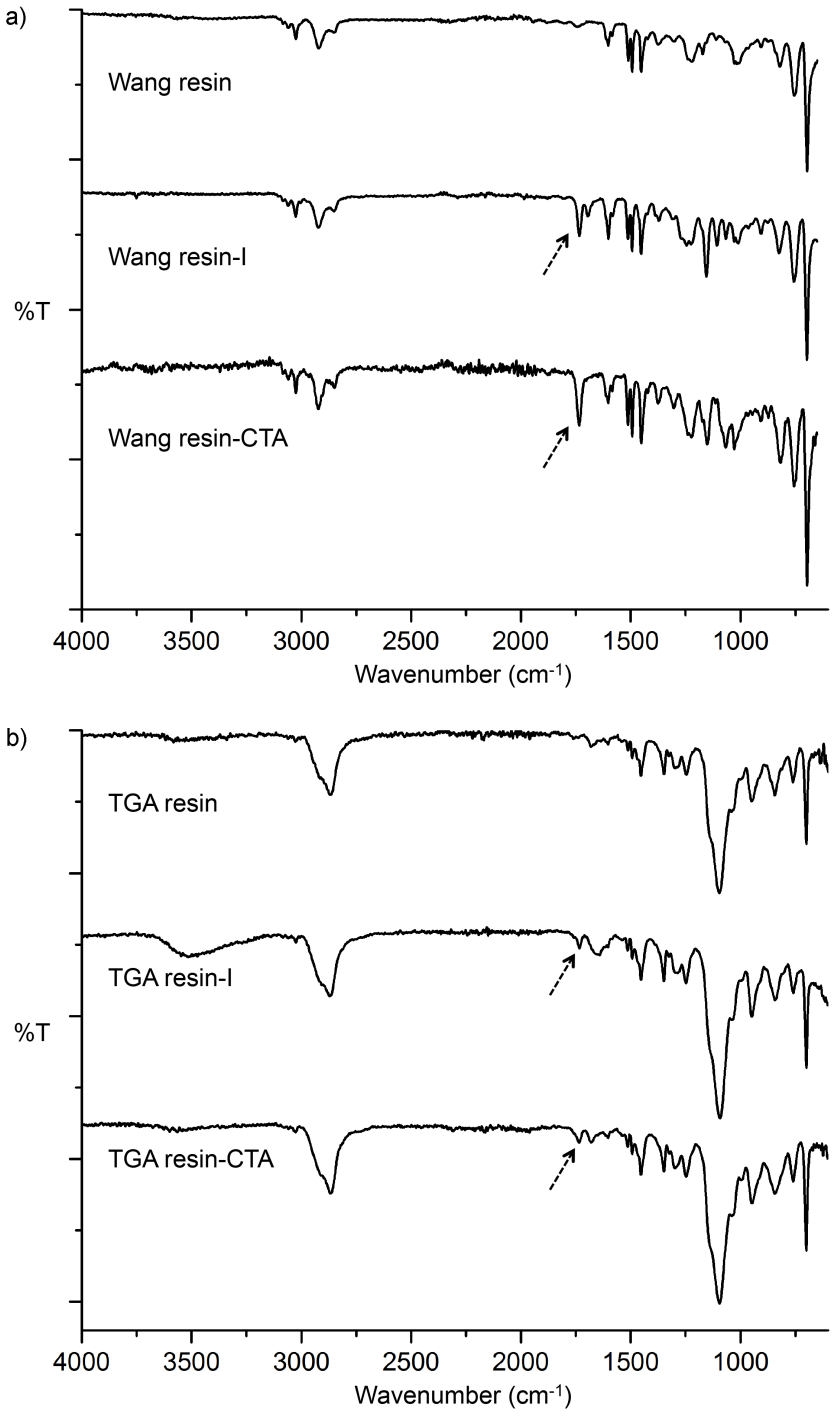

Figure 5-3. IR spectra overlays of modified a) Wang resins and b) TGA resins. The arrows are pointing to the appearance of carbonyl C=O stretches after esterification of the *para*-hydroxylbenzyl alcohols on the resin.

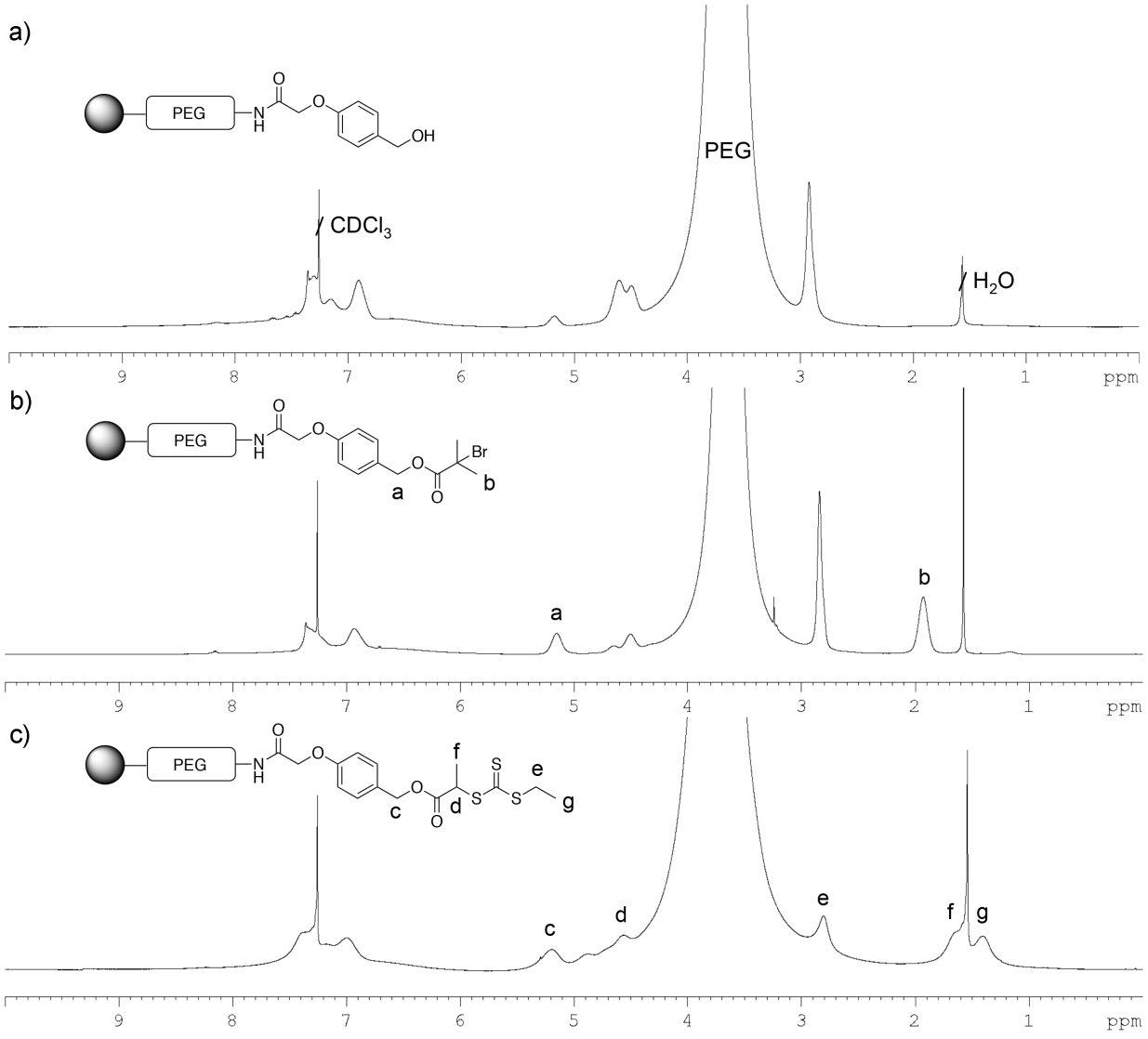

Figure 5-4. Gel-phase ^{1}H-NMR spectra of a) TGA resin, b) modified TGA-Br resin, and c) modified TGA-CTA resin.

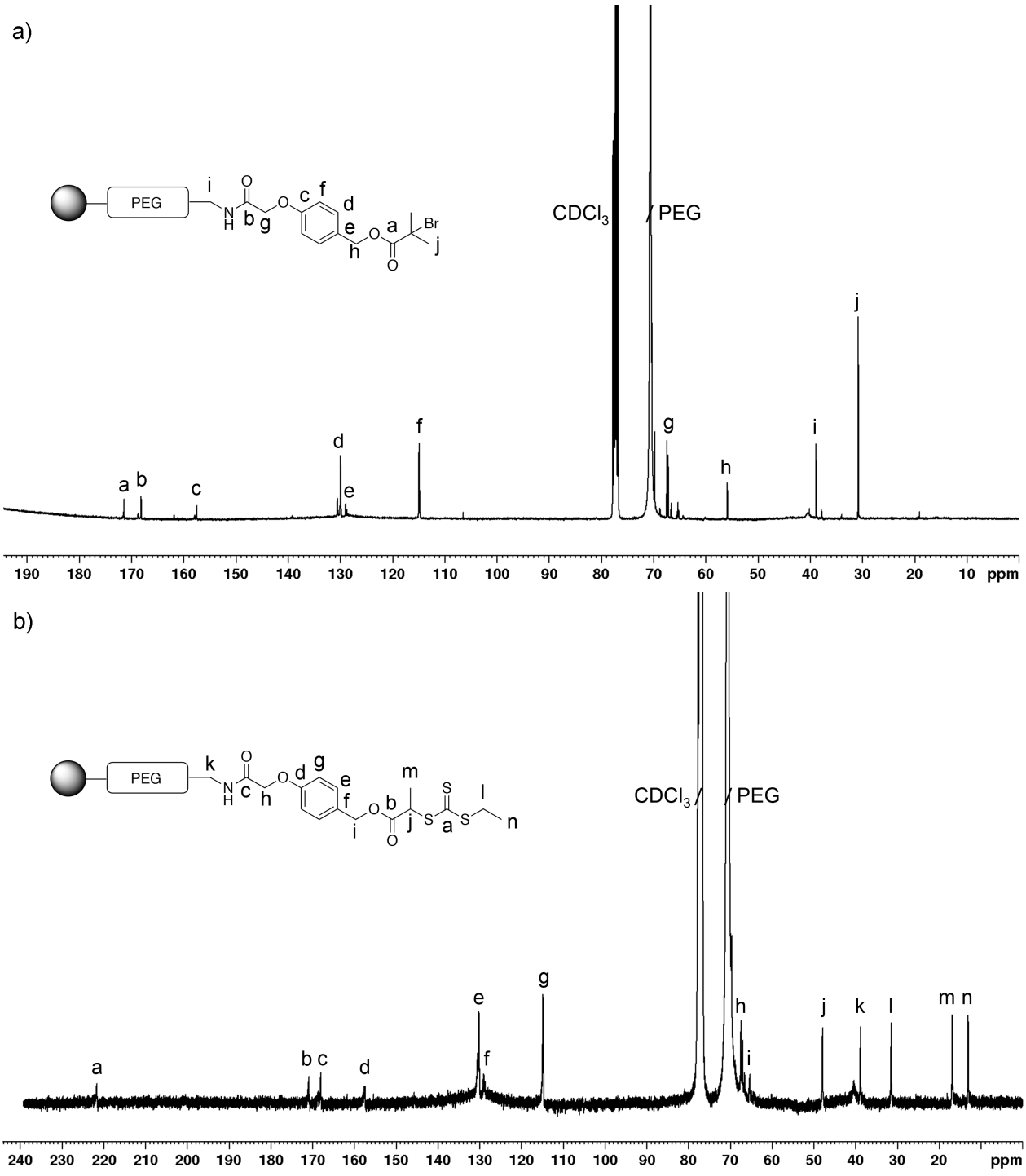

Figure 5-5. Gel-phase ^{13}C-NMR spectra of a) modified TGA-Br resin and b) modified TGA-CTA resin.

5.2.3 Optimization of RAFT Polymerization Conditions

Polymerizations in the presence of siRNA will require the use of aqueous buffer as solvent to retain its structure and functionality. Thus, polymerization conditions of PEGA were explored to find suitable conditions prior to the use of siRNA-CTA (**Scheme 5-5** and **Table 5-1**). For these studies, 2-(ethyl trithiocarbonate)propionic acid was used as the CTA, and azo initiator VA044 chosen for its water solubility and half-life at a low temperature. The polymerizations in pH 7.5 phosphate buffer saline (PBS) yielded high PDIs (PDI=1.56-2.20) and indicated that the polymerization was uncontrolled. This is likely due to the hydrolysis of the trithiocarbonate at neutral pH.[16] Changing the pH from 7.5 to 6.25 lowered the PDI significantly (PDI=1.17-1.30) and increased the rate of polymerization. We aimed to stop the polymerization at 40-50% conversion to prevent PEGA cross-linking and gelation. As a result, the condition selected was CTA:PEGA:VA044=1:100 (0.5 M):0.1 for 3 h at 40 °C in pH 6.5 PBS buffer, which was slightly less acidic than pH 6.25 and gave similar control over the polymerization.

Scheme 5-5. General scheme of RAFT polymerizations of PEGA.

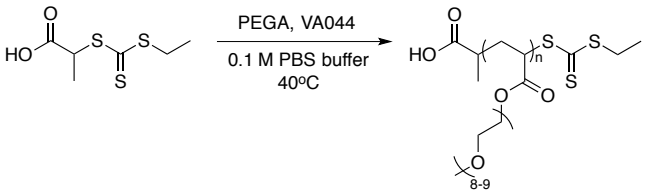

Table 5-1. RAFT polymerizations of PEGA under various conditions.

	pH	Solvent	CTA:PEGA:VA044	[PEGA]	Time (h)	Conversion	PDI
1	7.5	PBS	1: 100: 0.1	1	20	50%	2.20
2	7.5	PBS	1: 100: 1	1	4.3	46%	2.20
3	7.5	PBS	1: 30: 1	1	2	100%	1.69
4	7.5	PBS	1: (40+60): 1	1	3.5	45%	1.56
5	6.25	PBS	1: (40+60): 1	1	1	100%	1.17
6	6.25	PBS	1: 100: 0.2	1	1	89%	1.30
7	6.25	PBS	1: 100: 0.4	1	0.8	100%	1.20
8	6.5	PBS	1: 100: 0.2	0.7	1.25	90%	1.23
9	6.5	PBS	1: 100: 0.1	0.5	3.5	80%	1.23

5.2.4 RAFT Polymerizations with siRNA-CTA in the Presence of Sacrificial Resin

Polymerizations of PEGA from siRNA-CTA were attempted several times using previously selected conditions (**Scheme 5-6** and **Table 5-2**). The CTA concentration was calculated based on the Wang-CTA loading capacity (0.6 mmol/g), and the concentration of siRNA-CTA was neglected. From PAGE analysis, we could observe the sharp band of siRNA-CTA before polymerization (**Figure 5-6**, lane 2). In entry **RAFT-2**, a high molecular weight (MW) smear was observed, and the disulfide bond was cleaved under reducing conditions to release free siRNA as a sharp band (**Figure 5-6**, lane 3 and 4). For the remaining attempts, polymerization time was decreased to reduce the size of the polymer growth *grafted from* siRNA-CTA. However, the results were inconsistent and non-reproducible. In some attempts, Wang-CTA resin was not added. For example, **RAFT-5**, **RAFT-11**, **RAFT-14**, and **RAFT-15** were all conducted under the same condition (CTA:PEGA:VA044=1:100 (0.5 M):0.1 at 40 °C in pH 6.5 PBS buffer) for 60 min, but in **RAFT-5** and **RAFT-15**, no Wang-CTA resin was added.

The results varied from no reaction, to low polymer yield, or to gelation of the reaction (**Figure 5-6**). The high molecular weight smear observed in **RAFT-2** was not able to be reproduced, and further polymerization times of 3 h led to gelation of PEGA. This was probably caused by the occurrence of uncontrolled radical polymerizations of PEGA.

Scheme 5-6. RAFT polymerization of grafting PEGA from siRNA-CTA.

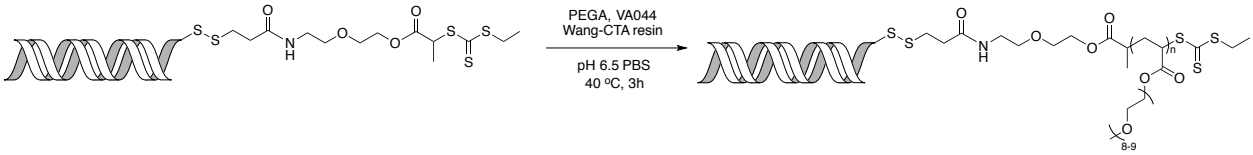

Table 5-2. RAFT polymerization attempts of grafting PEGA from siRNA-CTA.

Entry	Wang-CTA	Polymerization time (min)	Results (shown by PAGE gel)
RAFT-1	Yes	30	no reaction
***RAFT-2**	**Yes**	**180**	**high MW smear**
RAFT-3	Yes	30	low yield
RAFT-4	Yes	60	low yield
***RAFT-5**	**No**	**60**	**no reaction**
RAFT-6	No	90	no reaction
RAFT-7	Yes	120	gelation occurred
RAFT-8	Yes	130	gelation occurred
RAFT-9	Yes	90	gelation occurred
RAFT-10	Yes	30	low yield
***RAFT-11**	**Yes**	**60**	**gelation occurred**
RAFT-12	Yes	110	gelation occurred
RAFT-13	No	110	gelation occurred
***RAFT-14**	**Yes**	**60**	**low yield**
***RAFT-15**	**No**	**60**	**low yield**

* The PAGE analyses of the bolded entries are shown in the figure below.

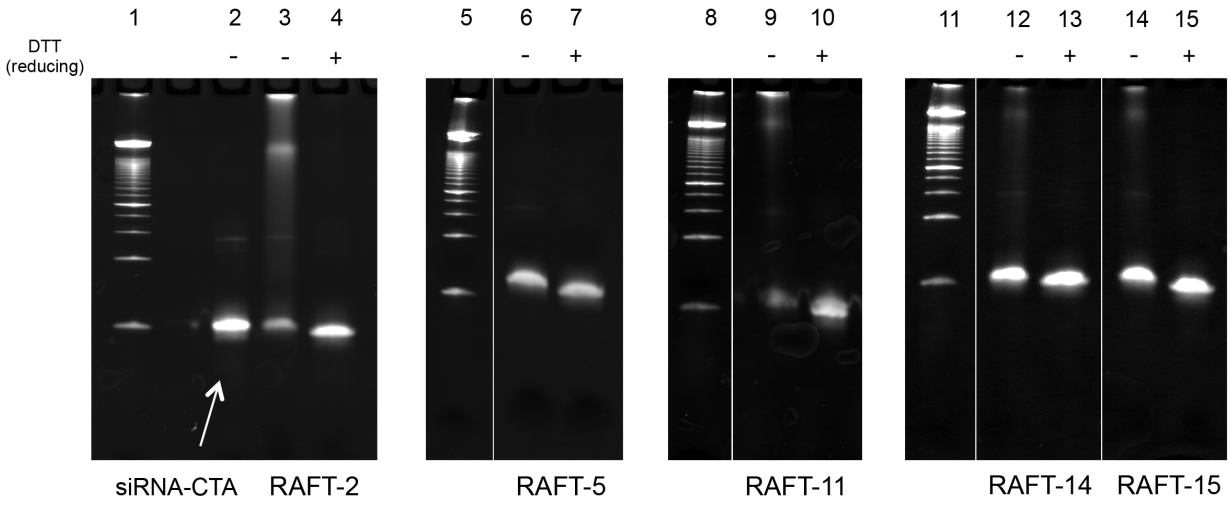

Figure 5-6. PAGE gel analysis of RAFT polymerizations of PEGA from siRNA-CTA (**RAFT-2**, **RAFT-5**, **RAFT-11**, **RAFT-14**, and **RAFT-15**). The white arrow is pointing to siRNA-CTA in lane 2.

After RAFT polymerizations, the Wang-CTA resins collected from the solution were analyzed gravimetrically and by IR spectroscopy. However, there was no increase in resin weight and no increase in C=O stretch intensity from pPEGA. Thus, no polymer growth from Wang-CTA occurred, even in **RAFT-2**, where polymer growth from siRNA-CTA was observed as a high MW smear. As mentioned in **Section 5.2.2**, it is likely due to the hydrophobic surface of Wang-CTA resins inhibiting surface-initiated polymerization. Therefore, several more RAFT polymerizations were conducted in the presence of TGA-CTA resin, which consists of a hydrophilic PEG surface, but still no polymer growth was observed (data not shown).

The effect of surface radical migration has been reported by Tsujii *et al*., who also reported the first surface-initiated graft polymerization using RAFT polymerization.[17] They

noticed a prominent low molecular weight shoulder while analyzing the cleaved graft chain by GPC analysis, which implied that there was significant undesired recombination. However, this phenomenon was nonexistent in polymer chains generated by the ATRP process. RAFT polymerization is mechanistically different from ATRP, and is based on the reversible chain transfer mediated by a chain transfer agent, most often a thiocarbonylthio group. In ATRP, the equilibrium between the dormant and active species is based on the reversible oxidative transfer of a halogen atom from the dormant species to the redox active transition metal catalyst complex to generate an active radical. They concluded that the high rate of termination in RAFT surface polymerizations was due to migration of radicals on the surface by chain transfer reactions. The exchange reaction should be highly dependent on the grafting density, and explains our results of not observing any polymer growth from both types of CTA-modified sacrificial resins due to the high loading density (0.28-1.0 mmol/g).

5.2.5 Normal ATRP with siRNA-I in the Presence of Wang-I Resin

To achieve *grafting from* siRNA-I, ATRP of PEGA was conducted in the presence of siRNA-I and Wang-I resin (**Scheme 5-7**). A negative control of unmodified siRNA was also subjected to the same polymerization conditions. As observed by PAGE analysis, a higher MW smear representing polymer growth was observed only when siRNA-I was added (**Figure 5-7**). In the siRNA control experiment, there was no difference or degradation before and after polymerization. Moreover, under reducing conditions, the resulting siRNA-pPEGA conjugate was reduced and completely released the free siRNA. This shows that the conjugate was through the disulfide bond and not a result of uncontrolled radical reaction on the siRNA. The results

showed that *grafting from* siRNA was achieved, and this experiment was referred to as **ATRP-1**. For the following experiments, the monomer was changed from PEGA to poly(ethylene glycol) methyl ether methacrylate (PEGMA, M_n=300), because methacrylates are generally a more appropriate choice for bromoisobutyrate initiators.

Scheme 5-7. ATRP of PEGA from siRNA-I in the presence of Wang-I resin.

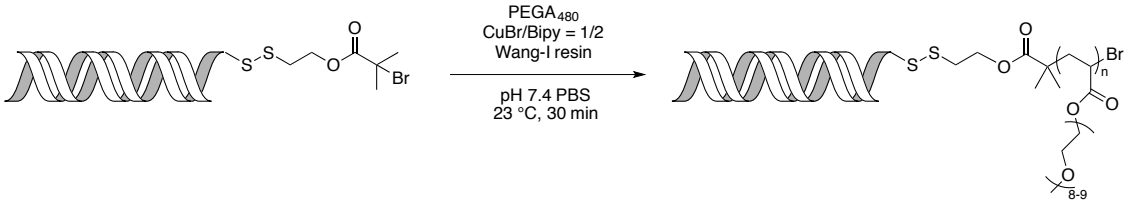

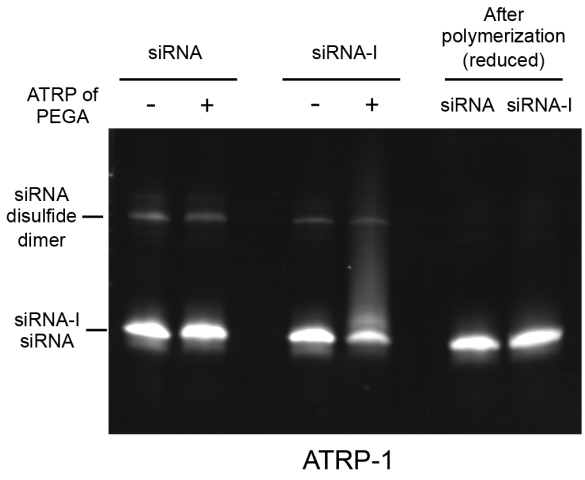

Figure 5-7. PAGE gel of conjugate samples after normal ATRP of PEGA conducted in the presence of siRNA control and siRNA-I, respectively. After polymerization, the samples were reduced with DTT, and both showed sharp bands of free siRNA after reduction.

The same ATRP conditions were performed using PEGMA as the monomer (**Scheme 5-8**). In PAGE analysis, a higher MW smear representing polymer growth was observed under non-reducing conditions, and released siRNA was observed under reducing conditions (**Figure 5-8**). The results were reproducible with two sets of results (out of many) shown here (**ATRP-2** and **ATRP-3**). However, most of the conjugates were retained in the stacking layer of the gel, meaning that the molecular weights were very large. To better control the polymer growth so that we could observe the conjugate within the gel, we re-investigated the polymerization conditions.

Scheme 5-8. ATRP of PEGMA from siRNA-I in the presence of Wang-I resin.

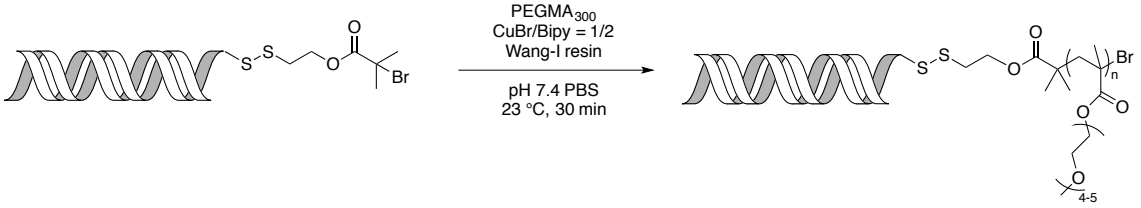

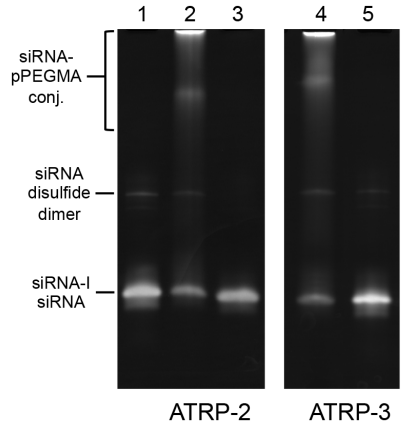

Figure 5-8. PAGE analysis of samples from normal ATRP of PEGMA initiated with siRNA-I. Lane 1: siRNA-I before polymerization; Lane 2 and 4: siRNA-I after polymerization of PEGMA; Lane 3 and 5: siRNA-I after polymerization of PEGMA, under reducing conditions.

5.2.6 Optimization of ATRP Conditions in Solution and in the Presence of Resin

Polymerization conditions of PEGMA for improved control in polymerization rate and PDI were explored. Tris-EDTA (TE) buffer is one of the widely utilized siRNA buffers. EDTA chelates metal ions necessary for nuclease activity, and protects siRNA from nuclease degradation.[18] However, we avoided the use of TE buffer during the polymerizations, since the EDTA would also chelate copper, replace the ligands, and deactivate the catalyst in ATRP. Instead, we used phosphate-buffered saline (PBS). However, ATRP in PBS may be problematic due to the possibility of the phosphate ions forming insoluble $Cu_3(PO_4)_2$ salt, or the chloride ions displacing the ligands, which would both consume copper and deactivate the catalyst.[19] Matyjaszewski and coworkers have conducted a systematic investigation of ATRP and AGET ATRP under such conditions, and their results have been adapted to this study.[19]

For the development of a model system, α-bromoisobutyric acid was used as the initiator for its water solubility (**Scheme 5-9** and **Table 5-3**). Normal ATRP with CuBr/Bipy catalyst complex in PBS yielded high PDIs (PDI=1.79-1.96) and indicated that the polymerizations were uncontrolled. Well-controlled ATRP in aqueous systems is challenging due to a number of factors. The polymerizations generally undergo high activation rate, dissociation of halide from the Cu(II)-X deactivating species, decreased stability of Cu/ligand complexes, disproportionation of Cu(I) and hydrolysis of C-X bonds. From entry 4 through 6, the catalyst system was changed to $CuCl/CuBr_2$/Bipy. Addition of $CuBr_2$ as deactivator increased the concentration of the deactivating species and reduced the activation rate. Also, Matyjaszewski and coworkers have reported that mixed halide initiation systems (i.e., R-Br as initiator and CuCl as catalyst) provide better control of ATRP because C-Cl bonds are more stable than C-Br bonds, and therefore should give faster initiation and slower propagation.[20] These changes in the catalyst system

lowered the PDI significantly (PDI=1.39-1.52). However, these results were still not considered well controlled (PDI<1.30).

To avoid instability of the active catalyst complex in the aqueous system, Activator Generated by Electron Transfer for ATRP (AGET ATRP) was employed. AGET ATRP combines higher oxidation state catalyst complexes with reducing agents, such as ascorbic acid (AA), to produce active catalyst complexes *in situ*.[21,22] Matyjaszewski's group demonstrated the use of $CuCl_2$/TPMA/AA for well-controlled polymerizations by aqueous AGET ATRP of OEOMA300 and OEOMA475.[22] Our results also demonstrated that AGET ATRP allowed improved control of the polymerization (PDI=1.20).

Scheme 5-9. General scheme of ATRP of PEGMA.

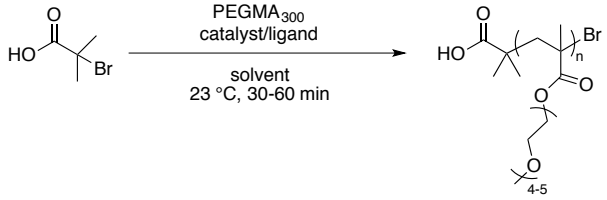

Table 5-3. ATRP and AGET ATRP of PEGMA under various conditions.

	Catalyst / ligand	[$PEGMA_{300}$]	M/ I/ catalyst/ ligand	Solvent	t (min)	Conv.	$M_{n,\,GPC}$	PDI
1	CuBr / Bipy	0.5	50/ 1/ 1/ 2.2	pH 7.4 PBS	30	68%	35 700	1.96
2	CuBr / Bipy	0.5	50/ 1/ 1/ 2.2	pH 6.5 PBS	30	47%	22 200	1.79
3	CuBr / $CuBr_2$ / Bipy	0.5	50/ 1/ 1/ 9/ 22	pH 7.4 PBS	60	0%	-	-
4	CuCl / $CuBr_2$ / Bipy	0.5	50/ 1/ 1/ 0.3/ 3	pH 7.4 PBS	30	35%	19 400	1.39
5	CuCl / $CuBr_2$ / Bipy	0.5	50/ 1/ 1/ 0.3/ 3	pH 7.4 PBS	60	44%	20 800	1.50
6	CuCl / $CuBr_2$ / Bipy	0.5	50/ 1/ 1/ 0.3/ 3	50mM NaCl	30	55%	18 900	1.52
7	$CuCl_2$ / TPMA / AA	0.5	50/ 1/ 1/ 1/ 0.6	pH 7.4 PBS	30	43%	18 000	1.20

To confirm that hydrophilic TGA-I resins allow surface-initiated polymer growth in aqueous buffered solvent systems, the selected polymerization conditions were applied to *grafting from* the TGA-I resin (**Scheme 5-10** and **Table 5-4**). ATRP with additional deactivators ($CuBr_2$) and AGET ATRP conditions were both conducted in the presence of TGA-I resin. The concentration of initiators was calculated based on the loading capacity of TGA resins (0.28 mmol/g). Besides PEGMA, diethylene glycol methyl ether methacrylate (m=2, later referred to as DEGMA) was used as another monomer choice. DEGMA can be analyzed by MALDI-TOF MS, which provided an additional characterization method that requires only small quantities of material.[23] After polymerization, the resin was separated by centrifugation and polymer growth was confirmed by IR analysis, as observed by the increase in carbonyl C=O stretch of the polymethacrylate esters at approximately 1750 cm^{-1} (**Figure 5.10 a** and **Figure 5.11 a**).

The polymers *grafted from* the resin were collected by acidic hydrolysis of the benzyl ester using 95% TFA. The cleaved polymers were analyzed by both ^{1}H-NMR and GPC (**Table 5-4**). The PDIs were slightly higher than the polymerizations conducted with α-bromoisobutyric acid as the initiator. With the addition of $CuBr_2$ as a deactivator, the ATRP of DEGMA gave PDI=1.74. With AGET ATRP, the polymerization of PEGMA and DEGMA gave PDI of 1.42 and 1.39, respectively. Therefore, identical AGET ATRP conditions were brought forward with siRNA-I incorporated in the polymerizations.

Scheme 5-10. General scheme of ATRP/AGET ATRP from TGA-I resin.

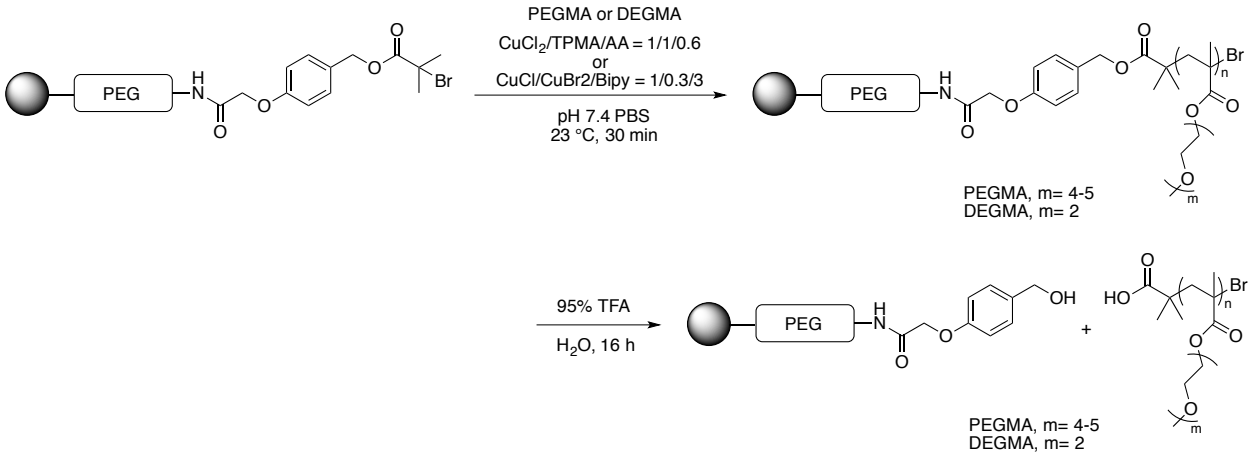

Table 5-4. Characterization of the polymers cleaved from TGA-I resin.

Cleaved polymer	ATRP	$M_{n,\ GPC}$	PDI
pPEGMA	AGET	11 700	1.42
pDEGMA	AGET	8 400	1.39
pDEGMA	normal	9 100	1.74

5.2.7 AGET ATRP with siRNA-I in the Presence of TGA-I Resin

After investigation of ATRP and AGET ATRP conditions in aqueous buffers and with TGA-I resins, we incorporated siRNA-I into the developed system (**Scheme 5-11**). To determine the role of TGA-I resin, AGET ATRP of PEGMA in the presence of siRNA-I was conducted with (**AGET-1**) and without (**AGET-2**) TGA-I resin. To examine if removing free siRNA before polymerization can increase the conjugation yield, AGET ATRP of DEGMA from siRNA-I that

had (**AGET-4**) and had not (**AGET-3**) been purified by HPLC (**Section 5.2.1**) was also performed.

Scheme 5-11. AGET ATRP of PEGMA/DEGMA from siRNA-I in the presence of sacrificial resin initiator, TGA-I resin.

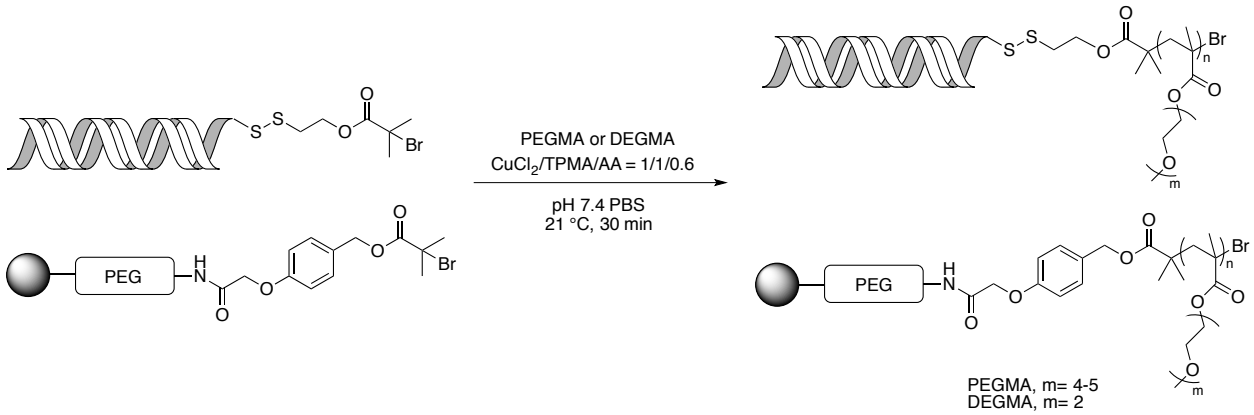

The resin and supernatant were separated by centrifugation after terminating the polymerization. By analyzing the supernatant (containing everything but the polymer-coated resin) with gel electrophoresis, higher molecular weight shifts in all PEGMA and DEGMA polymerization trials were observed (**Figure 5-9**, lanes 1, 3, 5, and 7). Also, all conjugate linkages were cleavable with DTT to release free siRNA under reducing conditions (lanes 2, 4, 6 and 8). By comparing **AGET-1** (lane 1) and **AGET-2** (lane 3), no noticeable differences in polymerization yield or polymer size was observed without the addition of TGA-I resin. The difference between **AGET-3** (lane 5) and **AGET-4** (lane 7) was also insignificant, implying that the unreacted siRNA in the conjugate mixture was mainly due to low initiator efficiency, instead

of unpurified starting material. This kind of inefficiency has been observed with similar pyridyl disulfide initiators.[24] The conjugates were similar to **ATRP-2** and **ATRP-3**, with the conjugate mainly retained in the stacking layer. However, it was essential for us to characterize the size and PDI of the grafted polymer to further improve the results.

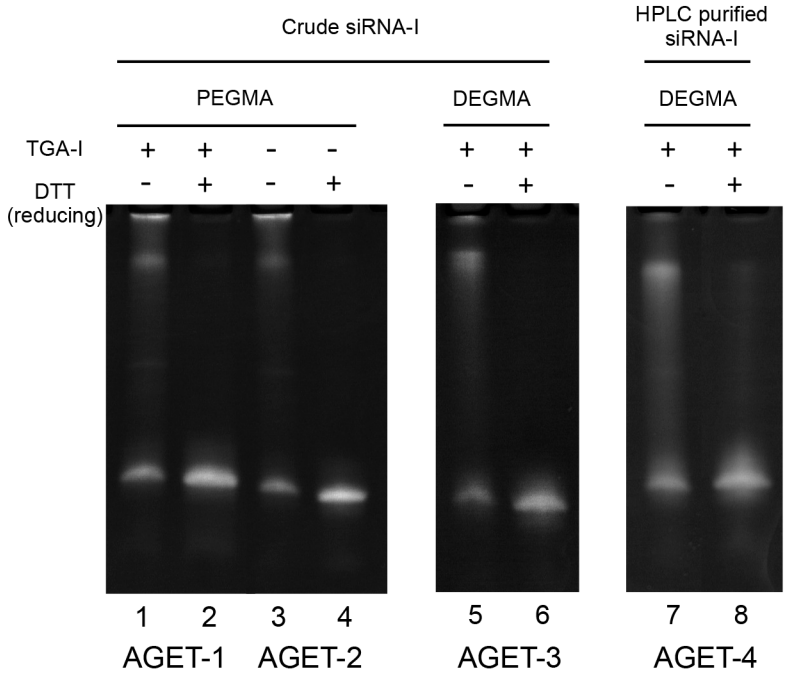

Figure 5-9. PAGE analysis of non-reduced and reduced **AGET-1** (siRNA-pPEGMA conjugate, AGET ATRP with TGA-I resin), **AGET-2** (siRNA-pPEGMA conjugate, AGET ATRP without TGA-I resin), **AGET-3** (siRNA-pDEGMA conjugate, AGET ATRP with TGA-I resin), and **AGET-4** (siRNA-pPEGMA conjugate, AGET ATRP with TGA-I resin and HPLC purified siRNA-I).

Since siRNA-I was only available in very small quantities (nanomoles), it would result in less than 5 micrograms of grafted polymers even if collected after disulfide bond cleavage. We first hypothesized that the polymers grafted from TGA-I resin and siRNA-I in the same polymerization vessel may result in similar and comparable sizes. This strategy is often utilized to determine molecular weight for example from surfaces.[13,17] Polymer growth from TGA-I resin was confirmed by IR analysis, as observed by the increase in carbonyl C=O stretch of the polymethacrylate esters around 1750 cm^{-1} (**Figure 5.10 b** and **Figure 5.11 b**). The polymers were cleaved by TFA and characterized by GPC (**Table 5-5**). All polymers showed average molecular weight around 7 kDa (6.5-7.7 kDa) with PDI around 1.40 (1.37-1.42).

Table 5-5. Characterization of the polymers cleaved from TGA-I resins in **AGET-1**, **AGET-3**, and **AGET-4**.

	Cleaved polymer	$M_{n,\ GPC}$	PDI
AGET-1	pPEGMA	7 300	1.42
AGET-3	pDEGMA	6 500	1.41
AGET-4	pDEGMA	7 700	1.37

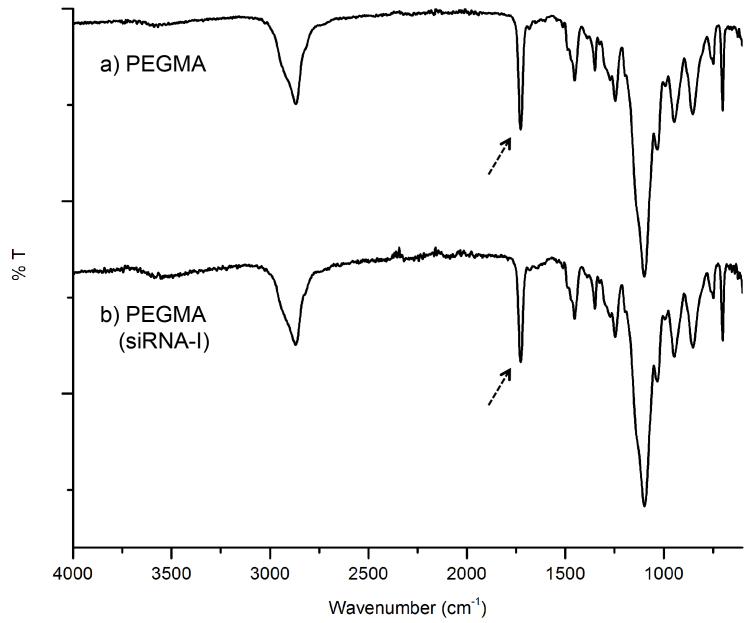

Figure 5-10. IR spectra of TGA-I resin after a) AGET ATRP of PEGMA, and b) AGET ATRP of PEGMA in the presence of siRNA-I.

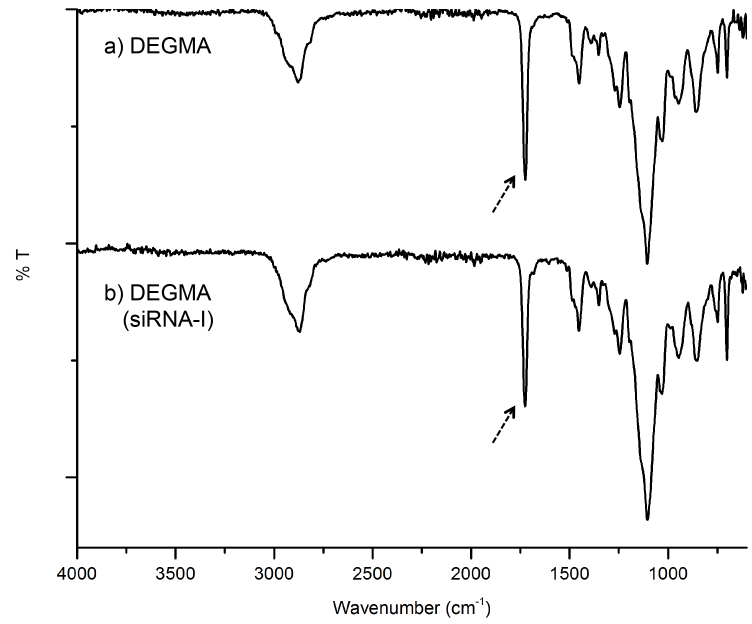

Figure 5-11. IR spectra of TGA-I resin after a) AGET ATRP of DEGMA, and b) AGET ATRP of DEGMA in the presence of siRNA-I.

pDEGMA cleaved from TGA-I resin in **AGET-3** was also characterized by MALDI-TOF (**Figure 5-12**). A typical mass spectrum of a polymer was obtained, with evenly distributed peaks, and the difference in between each peak corresponding to the mass of one monomer unit. The mass distribution (base peak m/z=5861.09) corresponded quite well to the average molecular weight obtained by gel permeation chromatography, which was 6500 Da. However, when *grafting from* a resin/surface, the grafting density reaches to a maximum due to the steric crowding of polymer chains. The molecular weights of the grafted polymers were likely not comparable to the polymers that were *grafted from* siRNA. Therefore, we needed other methods to determine the sizes of the siRNA-polymer conjugates.

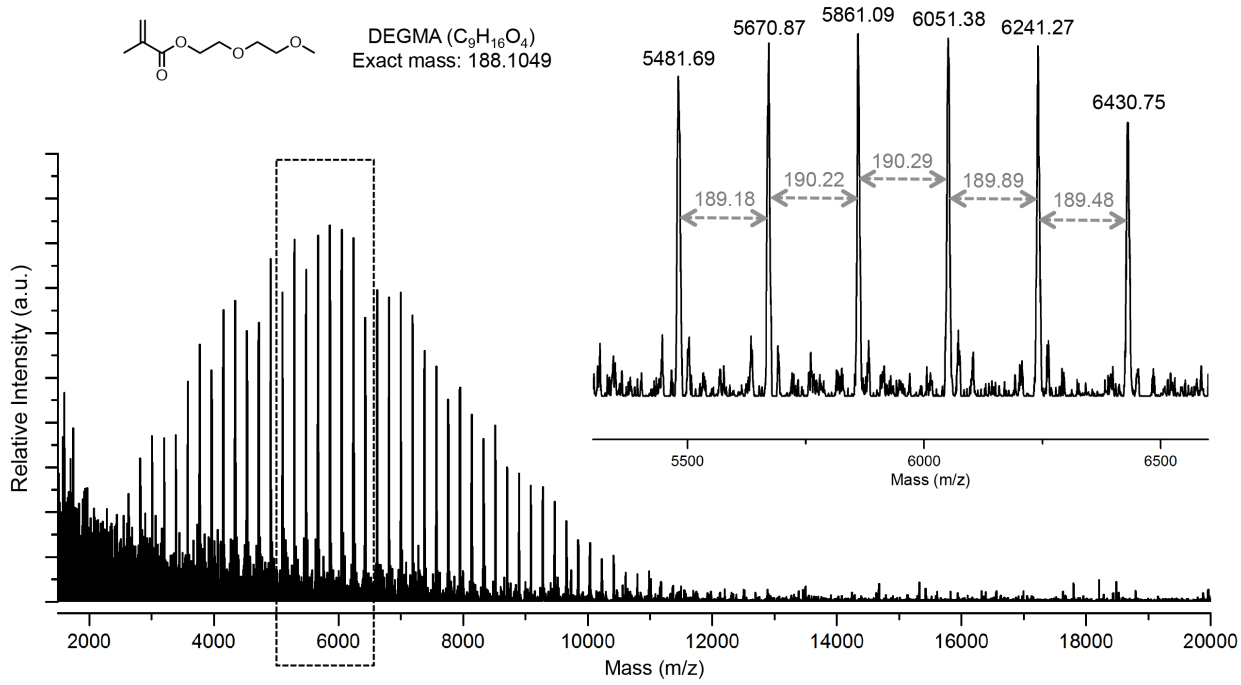

Figure 5-12. MALDI-TOF MS spectrum of pDEGMA cleaved from **AGET-3** resin. The distance between each peak corresponds closely to the mass of DEGMA monomer.

5.2.8 Determination of Molecular Weights of Grafted pDEGMA

Using previous polymerization conditions, the conjugates mainly retained in the stacking layer, which indicated that the grafted polymers had a much higher molecular weight comparing to siRNA. With the conjugates retained in the stacking layer or loading well, the relative size between each conjugate were not comparable. To overcome this issue, we changed the TBE polyacrylamide gels from 15% to a gradient of 4-20% for better separation within a larger molecular weight range. We also modified the polymerization conditions to decrease the monomer ratio (from 50 to 10 or 15), monomer concentration (from 0.5 M to 0.1 or 0.15 M), and polymerization time (from 30 minutes to 10 or 15 minutes), in order to reduce the size of the resulting conjugates (**Table 5-6** and **Figure 5-14,** lane 1 through 3).

Table 5-6. Summary of the polymerization conditions of **AGET-5** through **AGET-7**.

	[DEGMA] (M)	M:I[a]	Time (min)
AGET-5	0.10	10	10
AGET-6	0.15	15	15
AGET-7	0.15	15	30

[a] Monomer to initiator (TGA-I resin) ratio

To estimate the size of the siRNA conjugates, five pyridyl disulfide end-functionalized pDEGMAs (**pDEGMA-1** through **pDEGMA-5**) were synthesized by AGET ATRP (**Scheme 5-12**) and characterized by NMR and GPC to serve as molecular weight references (**Table 5-7**, see Appendix **Figure 5-22** through **Figure 5-26** for NMR spectra). The M_n (GPC) of the polymers

ranged from 8.8 kDa to 45.9 kDa with PDIs below 1.30, indicating that the polymerizations were well controlled (**Figure 5-13**).

Scheme 5-12. *Grafting from* siRNA and *grafting to* siRNA using AGET ATRP.

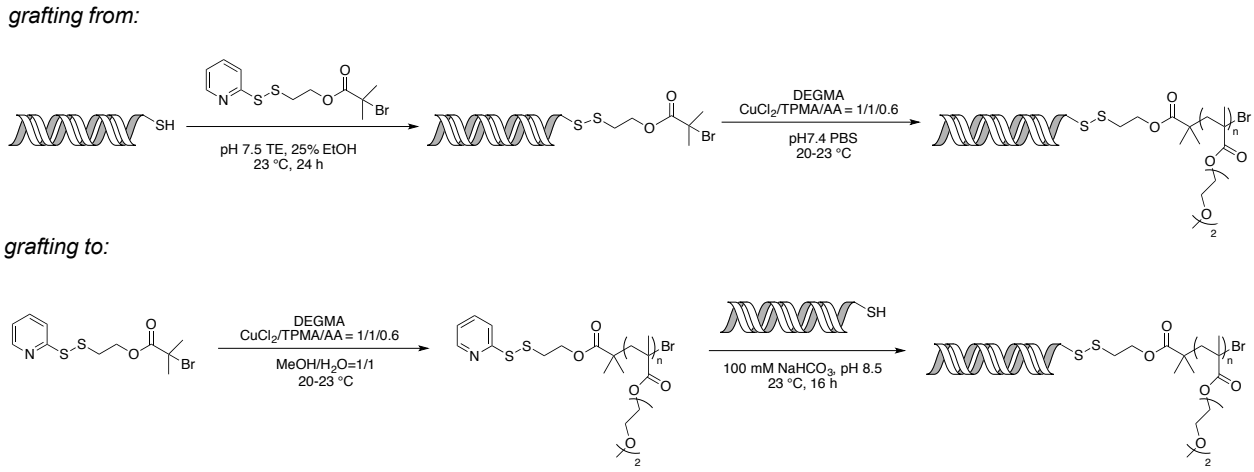

Table 5-7. Polymerization conditions and characterizations of **pDEGMA-1** through **pDEGMA-5**.

polymer	M:I[a]	Time (min)	Conversion (%)	M_n (theory)	M_n (NMR)	M_n (GPC)	PDI
pDEGMA-1	80:1	30	25	4 100	10 100	8 800	1.30
pDEGMA-2	200:1	45	30	11 600	16 400	12 300	1.20
pDEGMA-3	200:1	120	50	19 200	26 500	17 100	1.29
pDEGMA-4	500:1	100	30	28 600	38 000	29 900	1.24
pDEGMA-5	500:1	285	50	47 400	53 400	42 800	1.29

[a] Monomer (DEGMA) to initiator ratio

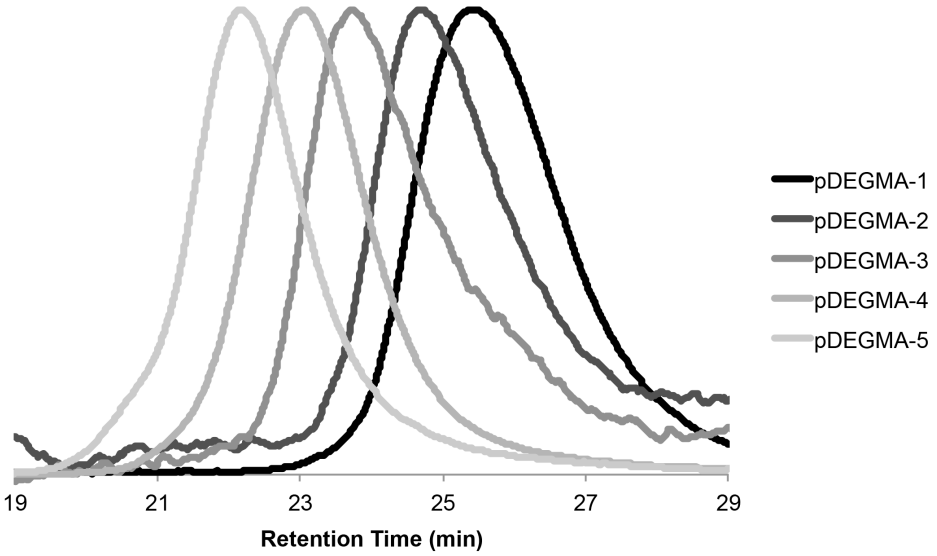

Figure 5-13. GPC traces overlay of **pDEGMA-1** (black) through **pDEGMA-5** (light gray).

The polymers were then *grafted to* siRNA, and the resulting conjugates were compared to conjugates that were prepared by the *grafting from* method (**AGET-5** through **AGET-7**) on 4-20% TBE polyacrylamide gels (**Scheme 5-12** and **Figure 5-14**). Using the five pre-synthesized and pre-characterized polymers as molecular weight references, the sizes of **AGET-5**, **AGET-6**, and **AGET-7** correlate well to the 8.8 kDa, 12.3 kDa, and 17.1 kDa conjugates, respectively.

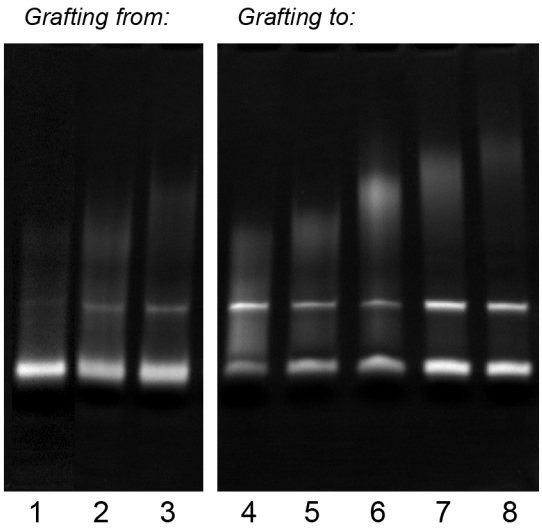

Lanes	Conjugate	Polymer M_n (kDa)	Conjugation Yield (%)
1	AGET-5	-	34
2	AGET-6	-	53
3	AGET-7	-	40
4	pDEGMA-1	8.8	82
5	pDEGMA-2	12.3	69
6	pDEGMA-3	17.1	78
7	pDEGMA-4	29.9	58
8	pDEGMA-5	42.8	49

Figure 5-14. PAGE analysis of siRNA-pDEGMA conjugates prepared by the *grafting from* method (lanes 1 through 3) and the *grafting to* method (lanes 4 through 8).

AGET-6 and **AGET-7** were also characterized by ^{1}H NMR spectroscopy to confirm the presence of pDEGMA (see Appendix **Figure 5-27** and **Figure 5-28**). A Shigemi tube, a microscale and magnetically susceptible NMR tube that requires smaller sample volume, was used for data acquisition of these samples. Also, an additional step of H_2O presaturation to suppress the water signal was necessary for such dilute samples in aqueous buffers. From ^{1}H NMR spectra, the presence of pDEGMA after polymerization from siRNA-I was confirmed in both samples.

5.2.9 Purification of siRNA-pPEG(M)A Conjugates by FPLC

One of the major drawbacks of *grafting to* is that purification is often a challenge, due to the similar molecular weights of the components and the excess amount of polymer required. On the other hand, *grafting from* provides easier purification due to significant mass differences between the bioconjugate and small molecule impurities. In **Chapter 4**, we described the synthesis a siRNA-pPEGA conjugate by the *grafting to* method. In **Section 5.2.4**, we described a siRNA-pPEGA conjugate (**RAFT-2**) synthesized by the *grafting from* method using RAFT polymerization. Also, in **Section 5.2.5**, we described the synthesis of siRNA-pPEGMA conjugates using (**ATRP-2** and **ATRP-3**) by the *grafting from* method using normal ATRP. These conjugates were collected and purified by Fast Protein Liquid Chromatography (FPLC) using a Superose 6 10/300 column and a UV detector set at 260 nm (**Figure 5-15**). For each sample, three fractions were collected and analyzed, labeled as 1 to 3. For siRNA-pPEGA conjugate that was prepared from the *grafting to* method, excess polymer interfered with the separation of siRNA, conjugate, and polymer. From the chromatogram and PAGE analysis, we observed that fraction 2 was mainly the conjugate, and fraction 3 consisted of mainly free siRNA and excess polymer (not stained on gel). The separation was not ideal, because the fractions overlapped and cross-eluted. For both **RAFT-2** and **ATRP-3** that were prepared by *grafting from*, the peaks in the chromatogram were highly resolved. By PAGE analysis, the fraction mainly consisted of the conjugate, without any free siRNA contamination. There was also no free polymer observed in the chromatogram. (Note: there was a peak at approximately 5 min retention time in **ATRP-3** that was not identified.) Therefore, the benefit of *grafting from* to increase the ease of purification has been demonstrated by preparing three similar conjugates through different synthetic methods.

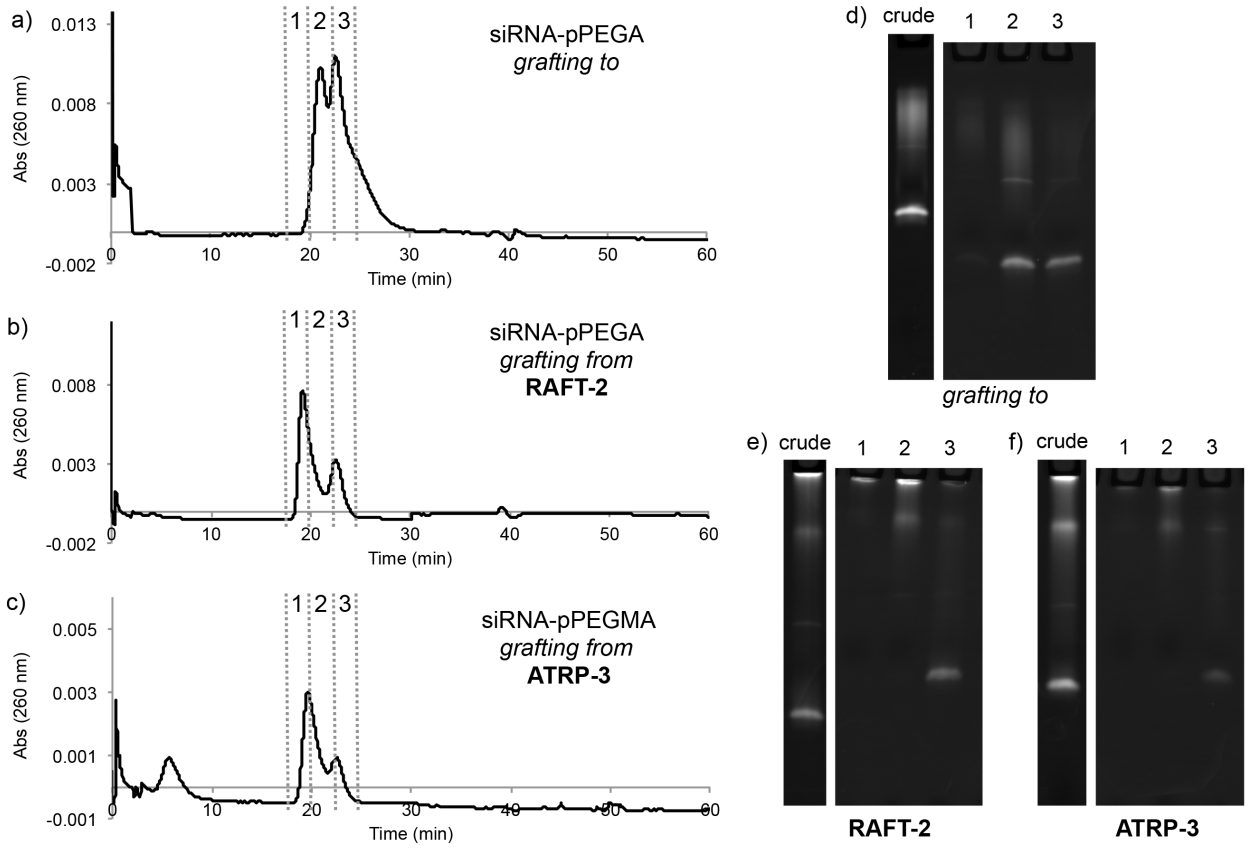

Figure 5-15. FPLC traces (a,b,c) and PAGE analysis (d,e,f) of siRNA-pPEGA conjugate prepared by *grafting to* (a,d), **RAFT-2** siRNA-pPEGA conjugate (b,e), and **ATRP-3** siRNA-pPEGMA conjugate (c,f). The "crude" lane shows the crude product before FPLC purification. As observed in the gels, **RAFT-2** and **ATRP-3** were successfully separated from unreacted siRNA (lane 2).

5.3 Conclusions

Herein, we demonstrated the first example towards preparing siRNA-polymer conjugates using the *grafting from* technique. We reported the synthesis of siRNA-I and siRNA-CTA as macroinitiators and macro-CTAs for ATRP and RAFT, respectively. We also prepared sacrificial initiators CTAs on hydrophobic and hydrophilic resin surfaces. RAFT polymerization conditions of PEGA were optimized for aqueous conditions at mild temperatures (40 °C). However, RAFT polymerizations in the presence of siRNA-CTA were non-reproducible, and we hypothesize the reason to be unsuccessful chain transfer process at low concentrations of siRNA-CTA. No polymer growth was observed from the resin surface of the sacrificial CTA, which could be due to surface radical migration effect and enhanced recombination.[17] In the ATRP system, we observed polymer growth (pPEGA) from siRNA-I, while no difference was observed for unmodified siRNA under the same conditions. By using AGET ATRP in pH 7.4 PBS, PEGMA and DEGMA were successfully *grafted from* siRNA-I and TGA-I resins, which were observed by PAGE analysis of the conjugates and IR analysis of the resin. The polymer *grafted from* TGA-I resin were cleaved and analyzed by ^{1}H-NMR, GPC, and MALDI-TOF MS, but the molecular weight did not correspond to the siRNA-polymer conjugates. The smaller polymer sizes on the resin were likely a result of reaching the maximum grafting density on the surface. To analyze the siRNA-polymer conjugates, tuning monomer-initiator ratio, monomer concentration, and polymerization time controlled the conjugate sizes. We estimated the siRNA-pDEGMA conjugate sizes (**AGET-5** through **AGET-7**) by synthesizing pyridyl disulfide end-functionalized pDEGMAs and using the *grafting to* technique to prepare siRNA-pDEGMA conjugates with pre-determined sizes, and concluded that the conjugate sizes were approximately 9, 13, and 17 kDa, respectively. The advantage of using the *grafting from* method was also

demonstrated by FPLC purification of the conjugates prepared by different methods. Conjugates prepared by *grafting to* required the addition of an excess of polymer, which was challenging to remove and also affected the separation of siRNA and the conjugate. As a conclusion, *grafting from* siRNA has been demonstrated for the first time, and can serve as an alternative method to prepare well-defined siRNA-polymer conjugates in the future.

5.4 Experimental Section

Materials

Chemicals were purchased from Sigma-Aldrich and Fisher Scientific and used as received unless otherwise specified. NovaSyn® TGA resin (130 μm) was purchased from Novabiochem®. Complementary 5'-thiol modified sense siRNA (5'ThioMC6-D-GCU GAC CCU GAA GUU CAU CUU-3') and antisense siRNA (5'-GAU GAA CUU CAG GGU CAG CUU-3') specific for enhanced green fluorescent protein (eGFP) mRNA and a scrambled sequence of complementary 5'-thiol modified sense siRNA (5'ThioMC6-D-GCC ACG UAU CGA UGU UUA CUU-3') and antisense siRNA (5'-AGG UAA ACA UCG AUA CGU GGC-3') were purchased from Integrated DNA Technologies. 15% Mini-PROTEAN® TBE-Urea Precast Gels were purchased from Bio-Rad. SYBR-Safe nucleic acid staining dye was purchased from Invitrogen.

Instrumentation

^{1}H and ^{13}C NMR spectra were obtained on Avance DRX 400, Bruker AV 500 and DRX 500 MHz spectrometers. Proton NMR spectra were acquired with a delay of 2 sec for small molecules, and a delay of 30 sec for all polymers. UV-Vis spectroscopy was performed using a Biomate 5 Thermo Spectronic spectrometer or Thermo Scientific NanoDrop 2000 (for small quantities such as siRNA samples). High-resolution electrospray ionization mass spectrum (HRESI-MS) was obtained on an IonSpec Ultima 7T ICR, (Varian Inc.) in the Molecular Instrumentation Center at UCLA. Infrared spectroscopy was performed using a PerkinElmer FT-IR equipped with an ATR accessory. Gel permeation chromatography was conducted on a Shimadzu HPLC system equipped with a refractive index detector RID-10A, one Polymer

Laboratories PLgel guard column, and two Polymer Laboratories PLgel 5 μm mixed D columns. DMF containing 0.10 M LiBr at 40 °C was used as the eluent (flow rate: 0.80 mL/min) and near-monodisperse poly(methyl methacrylate) from Polymer Laboratories were used for calibration. Gel electrophoresis was performed using 15% Tris Borate EDTA (TBE) polyacrylamide gel electrophoresis (PAGE) at a constant voltage of 200 V for 45 minutes using 1X TBE buffer (pH 8.0). The siRNA gel was stained with SYBR Safe stain (Invitrogen) in 1X TBE buffer for 20 minutes. Visualization was conducted with a Bio-Rad FX Pro Plus Fluorimager located in the DOE-Biochemistry Facility at UCLA. Fast protein liquid chromatography (FPLC) was performed on a Bio-Rad BioLogic DuoFlow chromatography system equipped with a GE Healthcare Life Sciences Superose 6 10/300 column and a QuadTec detector.

Methods

Synthesis of 3-(2-pyridyldithio)-propanoic acid 3. 1,2-Di(pyridin-2-yl)disulfane (3 g, 13.62 mmol) was dissolved in methanol and acetic acid (0.75 mL) and 3-mercapto-propanoic acid (0.482 g, 3.54 mmol) were added. The mixture stirred at 23 °C for 2 h. The viscous yellow oil was placed under vacuum to remove the acetic acid, and the crude product was purified using Hex/EtOAc=2/1+2% AcOH (89% yield). ^{1}H NMR (400 MHz in $CDCl_3$) δ: 8.54-8.45 (m, 1H), 7.74-7.66 (m, 1H), 7.66-7.58 (m, 1H), 7.23-7.15 (m, 1H), 3.11-3.04 (t, *J*=6.64 Hz, 2H), 2.82-2.74 (t, *J*=6.64 Hz, 2H). ^{13}C NMR (400 MHz in CDCl3) δ: 175.58, 159.22, 149.45, 137.47, 129.10, 121.30, 120.68, 34.20, 34.03. IR: ν = 3078, 3057, 2912, 2852, 2540, 1891, 1726, 1580, 1561, 1446, 1422, 1386, 1249, 1187, 1081, 1001, 770, 763 cm^{-1}.

Synthesis of N-(2-(2-hydroxyethoxy)ethyl)-3-(pyridin-2-yldisulfanyl)propanamide 4. **3** (200 mg, 1.08 mmol) was dissolved in ice cold DCM. 2-(2-aminoethoxy)ethanol (0.1 mL, 0.98 mmol) and

EDC (225 mg, 1.17 mmol) were added and the mixture was stirred on ice bath for 30 min, and then at 23 °C for 2 h. The crude product was purified using DCM/MeOH=9/1 (50% yield). ^{1}H NMR (400 MHz in $CDCl_3$) δ: 8.48-8.41 (m, 1H), 7.66-7.58 (m, 2H), 7.18-7.12 (bs, NH), 7.12-7.06 (m, 1H), 3.76-3.63 (m, 2H), 3.60-3.50 (m, 4H), 3.50-3.40 (m, 2H), 3.14-2.94 (t, *J*=6.88 Hz, 2H), 2.63-2.51 (t, *J*=6.88 Hz, 2H). ^{13}C NMR (400 MHz in CDCl3) δ: 171.10, 159.60, 149.51, 137.32, 120.07, 120.39, 72.33, 69.88, 61.61, 39.45, 35.67, 34.75. IR: ν = 3292, 3079, 2924, 2868, 1731, 1646, 1559, 1446, 1417, 1372, 1353, 1253, 1118, 1064, 760, 732, 717 cm^{-1}. ESI-MS (± 1.0) observed (predicted): H^+ 303.0824 (303.0832).

Synthesis of RAFT CTA 5. **4** (35 mg, 0.116 mmol) was dissolved in ice cold DCM. 2-(ethyl trithiocarbonate)propionic acid (21 mg, 0.10 mmol) and EDC (23 mg, 0.12 mmol) were added and stirred in ice bath for 30 min, then at 23 °C for 2 h. The crude product was purified using Hex/EtOAc=1/2 to yield a yellow oil (80% yield). ^{1}H NMR (400 MHz in $CDCl_3$) δ: 8.53-8.46 (m, 1H), 7.70-7.62 (m, 2H), 7.16-7.08 (m, 1H), 6.69-6.58 (bs, NH), 4.86-4.78 (q, *J*=7.37 Hz, 1H), 4.36-4.22 (m, 2H), 3.70-3.62 (m, 2H), 3.60-3.52 (m, 2H), 3.51-3.43 (m, 2H), 3.40-3.30 (q, *J*=7.44 Hz, 2H), 3.13-3.05 (t, *J*=6.86 Hz, 2H), 2.68-2.60 (t, *J*=6.86 Hz, 2H), 1.62-1.56 (d, *J*=7.40 Hz, 3H), 1.37-1.31 (t, *J*=7.42 Hz, 3H). ^{13}C NMR (500 MHz in CDCl3) δ: 221.82, 171.22, 170.78, 159.56, 149.49, 137.33, 121.02, 120.35, 69.90, 68.77, 64.65, 47.83, 39.39, 35.78, 34.82, 31.61, 16.79, 12.97. IR: ν = 3388, 3046, 2927, 1732, 1647, 1560, 1446, 1417, 1251, 1163, 1118, 1078, 1028, 813, 760 cm^{-1}. ESI-MS (± 1.0) observed (predicted): H^+ 495.0593 (495.0569). UV-Vis (H_2O) λ_{max} = 295 nm.

Synthesis of siRNA-I and siRNA-CTA. A solution of 5' ThioMC6 modified-siRNA (125 μL, 20 μM, in pH 8.0 TE buffer) was mixed with a DTT solution (12.5 μL, 200 mM, in pH 8.5 $NaHCO_3$ buffer) and kept for 2 h at 23 °C. To remove unreacted DTT, siRNA was precipitated by addition

of a 5 M NaCl solution (13.75 μL) and ethanol (400 μL), and kept at -20 °C for one hour. The precipitate was collected by centrifugation (16.1 rcf, 25 min) and washed five times using ice-cold 80% ethanol. The siRNA pellet was resuspended in 18.75 μL pH 8.0 TE buffer, and 6.25 μL of initiator **1**/CTA **5** solution (0.2 M in ethanol) was added to create a final concentration of 50 mM initiator **1**/CTA **5** (500 eq) in 25% ethanol. The reaction mixture was left at 23 °C for 24 h. To remove unreacted initiator/CTA, siRNA-I/siRNA-CTA was precipitated by addition of a 5 M NaCl solution (12.5 μL), pH 8.0 TE buffer (100 μL) and ethanol (400 μL), and kept at -20 °C for one hour. The precipitate was collected by centrifugation (16.1 rcf, 25 min) and washed five times using ice-cold 80% ethanol. The siRNA-I pellet was resuspended in 25 μL pH 7.4 PBS buffer, and siRNA-CTA pellet was resuspended in 25 μL pH 6.5 PBS buffer. The final concentration was determined by UV-Vis measurement at 260 nm.

MALDI-TOF MS Analysis of siRNA-I and siRNA-CTA. The matrix solution was a mixture of 2,4,6-trihydroxyacetophenone (THAP, 20 mg/mL in acetonitrile) diluted with an equal volume of diammonium hydrogen citrate (DAHC, 50 mg/mL in water).[25] 0.1 μL of siRNA sample was diluted in 1 μL of matrix solution, and subsequent dilutions (into the matrix solution) were also prepared to find the ideal concentration and sample/matrix ratio. The diluted samples were spotted on a 100-well plate and were mixed by pipetting to allow crystallization. The measurements were carried out in reflector mode with laser intensity set at 2200-2300.

HPLC Purification of siRNA-I and siRNA-CTA. HPLC was performed using a C18 column (150 x 4.6 mm^2, 5 μm, Phenomenex) and a photodiode array UV detector set at 260 nm. Chromatography was carried out with isocratic mobile phase of 75% 100 mM TEAA buffer (pH 7.0) and 25% acetonitrile; flow rate 0.5 mL/min; column at room temperature; 60 min runs. 100 mM TEAA buffer was prepared by mixing triethylamine (TEA, 5.56 mL) and acetic acid (2.29

mL) into water to a total volume of 400 mL, and the pH was tuned to pH 7.0. The fractions were collected, lyophilized, and then analyzed by MALDI-TOF MS. The concentration was estimated by UV-Vis measurement at 260 nm.

Wang Resin Modification (ATRP). This was synthesized by modifying literature procedure.[1] 150 mg of Wang resin (loading capacity 0.6-1.0 mmol/g) was reacted with 500 mg (3.0 mmol) of α-bromoisobutyric acid, 0.46 mL (3.0 mmol) of 1,3-diisopropylcarbodiimide, and 91.6 mg (0.75 mmol) of DMAP, in 10 mL of dry DMSO at 23 °C for 24 h. The beads were then washed with DMSO, water and THF and additionally Soxhlet extracted with THF for 8 h. The presence of the initiator fragment was verified by IR spectroscopy ($\nu_{C=O}$ = 1733 cm^{-1}).

NovaSyn® TGA Resin Modification (ATRP). 500 mg of NovaSyn® TGA resin (130 μm, loading capacity 0.28 mmol/g) was reacted with 467.6 mg (2.8 mmol) of α-bromoisobutyric acid, 805.2 mg (4.2 mmol) of EDC, and 85.5 mg (0.7 mmol) of DMAP, in 14 mL of dry DCM at 23 °C for 16 h. The beads were then washed with DCM, water and THF. The presence of the initiator fragment was verified by IR spectroscopy ($\nu_{C=O}$ = 1733 cm^{-1}) and gel-phase NMR spectroscopy. The large absorption at 1092 cm^{-1} corresponds to the C-O stretching of PEG. ^{1}H NMR (500 MHz in $CDCl_3$) δ: 7.50-6.75 (4H), 5.34-4.97 (2H), 4.61-4.41 (2H), 4.80-2.64 (300H), 2.16-1.75 (6H). ^{13}C NMR (500 MHz in CDCl3) δ: 171.55, 168.44, 157.79, 130.27, 115.18, 70.57, 69.73, 67.43, 67.18, 56.15, 39.06, 31.07.

Wang Resin Modification (CTA). Wang Resin (loading capacity 0.6-1.0 mmol/g, 0.1 g) was soaked in DMF for 1 h. The solution was then bubbled with argon and 2-(ethyl trithiocarbonate)propionic acid (0.35 g, 1.67 mmol), DCC (0.46 g, 2.22 mmol), and DMAP (0.003 g, 0.022 mmol) were added. The reaction proceeded at 23 °C for 3 h, and the solution

turned from bright red to yellow. Solvent was removed and the resin was rinsed thoroughly with DMF and DCM and dried overnight. This was followed by Soxhlet extraction with THF for 96 h. FT-IR (ATR) ν_{max}/cm^{-1}: 1732 ($\nu_{C=O}$). Furthermore, a small amount of modified resin (2 mg) was cleaved by stirring in 0.1 mL 50% (v/v) TFA/DCM. The solution was filtered and dried under high vacuum, and then characterized by TOF MS ES+ observed (predicted): H^+ 211.0833 (210.9876). The cleaved resin was characterized by FT-IR (ATR) and there was absence of peak at 1732 cm^{-1} ($\nu_{C=O}$).

NovaSyn® TGA Resin Modification (CTA). 300 mg of NovaSyn® TGA resin (130 μm, loading capacity 0.28 mmol/g) was reacted with 353.3 mg (1.7 mmol) of 3-mercapto-propanoic acid, 483.1 mg (2.5 mmol) of EDC, and 51.3 mg (0.4 mmol) of DMAP, in 8.4 mL of dry DCM at 23 °C for 16 h. The beads were then washed with DCM, water and THF. The color of the beads turned from pale yellow before modification, to bright yellow after washing. The presence of the CTA fragment was verified by IR spectroscopy ($\nu_{C=O}$ = 1734 cm^{-1}) and gel-phase NMR spectroscopy. The large absorption at 1095 cm^{-1} corresponds to the C-O stretching of PEG. ^{1}H NMR (500 MHz in $CDCl_3$) δ: 7.86-6.80 (4H), 5.48-5.05 (2H), 5.05-2.50 (300H), 1.91-1.62 (3H), 1.50-1.09 (3H). ^{13}C NMR (500 MHz in CDCl3) δ: 221.72, 171.01, 168.13, 157.61, 130.27, 114.93, 70.67, 67.52, 67.11, 47.99, 38.92, 31.58, 16.92, 13.14.

General Procedure for RAFT Polymerization of pPEGA. 2-(Ethyl trithiocarbonate)propionic acid (15 mg, 0.0713 mmol), PEGA (2.97 mL, 7.13 mmol), and VA044 (23.05 mg, 0.0713 mmol) were added to a Schlenk tube and subjected to 5-6 freeze-pump-thaw cycles. Degassed PBS buffer (pH 7.5, 6.25, or 6.5) was added and the vessel was heated to 40 °C. The polymerization was terminated by exposure to oxygen. The polymers were isolated by dialysis against water, followed by dialysis against acetone. Conversions and PDIs were determined by ^{1}H-NMR

spectroscopy and GPC, respectively.

General Procedures for RAFT Polymerization of pPEGA from siRNA-CTA. siRNA-CTA (3.25 μL, 100 μM), Wang-CTA resin (3.33 mg, 2×10^{-3} mmol) or TGA-CTA resin (7.14 mg, 2×10^{-3} mmol), PEGA (44 μL, 0.1 mmol), VA044 (64.8 μg, 2×10^{-4} mmol), and pH 6.5 PBS buffer (152.75 μL) were added to a micro Schlenk tube and subjected to 5-6 freeze-pump-thaw cycles. The flask was heated to 40 °C to start the polymerization, and was terminated by exposure to oxygen. The polymerization mixture was collected and centrifuged (16.1 rcf, 5 min) to separate the resin and supernatant. The resin was washed with water several times, and lyophilized to obtain weight. The residual monomer and VA044 in the supernatant was removed by centrifugal filtration (MWCO 10,000 Da) with pH 8.0 TE buffer (0.5 mL, 5 times). Half of the collected product (10 μL) was subjected as two samples (reduced/not reduced by DTT) for PAGE analysis.

PAGE analysis and intensity quantification. The TBE-Urea gels were imaged with a Bio-Rad FX Pro Plus Fluorimager and analyzed with the Quanti-One program. Each lane was selected by the rectangular selection tool, and plotted with the gel analysis function. The percentage peak area of the conjugate divided by the sum of the peak areas of the conjugate and unreacted siRNA was the conjugation efficiency (conjugation yield).

General Procedure for ATRP of PEGMA. α-bromoisobutyric acid (0.334 mg, 2.0 μmol), PEGMA (28.6 μL, 0.1 mmol), and pH 7.4 PBS (121.4 μL) were added to a micro Schlenk tube and subjected to 6 freeze-pump-thaw cycles. A catalyst stock solution (10x) was made of CuBr (2.87 mg, 20.0 μmol) and 2,2′-bipyridine (bipy, 6.87 mg, 44.0 μmol). The solid mixture was evacuated-refilled with argon 7 times, and then dissolved in degassed pH 7.4 PBS (500 μL). 50

μL of the catalyst stock solution was added to the Schlenk tube and stirred at 23 °C for 30 min under argon. The polymerization mixture was lyophilized to remove water, and then dissolved in D_2O to determine conversion by ^{1}H-NMR spectroscopy. The residual monomer and catalyst were removed by centrifugal filtration (MWCO 3000 Da) with 50% MeOH (0.5 mL, 4 times), and then H_2O (0.5 mL, 1 time). An aliquot was then lyophilized for GPC analysis to determine the molecular weight and PDI.

General Procedures for ATRP from siRNA-I in the presence of Wang-I Resin. siRNA-I (6.5 μL, 100 μM), Wang-I resin (3.33 mg, 2×10^{-3} mmol), PEGMA (28.6 μL, 0.1 mmol), and pH 7.4 PBS (114.9 μL) were added to a micro Schlenk tube and subjected to 6 freeze-pump-thaw cycles. A catalyst stock solution (10x) was made of CuBr (2.87 mg, 20.0 μmol) and 2,2′-bipyridine (bipy, 6.87 mg, 44.0 μmol). The solid mixture was evacuated-refilled with argon 7 times, and then dissolved in degassed pH 7.4 PBS (500 μL). 50 μL of the catalyst stock solution was added to the Schlenk tube and stirred at 23 °C for 30 min under argon. The polymerization mixture was collected and centrifuged (16.1 rcf, 5 min) to separate the resin and supernatant. The resin was washed with water several times, and lyophilized to obtain weight. The residual monomer and catalyst in the supernatant was removed by centrifugal filtration (MWCO 10,000 Da) with pH 8.0 TE buffer (0.5 mL, 5 times). Half of the collected product (14 μL) was subjected as two samples (reduced/not reduced by DTT) for PAGE analysis.

General Procedure for AGET ATRP from TGA-I Resins. A catalyst stock solution (10x) was made of $CuCl_2$ (2.28 mg, 20.0 μmol) and TPMA (5.81 mg, 20.0 μmol) in pH 7.4 PBS (400 μL). 40 μL of the catalyst solution was transferred into a micro Schlenk tube and allowed to stir for 5 min. TGA-I resin (7.14 mg, 2×10^{-3} mmol), PEGMA (28.6 μL, 0.1 mmol), and pH 7.4 PBS (81.4 μL) were then added to the flask and the mixture was subjected to 6 freeze-pump-thaw cycles.

Ascorbic acid (2.11 mg, 12×10^{-3} mmol) was dissolved in pH 7.4 PBS (500 μL) and degassed by bubbling Ar for 30 min. 50 μL of the ascorbic acid solution was added to the Schlenk tube and stirred at 23 °C for 30 min under argon. The polymerization mixture was collected and centrifuged (16.1 rcf, 5 min) to separate the resin and supernatant. The resin was washed with MeOH several times, and dried *in vacuo*. The weight of the resin was recorded, and the resin was then analyzed by IR spectroscopy.

Cleavage of Polymers Grown from TGA-I Resins. To TGA-I resin (9.8 mg) that was collected after polymerization, 95% TFA (0.2 mL) was added. The reaction was allowed to stir at 23 °C for 16 h, followed by *in vacuo* removal of TFA. The resin was washed with MeOH, centrifuged, and the supernatant was collected. This process was repeated for five times. The collected supernatant was dried *in vacuo*, and the cleaved polymers were then characterized by ^{1}H-NMR, GPC, and MALDI-TOF MS.

MALDI-TOF MS Analysis of pDEGMA. The matrix solution was DHB (10 mg/mL in 50% ACN and 0.1% TFA). 1 μL of pDEGMA sample (10 mg/mL in ACN) was diluted in 10 μL of matrix solution, and subsequent dilutions (into the matrix solution) were also prepared to determine the ideal concentration and sample/matrix ratio. The diluted samples were spotted on a 100-well plate and were mixed by pipetting to allow crystallization. The measurements were carried out in linear mode with laser intensity set at 1800-2000.

General Procedure for AGET ATRP of DEGMA from initiator 1. The procedure to synthesize **pDEGMA-1** is described here. $CuCl_2$ (1.2 mg, 8.9×10^{-3} mmol) and TPMA (2.6 mg, 8.9×10^{-3} mmol) in MeOH (200.0 μL) were allowed to stir in a micro Schlenk tube for 5 min. Initiator **1** (3.0 mg, 8.9×10^{-3} mmol), DEGMA (131.7 μL, 0.714 mmol), H_2O (0.45 mL) and MeOH (0.45

mL) were then added to the flask and the mixture was subjected to 6 freeze-pump-thaw cycles. Ascorbic acid (5x, 4.7 mg, 2.67×10^{-2} mmol) was dissolved in MeOH (1 mL) and degassed by bubbling Ar for 30 min. 200 μL of the ascorbic acid solution (1x) was added to the Schlenk tube to initiate the polymerization. The reaction mixture was stirred at 23 °C under argon, and aliquots were taken at pre-determined time points to monitor monomer conversion by ^{1}H-NMR spectroscopy in MeOD. The residual monomer and catalyst were removed by dialysis (MWCO 1000) against MeOH/H_2O=1/1 (4L), and then H_2O (4L), followed by lyophilization to obtain a clear, sticky polymer. ^{1}H NMR of **pDEGMA-1** (500 MHz in MeOD) δ: 8.53-8.39 (1H), 7.94-7.80 (2H), 7.34-7.21 (1H), 4.38-4.24 (2H), 4.22-4.00 (96H), 3.86-3.49 (303H), 3.46-3.34 (151H), 3.19-3.08 (2H), 2.18-1.45 (103H), 1.39-0.70 (159H). ^{1}H NMR of **pDEGMA-2** (500 MHz in MeOD) δ: 8.52-8.38 (1H), 7.93-7.81 (2H), 7.34-7.22 (1H), 4.35-4.24 (2H), 4.24-4.00 (160H), 3.88-3.50 (499H), 3.50-3.37 (245H), 3.18-3.08 (2H), 2.40-1.43 (174H), 1.43-0.70 (262H). ^{1}H NMR of **pDEGMA-3** (500 MHz in MeOD) δ: 8.50-8.39 (1H), 7.93-7.78 (2H), 7.33-7.20 (1H), 4.36-4.23 (2H), 4.22-4.01 (262H), 3.80-3.52 (817H), 3.50-3.34 (409H), 3.17-3.07 (2H), 2.16-1.68 (245H), 1.24-0.69 (410H). ^{1}H NMR of **pDEGMA-4** (500 MHz in MeOD) δ: 8.53-8.38 (1H), 7.93-7.77 (2H), 7.33-7.20 (1H), 4.36-4.23 (2H), 4.23-3.90 (384H), 3.83-3.50 (1175H), 3.47-3.35 (580H), 3.17-3.07 (2H), 2.38-1.39 (409H), 1.39-0.62 (603H). ^{1}H NMR of **pDEGMA-5** (500 MHz in MeOD) δ: 8.52-8.34 (1H), 7.98-7.77 (2H), 7.38-7.15 (1H), 4.35-4.23 (2H), 4.23-3.94 (544H), 3.86-3.48 (1666H), 3.48-3.34 (823H), 3.13-3.07 (2H), 2.39-1.42 (580H), 1.42-0.65 (846H).

Preparation of NMR samples of siRNA-pDEGMA conjugates (AGET-6 and AGET-7). The conjugate sample (10 μL in pH 8.0 TE buffer) was added to D_2O buffer (290 μL, pH 7.0, 10 mM phosphate, 0.1 M NaCl, 0.05 mM EDTA) to make the NMR sample. All bubbles were removed

from the Shigemi tube. Water presaturation procedure was carried out to suppress the large water signal.

FPLC Purification of siRNA-Polymer Conjugates. Fast protein liquid chromatography (FPLC) was performed on a Bio-Rad BioLogic DuoFlow chromatography system equipped with a GE Healthcare Life Sciences Superose 6 10/300 column and a QuadTec detector set at 214 nm and 260 nm. 50 mM Tris, 1 mM EDTA, pH 8.0 buffer was used as the solvent (4 °C, 0.5 ml/min). **RAFT-2**, **ATRP-3**, and pPEGA conjugate (from **Section 4.1**) were individually loaded into the column for purification. The fractions (1 mL each) were collected, desalted and concentrated by centrifugal filtration (MWCO 10,000), lyophilized, and then analyzed by PAGE. The concentration was estimated by UV-Vis measurement at 260 nm.

5.5 Appendix to Chapter 5: Supplementary Figures

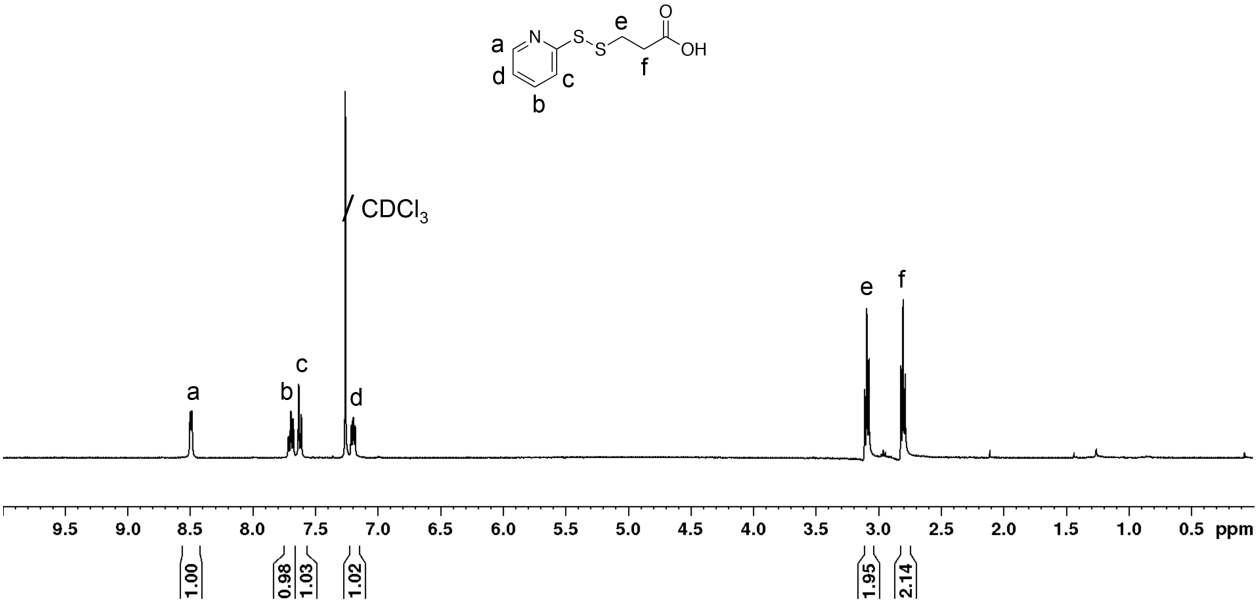

Figure 5-16. ^{1}H NMR spectrum of **3** (in $CDCl_3$).

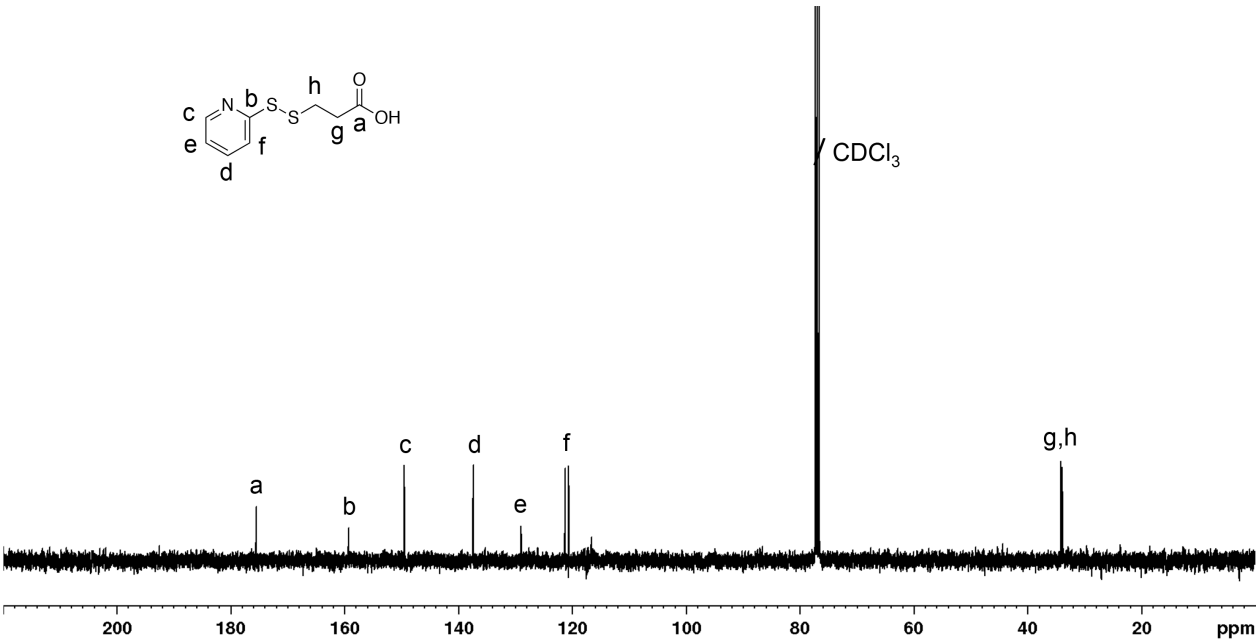

Figure 5-17. ^{13}C NMR spectrum of **3** (in $CDCl_3$).

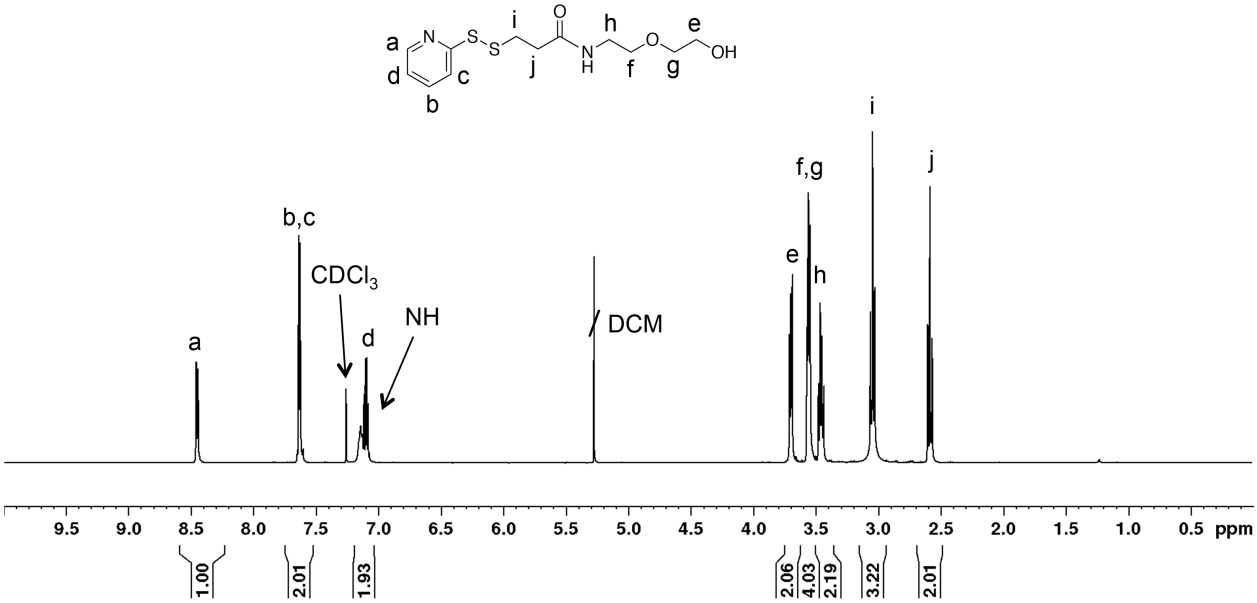

Figure 5-18. ^{1}H NMR spectrum of **4** (in $CDCl_3$).

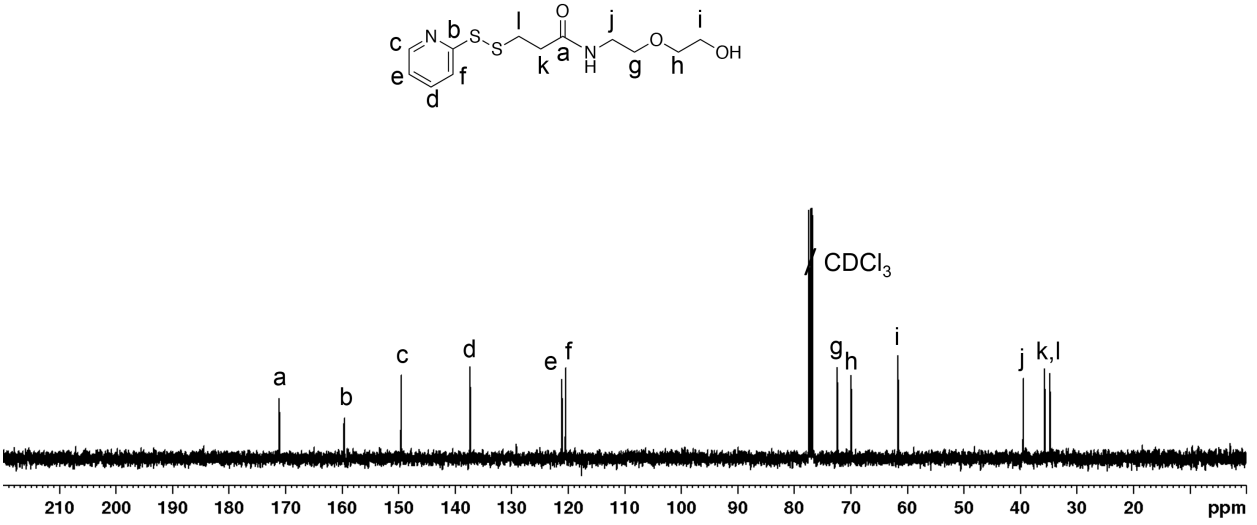

Figure 5-19. ^{13}C NMR spectrum of **4** (in $CDCl_3$).

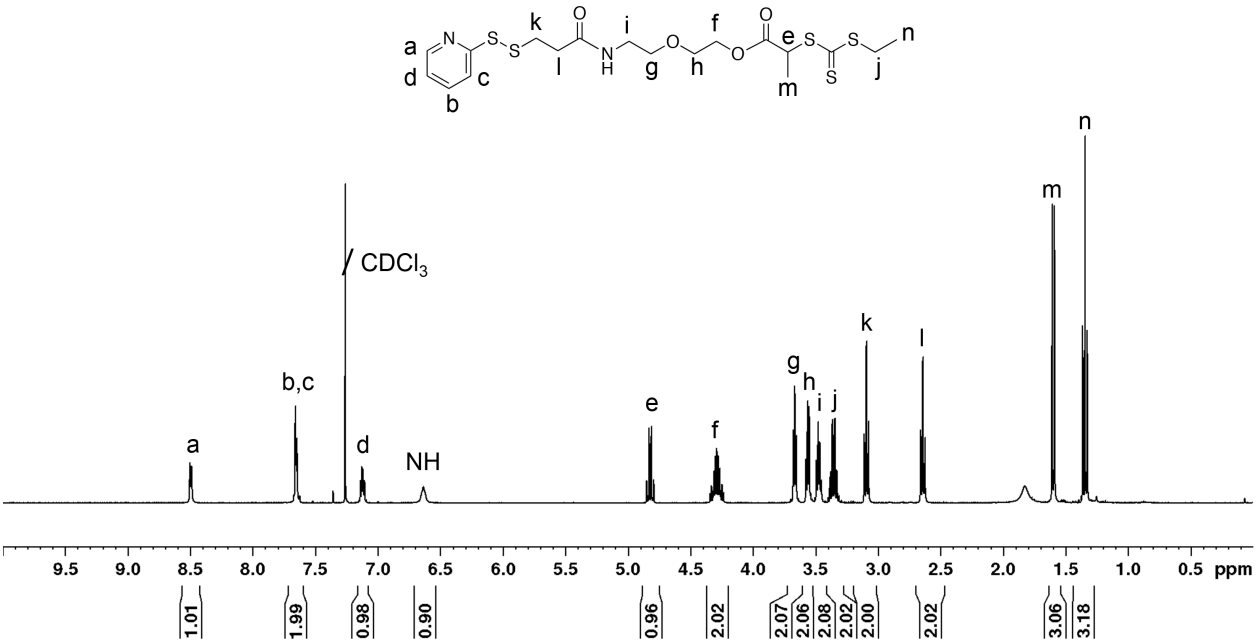

Figure 5-20. ^{1}H NMR spectrum of CTA **5** (in $CDCl_3$).

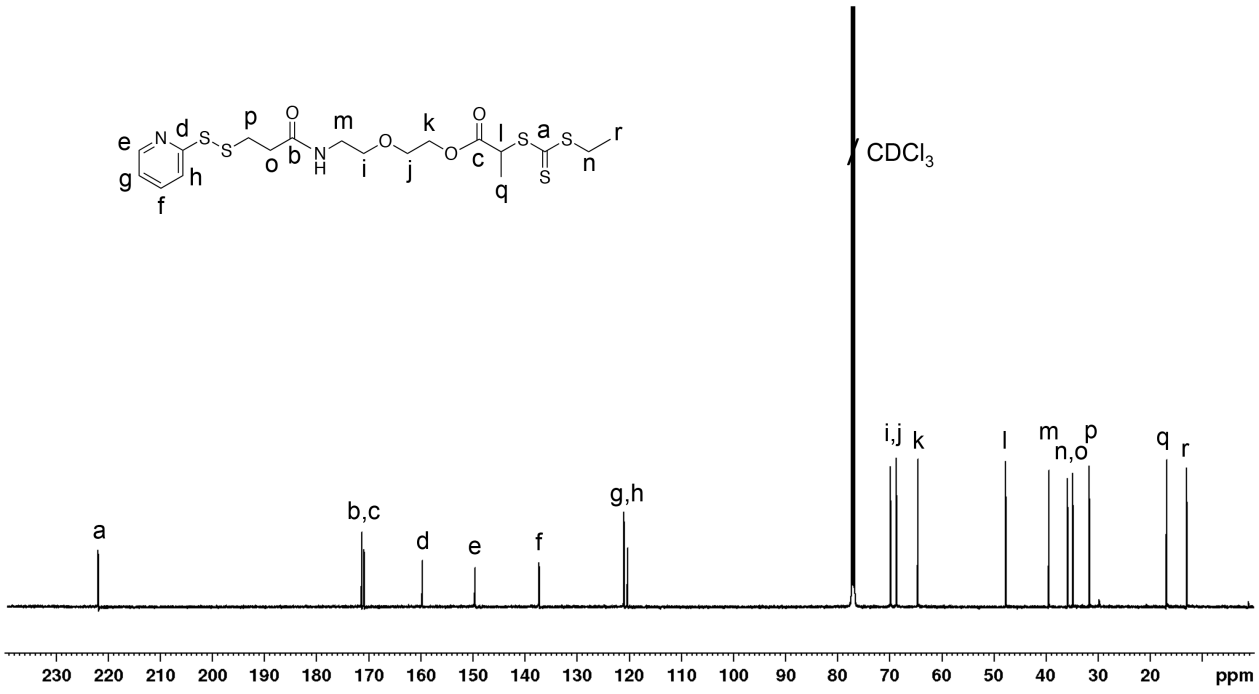

Figure 5-21. ^{13}C NMR spectrum of CTA **5** (in $CDCl_3$).

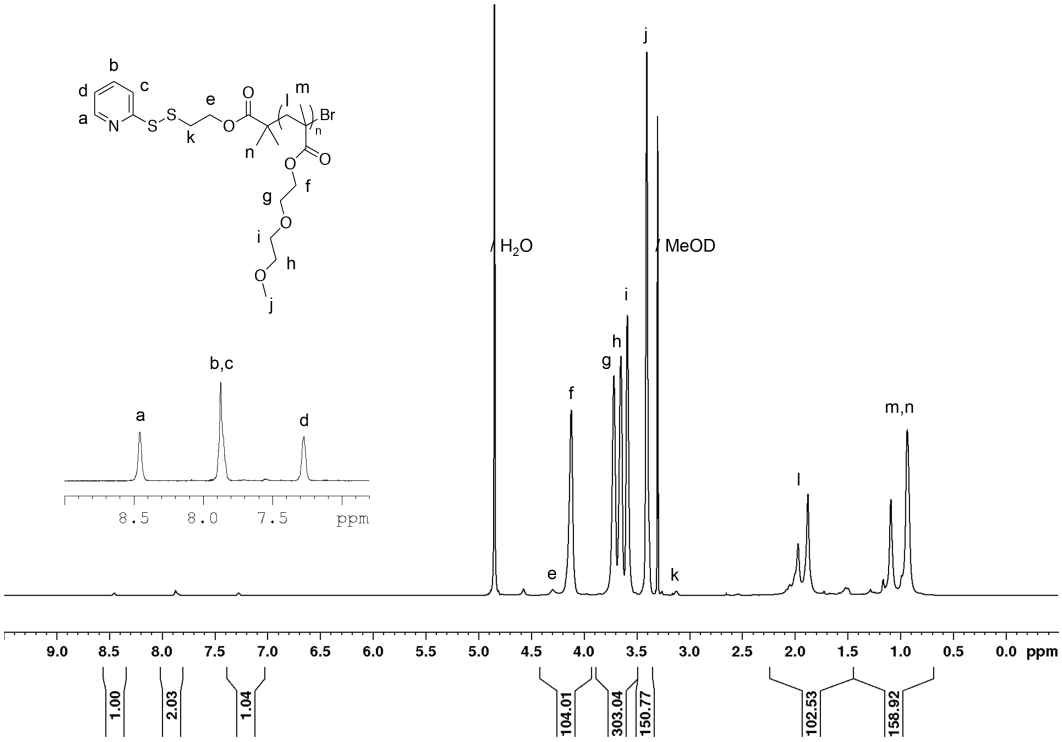

Figure 5-22. [1]H NMR spectrum of **pDEGMA-1** (in MeOD).

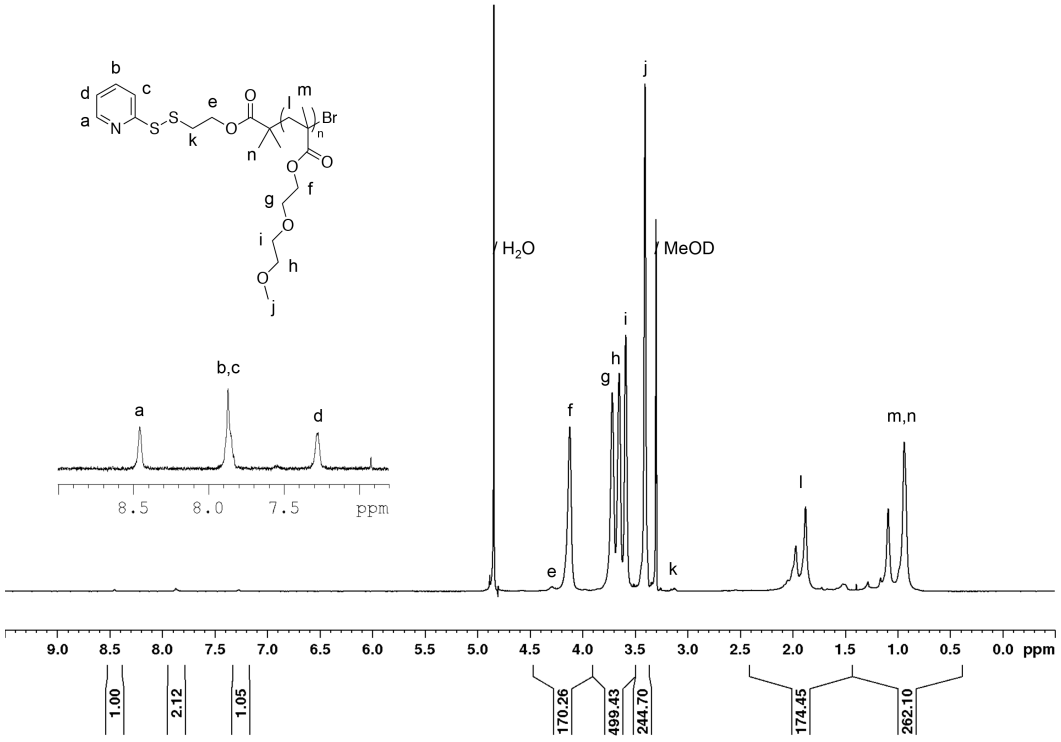

Figure 5-23. [1]H NMR spectrum of **pDEGMA-2** (in MeOD).

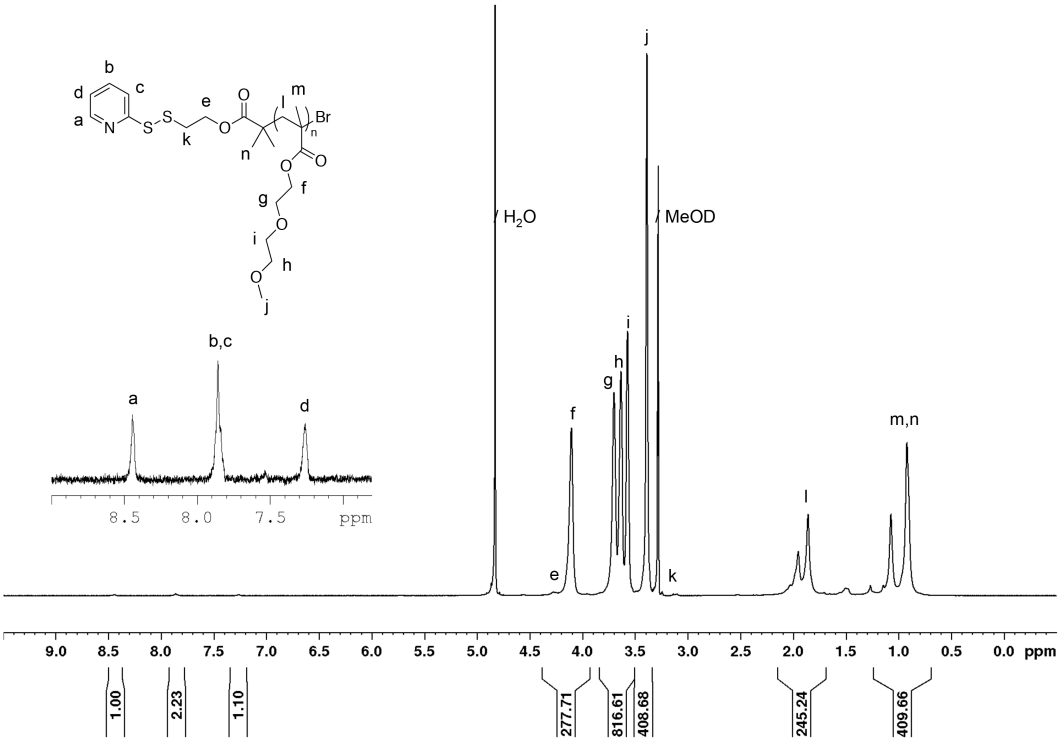

Figure 5-24. ^{1}H NMR spectrum of **pDEGMA-3** (in MeOD).

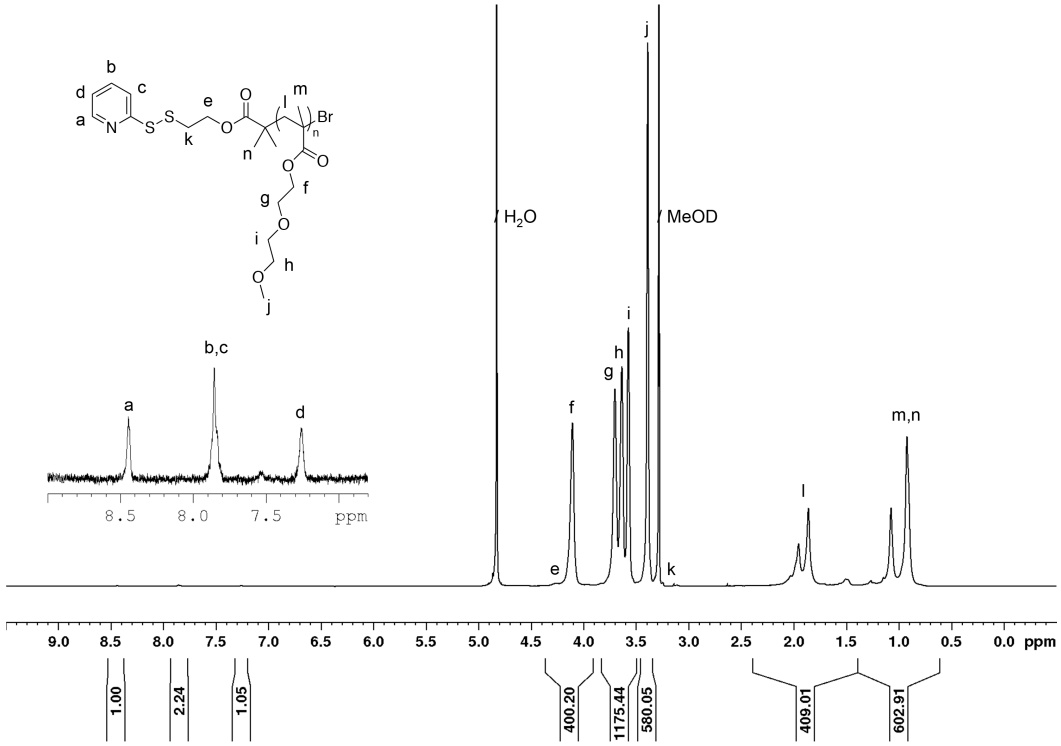

Figure 5-25. ^{1}H NMR spectrum of **pDEGMA-4** (in MeOD).

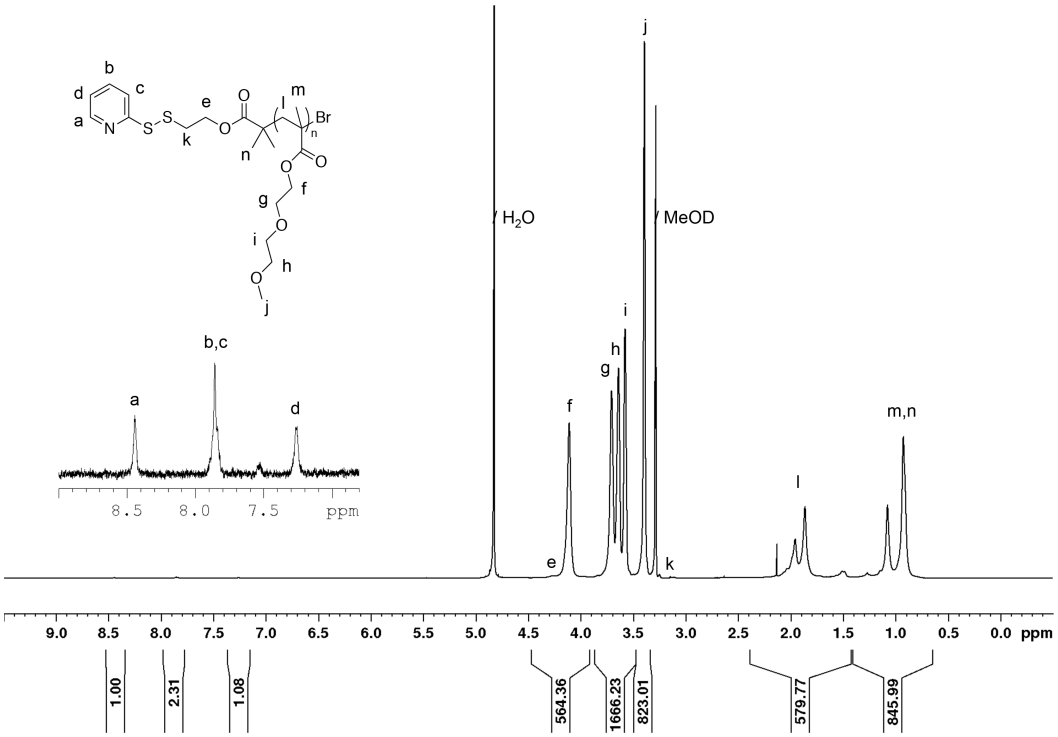

Figure 5-26. ^{1}H NMR spectrum of **pDEGMA-5** (in MeOD).

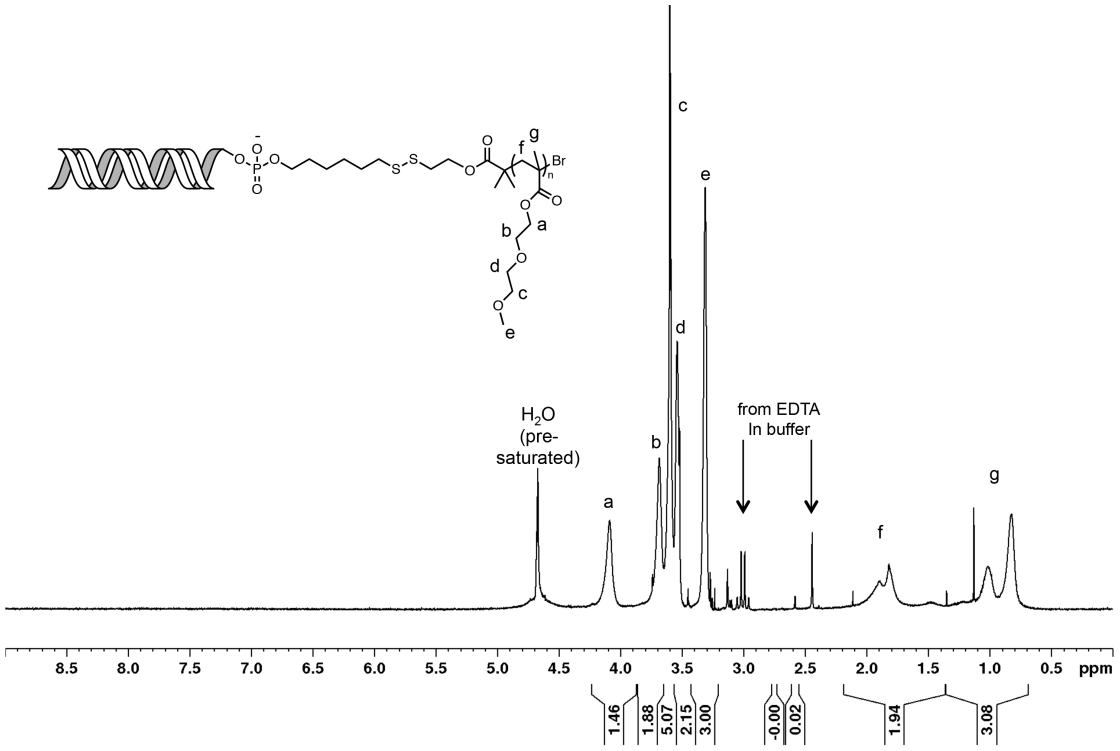

Figure 5-27. ^{1}H NMR spectrum of **AGET-6** (in buffered D_2O + 3.3% H_2O).

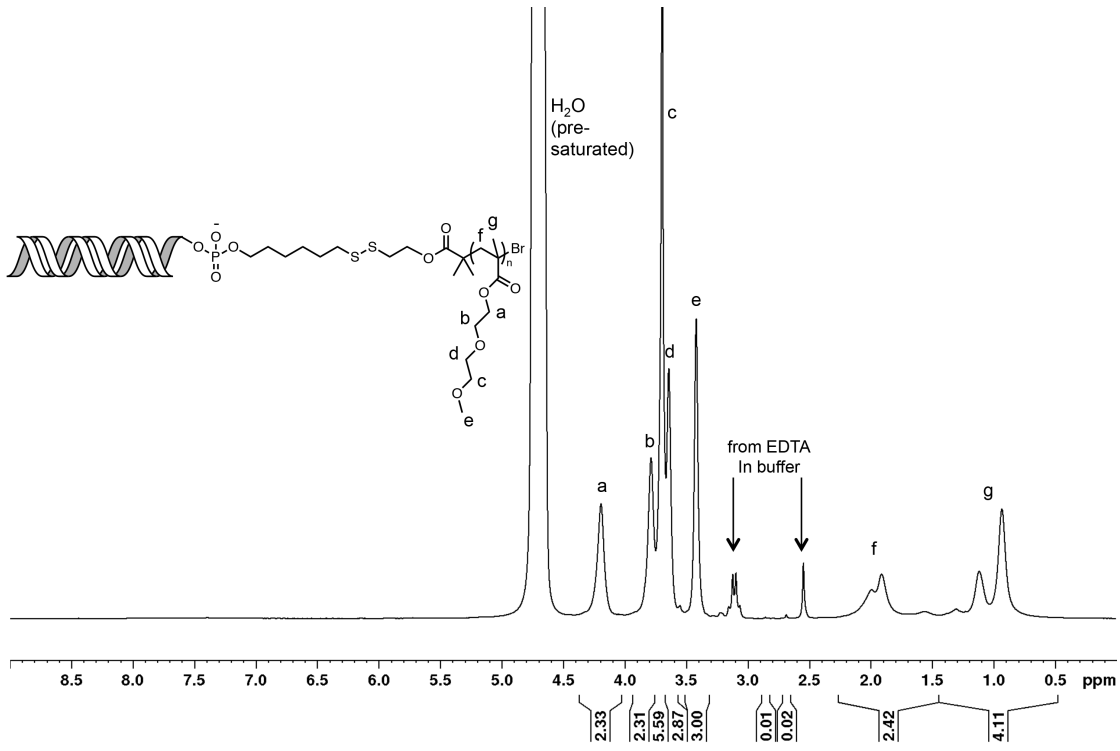

Figure 5-28. ^{1}H NMR spectrum of **AGET-7** (in buffered D_2O + 3.3% H_2O).

5.6 References

‡ Portions of this chapter is in preparation for publication as: Lin, E.-W.; Maynard, H. D., "Alternative Synthesis Route Toward siRNA-Polymer Conjugates: *Grafting From* siRNA," *in preparation*.

(1) Bontempo, D.; Maynard, H. D. "Streptavidin as a Macroinitiator for Polymerization: In Situ Protein-Polymer Conjugate Formation" *J. Am. Chem. Soc.* **2005**, *127*, 6508-6509.

(2) Lou, X. H.; Lewis, M. S.; Gorman, C. B.; He, L. "Detection of DNA Point Mutation by Atom Transfer Radical Polymerization" *Anal. Chem.* **2005**, *77*, 4698-4705.

(3) Lou, X. H.; He, L. "DNA-Accelerated Atom Transfer Radical Polymerization on a Gold Surface" *Langmuir* **2006**, *22*, 2640-2646.

(4) Lou, X. H.; Wang, C. Y.; He, L. "Core-Shell Au Nanoparticle Formation with DNA-Polymer Hybrid Coatings Using Aqueous ATRP" *Biomacromolecules* **2007**, *8*, 1385-1390.

(5) Okelo, G. O.; He, L. "Cu(0) as the Reaction Additive in Purge-Free ATRP-Assisted DNA Detection" *Biosens. Bioelectron.* **2007**, *23*, 588-592.

(6) Qian, H.; He, L. "Surface-Initiated Activators Generated by Electron Transfer for Atom Transfer Radical Polymerization in Detection of DNA Point Mutation" *Anal. Chem.* **2009**, *81*, 4536-4542.

(7) Qian, H.; He, L. "Polymeric Macroinitiators for Signal Amplification in AGET ATRP-Based DNA Detection" *Sens. Actuators, B* **2010**, *150*, 594-600.

(8) He, P.; Zheng, W. M.; Tucker, E. Z.; Gorman, C. B.; He, L. "Reversible Addition-Fragmentation Chain Transfer Polymerization in DNA Biosensing" *Anal. Chem.* **2008**, *80*, 3633-3639.

(9) He, P.; He, L. "Synthesis of Surface-Anchored DNA-Polymer Bioconjugates Using Reversible Addition-Fragmentation Chain Transfer Polymerization" *Biomacromolecules* **2009**, *10*, 1804-1809.

(10) Averick, S. E.; Dey, S. K.; Grahacharya, D.; Matyjaszewski, K.; Das, S. R. "Solid-Phase Incorporation of an ATRP Initiator for Polymer-DNA Biohybrids" *Angew. Chem., Int. Ed.* **2014**, *53*, 2739-2744.

(11) Heredia, K. L.; Bontempo, D.; Ly, T.; Byers, J. T.; Halstenberg, S.; Maynard, H. D. "In Situ Preparation of Protein - "Smart" Polymer Conjugates with Retention of Bioactivity" *J. Am. Chem. Soc.* **2005**, *127*, 16955-16960.

(12) Wang, S. S. "Para-Alkoxybenzyl Alcohol Resin and Para-Alkoxybenzyloxycarbonylhydrazide Resin for Solid-Phase Synthesis of Protected Peptide Fragments" *J. Am. Chem. Soc.* **1973**, *95*, 1328-1333.

(13) Angot, S.; Ayres, N.; Bon, S. A. F.; Haddleton, D. M. "Living Radical Polymerization Immobilized on Wang Resins: Synthesis and Harvest of Narrow Polydispersity Poly(methacrylate)s" *Macromolecules* **2001**, *34*, 768-774.

(14) Bontempo, D.; Tirelli, N.; Masci, G.; Crescenzi, V.; Hubbell, J. A. "Thick Coating and Functionalization of Organic Surfaces via ATRP in Water" *Macromol. Rapid Commun.* **2002**, *23*, 418-422.

(15) Braunshier, C.; Hametner, C. "Gel-Phase C-13 NMR Spectroscopy of Selected Solid Phase Systems" *QSAR Comb. Sci.* **2007**, *26*, 908-918.

(16) Baussard, J. F.; Habib-Jiwan, J. L.; Laschewsky, A.; Mertoglu, M.; Storsberg, J. "New Chain Transfer Agents for Reversible Addition-Fragmentation Chain Transfer (RAFT) Polymerisation in Aqueous Solution" *Polymer* **2004**, *45*, 3615-3626.

(17) Tsujii, Y.; Ejaz, M.; Sato, K.; Goto, A.; Fukuda, T. "Mechanism and Kinetics of RAFT-Mediated Graft Polymerization of Styrene on a Solid Surface. 1. Experimental Evidence of Surface Radical Migration" *Macromolecules* **2001**, *34*, 8872-8878.

(18) Napirei, M.; Wulf, S.; Eulitz, D.; Mannherz, H. G.; Kloeckl, T. "Comparative Characterization of Rat Deoxyribonuclease 1 (Dnase1) and Murine Deoxyribonuclease 1-Like 3 (Dnase1l3)" *Biochem. J.* **2005**, *389*, 355-364.

(19) Averick, S.; Simakova, A.; Park, S.; Konkolewicz, D.; Magenau, A. J. D.; Mehl, R. A.; Matyjaszewski, K. "ATRP under Biologically Relevant Conditions: Grafting from a Protein" *ACS Macro Lett.* **2012**, *1*, 6-10.

(20) Matyjaszewski, K.; Shipp, D. A.; Wang, J. L.; Grimaud, T.; Patten, T. E. "Utilizing Halide Exchange to Improve Control of Atom Transfer Radical Polymerization" *Macromolecules* **1998**, *31*, 6836-6840.

(21) Jakubowski, W.; Matyjaszewski, K. "Activator Generated by Electron Transfer for Atom Transfer Radical Polymerization" *Macromolecules* **2005**, *38*, 4139-4146.

(22) Oh, J. K.; Min, K.; Matyjaszewski, K. "Preparation of Poly(Oligo(Ethylene Glycol) Monomethyl Ether Methacrylate) by Homogeneous Aqueous AGET ATRP" *Macromolecules* **2006**, *39*, 3161-3167.

(23) Soeriyadi, A. H.; Li, G. Z.; Slavin, S.; Jones, M. W.; Amos, C. M.; Becer, C. R.; Whittaker, M. R.; Haddleton, D. M.; Boyer, C.; Davis, T. P. "Synthesis and Modification of Thermoresponsive Poly(Oligo(Ethylene Glycol) Methacrylate) via Catalytic Chain Transfer Polymerization and Thiol-Ene Michael Addition" *Polym. Chem.* **2011**, *2*, 815-822.

(24) Bontempo, D.; Heredia, K. L.; Fish, B. A.; Maynard, H. D. "Cysteine-Reactive Polymers Synthesized by Atom Transfer Radical Polymerization for Conjugation to Proteins" *J. Am. Chem. Soc.* **2004**, *126*, 15372-15373.

(25) Turner, J. J.; Jones, S. W.; Moschos, S. A.; Lindsay, M. A.; Gait, M. J. "MALDI-TOF Mass Spectral Analysis of siRNA Degradation in Serum Confirms an RNAse A-Like Activity" *Mol. BioSyst.* **2007**, *3*, 43-50.

Chapter 6

Morphing Hydrogel Patterns by

Thermo-Reversible Fluorescence Switching[‡]

6.1 Introduction

Stimuli responsive polymers (SRPs), materials that exhibit abrupt, dramatic, and reversible changes in one or more properties in response to an external trigger, have gained significant interest because of their versatility and tunable properties.[1] Some examples of triggers include temperature[2], pH[3], biomolecules[4], light[5], and electric[6] or magnetic field[7]. Thin films of stimuli responsive materials are particularly interesting for generating adaptive smart surfaces that can reversibly switch their properties such as wettability, adsorptivity, or optical properties.[1,8-14] As a result, such smart surfaces have broad applications in sensors, actuators, microfluidics, coatings, diagnostics, tissue engineering, and drug delivery. Of particular interest are surfaces designed to reversibly expose hidden patterns or encrypted messages.[8,15-17] To date, however, only smart surfaces that display a single pattern/message in response to stimuli were reported.[8,15-17] Herein, morphing surfaces capable of displaying multiple encrypted messages are presented. We envisioned that by utilizing the high resolution and alignment capabilities of electron beam (e-beam) lithography, we could generate complex multicomponent thermo-responsive hydrogel patterns. E-beam lithography is a maskless technique that irradiates focused high-energy electron beams onto polymer thin films. The electrons cause radical cross-linking of oligo(ethylene glycol) units and the silicon surface to form patterned hydrogels.[17] Such complex smart surfaces can be designed to reveal several different encrypted messages by morphing multiple times in response to stimuli.

Actuation of stimuli responsive thin films is most often characterized by atomic force microscopy (AFM), which is costly, time-consuming, and can be destructive to the sample. Monitoring the actuation of such films by more accessible and affordable optical techniques is highly desired.[14,18] Chilkoti *et al.* reported a simple gold nanoparticle based system for optical

monitoring of the lower critical solution temperature (LCST) of SRPs at the solid-liquid interface[18]. Yet, other techniques with simple readouts are critically needed.

Here we also describe for the first time, the use of the self-quenching property of fluorophores to monitor the actuation of stimuli responsive hydrogel patterns. Fluorescent probes are useful tools in research and clinical assays. Self-quenching is the quenching of fluorescence between identical molecules when they are in close proximity. The phenomenon has been used as a tool in many studies, such as protein folding[19], protease activities[20], volume change[21], distance measurement[22], and macromolecule association[23,24]. Naci Inci and coworkers have shown that dye-dye separation distance can be controlled by hydrating and dehydrating polyethylene glycol hydrogels modified with boradiazaindacene (BODIPY) dye molecules.[25] Liu's group has reported the use of Förster resonance energy transfer (FRET) pairs for monitoring the volume phase transition (VPT) of responsive microgels.[26,27] A few other examples have also shown the incorporation of fluorescent or luminescent sensing with thermoresponsive materials.[28,29] However, in our system, we do not need to synthesize fluorescent monomers. We hypothesize that fluorophore-conjugated hydrogels would be brightly fluorescent in the swollen state below their volume phase transition temperature (VPTT) whereas in the collapsed state (above the VPTT) of the gels, the fluorophores would self-quench due to being in close proximity. This should allow optical transduction of the dramatic volumetric change of the gel.

6.2 Results and Discussion

6.2.1 Synthesis of Amine Thermoresponsive Polymers

To prepare the fluorescence switching surfaces, we first synthesized thermo-responsive polymers based on oligo(ethylene glycol) methacrylate monomers. These monomers have been polymerized by a variety of techniques to obtain polymers with a range of LCSTs.[30-34] At temperatures above their LCST, hydrogen-bonded water molecules are released and the polymers become insoluble. The LCST can be tuned by altering the length of oligo(ethylene glycol) side chains or by adjusting the ratio of monomers with different lengths.[31,32] In our approach, atom transfer radical polymerization (ATRP) was used with an initiator containing a protected amine group for later fluorophore conjugation.

Initially, we synthesized (N-Boc-propylamino)-2-bromoisobutyrate **2** as the protected initiator (**Scheme 6-1**). The synthesis was modified from a procedure reported in literature (see Appendix **Figure 6-17** and **Figure 6-18** for NMR spectra).[35] With initiator **2**, we successfully synthesized a thermo-responsive polymer by ATRP with 1:1 monomer feed ratios of di(ethylene glycol) methyl ether methacrylate (DEGMA) and tri(ethylene glycol) methyl ether methacrylate (TEGMA) (**P_A'**, see Appendix **Figure 6-19** for NMR spectrum). The M_n measured by GPC was 25.6 kDa and the PDI was 1.18, which implied a controlled polymerization. The measured LCST was 38.8 °C with a sharp transition (see Appendix **Figure 6-20** for UV-Vis spectrum). However, we did not continue on this route. With the design of this ATRP initiator, there could be intramolecular exchange of the amine end-group to a hydroxyl group. We anticipate this happening if the free amine performs a nucleophilic attack at the carbonyl to form an amide bond through a six-membered ring intermediate. Therefore, we synthesized a new ATRP initiator that

will not encounter this potential issue to ensure the amine end-group is present for fluorophore conjugation (**Scheme 6-2**, see Appendix **Figure 6-21**, **6-22**, and **6-23** for NMR spectra).[36]

Scheme 6-1. Synthesis of ATRP initiator **2** and thermoresponsive polymer $\mathbf{P_A}$'.

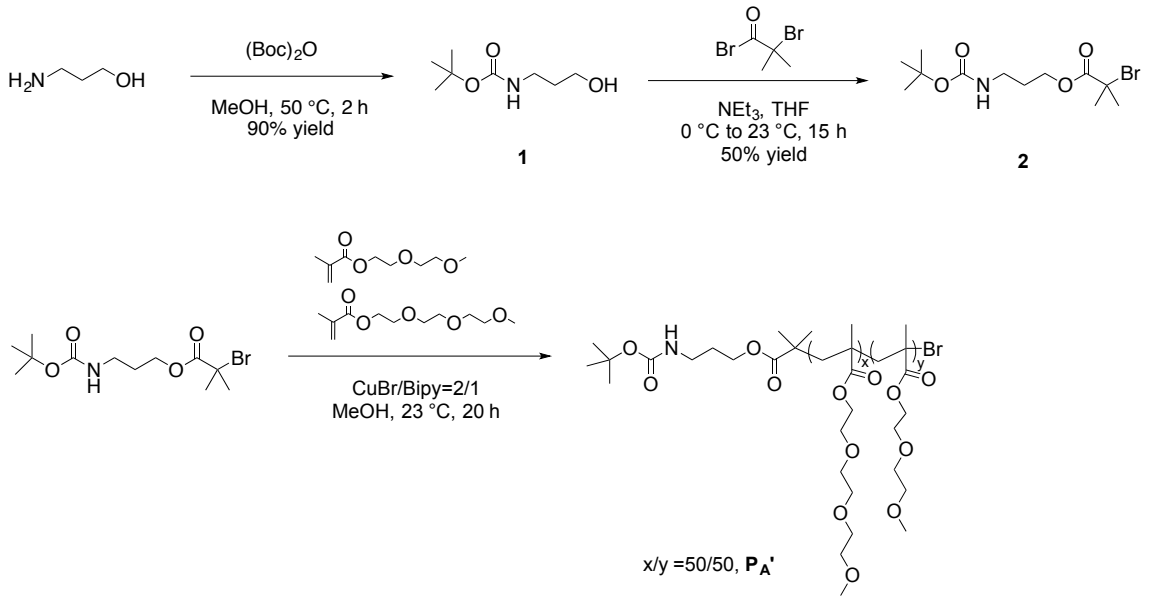

With ATRP initiator **4**, two copolymerizations were carried out with DEGMA and TEGMA using monomer feed ratios of 7:3 and 3:7 (**Table 6-1** and **Scheme 6-2**, and see **Table 6-2** for monomer ratio determination). This yielded two copolymers: $\mathbf{P_{30}}$ and $\mathbf{P_{40}}$ with LCSTs of 33.1 °C and 40.0 °C, respectively. A homopolymer of poly(ethylene glycol) methyl ether methacrylate (PEGMA, M_n= 300 g/mol, OEG units = 4-5), $\mathbf{P_{65}}$, with a higher LCST of 62.1 °C was also prepared. In accordance with the earlier reports, the LCST of the synthesized polymers

increased as the average length of the oligo(ethylene glycol) units in the polymer increased.[30-34] After deprotection of the amine end-group, the LCST values increased slightly to 33.3 °C, 41.4 °C, and 65.6 °C for $\mathbf{P_{30}}$, $\mathbf{P_{40}}$, and $\mathbf{P_{65}}$, respectively (see **Figure 6-1** through **Figure 6-6** for ^{1}H NMR spectra). This is expected and can be attributed to an increase in hydrophilicity of the polymers after removal of the Boc group. ATRP was preferred over conventional free radical polymerization because it yielded polymers with amine end-groups and generally results in polymers with narrow polydispersities. It has been shown in literature that this protected initiator had low initiation efficiency in the ATRP of poly(methyl methacrylate) and resulted in polymers with rather broad polydispersity indices (PDIs) and higher molecular weight than expected, which is also observed in our case.[36] However, despite the broad PDI's, importantly the polymers exhibited sharp phase transitions at the desired temperatures (**Figure 6-7**).

Scheme 6-2. Synthesis of the ATRP initiator and thermoresponsive polymers.

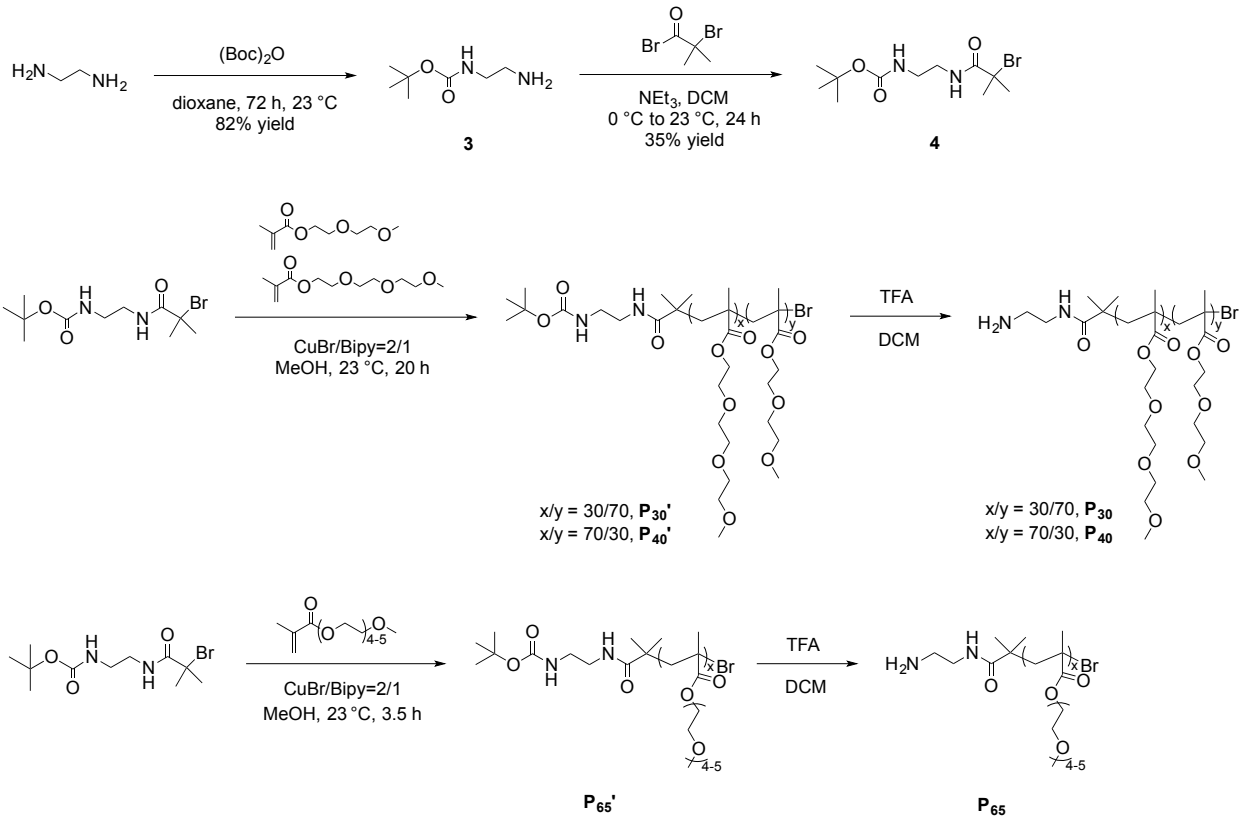

Table 6-1. The characteristics of the synthesized polymers, $\mathbf{P_{30}}$, $\mathbf{P_{40}}$, and $\mathbf{P_{65}}$, before and after deprotection of the amine end-group.

Monomer	Polymer	M_n (kg/mol)[a]	PDI	LCST (°C)
DEGMA/TEGMA (70/30)	N-Boc-P_{30}'	33.6	1.53	33.1
	NH_2-P_{30}	29.5	1.67	33.3
DEGMA/TEGMA (30/70)	N-Boc-P_{40}'	55.1	1.46	40.0
	NH_2-P_{40}	59.8	1.32	41.4
PEGMA (M_n = 300 g/mol)	N-Boc-P_{65}'	62.4	2.17	62.1
	NH_2-P_{65}	59.8	2.20	65.6

[a] As determined by gel permeation chromatography.

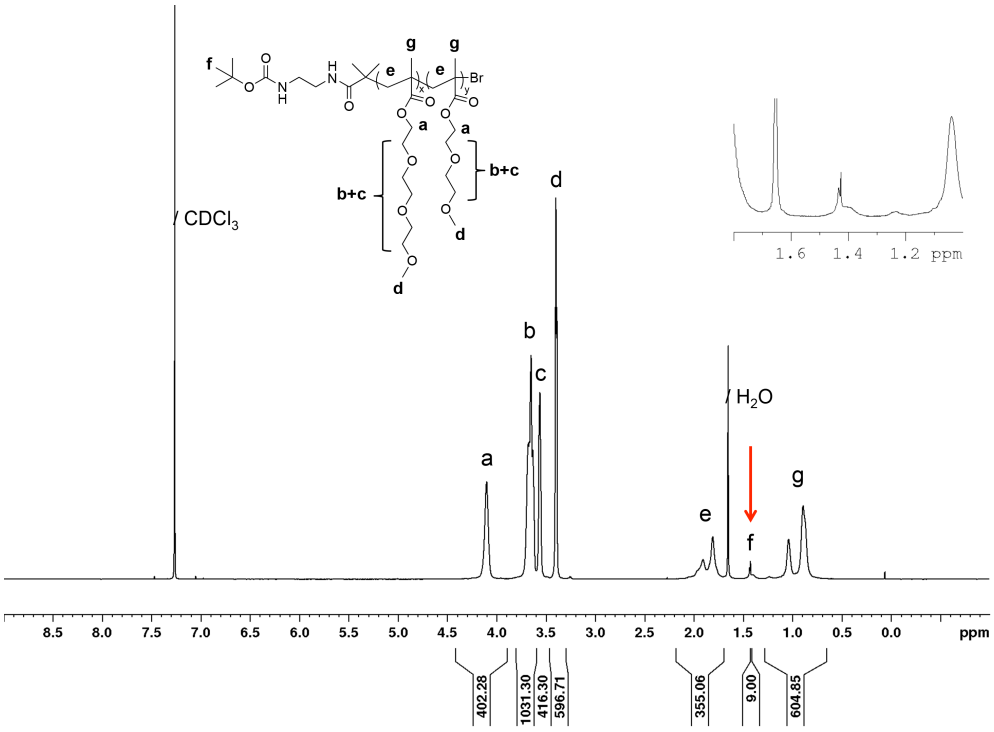

Figure 6-1. ^{1}H NMR spectrum of **P_{30}'** in $CDCl_3$. The arrow is pointing to the peak showing the Boc group protons.

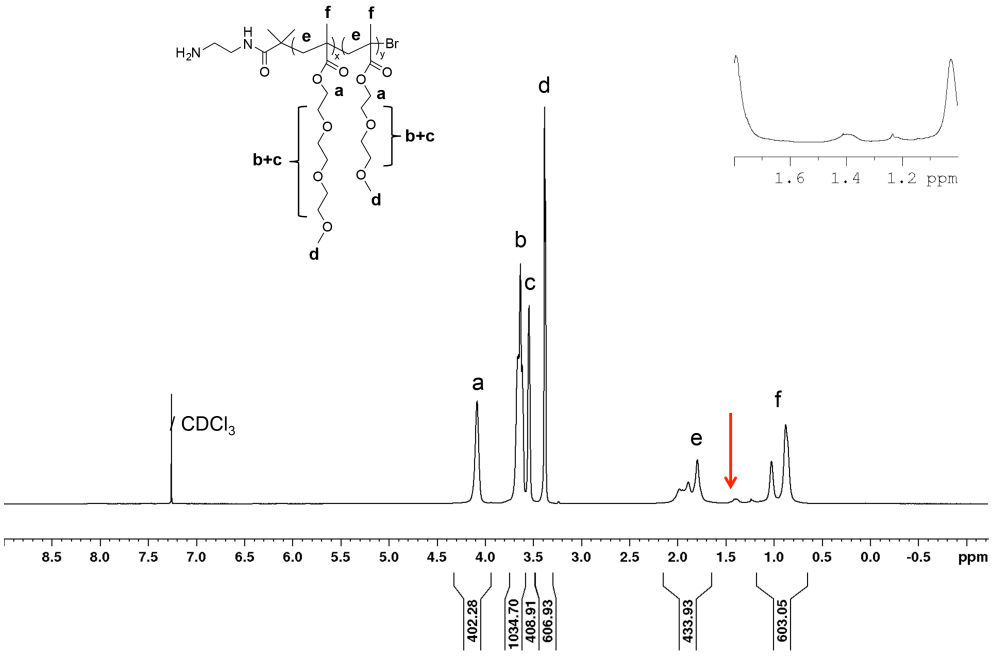

Figure 6-2. ^{1}H NMR spectrum of **P_{30}** in $CDCl_3$. The arrow is pointing to the disappearance of the Boc group protons after deprotection.

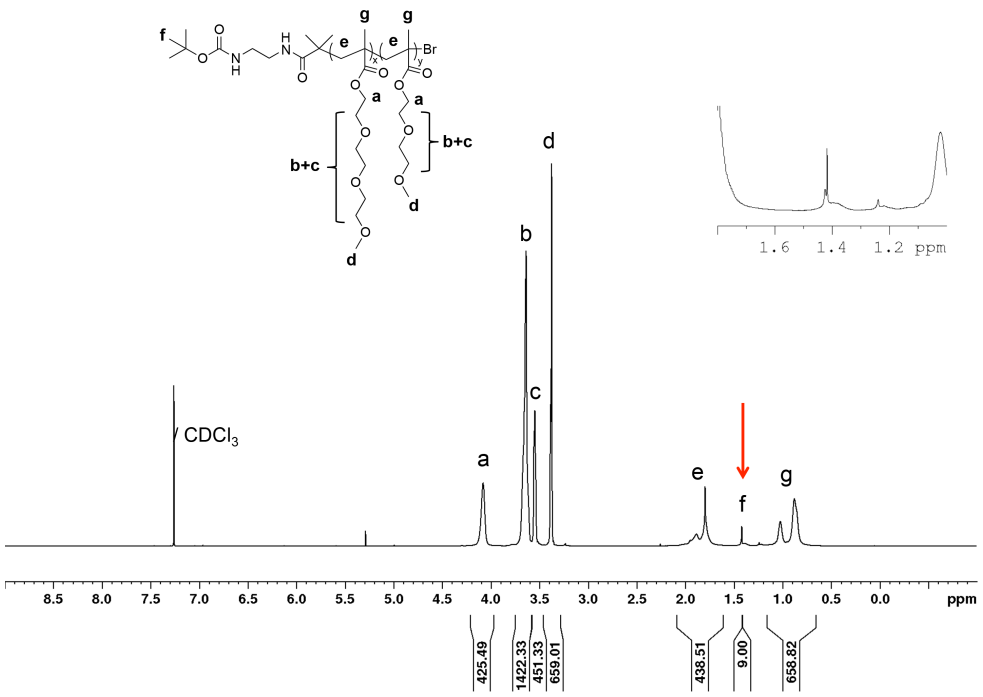

Figure 6-3. ^{1}H NMR spectrum of **P_{40}'** in $CDCl_3$. The arrow is pointing to the peak of the Boc group protons.

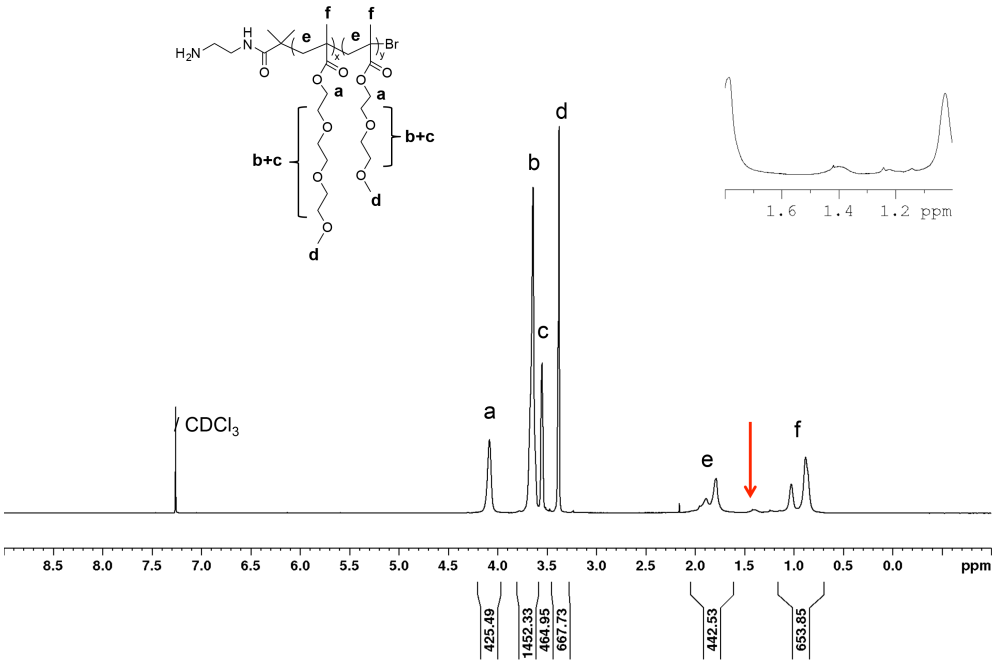

Figure 6-4. ^{1}H NMR spectrum of **P_{40}** in $CDCl_3$. The arrow is pointing to the disappearance of the Boc group protons after deprotection.

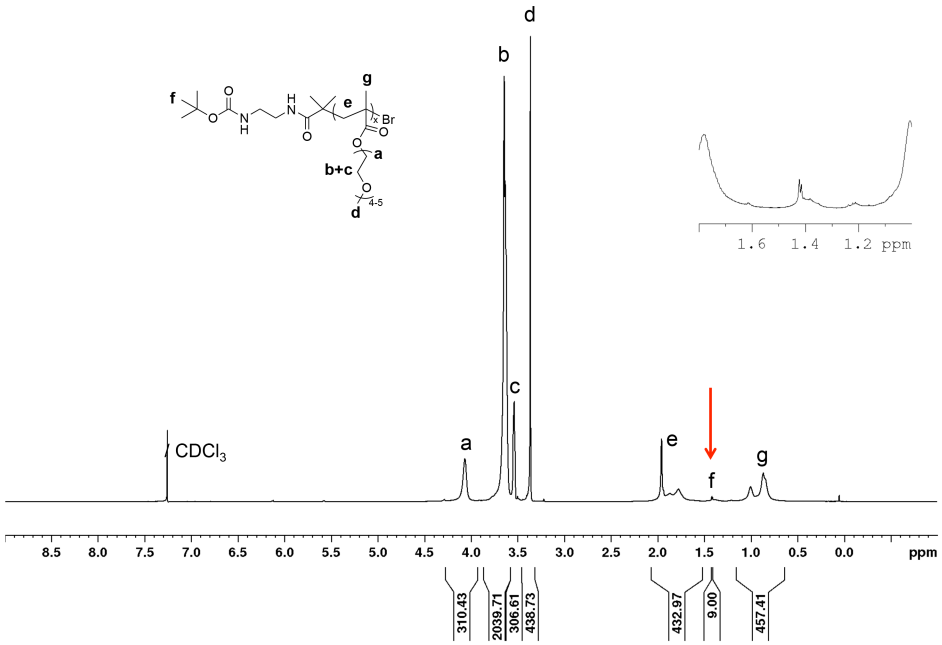

Figure 6-5. ^{1}H NMR spectrum of **P_{65}'** in $CDCl_3$. The arrow is pointing to the peak of the Boc group protons.

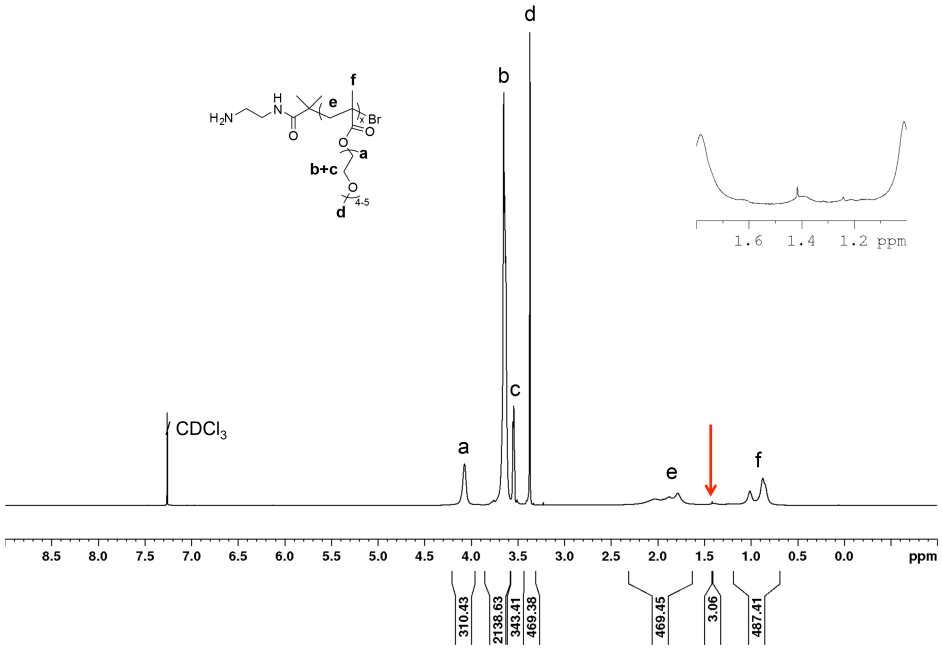

Figure 6-6. ^{1}H NMR spectrum of **P_{65}** in $CDCl_3$. The arrow is pointing to the disappearance of the Boc group protons after deprotection. The deprotection did not go to completion using the same condition as **P_{30}** and **P_{40}**.

Table 6-2. The calculated monomer ratio and M_n of the copolymers from ^{1}H NMR.

Polymer	Feed ratio		Calculated units		Calculated ratio		M_n (kDa)
	TEGMA	DEGMA	TEGMA	DEGMA	TEGMA	DEGMA	
P_{30}'	30	70	60.2	134.6	30.9	69.1	39.6
P_{30}	-	-	59.2	146.2	28.8	71.2	41.6
P_{40}'	70	30	149.3	68.5	68.5	31.5	47.9
P_{40}	-	-	160.2	58.4	73.3	26.7	48.5

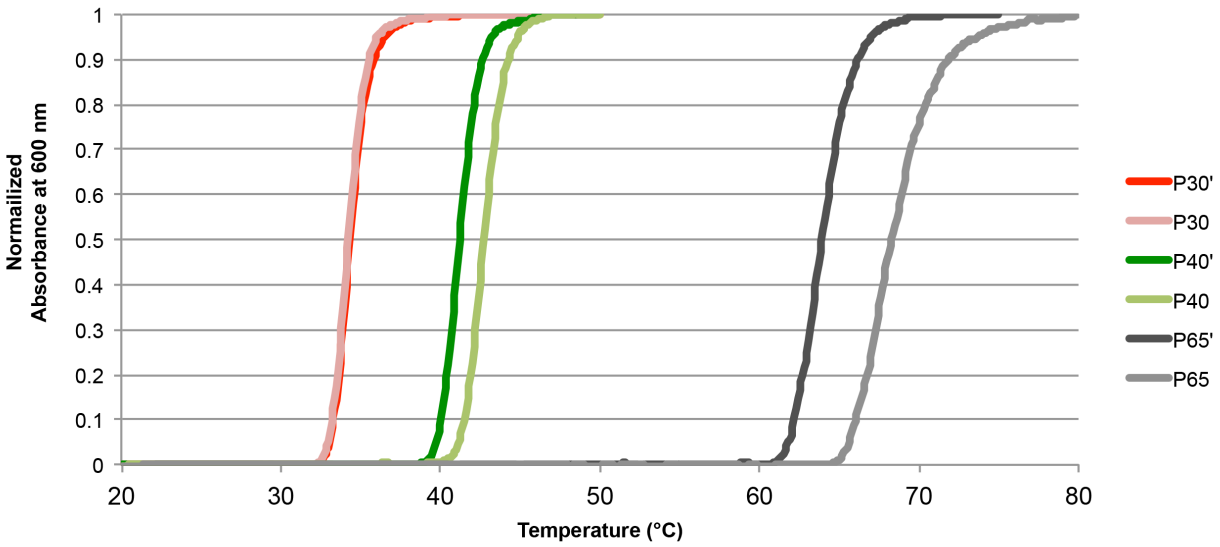

Figure 6-7. UV-Vis spectrum for the LCST determination of the polymers.

6.2.2 Preparation of Hydrogel Patterns by E-Beam Lithography

After characterizing the thermo-responsive properties of the polymers, we investigated their patterning by electron beam lithography **(Figure 6-8)**. Upon e-beam irradiation, oligo(ethylene glycol) based polymers are cross-linked to themselves and to the underlying

native oxide layer on silicon surfaces forming stable patterns.[17] Very low area doses (0.4 mC/cm^2) were required to pattern the polymers. After e-beam exposure, amine-reactive fluorophores were easily conjugated to the patterned hydrogels.

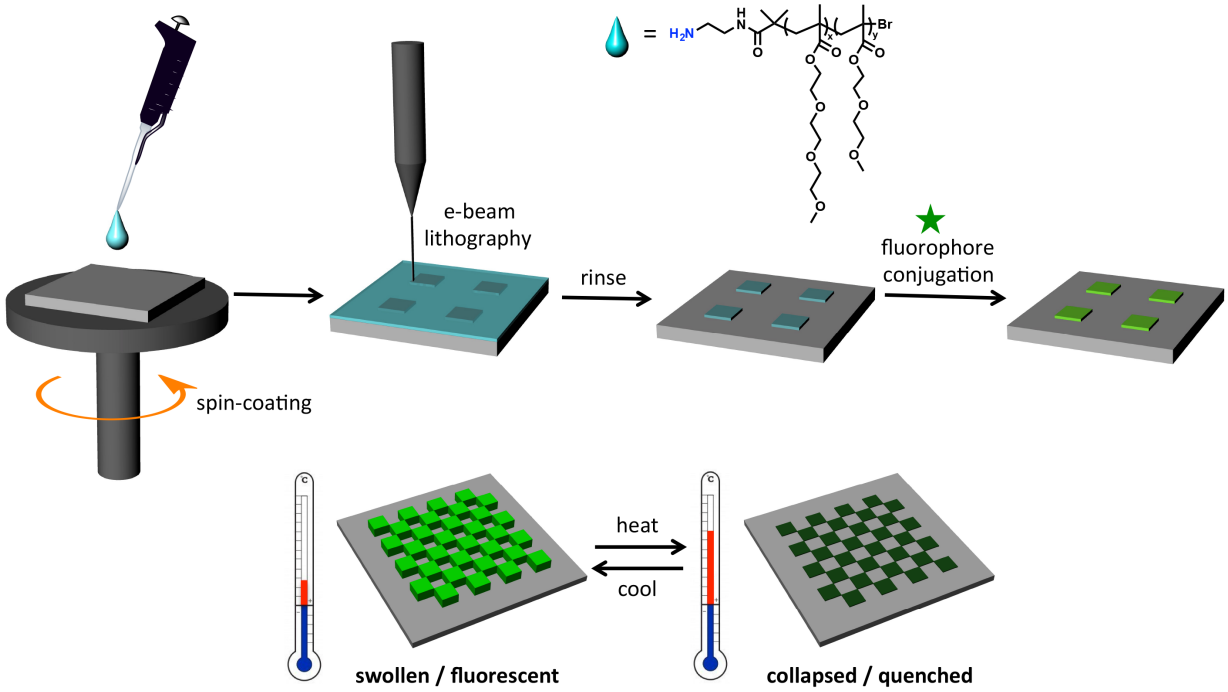

Figure 6-8. Preparation of thermo-responsive fluorescent hydrogel patterns by e-beam lithography and schematic representation of their fluorescence switching behavior in response to temperature change.

6.2.3 Screening Amine-Reactive Fluorophores

We first chose fluorescein isothiocyanate (FITC, Ex/Em 495/519 nm), a green fluorescent dye, to attach to the amine-functionalized $\mathbf{P_{30}}$ hydrogel. The hydrogels are brightly fluorescent at ambient temperature when immersed in water, and exhibit no fluorescent when the chip is dry. This correlates to our hypothesis that when the hydrogel is hydrated, the distance

between each fluorophore is larger, but when the gel is collapsed, the fluorophores come close to each other and the fluorescence is quenched. When the FITC-modified $\mathbf{P_{30}}$ hydrogel was heated in water from 25 °C to 40 °C, the fluorescent intensity significantly dropped, and increased again after cooling the surface back to 25 °C. However, the photobleaching effect of FITC was very significant, and the fluorescent intensity decreased to 13% after four cycles (**Figure 6-10a**).[37]

Alexa Fluor® 488 (AF488, Ex/Em 495/519 nm) is a fluorescein derivative tailored with greater photostability.[38] However, the AF488-modified $\mathbf{P_{30}}$ hydrogel did not show self-quenching properties in heating-cooling cycles (data not shown). Though not directly comparable, it has been reported that Alexa Fluor® dyes undergo much less self-quenching compared to Cyanine dyes.[39] The more hydrophobic the fluorophore, the more likely self-quenching will occur, perhaps due to the decreased contact with water and increased stacking through aromatic interactions.

By comparing the structures of fluorescein dyes, Rhodamine Green (RhodG, Ex/Em 502/527 nm) does not have the hydrophilic sulfonate groups like AF488, and is more hydrophobic (**Figure 6-9**). RhodG is also known to be more photostable than FITC,[40] and we have confirmed this by performing multiple heating and cooling cycles. The FITC-modified hydrogels suffered significant photobleaching (fluorescence intensity decreased to 10%) within 4 cycles; on the other hand, RhodG-modified hydrogels still exhibited significant difference in fluorescence between heating and cooling (decreased to 60%) after 8 cycles. (**Figure 6-10**).

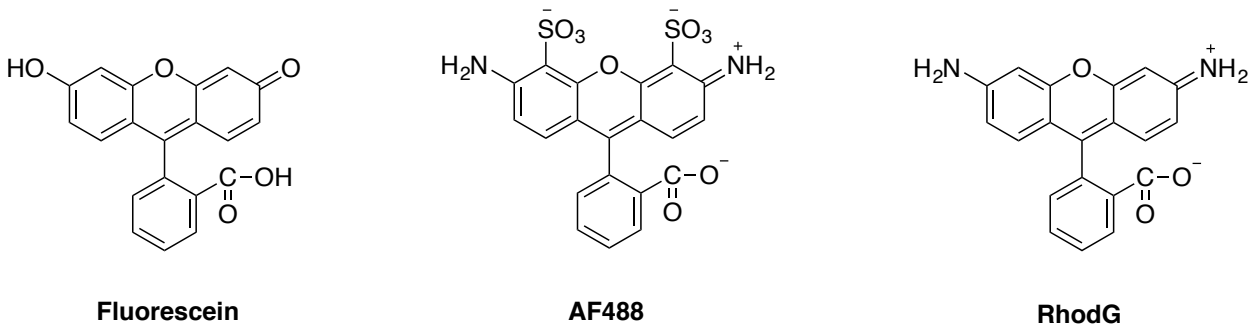

Figure 6-9. The chemical structures of the three green fluorescent dyes compared in this study. Shown from left to right: Fluorescein, Alexa Fluor® 488 (AF488), and Rhodamine Green (RhodG).

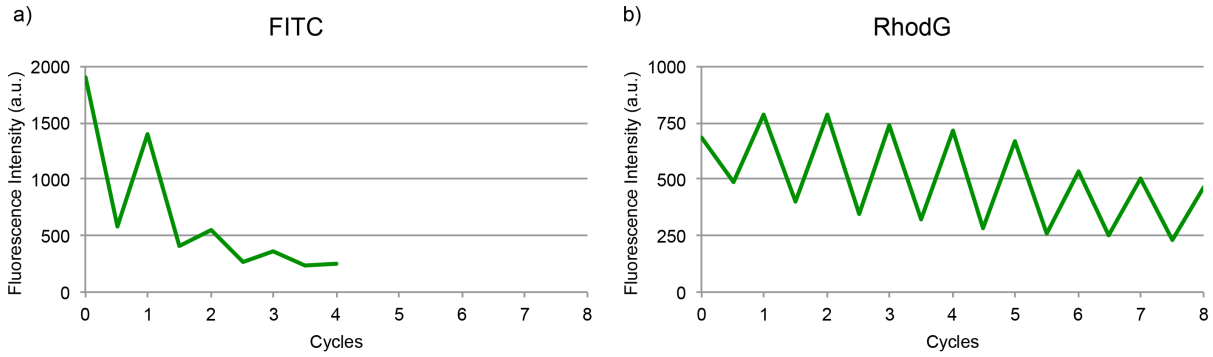

Figure 6-10. Fluorescence data of the heating and cooling cycles of a) FITC-modified and b) RhodG-modified $\mathbf{P_{30}}$ hydrogels. Between each heating and cooling step, the surface was allowed to equilibrate for 30 min. Exposure time: 2 sec.

After screening a few amine-reactive fluorophores, Rhodamine Green™-X carboxylic acid, succinimidyl ester, hydrochloride (RhodG) and Lissamine™ rhodamine B sulfonyl chloride (Lissamine Red) were chosen because of their photostability and efficient self-quenching properties.

6.2.4 Thermoresponsive Hydrogels at Different Temperatures

When the fluorophore-conjugated chips were heated to temperatures above the VPTT of the gels, a dramatic decrease in the fluorescence intensity was readily observed **(Figure 6-11)**. Once $\mathbf{P_{30}}$ hydrogels labeled with RhodG were heated to 37 °C, the fluorescence intensity reduced to 11.9 % of the original, and $\mathbf{P_{30}}$ hydrogels labeled with Lissamine Red dropped to 14.0 % (**Figure 6-11a** and **Figure 6-12**). Thus, the fluorescence quenching effect due to temperature change was significant for both $\mathbf{P_{30}}$ and $\mathbf{P_{40}}$ hydrogels (**Figure 6-11b**). Importantly, the fluorescence was recovered by lowering the temperature back to values below the VPTT, indicating that the fluorescence switching was reversible. These observations support our hypothesis that temperature-induced collapse of the gel led to self-quenching of the conjugated fluorophores.

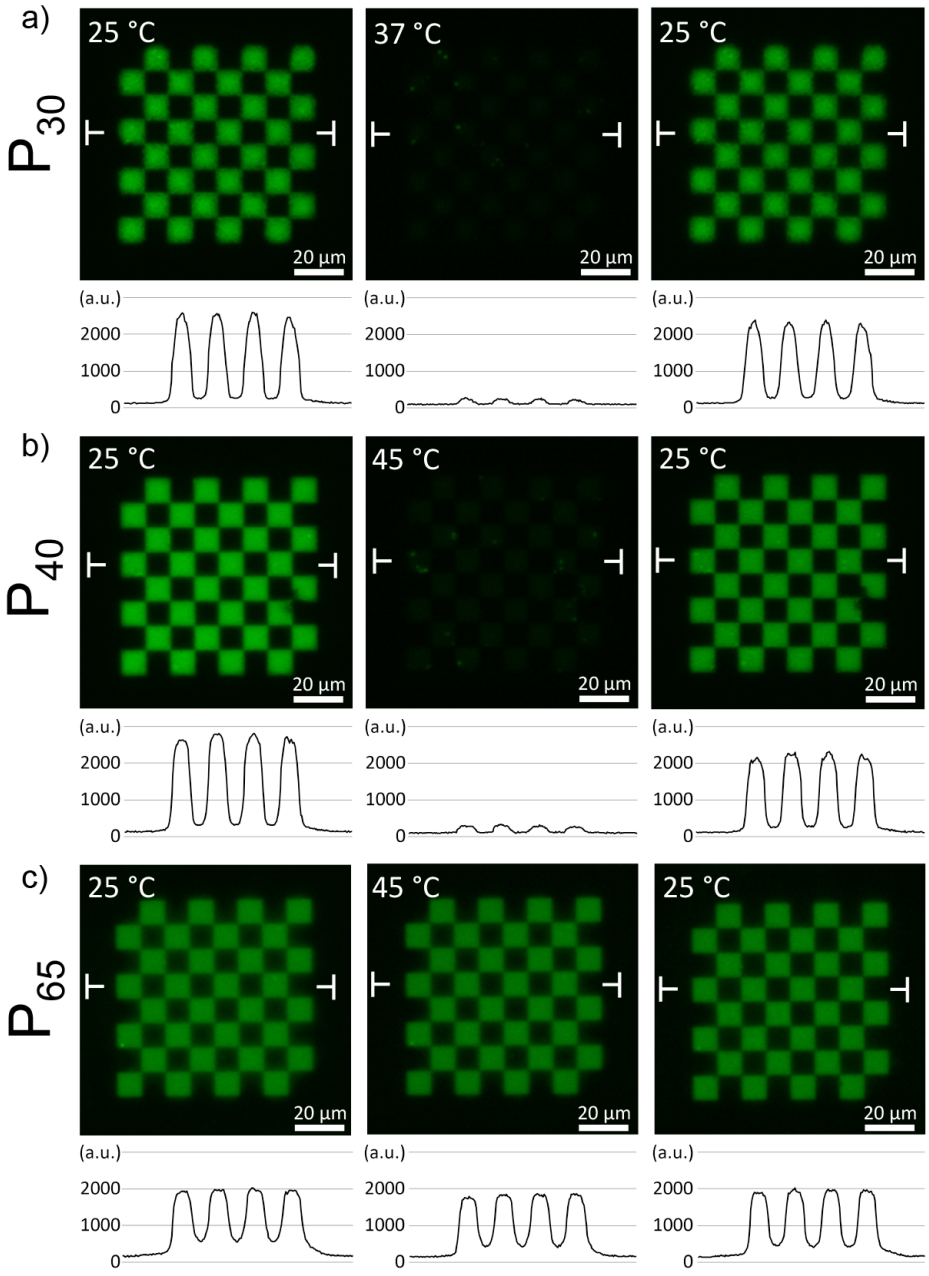

Figure 6-11. Fluorescence micrographs of the gels with intensity profiles of $\mathbf{P_{30}}$ (a), $\mathbf{P_{40}}$ (b), and $\mathbf{P_{65}}$ (c) at room temperature, above their VPTTs and after cooling back to room temperature. At temperatures above the VPTT, fluorescence quenching is observed, and upon cooling, the fluorescence is recovered.

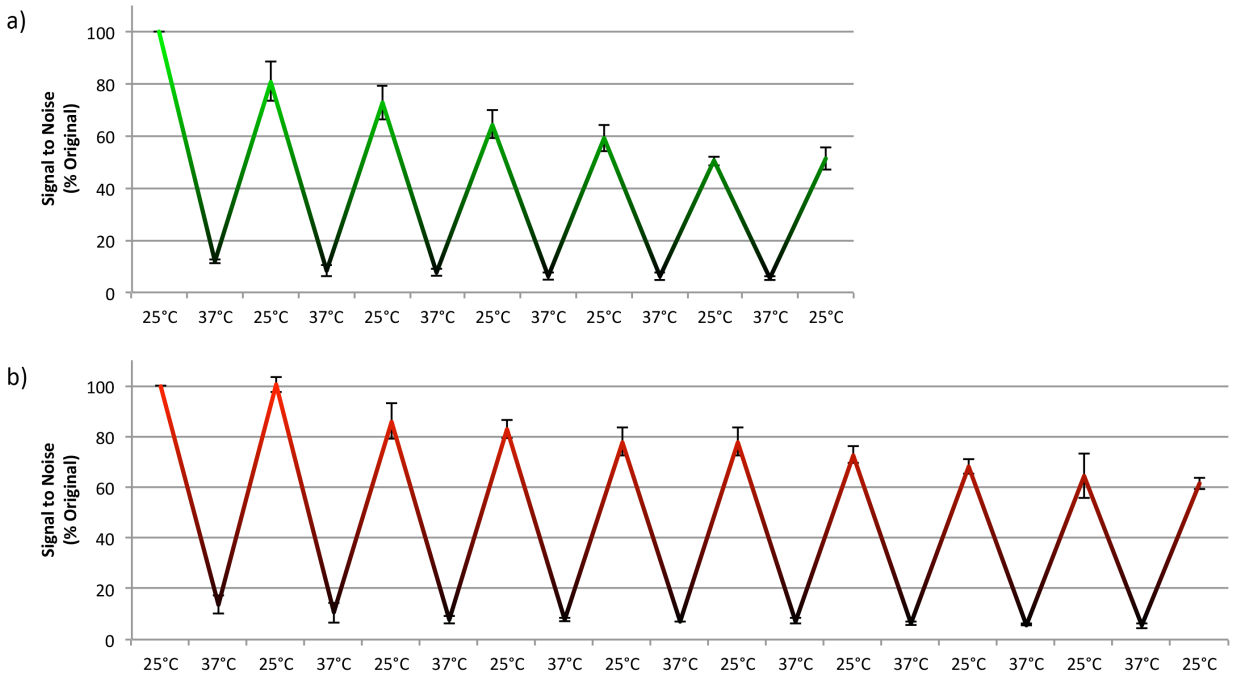

Figure 6-12. Fluorescence data from the heating and cooling cycles of $\mathbf{P_{30}}$ hydrogels modified with a) Rhodamine Green and b) Lissamine Red.

We performed heating-cooling cycles to investigate the reversibility of fluorescence switching behavior for $\mathbf{P_{30}}$. A gradual decrease in fluorescence signal was observed with increasing number of cycles due to photobleaching of the dyes. The intensity of RhodG conjugated gels dropped to 51.4 % after 7 cycles (14 times excitation/exposure), whereas Lissamine Red conjugated hydrogels retained 61.4 % of their initial fluorescence after 10 cycles (**Figure 6-12**). To investigate the effect of photobleaching on this fluorescence decay behavior, we imaged a RhodG conjugated control pattern before starting the heating-cooling cycles and after the 7th cycle. After 7 heating-cooling cycles (but only twice excitation/exposure), the fluorescence signal was retained at 87.2 % (versus 51.4 %) (**Figure 6-13**). This suggested that

photobleaching of the fluorophores was the major factor in the observed gradual decrease of the fluorescence signal. To investigate the effect of temperature induced quenching of fluorophores, we prepared hydrogel patterns with $\mathbf{P_{65}}$ and monitored the fluorescence signal from 25 to 45 °C. As expected, the fluorescence intensity of $\mathbf{P_{65}}$ hydrogels decreased much less than that observed for $\mathbf{P_{30}}$ and $\mathbf{P_{40}}$ at temperatures of 37 °C and 45 °C, as these temperatures are well below the VPTT for $\mathbf{P_{65}}$. An increase from 25 °C to 45 °C caused only 5.3 % and 36.5 % decrease in fluorescence signal for RhodG and Lissamine Red conjugated patterns, respectively (**Figure 6-11c** and **Figure 6-14**).

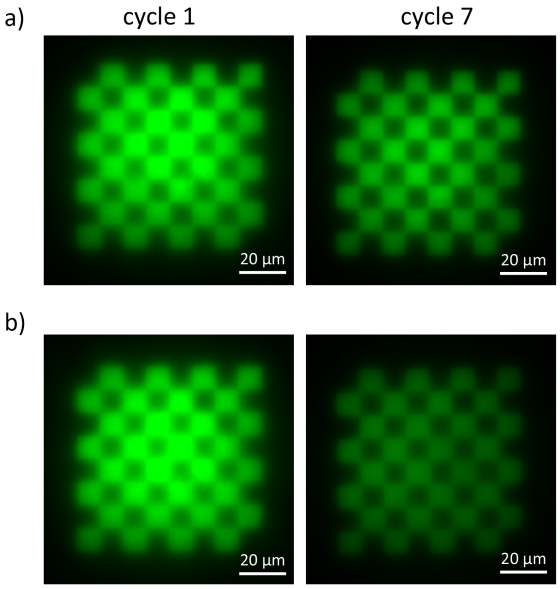

Figure 6-13. The photobleaching effect of Rhodamine Green conjugated to $\mathbf{P_{30}}$ hydrogels after a) 2 times and b) 14 times of exposure. The intensity of RhodG conjugated gels dropped to 51.4 % after 7 heating-cooling cycles (14 times excitation/exposure), while the control was retained at 87.2 %. This suggested that photobleaching of the fluorophores was the major factor in the observed gradual decrease of the fluorescence signal.

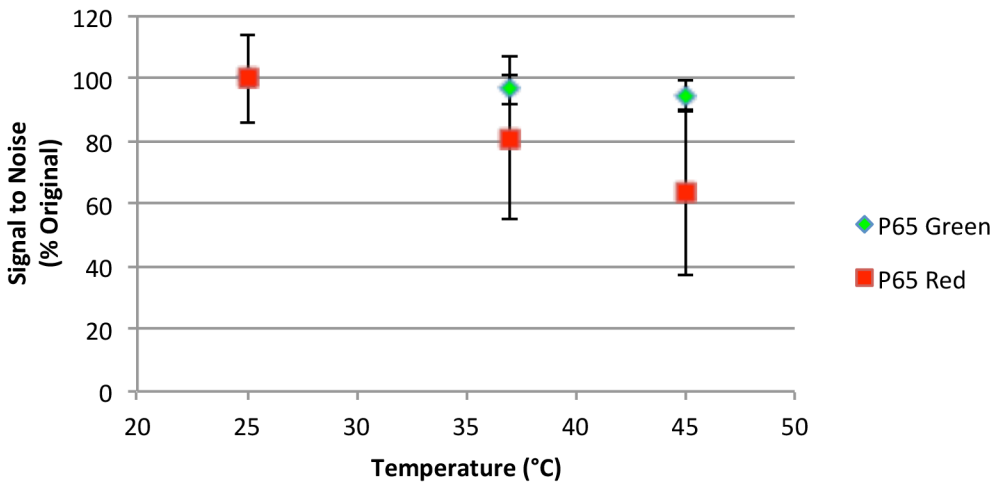

Figure 6-14. The response of fluorophores (Green diamond – Rhodamine Green; Red square – Lissamine Red) toward temperature increase measured with $\mathbf{P_{65}}$ hydrogels that did not collapse at this temperature range.

6.2.5 AFM Measurements

We also performed AFM measurements to verify that the observed fluorescence switching behavior was due to temperature-induced swelling-collapse of the hydrogels (**Figure 6-15**). Above the VPTT, the thicknesses of the hydrogels sharply decreased to less than 25 % of their initial thickness, which supports the fluorescence microscopy observations. AFM measurements also showed that the thermo-responsive swelling-collapse behavior was reversible.

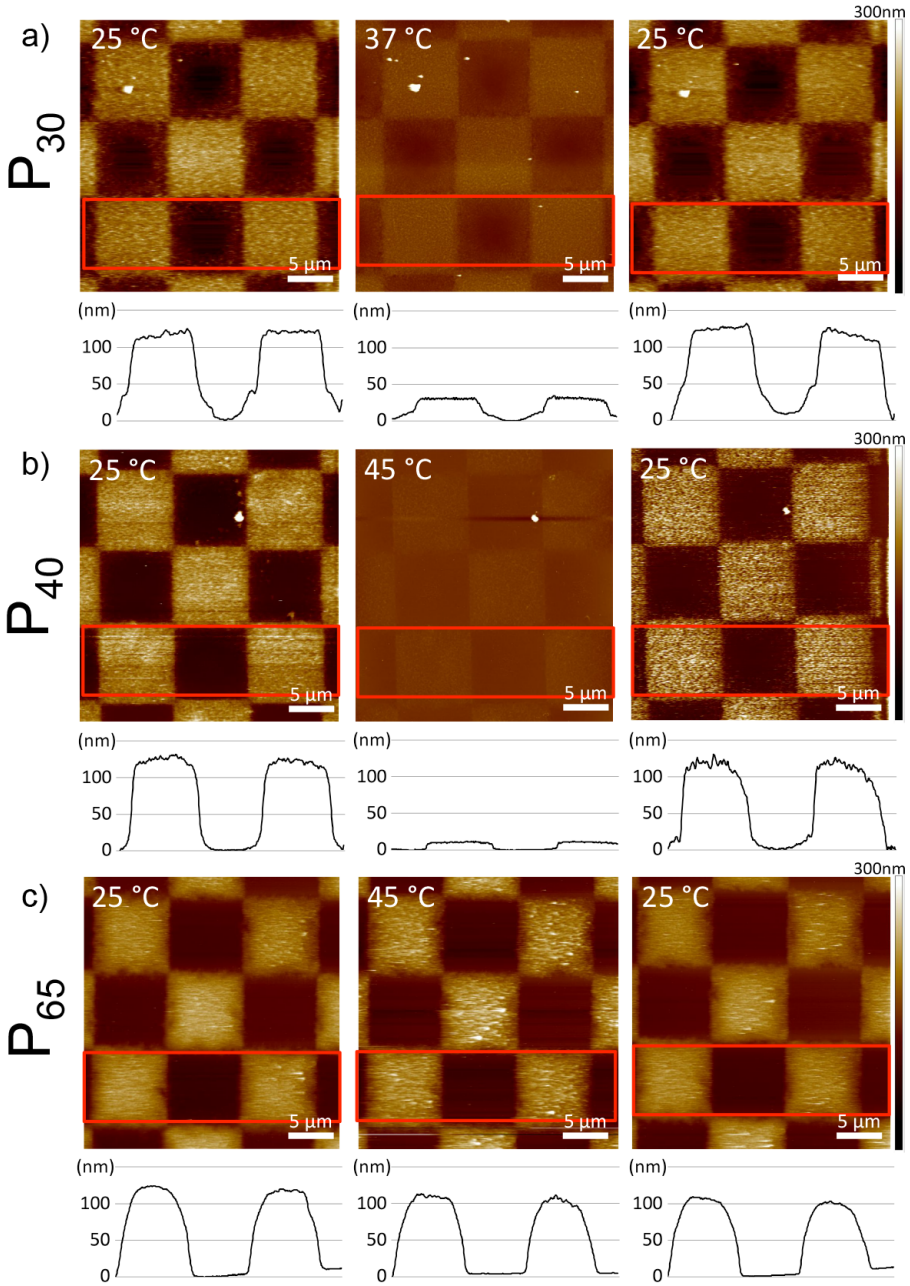

Figure 6-15. AFM images with height of $\mathbf{P_{30}}$ (d); $\mathbf{P_{40}}$ (e), and $\mathbf{P_{65}}$ (f) at room temperature, above their VPTTs and after cooling back to room temperature. At temperatures above the VPTT, gels shrink, and upon cooling, swelling is observed.

6.2.6 Multicomponent Patterns

To demonstrate the utility of the fluorescent hydrogel patterns as dynamic displays, we patterned the three polymers in a design that revealed encrypted messages at different temperatures. Sequential e-beam writing of different polymers generated multicomponent patterns. The entire pattern was then conjugated with RhodG. At room temperature, all hydrogels were swollen and brightly fluorescent upon excitation **(Figure 6-16a)**. When heated to 37 °C, only the $\mathbf{P_{30}}$ hydrogels collapsed and their fluorescence intensity decreased significantly. At this temperature, the surface pattern changed from displaying "888" to "037". When heating further to 45 °C, the $\mathbf{P_{40}}$ hydrogels also collapsed, and only $\mathbf{P_{65}}$ hydrogels remained bright. The fluorescent pattern became "111". Upon cooling down to 37 and 25 °C, the surface sequentially displayed "037" and "888", respectively. To the best of our knowledge, this is the first study demonstrating smart surfaces that display morphing images in response to changes in environmental conditions.

We then investigated incorporating two fluorophores into a dual hydrogel pattern **(Figure 6-16b)**. First a checkerboard pattern with $\mathbf{P_{30}}$ and Lissamine Red was generated. Then, a complementary pattern was written with $\mathbf{P_{40}}$ followed by conjugation of RhodG. This resulted in a checkerboard pattern with green and red squares. Upon heating to 37 °C, the red fluorescence diminished, while the green was still preserved to a large extent. The collapse of $\mathbf{P_{30}}$ gels at 37 °C appeared to reduce the height of $\mathbf{P_{40}}$ gels and led to a decrease in the intensity of green fluorophore, likely because both gels were in contact. However, the decrease in green fluorescence was much lower than that observed for red fluorescence. At 45 °C, both hydrogels collapsed, leading to a significant decrease in the fluorescence intensity in both channels. These

dual dye patterns were also thermo-reversible and showed gradual fluorescence recovery upon cooling.

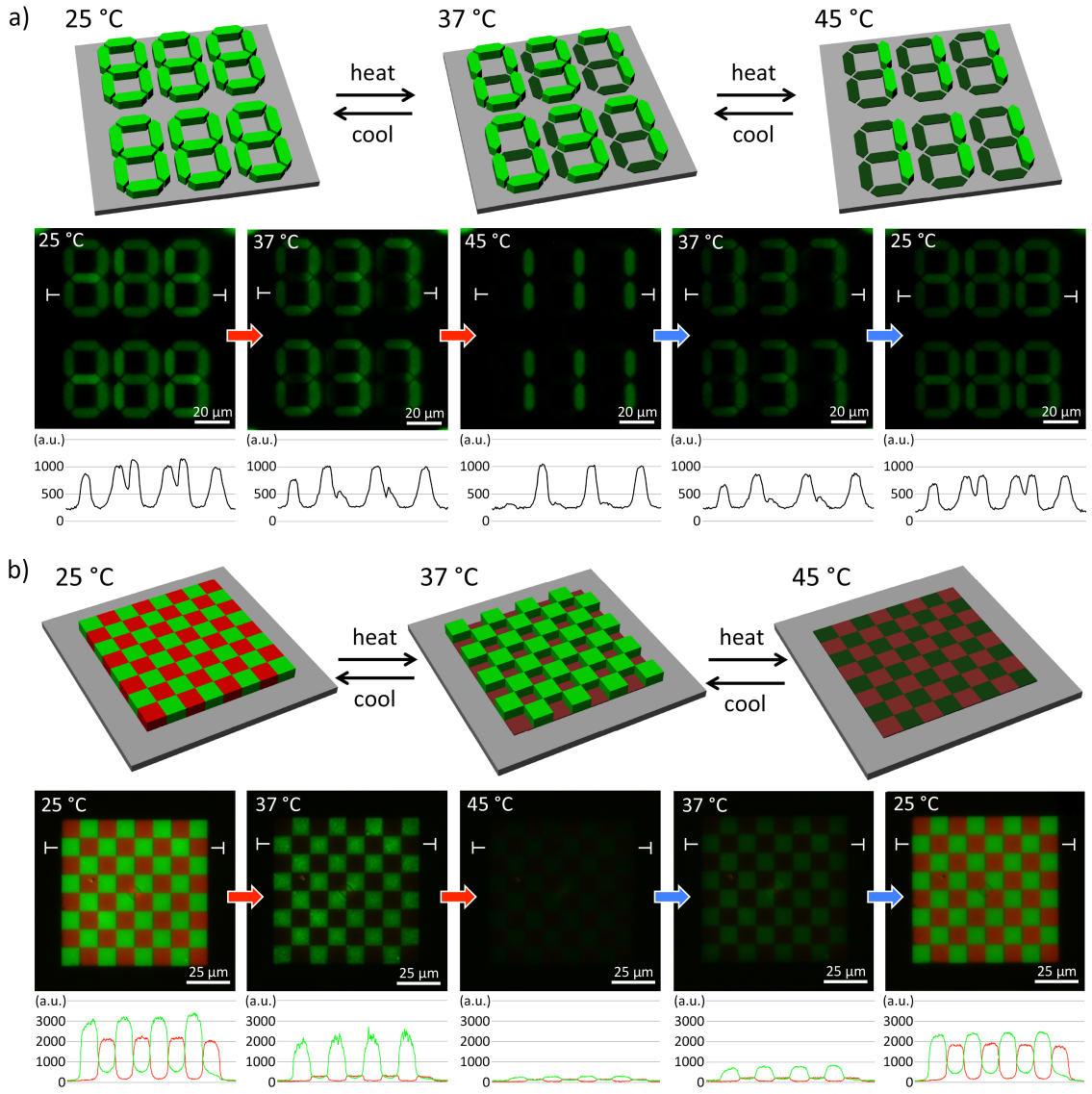

Figure 6-16. 3-D representations, fluorescence micrographs, and intensity profiles of multicomponent single dye (a) and dual dye (b) conjugated hydrogel patterns. (a) At room temperature, single dye patterned multicomponent surfaces display “888”. Upon increasing the temperature to 37 °C and 45 °C, the displayed patterns become “037” and “111”, respectively.

(b) The red and green colors in checkerboard patterns are sequentially switched off with increasing temperature and then switched back on with decreasing temperature.

6.3 Conclusions

In this study, we demonstrated that by using thermo-responsive hydrogels and self-quenching fluorophores, fluorescence switching of the surfaces could be controlled by temperature-induced volume phase transition behavior of the hydrogels. The fluorescence microscopy observations were corroborated with AFM data. Surfaces revealing encrypted messages upon external stimuli were readily prepared by patterning multiple stimuli responsive polymers. Two fluorophores were incorporated without changing the functional groups of the polymers, which greatly simplifies the system. These multicomponent, morphing fluorescent hydrogel patterns may be useful in a diverse range of applications such as (bio)sensors, encryptions, biomedical microdevices, and self-reporting surfaces.

6.4 Experimental Section

Materials

All chemicals were purchased from Sigma-Aldrich and used without further purification unless otherwise specified. Copper bromide (CuBr) was purified by stirring in glacial acetic acid for 12 h and rinsing with ethanol and diethyl ether. Silicon wafers were purchased from Cemat Silicon S.A. Rhodamine Green™ carboxylic acid, succinimidyl ester, hydrochloride, Lissamine™

rhodamine B sulfonyl chloride, Fluorescein isothiocyanate, and Alexa Fluor® 488 caboxylic acid, succinimidyl ester were purchased from Life Technologies.

Instrumentation

NMR spectra were obtained on a Bruker DRX 500 MHz spectrometer. Gel permeation chromatography (GPC) was performed on a Shimadzu HPLC system equipped with a RID-10A detector and two PLgel 5 μm mixed D columns (Polymer Laboratories) at 40 °C with 0.1 M lithium bromide in N,N-dimethylformamide (DMF) (flow rate: 0.60 mL/min). Monodisperse poly(methyl methacrylate) (PMMA) samples (Polymer Laboratories) were employed as the standards for calibration. Chromatograms were processed with the EZStart 7.2 chromatography software to obtain the number-average molecular weight (M_n) and polydispersity index (PDI).

Methods

Synthesis of 3-(N-Boc-amino)propanol **1.** The synthesis was modified from a procedure reported in literature.[35] 3-Aminopropanol (0.5 mL, 6.57mmol) was added drop wise to di-tert-butyl dicarbonate (1.42 g, 6.5 mmol) in 5 mL methanol. The reaction mixture was heated at 50 °C for 2 h. Methanol was then evaporated and the pH was reduced to 2–3 with a 1 N solution of hydrochloric acid. The reaction mixture was extracted three times with ethyl acetate and the organic layer was dried over $MgSO_4$ then evaporated to give 1.02 g of colorless liquid with 90% yield. ^{1}H NMR (500 MHz in $CDCl_3$) δ: 4.78 (bs, 1H, NH), 3.65 (bs, 2H, C**H$_2$**OH), 3.30-3.25 (m, 2H, C**H$_2$**NH), 2.99 (bs, 1H, OH), 1.68-1.62 (m, 2H, CH_2**C**H$_2$**C**H_2), 1.43 (s, 9H, $(CH_3)_3C$).

Synthesis of ATRP Initiator (N-Boc-propylamino)-2-bromoisobutyrate **2.** The synthesis was modified from a procedure reported in literature.[35] **1** (0.6 g, 3.42 mmol) and THF (10 mL) were

mixed in a round bottom flask. At 0 °C, triethylamine (0.93 mL, 6.67 mmol) and 2-bromoisobutyrylbromide (0.69 mL, 5.58 mmol) were added drop wise. The reaction mixture was stirred at 0-23 °C for 15 h. The mixture was then filtered and the white solid was washed with THF. After the evaporation of the solvent, the crude material was dissolved in dichloromethane and washed with water, a saturated solution of sodium bicarbonate and then water again. The organic phase was dried over $MgSO_4$ and evaporated. The crude was purified by silica gel flash chromatography with EtOAc : Hexane = 1 : 8 to obtain 0.55 g of the initiator (N-Boc-propylamino)-2-bromoisobutyrate with 50% yield. ^{1}H NMR (500 MHz in $CDCl_3$) δ: 4.77 (bs, 1H, NH), 4.26-4.23(t, 2H, CH_2O), 3.26-3.21 (m, 2H, C**H$_2$**NH), 1.93 (s, 6H, $(CH_3)_2CBr$), 1.91-1.81 (m, 2H, CH_2**CH$_2$**CH_2), 1.43 (s, 9H, $(CH_3)_3C$).

Synthesis of 2-(N-Boc-amino)-ethylamine **3.** The synthesis was modified from a procedure reported in literature.[36] A solution of di-tert-butyl dicarbonate (2.105 mL, 9.16 mmol) in 25 mL of 1,4-dioxane was slowly added drop wise into a stirred solution of diaminoethane (4.6 mL, 68.7 mmol) in 25 mL of 1,4-dioxane over a period of 1 h. After 72 h, the precipitate that formed was filtered off and the 1,4-dioxane and excess diaminoethane were removed under vacuum from the filtrate. Water (30 mL) was added to the residue and the water-insoluble bis(N,N'-tert-butyloxycarbonyl)-1,2-diaminoethane was removed by filtration. From the aqueous solution saturated with sodium chloride, the product was extracted with dichloromethane. The collected organic phase was dried over $MgSO_4$ and evaporated under reduced pressure to give 1.2 g of tert-butyl-N-(2-amino-ethyl) carbonate as a colorless oil with 82% yield containing slight amount of impurities. ^{1}H NMR (500 MHz in $CDCl_3$) δ: 4.89 (bs, 1H, NH), 3.19-3.15 (m, 2H, NHC**H$_2$**CH_2), 2.81-2.78 (m, 2H, CH_2**CH$_2$**NH_2), 1.44 (s, 9H, $(CH_3)_3C$). ESI-MS (± 1.0) observed (predicted): H^+ 161.1290 (161.1290).

***Synthesis of ATRP initiator* 4.** The synthesis was modified from a procedure reported in literature.[36] **3** (1.2 g, 7.49 mmol), triethylamine (1.04 mL, 7.49 mmol), and dry dichloromethane (10 mL) were placed in a round-bottomed flask. 2-Bromoisobutyryl bromide (0.93 mL, 7.49 mmol) was added slowly with stirring at 0 °C. The reaction was left to warm to 23 °C with continuous stirring for 24 h. Triethylammonium bromide formed as a white precipitate was filtered off. After removal of the solvent under vacuum from the filtrate, a yellow solid was left. The product was dissolved in methanol and precipitated into saturated sodium carbonate. The precipitant was dissolved in dichloromethane and washed with water twice. The organic layer was dried over $MgSO_4$ and evaporated. The crude was then purified by silica gel flash chromatography with EtOAc : Hexane = 1 : 2 to obtain 0.81 g of the initiator as a white solid with 35% yield. ^{1}H NMR (500 MHz in $CDCl_3$) δ: 4.84 (bs, 1H, NH), 3.39-3.33 (m, 4H, CH_2CH_2), 1.93 (s, 6H, $(CH_3)_2CBr$), 1.44 (s, 9H, $(CH_3)_3C$). ^{13}C NMR (500 MHz in $CDCl_3$) δ: 172.75, 156.92, 79.85, 61.72, 41.83, 39.80, 32.35, 28.54. ESI-MS (± 1.0) observed (predicted): H^+ 331.0638 (331.0633).

General procedure of atom transfer radical polymerizations. With NBoc-protected **P_{30}**' as an example: **2** (20 mg, 0.0647 mmol), triethylene glycol methyl ether methacrylate (0.44 mL, 1.94 mmol), diethylene glycol methyl ether methacrylate (0.836 mL, 4.53 mmol) and MeOH (0.625 mL) were added to a Schlenk tube and subjected to 6 freeze-pump-thaw cycles. A catalyst stock solution (4x) was made of CuBr (37.12 mg, 0.26 mmol) and 2,2′-bipyridine (bipy, 80.8 mg, 0.52 mmol). The solid mixture was evacuated-refilled with argon 7 times, and then dissolved in degassed MeOH (500 μL). 125 μL of the catalyst stock solution was added to the Schlenk tube and stirred at 23 °C for 20 h under argon. The polymerization reached 34% conversion (calculated by comparing the integration of 4.1-4.3 ppm ester signals to alkene signals).

Methanol was removed under reduced pressure. The crude was re-dissolved in THF and filtered through silica to remove the copper. The excess monomer was removed by dialysis (MWCO 3500 Da) against H_2O (4 L, 5 times). After lyophilization, a clear sticky polymer was obtained. Following the same procedure, three polymers were synthesized from various monomer compositions, and are summarized in Table 1.

Deprotection of NBoc-terminated polymers. **P_{30}'** (23.5 mg) was dissolved in 500 μL dry dichloromethane. Trifluoroacetic acid (TFA, 100 μL) was added, and the solution was stirred at 23 °C for 30 min. The reaction mixture was dried *in vacuo* to remove solvent and TFA, and then redissolved in H_2O. The aqueous solution was then dialyzed (MWCO 3500 Da) against H_2O for 2 days, followed by 10 mM EDTA solution for 2 more days. After lyophilization, a clear sticky polymer was obtained.

LCST Determination. The absorbance of polymer solutions (1 mg/mL in H_2O) at 600 nm was measured with a Hewlett-Packard HP8453 diode-array UV-Vis spectrophotometer with Peltier temperature control. The following temperature program was used: temperature was elevated at 0.5 °C/min and held for 30 s prior to measuring the absorbance at 600 nm. At temperatures close to the LCST, the absorbance values started increasing and reached a plateau maximum as the solutions became completely turbid. The temperature at which 10% of the maximum absorbance occurred was assigned as the LCST.

Calculation of monomer ratio in copolymers. The integrations of peaks for the protected polymers (**P_{30}'**, **P_{40}'**, and **P_{65}'**) were calibrated with respect to the Boc group at 1.4 ppm. The integration of deprotected polymers (**P_{30}**, **P_{40}**, and **P_{65}**) were based on setting the integration value of peak **a** (the methylene protons next to the ester unit) to the same value as its protected

polymer. To show the calculation of monomer ratio determination, **P_{30}'** is described as an example below. Setting x=TEGMA units and y=DEGMA units, the following equation was obtained from the integration of peak **a**: 2x+2y=402.28. Then, from the total integration of peak **b**+**c** (methylene protons of the ethylene glycol units), another formula was obtained: 10x+6y=1447.6. The monomer units were calculated by the two underlined formulas to get x=60.19 and y=134.61. The ratio of TEGMA and DEGMA units were then calculated to be 30.9 % and 69.1 %, which is very close to the feed ratio of 30/70. Similar results can be obtained using integrations of **d**, **e**, or **g** as the first formula. The integrals match well with **d** (3x+3y, methyl protons of the methoxy group) and **g** (3x+3y, methyl protons of the methacrylates). It is noted that peak **e** (2x+2y, methylene protons of polymer backbone) doesn't always correlate well, perhaps due to the overlap of the protons from H_2O.

Preparation of Thermo-responsive Polymer Patterned Surfaces by e-Beam Lithography. Silicon chips were cleaned by immersing into freshly prepared piranha solution (3:1 H_2SO_4/H_2O_2, *Caution! Piranha solution reacts violently with organic materials*). The chips were then washed with a large excess of MilliQ water and dried under a stream of air. Cleaned Si chips were spin-coated (2000 rpm for 20 s, 4000 rpm for 10 s) with 1 wt% polymer solutions in 1,2-dichloroethane. The coated chips were then used directly without any drying or baking steps. Pattern files for electron beam lithography were created using DesignCAD Express 16 software. The designed patterns were generated using a JC Nabity e-beam lithographic system (Nanometer Pattern Generation System, version 9.0) modified from a JEOL JSM-6610 scanning electron microscope. An accelerating voltage of 30 kV was used, with a beam current of ~15 pA, a spot size of 32 nm, and using an area dose of 0.4 $\mu C/cm^2$. After e-beam exposure, any non-crosslinked polymer on the chips was rinsed with methanol, water, and methanol (10 s each) and

the substrates were dried under a stream of nitrogen. Pattern formation was confirmed using an upright bright-field microscope.

Conjugation of Fluorescent Dyes onto Surfaces. Immediately after developing the e-beam patterned surfaces, a 10 μL solution (10 mg/mL in DMSO or DMF containing 1 % triethylamine) of either Rhodamine Green™ carboxylic acid succinimidyl ester hydrochloride, Fluorescein isothiocyanate, Alexa Fluor® 488 caboxylic acid, succinimidyl ester, mixed isomers (10 mg/mL in DMSO) or Lissamine™ rhodamine B sulfonyl chloride was placed on the chips for one hour. Then, the chips were rinsed thoroughly with DMF and MilliQ water. Dye conjugation was assessed by fluorescence microscopy.

Preparation of Multicomponent Fluorescence Switching Surfaces. For multicomponent patterns, silicon wafers with gold alignment reference marks fabricated by conventional photolithography and Ti/Au deposition were used.[41] Dual dye patterns were created by first writing a checkerboard pattern with $\mathbf{P_{30}}$ and conjugating the patterned hydrogels with Lissamine™ rhodamine B sulfonyl chloride as described above. Then, $\mathbf{P_{40}}$ was spin-coated and after alignment to the first layer, a complementary checkerboard pattern with $\mathbf{P_{40}}$ was written in the same way at the desired position. These patterns were conjugated with Rhodamine Green™ carboxylic acid succinimidyl ester hydrochloride. The dye conjugation was done in the order described above to avoid the reaction of Lissamine™ rhodamine B sulfonyl chloride with the amine group of RhodG. Single dye, multicomponent patterns were written as described above except the dye conjugation was performed at once after all the layers had been written.

Fluorescence Microscopy and Thermoresponsive Fluorescence Switching. To assess the thermo-responsive fluorescence switching behavior, chips having fluorophore conjugated

hydrogel patterns were fixed onto a Peltier heating-cooling device. Then, a glass slide with spacers was placed on top of the device to create a slit. The whole surface of the chips was covered with water by filling the slit with MilliQ water. The temperature on the surface of the chip was adjusted with the Peltier device and measured with an infrared thermometer. The samples were kept at predetermined temperatures for 30 min to ensure that equilibrium had been reached although fluorescence switching could be observed in less than 1 min and 5 min during heating and cooling, respectively. Then, the surfaces were visualized with fluorescence microscopy using a Zeiss Axiovert 200 fluorescent microscope equipped with an AxioCam MRm monochrome camera. For RhodG, a 485/20 band pass excitation filter and a 515 band pass emission filter was used whereas for Lissamine Rhodamine B a 546/12 band pass excitation filter and a 509 band pass emission filter was used. The pictures were acquired and processed using AxioVision LE 4.6 software. For a given experiment, the acquisition and processing parameters were kept the same for different cycles and temperatures to allow a fair comparison of the samples under different conditions. NIH ImageJ software was used to calculate the signal-to-noise ratio as (signal – background)/standard deviation of background.

Atomic Force Microscopy. For height characterization of thermo-responsive hydrogel patterns, a Bruker Dimension Icon AFM equipped with an automated heating-cooling stage was used in Peak Force tapping mode with ScanAsyst Fluid probes. The samples were mounted on the stage with a double sided copper tape and AFM imaging was performed while samples were immersed in water. The oscillation frequency was 2 kHz. Each set of height measurement corresponds to a 512 × 512 force separation curves obtained over an area of 35 × 35 μm at a scan rate of 0.5 Hz.

6.5 Appendix to Chapter 6: Supplementary Figures

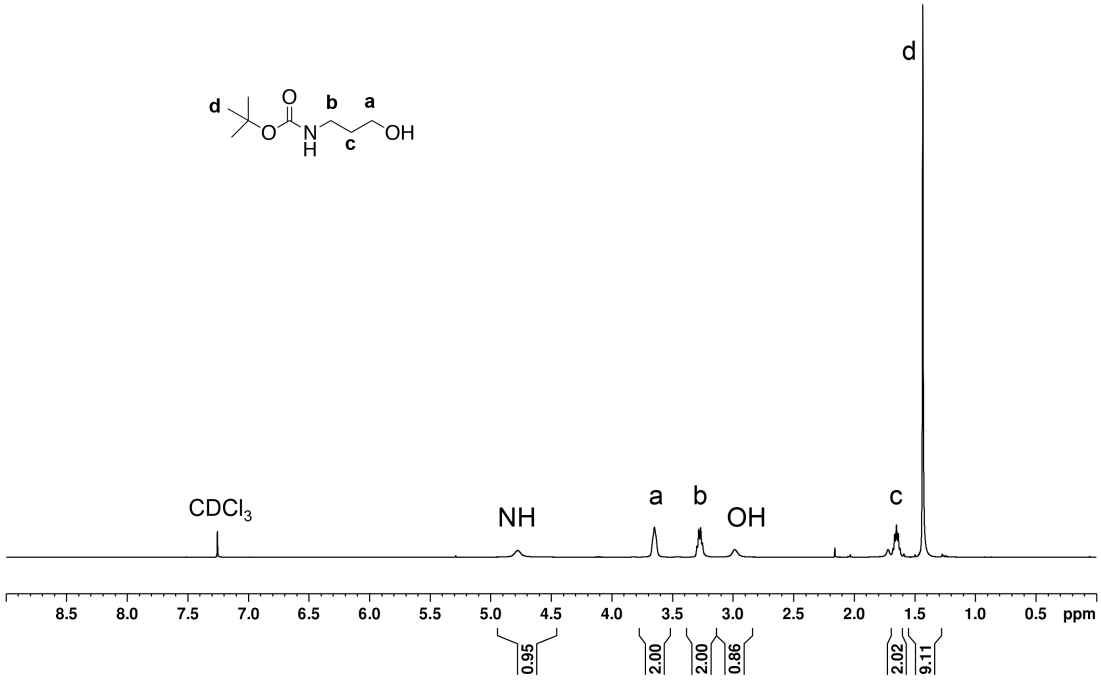

Figure 6-17. ^{1}H NMR spectrum of **1** in $CDCl_3$.

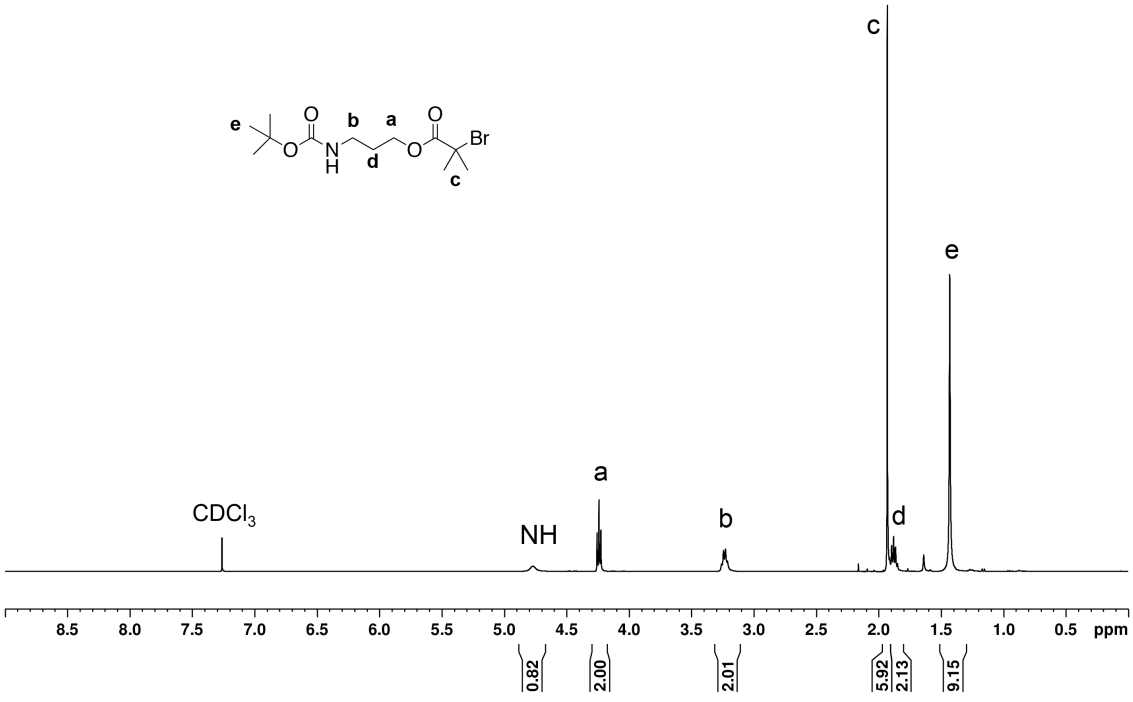

Figure 6-18. ^{1}H NMR spectrum of **2** in $CDCl_3$.

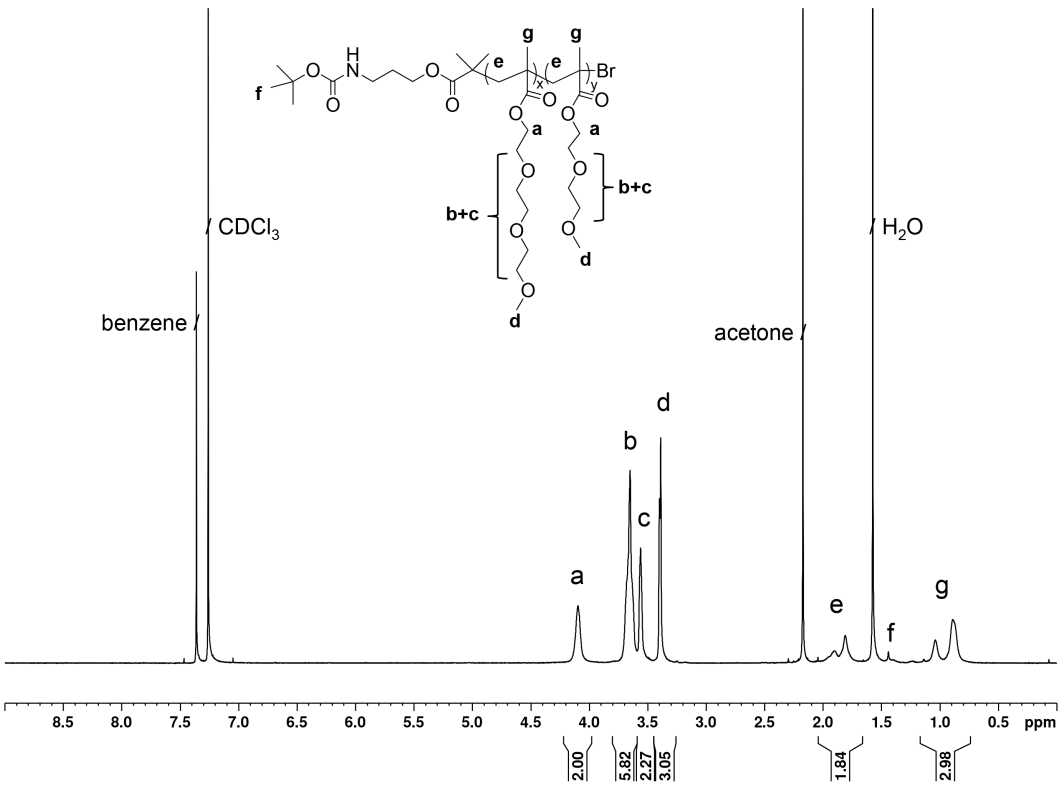

Figure 6-19. ^{1}H NMR spectrum of $\mathbf{P_A}$**'** in $CDCl_3$.

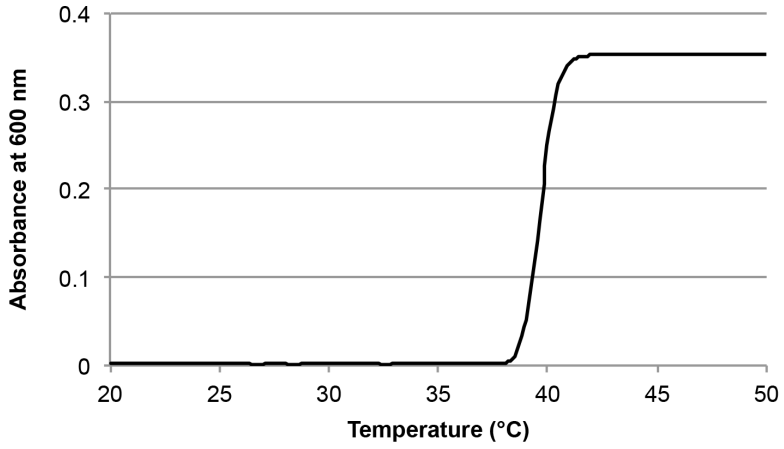

Figure 6-20. UV-Vis spectrum for the LCST determination of $\mathbf{P_A}$**'**.

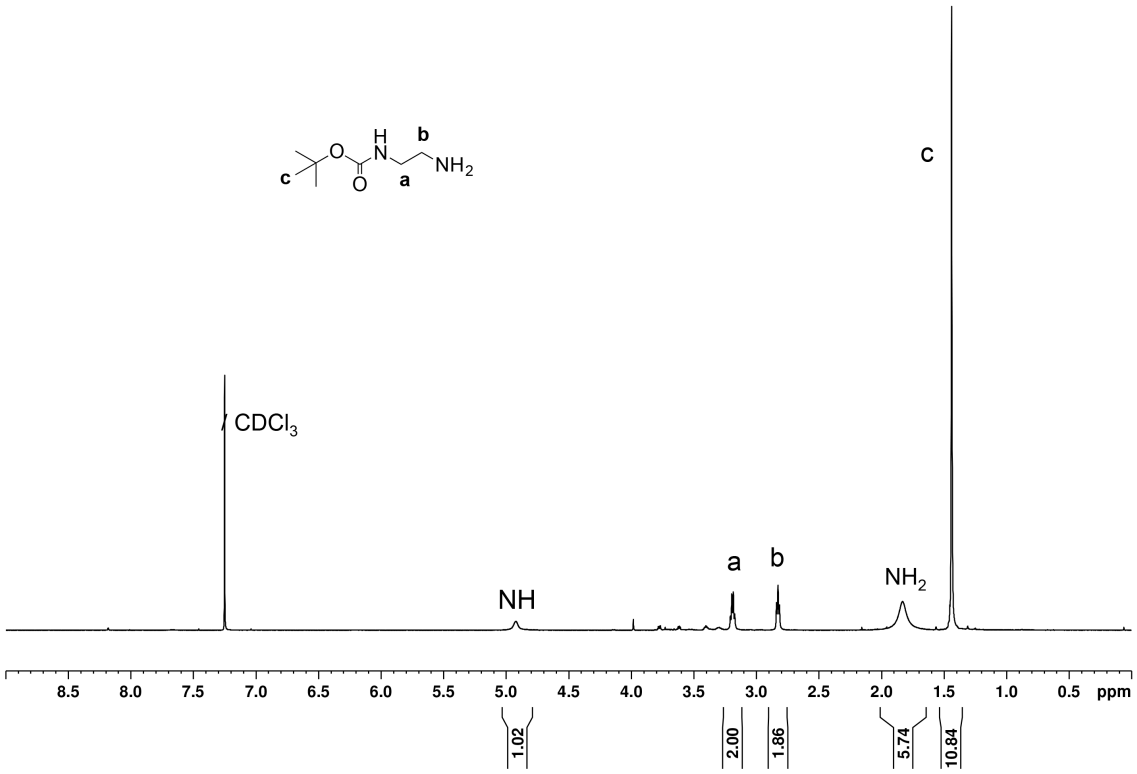

Figure 6-21. ^{1}H NMR spectrum of **3** in $CDCl_3$.

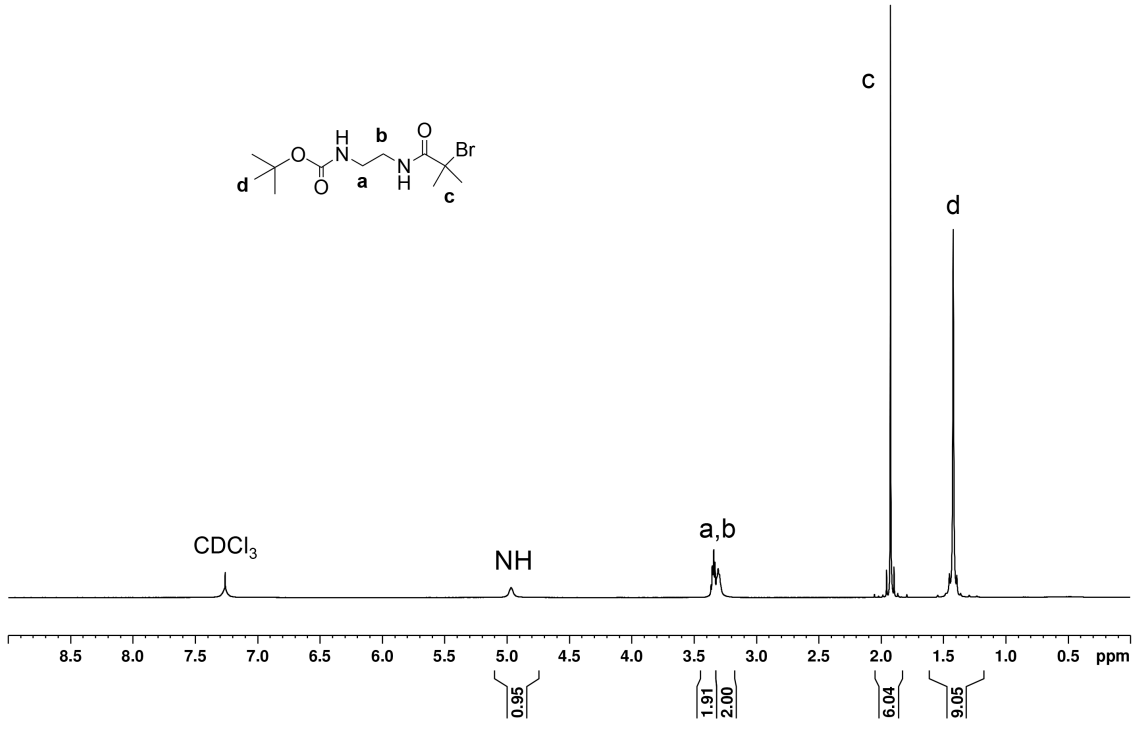

Figure 6-22. ^{1}H NMR spectrum of **4** in $CDCl_3$.

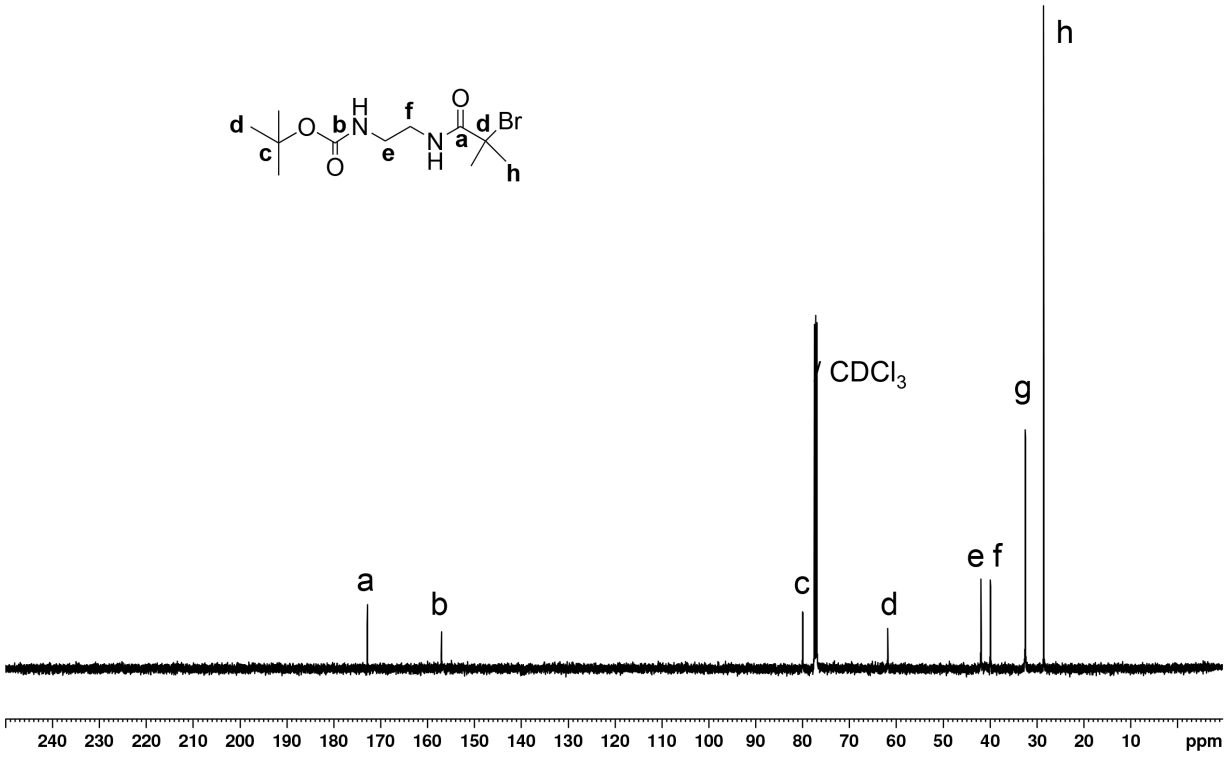

Figure 6-23. ^{13}C NMR spectrum of **4** in $CDCl_3$.

6.6 References

‡ Portions of this chapter have been published as: Bat, E.; Lin, E.-W.; Saxer, S.; Maynard, H. D., "Morphing Hydrogel Patterns by Thermo-Reversible Fluorescence Switching," *Macromol. Rapid Commun*. **2014**, *35*, 1260-1265.

(1) Stuart, M. A. C.; Huck, W. T. S.; Genzer, J.; Muller, M.; Ober, C.; Stamm, M.; Sukhorukov, G. B.; Szleifer, I.; Tsukruk, V. V.; Urban, M.; Winnik, F.; Zauscher, S.; Luzinov, I.; Minko, S. "Emerging Applications of Stimuli-Responsive Polymer Materials" *Nat. Mater*. **2010**, *9*, 101-113.

(2) Chung, J. E.; Yokoyama, M.; Yamato, M.; Aoyagi, T.; Sakurai, Y.; Okano, T. "Thermo-Responsive Drug Delivery from Polymeric Micelles Constructed Using Block Copolymers of Poly(*N*-Isopropylacrylamide) and Poly(Butylmethacrylate)" *J. Controlled Release* **1999**, *62*, 115-127.

(3) Dong, L. C.; Hoffman, A. S. "A Novel-Approach for Preparation of pH-Sensitive Hydrogels for Enteric Drug Delivery" *J. Controlled Release* **1991**, *15*, 141-152.

(4) Miyata, T.; Asami, N.; Uragami, T. "A Reversibly Antigen-Responsive Hydrogel" *Nature* **1999**, *399*, 766-769.

(5) Lendlein, A.; Jiang, H. Y.; Junger, O.; Langer, R. "Light-Induced Shape-Memory Polymers" *Nature* **2005**, *434*, 879-882.

(6) Murdan, S. "Electro-Responsive Drug Delivery from Hydrogels" *J. Controlled Release* **2003**, *92*, 1-17.

(7) Szabo, D.; Szeghy, G.; Zrinyi, M. "Shape Transition of Magnetic Field Sensitive Polymer Gels" *Macromolecules* **1998**, *31*, 6541-6548.

(8) Ionov, L.; Minko, S.; Stamm, M.; Gohy, J. F.; Jerome, R.; Scholl, A. "Reversible Chemical Patterning on Stimuli-Responsive Polymer Film: Environment-Responsive Lithography" *J. Am. Chem. Soc*. **2003**, *125*, 8302-8306.

(9) Lahann, J.; Mitragotri, S.; Tran, T. N.; Kaido, H.; Sundaram, J.; Choi, I. S.; Hoffer, S.; Somorjai, G. A.; Langer, R. "A Reversibly Switching Surface" *Science* **2003**, *299*, 371-374.

(10) Mendes, P. M. "Stimuli-Responsive Surfaces for Bio-Applications" *Chem. Soc. Rev.* **2008**, *37*, 2512-2529.

(11) Russell, T. P. "Surface-Responsive Materials" *Science* **2002**, *297*, 964-967.

(12) Sidorenko, A.; Krupenkin, T.; Taylor, A.; Fratzl, P.; Aizenberg, J. "Reversible Switching of Hydrogel-Actuated Nanostructures into Complex Micropatterns" *Science* **2007**, *315*, 487-490.

(13) Tokarev, I.; Minko, S. "Stimuli-Responsive Hydrogel Thin Films" *Soft Matter* **2009**, *5*, 511-524.

(14) Nath, N.; Chilkoti, A. "Creating "Smart" Surfaces Using Stimuli Responsive Polymers" *Adv. Mater.* **2002**, *14*, 1243-1247.

(15) Hu, Z. B.; Chen, Y. Y.; Wang, C. J.; Zheng, Y. D.; Li, Y. "Polymer Gels with Engineered Environmentally Responsive Surface Patterns" *Nature* **1998**, *393*, 149-152.

(16) Kim, J.; Yoon, J.; Hayward, R. C. "Dynamic Display of Biomolecular Patterns through an Elastic Creasing Instability of Stimuli-Responsive Hydrogels" *Nat. Mater.* **2010**, *9*, 159-164.

(17) Kolodziej, C. M.; Maynard, H. D. "Shape-Shifting Micro- and Nanopatterns Controlled by Temperature" *J. Am. Chem. Soc.* **2012**, *134*, 12386-12389.

(18) Nath, N.; Chilkoti, A. "Interfacial Phase Transition of an Environmentally Responsive Elastin Biopolymer Adsorbed on Functionalized Gold Nanoparticles Studied by Colloidal Surface Plasmon Resonance" *J. Am. Chem. Soc.* **2001**, *123*, 8197-8202.

(19) Zhuang, X. W.; Ha, T.; Kim, H. D.; Centner, T.; Labeit, S.; Chu, S. "Fluorescence Quenching: A Tool for Single-Molecule Protein-Folding Study" *Proc. Natl. Acad. Sci. U. S. A.* **2000**, *97*, 14241-14244.

(20) Jones, L. J.; Upson, R. H.; Haugland, R. P.; PanchukVoloshina, N.; Zhou, M. J. "Quenched BODIPY Dye-Labeled Casein Substrates for the Assay of Protease Activity by Direct Fluorescence Measurement" *Anal. Biochem.* **1997**, *251*, 144-152.

(21) Hamann, S.; Kiilgaard, J. F.; Litman, T.; Alvarez-Leefmans, F. J.; Winther, B. R.; Zeuthen, T. "Measurement of Cell Volume Changes by Fluorescence Self-Quenching" *J. Fluoresc.* **2002**, *12*, 139-145.

(22) Kalinin, S.; Molothovsky, J. G.; Johansson, L. B. A. "Distance Measurements Using Partial Donor-Donor Energy Migration within Pairs of Fluorescent Groups in Lipid Bilayers" *J. Phys. Chem. B* **2003**, *107*, 3318-3324.

(23) Karolin, J.; Fa, M.; Wilczynska, M.; Ny, T.; Johansson, L. B. A. "Donor-Donor Energy Migration for Determining Intramolecular Distances in Proteins: I. Application of a Model to the Latent Plasminogen Activator Inhibitor-1 (PAI-1)" *Biophys. J.* **1998**, *74*, 11-21.

(24) Runnels, L. W.; Scarlata, S. F. "Theory and Application of Fluorescence Homotransfer to Melittin Oligomerization" *Biophys. J.* **1995**, *69*, 1569-1583.

(25) Acikgoz, S.; Aktas, G.; Inci, M. N.; Altin, H.; Sanyal, A. "FRET Between BODIPY Azide Dye Clusters within PEG-Based Hydrogel: A Handle to Measure Stimuli Responsiveness" *J. Phys. Chem. B* **2010**, *114*, 10954-10960.

(26) Yin, J.; Hu, H. B.; Wu, Y. H.; Liu, S. Y. "Thermo-and Light-Regulated Fluorescence Resonance Energy Transfer Processes within Dually Responsive Microgels" *Polym. Chem.* **2011**, *2*, 363-371.

(27) Wang, D.; Liu, T.; Yin, J.; Liu, S. Y. "Stimuli-Responsive Fluorescent Poly(*N*-Isopropylacrylamide) Microgels Labeled with Phenylboronic Acid Moieties as Multifunctional Ratiometric Probes for Glucose and Temperatures" *Macromolecules* **2011**, *44*, 2282-2290.

(28) Gota, C.; Okabe, K.; Funatsu, T.; Harada, Y.; Uchiyama, S. "Hydrophilic Fluorescent Nanogel Thermometer for Intracellular Thermometry" *J. Am. Chem. Soc.* **2009**, *131*, 2766-2767.

(29) Pinaud, F.; Russo, L.; Pinet, S.; Gosse, I.; Ravaine, V.; Sojic, N. "Enhanced Electrogenerated Chemiluminescence in Thermoresponsive Microgels" *J. Am. Chem. Soc.* **2013**, *135*, 5517-5520.

(30) Han, S.; Hagiwara, M.; Ishizone, T. "Synthesis of Thermally Sensitive Water-Soluble Polymethacrylates by Living Anionic Polymerizations of Oligo(Ethylene Glycol) Methyl Ether Methacrylates" *Macromolecules* **2003**, *36*, 8312-8319.

(31) Ishizone, T.; Seki, A.; Hagiwara, M.; Han, S.; Yokoyama, H.; Oyane, A.; Deffieux, A.; Carlotti, S. "Anionic Polymerizations of Oligo(Ethylene Glycol) Alkyl Ether Methacrylates: Effect of Side Chain Length and Omega-Alkyl Group of Side Chain on Cloud Point in Water" *Macromolecules* **2008**, *41*, 2963-2967.

(32) Lutz, J. F.; Hoth, A. "Preparation of Ideal PEG Analogues with a Tunable Thermosensitivity by Controlled Radical Copolymerization of 2-(2-Methoxyethoxy)Ethyl Methacrylate and Oligo(Ethylene Glycol) Methacrylate" *Macromolecules* **2006**, *39*, 893-896.

(33) Yamamoto, S. I.; Pietrasik, J.; Matyjaszewski, K. "The Effect of Structure on the Thermoresponsive Nature of Well-Defined Poly(Oligo(Ethylene Oxide) Methacrylates) Synthesized by ATRP" *J. Polym. Sci., Part A: Polym. Chem.* **2008**, *46*, 194-202.

(34) Hua, F. J.; Jiang, X. G.; Li, D. J.; Zhao, B. "Well-Defined Thermosensitive, Water-Soluble Polyacrylates and Polystyrenics with Short Pendant Oligo (Ethylene Glycol) Groups Synthesized by Nitroxide-Mediated Radical Polymerization" *J. Polym. Sci., Part A: Polym. Chem.* **2006**, *44*, 2454-2467.

(35) Toquer, G.; Monge, S.; Antonova, K.; Blanc, C.; Nobili, M.; Robin, J. J. "Synthesis via ATRP and Anchoring Properties of Ammonium-Terminated Monofunctional or Telechelic Polystyrenes" *Macromol. Chem. Phys.* **2007**, *208*, 94-102.

(36) Sadhu, V. B.; Pionteck, J.; Voigt, D.; Komber, H.; Fischer, D.; Voit, B. "Atom-Transfer Radical Polymerization: A Strategy for the Synthesis of Halogen-Free Amino-Functionalized Poly(Methyl Methacrylate) in a One-Pot Reaction" *Macromol. Chem. Phys.* **2004**, *205*, 2356-2365.

(37) Song, L. L.; Hennink, E. J.; Young, I. T.; Tanke, H. J. "Photobleaching Kinetics of Fluorescein in Quantitative Fluorescence Microscopy" *Biophys. J.* **1995**, *68*, 2588-2600.

(38) Panchuk-Voloshina, N.; Haugland, R. P.; Bishop-Stewart, J.; Bhalgat, M. K.; Millard, P. J.; Mao, F.; Leung, W. Y. "Alexa Dyes, a Series of New Fluorescent Dyes That Yield Exceptionally Bright, Photostable Conjugates" *J. Histochem. Cytochem.* **1999**, *47*, 1179-1188.

(39) Berlier, J. E.; Rothe, A.; Buller, G.; Bradford, J.; Gray, D. R.; Filanoski, B. J.; Telford, W. G.; Yue, S.; Liu, J. X.; Cheung, C. Y.; Chang, W.; Hirsch, J. D.; Beechem, J. M.; Haugland, R. P. "Quantitative Comparison of Long-Wavelength Alexa Fluor Dyes to Cy Dyes: Fluorescence of the Dyes and Their Bioconjugates" *J. Histochem. Cytochem.* **2003**, *51*, 1699-1712.

(40) Hama, Y.; Urano, Y.; Koyama, Y.; Bernardo, M.; Choyke, P. L.; Kobayashi, H. "A Comparison of the Emission Efficiency of Four Common Green Fluorescence Dyes after Internalization into Cancer Cells" *Bioconjugate Chem.* **2006**, *17*, 1426-1431.

(41) Christman, K. L.; Schopf, E.; Broyer, R. M.; Li, R. C.; Chen, Y.; Maynard, H. D. "Positioning Multiple Proteins at the Nanoscale with Electron Beam Cross-Linked Functional Polymers" *J. Am. Chem. Soc.* **2009**, *131*, 521-527.